

Carl Fredrik Andresen

Quark, Hybrid, and Unified Hybrid Stars with the Quark-Meson Model

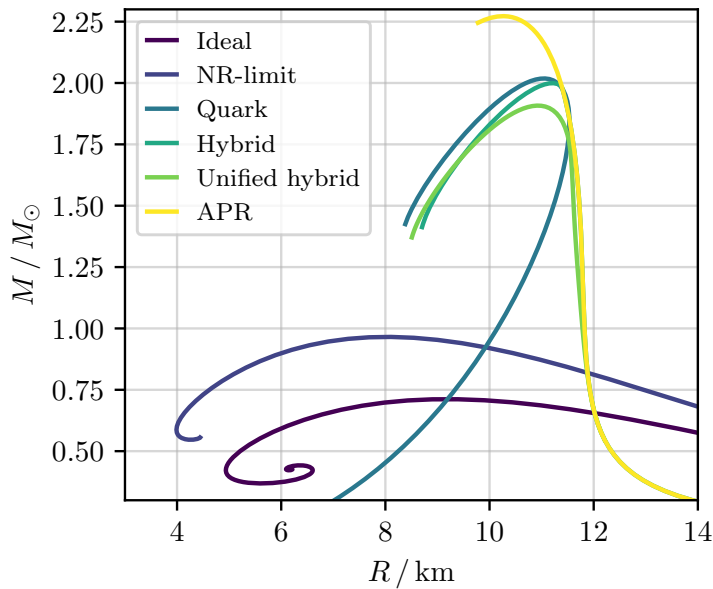
Including Ideal Neutron Stars

Master's thesis in Applied Physics and Mathematics

Supervisor: Jens Oluf Andersen

June 2023

Mass-Radius Relations for Compact Stars



Carl Fredrik Andresen

Quark, Hybrid, and Unified Hybrid Stars with the Quark-Meson Model

Including Ideal Neutron Stars

Master's thesis in Applied Physics and Mathematics
Supervisor: Jens Oluf Andersen
June 2023

Norwegian University of Science and Technology
Faculty of Natural Sciences
Department of Physics



Acknowledgements

First and foremost, I would like to thank my supervisor, Professor Jens Oluf Andersen. For one whole year, you have guided me on the challenging path towards describing a hybrid star. Our weekly meetings with feedback and insightful discussion have both motivated and sparked a growing curiosity in me for matter under extreme conditions. Having talked to other students about help and feedback on thesis work, it is clear to me that your thesis supervision is certainly top-notch – I have yet to find another student who has received feedback more frequently. Thank you!

Secondly, both the project and Master's thesis have been inspired by the works of Herman Sletmoen, Ref. [1]. In many places, I have followed in your footsteps, making it easy to correct errors I have made and also giving hints on where to look next. I know that not only I, but also several other students writing about entirely different topics, have been inspired by the effort you put into your thesis – thank you for setting an example of how it should be done.

Thirdly, I would like to thank my family and friends for proof reading parts of, or, for some, even the whole document. I can only imagine what it is like trying to get a hold of all the equations and jargon without having a background in physics.

Lastly, being a student in Trondheim is not only about studying – so thanks to all who have made my five years here entertaining!

Disclaimer to the External Examiner

This document represents the work two semesters. It consists of two main parts.

1. Part I is the project thesis, the work of the autumn semester, 2022.
2. Part II is the Master's thesis, the work of the spring semester, 2023.

In addition comes the Appendices. Appendices A–D belong to the project thesis. This leaves Appendices E–I to the Master's thesis.

Important: *Only Part II and Appendices E, F, G, H, and I are to be evaluated.*

There are a couple of reasons why I have chosen to include both the project and the Master's thesis in a single document. The two parts are very much connected. Specifically, the Master's thesis rests on some important results from the project thesis. Instead of deriving results twice, spending time writing the same contents in a different manner, the inclusion of both in one document allows free referencing of the project thesis results. Furthermore, the results in the Master's thesis are a natural continuation of where the project thesis ends.

Abstract

Part I: Ideal Neutron Stars (project thesis)

In this project, we set out to describe a spherical compact star composed of cold, non-interacting neutron matter. Along the way, we derive general equations which we can use later to build more complex, and more realistic, neutron star models. The main goal is to calculate the mass-radius relations parameterised by the central pressure of the star. The pressure, mass and radius are related by the Tolman-Oppenheimer-Volkoff-equation, which we derive from the theory of general relativity. This equation alone is not enough for a full description of a star – we need an equation which describes how the matter in the star behaves, called an equation of state. We derive one such equation by considering a free fermionic gas at $T = 0$. We call it the ideal equation of state. Then we combine these results to calculate the mass-radius relations for a sequence of ideal neutron stars. This reproduces the original work of Oppenheimer and Volkoff from 1939. Finally, we investigate the stability of ideal neutron stars through perturbation analysis, following the idea of Chandrasekhar from 1964. Although the ideal model is too simple to predict results in accordance with observations, it will lay the foundation for more realistic models.

Part II: Quark, Hybrid, and Unified Hybrid Stars (Master's thesis)

In part II, the Master's thesis, we describe cold, spherically symmetric, compact stars with the two-flavour quark-meson model. At first, we derive important thermodynamic quantities from quantum field theory at finite chemical potential. Plugging the quark-meson Lagrangian density into this framework, we obtain an equation of state for two-flavour quark matter, allowing us to model quark stars. With the Tolman-Oppenheimer-Volkoff-equations, we calculate mass maxima in the range $[1.77, 2.02] M_{\odot}$ (solar mass), depending on the quark-meson model parameters. Introducing the Akmal-Pandharipande-Ravenhall equation of state for nuclear matter, we also model compact stars consisting of both nuclear and quark matter: Hybrid stars. For an abrupt transition from nuclear to quark matter in the star core, we find maximum masses in the range $[2.00, 2.08] M_{\odot}$, again depending on the quark-meson model parameters. Using an interpolating phase between the nuclear and quark matter instead of the abrupt transition, we find that the range shifts to $[1.67, 1.95] M_{\odot}$. The choice of where to start and end the interpolating phase significantly influences the maxima, hence the difference in the size of the intervals for the two hybrid star models.

The cover plot displays a selection of the mass-radius relations we encounter throughout the project and Master's thesis.

Sammendrag

Del I: Ideelle nøytronstjerner (prosjektoppgave)

I prosjektoppgaven beskriver vi en sfærisk kompakt stjerne som består av kalde, ikke-interagerende nøytroner. Underveis utleder vi generelle likninger som vi kan bruke senere til å lage mer kompliserte og realistiske nøytronstjernemodeller. Hovedmålet er å regne ut masse-radius-relasjoner parametrisert ved stjernens sentraltrykk. Trykket, massen og radien kobles sammen av Tolman-Oppenheimer-Volkoff-likningen, som vi utleder fra generell relativitetsteori. Denne likningen alene er ikke nok til en fullstendig beskrivelse av en stjerne – vi trenger en likning som beskriver hvordan materien i stjernen oppfører seg, en tilstandslikning. Vi utleder en slik likning ved å betrakte en gass av frie fermioner ved $T = 0$. Vi kaller denne likningen for den ideelle tilstandslikningen. Deretter kombinerer vi resultatene til å regne ut masse-radius-relasjonene for en rekke av ideelle nøytronstjerner. Dette gjensker originalarbeidet til Oppenheimer og Volkoff fra 1939. Til slutt undersøker vi stabiliteten til ideelle nøytronstjerner ved hjelp av perturbasjonsteori. Denne delen er i tråd med arbeidet til Chandrasekhar fra 1964. Selv om den ideelle modellen er for enkel til å produsere resultater som stemmer overens med observasjoner, vil den legge grunnlaget for mer realistiske modeller.

Del II: Kvark-, hybrid- og forente hybridstjerner (masteroppgave)

I del II, masteroppgaven, beskriver vi kalde, sfærisk-symmetriske, kompakte stjerner med kvark-mesonmodellen med to kvarker. Til å begynne med utleder vi relevante termodynamiske størrelser fra kvantefeltteori ved endelig kjemisk potensial. Vi bruker deretter dette rammeverket på den fenomenologiske kvark-mesonmodellen for å finne en tilstandslikning for kvarkmaterie bestående av de to letteste kvarkene, u - og d -kvarken. Med TOV-likningene regner vi ut massemaksimum i intervallet $[1.77, 2.02] M_{\odot}$ for kvarkstjerner. Maksimalverdien avhenger av parameterne vi bruker i kvark-mesonmodellen. Ved hjelp av Akmal-Pandharipande-Ravenhall-tilstandslikningen modellerer vi også kompakte stjerner bestående av både nukleær- og kvarkmaterie: Såkalte hybridstjerner. Ved å bruke en brå overgang fra nukleærmaterie til kvarkmaterie i stjernens kjerne, finner vi maksimalmasser i intervallet $[2.00, 2.08] M_{\odot}$. På ny avhenger verdien av modellparameterne. Til slutt bruker vi også en interpolerende fase mellom nukleær- og kvarkmaterien i det vi kaller en forent hybridstjerne. Da finner vi at maksimalmassene flyttes til intervallet $[1.67, 1.95] M_{\odot}$. Maksimalmassene er følsomme for hvor vi velger å begynne og slutte den interpolerende fasen, og derfor spenner dette siste intervallet over flere verdier enn det forrige.

Illustrasjonen på fremsiden viser noen av masse-radius-relasjonene vi regner ut i løpet av prosjekt- og masteroppgaven.

Table of Contents

Acknowledgement	i
Abstract	v
Sammendrag	vii
Part I: Ideal Neutron Stars	1
1 Introduction	3
2 General Relativity and the TOV-equation	5
2.1 Deriving the Einstein Equation	5
2.2 The Spherically Symmetric Star	8
3 Solution to the TOV-equation for an Incompressible Fluid	13
3.1 TOV-solution for an Incompressible Fluid	13
3.2 Newtonian Gravity and an Incompressible Fluid	15
3.3 Comparing TOV and Newtonian Solution for an Incompressible Fluid	17
4 Equation of State for an Ideal Fermi Gas	21
4.1 Fermion Statistics and the Ideal Equation of State	21
4.2 Limiting Behavior of the Ideal Equation of State	24
5 TOV-solutions for the free Fermi gas	29
5.1 TOV Solution for an Ultrarelativistic Equation of State for a Free Fermi Gas	29
5.2 Numeric Solution to the TOV-equation for the Free Fermi Gas	30
6 Stability of Compact Stars	35
6.1 Qualitative Argument for Stability	35
6.2 Stability Analysis Through Perturbation Theory	37
6.2.1 Defining the Radial Perturbation	37
6.2.2 Constraining the Radial Perturbation	41
6.2.3 Finding the Eigenfrequencies of the Radial Perturbation	45
6.3 Stability of Ideal Neutron Stars	47
7 Summary and outlook	51
7.1 Summary	51
7.2 Outlook	52

Part II: Quark, Hybrid, and Unified Hybrid Stars with the Quark-Meson Model	54
8 Introduction	55
9 Quantum Fields at Finite Chemical Potential	57
9.1 Deriving Thermodynamical Quantities from the Grand Potential	57
9.2 The Grand Canonical Partition Function from a Quantum Field Theory Description . . .	58
9.2.1 Grand Partition Function for Bosons	61
9.3 Grand Partition Function for Fermions	65
9.3.1 Grassmann Numbers	66
9.3.2 Path Integral Tools for Fermions	69
9.4 The Number Density Operator \hat{N}	75
10 Two-Flavour Quark-Meson Model	77
10.1 From QCD to the Quark-Meson Model	77
10.2 The Two-Flavour Quark-Meson Lagrangian	81
11 Quark Stars with the QM-model	85
11.1 The Grand Potential in the Mean-Field Approximation	85
11.1.1 Matsubara Frequency Summation	89
11.2 Divergence in the Quark-Meson Model in the Mean Field Approximation	92
11.3 Pressure and Energy Density in the Quark-Meson Model at Zero Temperature	93
11.4 Parameter Fit at Tree Level	96
11.4.1 Determining the Bag Constant	102
11.5 Consistent Renormalising of the Quark-Meson model	105
12 Hybrid Stars	111
12.1 The Akmal-Pandharipande-Ravenhall Equation of State	111
12.2 First-Order Transition Between Nucleon Matter and Quark Matter	113
12.3 Interpolating Between the Nucleonic Phase and the Quark Phase	116
12.4 Comparing the Quark and Hybrid Stars to Observed Neutron Stars	123
13 Summary & Outlook	125
13.1 Summary	125
13.2 Outlook	128
A Relativistic Thermo- and Fluid Dynamics	129
A.1 Energy-momentum Tensor for Ideal Fluid	129
A.2 Thermodynamics for an Ideal Fluid	130
B Energy-Momentum Conservation	135
B.1 The Euler-Lagrange Equation	135
B.2 Spacetime Translation Symmetry	136
C Time-Dependent Schwarzschild Metric	139
D Numerical Methods of Part I	143
D.1 Numerical Solution to the TOV-system of Equations	143
D.2 Eigenfrequencies for the Radially Oscillating Ideal Neutron Star	147
E Gaussian Integrals	151
E.1 Ordinary Gaussian Integrals	151
E.2 Grassmannian Gaussian Integrals	154
F Noether's Theorem	157

G Feynman Diagrams	159
G.1 Feynman Rules for the Quark-Meson Model	159
G.2 Diagram Calculation	160
H Dimensional Regularisation	161
I Numerical Methods of Part II	165
I.1 Dimensionless Form of Ω	165
I.2 Construction of Interpolating Polynomials in a Unified Equation of State	167
References	173

Notation

Throughout both Part I and Part II of this project, we will use the Einstein summation convention. This means repeated indices are summed over. We say that we contract the indices. Greek indices, e.g. μ and ν , denote spacetime indices and are consequently summed from 0 to 3. Latin alphabet indices, e.g. i and n , denote Euclidean indices. These indices are summed from 1 to 3. This is, of course, unless anything else is specified.

$$T^\mu = T^0 + T^1 + T^2 + T^3 \quad \text{and} \quad T^i = T^1 + T^2 + T^3. \quad (0.1)$$

For the metric tensor, we will use the mostly negative convention. For a flat spacetime, this means that the Minkowski metric $\eta_{\mu\nu}$ takes the form

$$\eta_{\mu\nu} = \begin{pmatrix} 1 & 0 & 0 & 0 \\ 0 & -1 & 0 & 0 \\ 0 & 0 & -1 & 0 \\ 0 & 0 & 0 & -1 \end{pmatrix}. \quad (0.2)$$

To describe a spacetime vector, we will use both \mathbf{x} and x^μ . The two notations are equivalent. For a spatial 3-dimensional vector, we will use the notation \vec{x} . As a shorthand for partial derivative of a spacetime coordinate x^μ , we will write

$$\partial_\mu \equiv \frac{\partial}{\partial x^\mu} = \left(\frac{1}{c} \frac{\partial}{\partial t}, \frac{\partial}{\partial x^1}, \frac{\partial}{\partial x^2}, \frac{\partial}{\partial x^3} \right). \quad (0.3)$$

For the project thesis, we will, unlike many texts on general relativity and special relativity, we keep all the natural constants as they appear, i.e. the speed of light c , Planck's reduced constant \hbar and Newton's gravitational constant G will not be set to unity.

However, in Part II, the Master's thesis, we will take

$$\hbar = c = 1. \quad (0.4)$$

Fermions and γ -matrices

Fermions are described by a complex 4-component vector $\Psi = (\Psi_0, \Psi_1, \Psi_2, \Psi_3)$. In the fermionic sector of a Lagrangian density, the γ -matrices appear. These matrices mix the components of fermion-vectors. We denote them with Lorentz-indices. They satisfy the following anti-commutation relation

$$\{\gamma^\mu, \gamma^\nu\} = 2\eta^{\mu\nu}. \quad (0.5)$$

Explicitly, they read

$$\begin{aligned} \gamma^0 &= \begin{pmatrix} 1 & 0 & 0 & 0 \\ 0 & 1 & 0 & 0 \\ 0 & 0 & -1 & 0 \\ 0 & 0 & 0 & -1 \end{pmatrix}, & \gamma^1 &= \begin{pmatrix} 0 & 0 & 0 & 1 \\ 0 & 0 & 1 & 0 \\ 0 & -1 & 0 & 0 \\ -1 & 0 & 0 & 0 \end{pmatrix}, \\ \gamma^2 &= \begin{pmatrix} 0 & 0 & 0 & -i \\ 0 & 0 & i & 0 \\ 0 & i & 0 & 0 \\ -i & 0 & 0 & 0 \end{pmatrix}, & \gamma^3 &= \begin{pmatrix} 0 & 0 & 1 & 0 \\ 0 & 0 & 0 & -1 \\ -1 & 0 & 0 & 0 \\ 0 & 1 & 0 & 0 \end{pmatrix}. \end{aligned} \quad (0.6)$$

In addition to these, we will encounter γ^5 , which is defined as

$$\gamma^5 = i\gamma^0\gamma^1\gamma^2\gamma^3 = \begin{pmatrix} 0 & 0 & 1 & 0 \\ 0 & 0 & 0 & 1 \\ 1 & 0 & 0 & 0 \\ 0 & 1 & 0 & 0 \end{pmatrix}. \quad (0.7)$$

Considering a fermion as a complex 4 vector, we see that the γ^5 -matrix acts upon the fermion by swapping the upper components, Ψ^0, Ψ^1 , with the lower two, Ψ^2, Ψ^3 . The γ^5 -matrix has the property that it anti-commutes with all the other γ^μ . In addition, it is Hermitian and it squares to unity.

$$\{\gamma^5, \gamma^\mu\} = 0, \quad (\gamma^5)^\dagger = \gamma^5, \quad \text{and} \quad \gamma^5\gamma^5 = \mathbb{1}_{4 \times 4}. \quad (0.8)$$

Although $(\gamma^5)^2$ is a matrix, we will favour writing simply 1 instead of $\mathbb{1}_{4 \times 4}$. This is for brevity of notation, as there are other indices to sum over as well, e.g. colour and flavour indices for quarks. Whenever quarks enter the Lagrangian, they are represented by 4-component vectors, and we will not always be explicit about this.

Pauli Matrices

The Pauli matrices, τ_i , are frequently occurring in physics, and this thesis is no exception. On matrix form, the Pauli matrices read

$$\tau_1 = \begin{pmatrix} 0 & 1 \\ 1 & 0 \end{pmatrix}, \quad \tau_2 = \begin{pmatrix} 0 & -i \\ i & 0 \end{pmatrix}, \quad \tau_3 = \begin{pmatrix} 1 & 0 \\ 0 & -1 \end{pmatrix}. \quad (0.9)$$

For us, they will be particularly important as the generators of the $SU(2)$ -group, the group of all complex 2×2 -matrices where a matrix $U^\dagger = U^{-1}$, with a determinant of absolute value 1. Being the generators means that we can write any element $U \in SU(2)$ as $U = \exp(i\alpha_j\tau_j)$. It also comes with the properties of being Hermitian and traceless.

$$(\tau_i)^\dagger = \tau_i, \quad \text{and} \quad \text{Tr}(\tau_i) = 0. \quad (0.10)$$

In addition, it is possible to show that

$$\text{Tr}(\tau_i\tau_j) = 2\delta_{ij}, \quad (0.11)$$

where δ_{ij} is the Kronecker delta. We will also encounter the Gell-Mann-matrices, which are the standard matrices to represent the basis for the generators of the $SU(3)$ -group. We denote these by T^A , where $A \in \{1, \dots, 8\}$. These are, in some sense, the bigger brothers of the Pauli-matrices.

Conversion Factors and Useful Constants

As we use the unit conversion in Eq. (0.4) in the Master's thesis, we express e.g. masses, number densities, and pressures in different powers of an energy scale, often with units of MeV. Consequently, when we have performed all calculations, the answer is not expressed in terms of familiar SI-units. In order to keep the numeric values low, we will also often use $f_\pi = 93 \text{ MeV}$ as the energy scale. Restoring the c and \hbar is a simple exercise when we know what SI-unit we are going back to. We need conversions for energy densities, pressures and number densities. The most relevant conversions are

$$f_\pi^4 \xrightarrow{\text{Restore } \hbar, c} 9.74 \times 10^{-3} \text{ GeV fm}^{-3} = 1.56 \times 10^{33} \text{ Pa}, \quad (\text{energy density, pressure}) \quad (0.12)$$

$$f_\pi^3 \xrightarrow{\text{Restore } \hbar, c} 0.1047 \text{ fm}^{-3}. \quad (\text{number density}) \quad (0.13)$$

A practical scale to compare neutron star number densities against, is the nuclear saturation density, n_0 , which is the number density in atomic nuclei. The neutron star masses are often comparable to the solar mass, M_\odot . We use

$$n_0 \approx 0.16 \text{ fm}^{-3} \xrightarrow{\hbar=c=1} 1.53 f_\pi^3, \quad (0.14)$$

$$M_\odot = 1.988 \times 10^{30} \text{ kg}, \quad (0.15)$$

as their values, see Refs. [2] and [3].

We will mostly try to omit abbreviations, with some exceptions. The words we abbreviate will be explained at their first occurrence in the main text. To have them all in one place, we list them here.

SR = Special relativity,	GR = General relativity,
TOV = Tolman-Oppenheimer-Volkoff,	QFT = Quantum field theory,
TFT = Thermal field theory,	APR = Akmal-Pandharipande-Ravenhall.

Part I
Ideal Neutron Stars

Project Thesis

Autumn 2022

Introduction

Stars have fascinated mankind for a long time. And for good reason, as our existence is dependent on one. But not only are stars intriguing due to their importance to us, they also exhibit interesting physics throughout their entire lifespan. From thermo-nuclear fusion processes, relativistic gravitational effects to supernovae: The life of a star is certainly worthwhile giving a bit of extra attention. Trying to describe a star forces us to combine many important branches of physics into one exciting description.

When thinking of a star, most people imagine luminous objects powered by fusion reactions in the core. But this is just one part of the life cycle of a star. Every star evolves through several phases before ending up as either a white dwarf, a neutron star or a black hole. In the beginning, a star forms as a cloud of interstellar gas gathers into a cluster. Gravity attracts more gas into the cluster as time passes. The gravitational energy released from the attraction is converted to thermal energy, and the temperature in the cluster rises along with the energy density and the pressure. At a certain temperature, fusion processes start at the core. At this point, the star has entered its luminous stage. We say that it has become a main sequence star. During the luminous stage, the radiation pressure balances the gravitational pull. The fusion processes start with hydrogen, until all the hydrogen has run out in the core. Then the core starts to contract, enabling fusion of helium due to the increase in temperature. This goes on with heavier and heavier elements, until the core can no longer reach the temperature to start the next fusion stage. For the most massive stars, iron marks the end of the fusion processes, as iron can no longer produce energy by fusion. This means that at some point, every star runs out of fuel and the fusion processes stop. Then the star starts to contract due to the force of gravity. The next stage depends on the mass of the star. A white dwarf is the end state for a star of relatively low mass. By relatively low, we mean stars with mass $< 8M_{\odot}$. Much of the mass is lost in the process of becoming a white dwarf, as a white dwarf typically has a mass of $\sim 0.5M_{\odot}$. The dwarf is a hot, compact object. A white dwarf usually has a radius of a few kilometers, and a mass density about a million times higher than that of the earth. A massive star, i.e. $M > 8M_{\odot}$, may end up as a neutron star after a great explosion called a supernova. A neutron star is smaller and way more compact than a white dwarf. A typical neutron star has a radius of about ten kilometers and a mass of $\sim 1.4M_{\odot}$. This means that the neutron star is incredibly dense! In comparison, the radius of the sun is about 70000 times larger than that of the average neutron star, and the masses are comparable. We call both white dwarves and neutron stars compact stars. The most massive stars create black holes, also after a supernova. We will not consider black holes here. For a more detailed introduction to the life cycle of a star, see Ref. [4](pp. 62-69).

In this thesis, we are particularly interested in the compact remnants of a main sequence star. Both the white dwarf and the neutron star will after their formation gradually cool down through thermal radiation. Compact stars are dense objects where the force of gravity is balanced by an internal pressure. Such a pressure can stem from the Pauli exclusion principle, which states that fermions cannot occupy the

same state. We call this type of pressure the quantum pressure or the degeneracy pressure. The internal pressure in a compact star can also be caused by repulsive forces between the particles. For instance, in a low temperature white dwarf, the pressure comes from the quantum pressure from degenerate, non-relativistic electrons. A neutron star is also sustained by the degeneracy pressure, but due to its large internal energy it cannot be treated non-relativistically. The high mass densities are not suitable for a Newtonian gravity-description. This means that matter should be treated with a relativistic description, and the strong gravitational force should be described by the theory of general relativity. The compact stars are interesting because of the extreme conditions imposed on the matter inside. This is particularly true for a neutron star. In this thesis, we are going to describe a neutron star composed of cold non-interacting neutron matter in the framework of general relativity and statistical physics. This is a preliminary to the study of more complex neutron star models consisting of interacting matter with more than one species of particle.

General Relativity and the TOV-equation

The main goal of this chapter is to derive the Tolman-Oppenheimer-Volkoff-equation (TOV). This is a differential equation which we will use to describe compact stars. To do so, we must first derive the Einstein equation from general relativity. Then we solve the Einstein equation for a spherically symmetric geometry. Although we assume the reader is familiar with GR, we give a quick recapitulation of the most essential ideas and quantities. This also serves to explain the notation.

2.1 Deriving the Einstein Equation

In GR, and hence SR, we do not treat space and time separately. In the Newtonian description of reality, we are used to treat space and time separately. We use 3-dimensional vectors for space, and time is treated as an independent parameter. In GR, however, we treat space and time together, as one 4-dimensional vector in spacetime. A coordinate is then $\mathbf{x} = x^\mu = (cx^0, x^1, x^2, x^3)$, where we put the time coordinate first. In a Cartesian coordinate system, this vector takes the form $x^\mu = (ct, x, y, z)$. In addition to including the time coordinate to construct a 4-vector, we use a special metric when we take the scalar product. This metric is called the Minkowski metric, and it is written out in Eq. (0.2). Taking the scalar product of a vector with itself gives a measure of distance in spacetime. For an infinitesimal vector, it reads

$$\begin{aligned} \mathbf{dx} \cdot \mathbf{dx} &= dx^\mu \eta_{\mu\nu} dx^\nu = \eta_{\mu\nu} dx^\mu dx^\nu \\ &= (cdx^0)^2 - (dx^1)^2 - (dx^2)^2 - (dx^3)^2 \\ &= c^2 dt^2 - dx^2 - dy^2 - dz^2. \end{aligned} \tag{2.1}$$

In the first line, we are free to move $\eta_{\mu\nu}$ around since it is just a number when we write the equation in component form. Why is this a natural formalism? There are many reasons, and we shall consider one particular example. We see that the positive term is equal to how far the speed of light can travel during the time t . The sum of the negative terms is equal to the usual length of a 3-dimensional vector. From this, we see that a vector \mathbf{x} with negative spacetime distance has a spatial component \vec{x} which is longer than than the speed of light can travel during the time t . To see why this is useful, we now let \mathbf{x} and \mathbf{y} describe two separate spacetime events. Imagine for instance that the event $\mathbf{x} = (t, \vec{x})$ is a light signal being emitted at some point in space \vec{x} at a time t , and similarly for \mathbf{y} . The difference between the two events $\mathbf{x} - \mathbf{y}$ describes their separation both temporally and spatially. If the length of the difference $\mathbf{x} - \mathbf{y}$ is smaller than zero, we know that the two events cannot be connected to each other, as the light emitted from \mathbf{x} would not have had the time to reach \mathbf{y} or the other way around. This is due to the fact that no signal can, of course, travel faster than light. This feature is very useful, as it easily allows us to

determine whether two events are causally connected or not. In addition, the path of light will always have a spacetime distance which is zero.

The case we have described above is only applicable to flat spacetime. We are interested in GR, where spacetime is in general curved. We can generalise the flat spacetime formalism through the mathematical description of spacetime as a Riemannian manifold. We will not go into detail about the mathematical definition here, but a main feature of a Riemannian manifold is that at any point, it is locally flat. This means that in a small neighbourhood, we can find a coordinate system in which the metric is Minkowski. This property is called the equivalence principle. Physically, it means that in a neighbourhood, the laws of physics from flat space are valid. This has the consequence that the analysis of a flat spacetime carries over to the general spacetime. In particular, the notion of distance we introduced above is valid in a small neighbourhood around any point.

To describe a Riemannian manifold, we promote the Minkowski metric to a more general, spacetime dependent metric $\eta_{\mu\nu} \rightarrow g_{\mu\nu}(\mathbf{x})$. In a scalar product, we now use $g_{\mu\nu}$. The distance between two infinitesimally separated points, also called a line element ds^2 , now reads

$$ds^2 = g_{\mu\nu} dx^\mu dx^\nu. \quad (2.2)$$

The notion of distance holds for two infinitesimally separated points, because they belong in the same neighbourhood. Eq. (2.2) is similar to the case for the flat spacetime Eq. (2.1), except for the change of the metric. In order to measure distances between well-separated events, we would have to integrate the line elements between the two events.

We see that the metric tensor can be taken to be symmetric in its indices: $g_{\mu\nu} = g_{\nu\mu}$, because any anti-symmetric component does not contribute to ds^2 .

Next, we are interested in performing coordinate transformations from one coordinate system described by x^μ to another coordinate system described by $x'^\mu = x'^\mu(\mathbf{x})$. We can use the product rule to express the transformation for an infinitesimal vector dx'^μ . We can also do this the other way around, for $x^\mu = x^\mu(\mathbf{x}')$. We find

$$dx'^\mu = \frac{\partial x'^\mu}{\partial x^\nu} dx^\nu \quad \text{and} \quad dx^\mu = \frac{\partial x^\mu}{\partial x'^\nu} dx'^\nu. \quad (2.3)$$

Going from one coordinate system to the other and then back again, we see that these transformations are inverses of each other. Mathematically speaking, we write $\frac{\partial x'^\mu}{\partial x^\rho} \frac{\partial x^\rho}{\partial x'^\nu} = \delta_\nu^\mu$, where δ_ν^μ denotes the elements of the identity matrix. We require that the line element is invariant under coordinate transformations. Otherwise, there would be no properly defined notion of distance. Let now $g'_{\mu\nu}$ denote the metric tensor in the coordinate system described by coordinates x'^μ . Asserting the invariance of the line element in Eq. (2.2) allows us to write

$$\begin{aligned} g'_{\mu\nu} dx'^\mu dx'^\nu &= g_{\alpha\beta} dx^\alpha dx^\beta \\ g'_{\mu\nu} \frac{\partial x'^\mu}{\partial x^\alpha} \frac{\partial x'^\nu}{\partial x^\beta} dx^\alpha dx^\beta &= g_{\alpha\beta} dx^\alpha dx^\beta, \end{aligned} \quad (2.4)$$

or

$$g'_{\mu\nu} = g_{\alpha\beta} \frac{dx^\alpha}{dx'^\mu} \frac{dx^\beta}{dx'^\nu}. \quad (2.5)$$

In going from Eq. (2.4) to Eq. (2.5), we have cancelled the equal differentials on each side, and we have applied the inverse transformation to both sides to express $g'_{\mu\nu}$ in terms of $g_{\mu\nu}$ and the transformation. We see that each index of the metric transforms inversely the vector dx^μ . This motivates us to define tensors with covariant upper indices and contravariant with lower indices. A tensor is an object with one or more indices, upper or lower, which abides specific transformation rules under a change of coordinate systems. For a tensor with one index, also called a vector, the transformation property looks like

$$V^\mu \rightarrow V'^\mu = \frac{\partial x'^\mu}{\partial x^\nu} V^\nu \quad \text{and} \quad V_\mu \rightarrow V'_\mu = \frac{\partial x^\nu}{\partial x'^\mu} V_\nu. \quad (2.6)$$

For a tensor with more than one index, each upper index μ will transform as $\frac{\partial x'^{\mu}}{\partial x^{\nu}}$, and each lower index μ as $\frac{\partial x^{\nu}}{\partial x'^{\mu}}$. The metric tensor is an example of this, as seen in Eq. (2.5).

We define the metric tensor with upper indices, $g^{\mu\nu}$, to be the inverse of $g_{\mu\nu}$. This means that $g_{\mu\alpha}g^{\alpha\nu} = \delta_{\mu}^{\nu}$. We confirm that the inverse property also holds after a coordinate transformation, which it should if the transformation rules for tensors are properly defined.

$$\begin{aligned}\delta_{\nu}^{\mu} &= g^{\mu\rho}g_{\rho\nu} \rightarrow g'^{\mu\rho}g'_{\rho\nu} = g^{\alpha\beta}\frac{dx'^{\mu}}{dx^{\alpha}}\frac{dx'^{\rho}}{dx^{\beta}}g_{\sigma\omega}\frac{\partial x^{\sigma}}{\partial x'^{\rho}}\frac{\partial x^{\omega}}{\partial x'^{\nu}} \\ &= g^{\alpha\beta}g_{\sigma\omega}\delta_{\beta}^{\sigma}\frac{dx'^{\mu}}{dx^{\alpha}}\frac{\partial x^{\omega}}{\partial x'^{\nu}} = \delta_{\omega}^{\alpha}\frac{\partial x^{\omega}}{\partial x'^{\nu}} = \delta_{\nu}^{\mu}.\end{aligned}\quad (2.7)$$

Going on, we use the metric tensor to lower and raise indices of tensors by contraction, e.g.

$$V_{\mu} = g_{\mu\nu}V^{\nu} \quad \text{and} \quad V^{\mu} = g^{\mu\nu}V_{\nu}.\quad (2.8)$$

This is also consistent with the tensorial transformation rules, of course. From the raising or lowering property, we notice that the metric with one upper and one lower index is equal to the identity matrix, $g_{\mu}^{\nu} = g_{\mu\alpha}g^{\alpha\nu} = \delta_{\mu}^{\nu}$.

Until now, we have not mentioned any other vector quantities besides the position coordinates dx^{μ} . An example of another vector, is the four-velocity u^{μ} . Here it is written in its contravariant form. The 4-velocity will be important later. Let r^{μ} denote some position 4-vector, and we would like to find its velocity. Typically, one would differentiate with respect to the coordinate time. This will not work now, as we want to preserve the tensorial transformation property of the position 4-vector r^{μ} . We know that the time coordinate in general transforms, so differentiating a vector with respect to the time coordinate, would in total not transform with the transformation property defined above, in Eq. (2.6). Both the position 4-vector component and the derivative itself would transform under a change of coordinate system, ruining the linear transformation property we want. We need to differentiate with respect to something which is invariant with respect to a coordinate transform. We have already defined one such quantity: The line element. From the line element, we can define the proper time τ .

$$d\tau^2 = \frac{ds^2}{c^2}.\quad (2.9)$$

The proper time has a nice physical interpretation. We imagine an observer moving along a spacetime curve. This observer perceives it as the surroundings are moving, and that he/she is at rest. The time this observer would measure going from one point on the spacetime curve to another, is the proper time. We can use the proper time instead of t to parameterise the differentiation. For a position vector r^{μ} with non-zero $d\tau$, we define the four-velocity of as

$$u^{\mu} = \frac{dr^{\mu}}{d\tau} = \left(c \frac{dr^0}{d\tau}, \frac{dr^1}{d\tau}, \frac{dr^2}{d\tau}, \frac{dr^3}{d\tau} \right).\quad (2.10)$$

We need a few more definitions before we can write down the Einstein equation. With the metric tensor, we can write the Christoffel symbols, also called the metric connection, as

$$\Gamma_{\mu\nu}^{\lambda} = \frac{1}{2}g^{\lambda\sigma}(\partial_{\mu}g_{\sigma\nu} + \partial_{\nu}g_{\sigma\mu} - \partial_{\sigma}g_{\mu\nu}).\quad (2.11)$$

Firstly, we notice that the symmetry of exchanging the indices in $g_{\mu\nu}$, implies a symmetry of interchanging the lower indices in $\Gamma_{\mu\nu}^{\lambda}$. We mentioned earlier that in GR, we can at any point erect a coordinate system such that a neighbourhood around the point is described by the Minkowski metric. The Christoffel symbols describe the connection between a locally flat coordinate system with another coordinate system. From their definition, we see that the Christoffel symbols vanish if space becomes flat. This happens because the metric then becomes independent of spacetime coordinates, and all partial derivatives in the parenthesis vanish. Despite appearing to be so, the Christoffel symbols are not tensorial. However, they

appear in the expression for the covariant derivative ∇_μ , which, when acting on a tensor quantity, is a tensor.

$$\nabla_\lambda T^{\mu\nu\dots}_{\rho\sigma\dots} = \partial_\lambda T^{\mu\nu\dots}_{\rho\sigma\dots} + \Gamma^\mu_{\lambda\alpha} T^{\alpha\nu\dots}_{\rho\sigma\dots} + \Gamma^\nu_{\lambda\alpha} T^{\mu\alpha\dots}_{\rho\sigma\dots} + \dots - \Gamma^\alpha_{\lambda\rho} T^{\mu\nu\dots}_{\alpha\sigma\dots} - \Gamma^\alpha_{\lambda\sigma} T^{\mu\nu\dots}_{\rho\alpha\dots} - \dots \quad (2.12)$$

Loosely speaking, the covariant derivative ∇_μ generalises the partial derivative ∂_μ . Going from a curved spacetime to a flat one, the covariant derivative simplifies to the partial derivative because the Christoffel symbols vanish. Now we are ready to introduce a very important principle: The principle of general covariance. This principle states that any result valid in SR is valid also in GR with the exception that the Minkowski metric $\eta_{\mu\nu}$ takes the form of the general metric $g_{\mu\nu}$ and partial derivatives ∂_μ turn into covariant derivatives ∇_μ . This follows from the equivalence principle. A good discussion can be found in [5], (pp. 385-387).

Acting with the covariant derivative upon the metric tensor gives 0, i.e. $\nabla_\lambda g_{\mu\nu} = 0$. This can be found by combining Eqs. (2.11) and (2.12). Now everything is set up to define the Riemann curvature tensor $R^\lambda_{\mu\nu\rho}$. The Riemann curvature tensor arises from the fact that covariant derivatives no longer commute, as ordinary partial derivatives do. We investigate the commutator acting on a vector

$$[\nabla_\mu, \nabla_\nu]V_\rho = \nabla_\mu \nabla_\nu V_\rho - \nabla_\nu \nabla_\mu V_\rho \equiv -R^\lambda_{\mu\nu\rho} V_\lambda. \quad (2.13)$$

From the definition above, the Riemann curvature tensor $R^\lambda_{\mu\nu\rho}$ takes the form

$$R^\lambda_{\mu\nu\rho} = \partial_\mu \Gamma^\lambda_{\nu\rho} - \partial_\nu \Gamma^\lambda_{\mu\rho} + \Gamma^\alpha_{\mu\rho} \Gamma^\lambda_{\nu\alpha} - \Gamma^\alpha_{\nu\rho} \Gamma^\lambda_{\mu\alpha}. \quad (2.14)$$

A discussion of the Riemann curvature tensor can be found in [6] (pp. 77-81). Flat space is equivalent to the vanishing of the Riemann curvature tensor. If we contract the first index in the Riemann curvature tensor with its third, we get the Ricci tensor $R_{\mu\nu}$. Contracting the indices of the Ricci tensor gives the Riemann scalar R .

$$R^\lambda_{\mu\lambda\nu} = R_{\mu\nu} \quad \text{and} \quad g^{\mu\alpha} R_{\alpha\mu} = R^\mu_\mu = R. \quad (2.15)$$

Finally, we have defined all tensors we need to state the equation which governs how matter and momentum curves spacetime. This equation is called the Einstein equation. A derivation of this from physical principles can be found in [5] (pp. 405-407). In component form, it is

$$R_{\mu\nu} - \frac{1}{2} R g_{\mu\nu} = -\frac{8\pi G}{c^4} T_{\mu\nu}, \quad (2.16)$$

which is ten equations - one for each index combination, subtracting six of them due to the $(\mu \leftrightarrow \nu)$ -symmetry. Note the minus sign on the right hand side. This is a consequence of our choice of the mostly negative metric. $T_{\mu\nu}$ is the energy-momentum tensor. In general, we have to add another term $\Lambda g_{\mu\nu}$ to the left hand side, where Λ is called the cosmological constant. This extra term plays an important role in the expansion of the universe, but close to a massive object, it is so small that we can neglect it.

2.2 The Spherically Symmetric Star

The next goal is to solve Eq. (2.16) for the metric $g_{\mu\nu}$ for a spherically symmetric star. In spherical coordinates, we use spacetime coordinates $x^\mu = (ct, r, \theta, \phi)$. Having a stationary spherical symmetry, there should be neither time dependence nor angular dependence in the metric. In addition, the line element ds^2 should be invariant under time inversion, $t \rightarrow -t$, and to independent inversions of the spatial axes, namely $\theta \rightarrow \pi - \theta$ and $\phi \rightarrow -\phi$. Performing these inversions corresponds to sending $dt \rightarrow -dt$, $d\theta \rightarrow -d\theta$ and $d\phi \rightarrow -d\phi$ in Eq. (2.2). In order for ds^2 to be invariant, we have to require that g_{rt} , $g_{r\theta}$, $g_{r\phi}$, $g_{t\theta}$, $g_{t\phi}$ and $g_{\theta\phi}$ all vanish. For the angular part, we should also have $g_{\theta\theta}d\theta^2 + g_{\phi\phi}d\phi^2 = f(r)[d\theta^2 + \sin^2(\theta)d\phi^2] = f(r)d\Omega^2$, due to the spherical symmetry. This is the customary angular element scaled with some function of the radial coordinate r . We are left with

$$ds^2 = g_{\mu\nu} dx^\mu dx^\nu = g_{tt}(r)c^2 dt^2 + g_{rr}(r)dr^2 - f(r)d\Omega^2. \quad (2.17)$$

We still have the freedom to choose the radial coordinate. A convenient choice is $r' = r'(r)$ such that $r'^2 = -f(r)$, which makes the angular part of the metric the customary one from flat space in spherical coordinates. We also rename $r' \rightarrow r$, $g_{tt}(r) = \alpha(r)$ and $g_{rr} = -\beta(r)$. In this way, we have arrived at the most general form for the metric for a spherically symmetric geometry

$$ds^2 = \alpha(r)c^2 dt^2 - \beta(r)dr^2 - r^2 d\Omega^2. \quad (2.18)$$

We also assume that the star is composed of an ideal fluid. In Appendix A, we discuss the ideal fluid and derive its energy-momentum tensor. It reads

$$T_{\mu\nu} = \frac{u_\mu u_\nu}{c^2}(\epsilon + p) - g_{\mu\nu}p, \quad (2.19)$$

where u^μ denotes the 4-velocity. In the rest frame of the fluid, the four velocity squared is $u_\mu u^\mu = c^2$, with the three vector part $\vec{u} = 0$. Writing out the square of the velocity in the restframe gives us

$$c^2 = u_\mu u_\nu g^{\nu\mu} = \alpha(r)u_0^2. \quad (2.20)$$

Now, we insert the expression above into $T_{\mu\nu}$ to find the energy momentum tensor $T_{\mu\nu} = \alpha(r)(\epsilon + p)\delta_\mu^0 \delta_\nu^0 - pg_{\mu\nu}$. Writing it out in matrix form, we find

$$T_{\mu\nu} = \begin{pmatrix} \alpha(r)\epsilon & 0 & 0 & 0 \\ 0 & \beta(r)p & 0 & 0 \\ 0 & 0 & r^2 p & 0 \\ 0 & 0 & 0 & r^2 \sin^2(\theta)p \end{pmatrix}. \quad (2.21)$$

The next task is to find the right hand side of Eq. (2.16). We start by calculating the Christoffel symbols in terms of the unknown functions $\alpha(r)$ and $\beta(r)$. Since we know the form of $g_{\mu\nu}$, and thus also know $g^{\mu\nu}$, we can express Eq. (2.11) in terms of α and β . Since the metric is diagonal and only depends on r and θ , there are not many non-zero Christoffel symbols. To exemplify the calculation, let us consider Γ_{rt}^t .

$$\begin{aligned} \Gamma_{rt}^t &= \frac{1}{2}g^{t\sigma}(\partial_r g_{t\sigma} + \partial_t g_{r\sigma} - \partial_\sigma g_{rt}) = \frac{1}{2}g^{tt}(\partial_r g_{tt}) \\ &= \frac{1}{2} \frac{\alpha'(r)}{\alpha(r)}, \end{aligned} \quad (2.22)$$

where the prime ' denotes the derivative with respect to r . Performing this calculational exercise for all Christoffel symbols, one finds that there are 9, not counting the terms we know from symmetry of the lower index-pair. They are

$$\begin{aligned} \Gamma_{rr}^r &= \frac{1}{2} \frac{\beta'}{\beta}, & \Gamma_{\theta\theta}^r &= -\frac{r}{\beta}, \\ \Gamma_{tt}^r &= \frac{1}{2} \frac{\alpha'}{\beta}, & \Gamma_{\phi\phi}^r &= -\frac{r \sin^2(\theta)}{\beta}, \\ \Gamma_{rt}^t &= \frac{1}{2} \frac{\alpha'}{\alpha}, & \Gamma_{\theta\phi}^\phi &= \frac{\cos(\theta)}{\sin(\theta)}, \\ \Gamma_{r\theta}^\theta &= \frac{1}{r}, & \Gamma_{r\phi}^\phi &= \frac{1}{r}, \\ \Gamma_{\phi\phi}^\theta &= -\sin(\theta) \cos(\theta). \end{aligned} \quad (2.23)$$

Next, we can insert these into Eq. (2.14) and contract as in Eq. (2.15) to find the Ricci tensor components. Doing it explicitly for R_{tt} , we get the following

$$\begin{aligned} R_{tt} &= \partial_t \Gamma_{\sigma t}^\sigma - \partial_\sigma \Gamma_{tt}^\sigma + \Gamma_{t\sigma}^\rho \Gamma_{\rho t}^\sigma - \Gamma_{tt}^\rho \Gamma_{\rho\sigma}^\sigma \\ &= -\partial_r (\Gamma_{tt}^r) + \Gamma_{tr}^t \Gamma_{tt}^r + \Gamma_{tt}^r \Gamma_{rt}^t - \Gamma_{tt}^r \Gamma_{rt}^t - \Gamma_{tt}^r \Gamma_{rr}^r - \Gamma_{tt}^r \Gamma_{r\theta}^\theta - \Gamma_{tt}^r \Gamma_{r\phi}^\phi \\ &= -\partial_r \left(\frac{\alpha'}{2\beta} \right) + \frac{\alpha'}{2\beta} \left(\frac{\alpha'}{2\alpha} - \frac{2}{r} - \frac{\beta'}{2\beta} \right) = -\frac{\alpha''}{2\beta} + \frac{\alpha'}{2\beta} \left(\frac{\alpha'}{2\alpha} + \frac{\beta'}{2\beta} \right) - \frac{\alpha'}{r\beta} \end{aligned} \quad (2.24)$$

In the same manner, we find R_{rr} and $R_{\theta\theta}$. Performing the calculation, we find

$$R_{rr} = \frac{\alpha''}{2\alpha} - \frac{\alpha'}{2\alpha} \left(\frac{\alpha'}{2\alpha} + \frac{\beta'}{2\beta} \right) - \frac{\beta'}{r\beta}, \quad (2.25)$$

$$R_{\theta\theta} = \frac{1}{\beta} + \frac{r}{\beta} \left(\frac{\alpha'}{2\alpha} - \frac{\beta'}{2\beta} \right) - 1. \quad (2.26)$$

In order to proceed, we wish to express R in terms of ϵ and p . We can trace the Einstein equation (2.16), i.e. contracting it with $g^{\mu\nu}$. The energy-momentum tensor trace reads $T_{\mu\nu}g^{\mu\nu} = \epsilon - 3p$. Consequently, we find

$$R = \frac{8\pi G}{c^4}(\epsilon - 3p). \quad (2.27)$$

As the next step, we substitute Eq. (2.27) into Eq. (2.16) and consider the three cases when $(\mu, \nu) = (t, t)$, (r, r) and (θ, θ) .

$$R_{tt} = -\frac{8\pi G}{c^4}T_{tt} + \frac{1}{2}Rg_{tt} = -\frac{4\pi G}{c^4}\alpha(r)(\epsilon + 3p), \quad (2.28)$$

$$R_{rr} = -\frac{4\pi G}{c^4}\beta(r)(\epsilon - p), \quad (2.29)$$

$$R_{\theta\theta} = -\frac{4\pi G}{c^4}r^2(\epsilon - p). \quad (2.30)$$

Now we are nearly at our goal, namely expressing β in terms of the pressure p and the energy density ϵ . By making a particular linear combination of R_{tt} , R_{rr} and $R_{\theta\theta}$, we can simplify the equations for α and β . Firstly, we see that $\frac{R_{tt}}{\alpha} + \frac{R_{rr}}{\beta} = -\frac{\alpha'}{r\alpha\beta} - \frac{\beta'}{r\beta^2}$, where we only have first order derivatives. If we additionally include $R_{\theta\theta}$, we can totally eliminate α , as in

$$\begin{aligned} \frac{R_{tt}}{2\alpha} + \frac{R_{rr}}{2\beta} + \frac{R_{\theta\theta}}{r^2} &= -\frac{\alpha'}{2r\alpha\beta} - \frac{\beta'}{2r\beta^2} + \frac{1}{r^2\beta} + \frac{\alpha'}{2r\alpha\beta} - \frac{\beta'}{2r\beta^2} - \frac{1}{r^2} = \frac{1}{r^2\beta} - \frac{\beta'}{r\beta^2} - \frac{1}{r^2} \\ &= -\frac{2\pi G}{c^2}(\epsilon + 3p + \epsilon - p + 2\epsilon - 2p) = -\frac{8\pi G}{c^4}\epsilon. \end{aligned} \quad (2.31)$$

In the second line, Eqs. (2.28), (2.29) and (2.30) were used. This expression can be rearranged into

$$\frac{1}{\beta} - \frac{r\beta'}{\beta^2} = \frac{d}{dr} \left(\frac{r}{\beta} \right) = 1 - \frac{8\pi G}{c^4}\epsilon r^2. \quad (2.32)$$

We can integrate both sides of this expression from $r' = 0$ to $r' = r$. The left hand side immediately evaluates to $\frac{r}{\beta(r)} - \lim_{r' \rightarrow 0} \frac{r'}{\beta(r')}$. If we assume that β does not approach 0 (or at least that it approaches 0 more slowly than r) in the limit $r \rightarrow 0$, the second term disappears, and we are left with $\frac{r}{\beta}$ on the left hand side.

$$\frac{r}{\beta(r)} = r + \frac{2G}{c^2} \int_0^r dr' 4\pi r'^2 \frac{\epsilon(r')}{c^2}. \quad (2.33)$$

We define the integral to be $M(r)$. This has the interpretation of being the gravitational mass, that is the mass that curves spacetime and thus affects the path of other objects moving in space and time. Having defined $M(r)$, we can continue to solve for $\beta(r)$. We arrive at

$$\beta(r) = \frac{1}{1 - \frac{2GM(r)}{c^2 r}}. \quad (2.34)$$

This is self consistent with the assumption of β not going to zero as $r \rightarrow 0$. Now we have found one of the metric functions, and it turns out that this is the only one we need an explicit expression for to derive the TOV-equation. In order to proceed, we make use of energy-momentum conservation. We derive this relation in Appendix B. In general relativity, the conservation law is expressed as

$$\nabla_{\mu} T^{\mu\nu} = 0. \quad (2.35)$$

We consider this equation for $\nu = r$. Firstly, we raise the indices of $T_{\mu\nu}$ for an ideal fluid found in Eq. (2.21). This has the effect of sending $\alpha \rightarrow \frac{1}{\alpha}, \beta \rightarrow \frac{1}{\beta}, r^2 \rightarrow \frac{1}{r^2}$, and $r^2 \sin^2(\theta) \rightarrow \frac{1}{r^2 \sin^2(\theta)}$. Secondly, we use the definition of the covariant derivative to find

$$\begin{aligned}
 \nabla_\mu T^{\mu r} &= \partial_\mu T^{\mu r} + \Gamma_{\mu\alpha}^\mu T^{\alpha r} + \Gamma_{\mu\alpha}^r T^{\alpha\mu} \\
 &= \partial_r T^{rr} + \left(\Gamma_{rr}^r + \Gamma_{tr}^t + \Gamma_{\theta r}^\theta + \Gamma_{\phi r}^\phi \right) T^{rr} + \Gamma_{rr}^r T^{rr} + \Gamma_{tt}^r T^{tt} + \Gamma_{\theta\theta}^r T^{\theta\theta} + \Gamma_{\phi\phi}^r T^{\phi\phi} \\
 &= \partial_r \left(\frac{p}{\beta} \right) + \frac{\beta'}{\beta^2} p + \frac{\alpha'}{2\alpha\beta} p + \frac{2}{r\beta} p + \frac{\alpha'}{2\alpha\beta} \epsilon - \frac{2}{r\beta} p \\
 &= \frac{1}{\beta} p' + \frac{\alpha'}{2\alpha\beta} (\epsilon + p) = 0.
 \end{aligned} \tag{2.36}$$

We gather the α s on one side, and find that the above expression is equivalent to

$$\frac{\alpha'}{2\alpha} = \frac{-p'}{\epsilon + p}, \tag{2.37}$$

which is the important energy-momentum conservation constraint. This will, in addition to its immediate application, be applied in the case of radially perturbed stars. The final step to find the desired TOV-equation, is to insert Eq. (2.37) into the expression for $R_{\theta\theta}$ that we found in Eq. (2.26). Then, we apply our other equation for $R_{\theta\theta}$, namely Eq. (2.30).

$$R_{\theta\theta} = \frac{1}{\beta} + \frac{r}{\beta} \left(\frac{-p'}{\epsilon + p} - \frac{\beta'}{2\beta} \right) - 1 = -\frac{4\pi G}{c^4} r^2 (\epsilon - p) \tag{2.38}$$

Here, the derivative of p with respect to r appears, which is exactly what we want for a differential equation describing p . Therefore, we isolate $\frac{dp}{dr}$ and insert β from Eq. (2.34). To make the second step in the calculation easier to see, we note that $1 - \frac{1}{\beta} + \frac{r\beta'}{2\beta^2} = \frac{GM}{c^2 r} + \frac{4\pi G}{c^4} \epsilon r^2$.

$$\begin{aligned}
 \frac{dp}{dr} &= \frac{\epsilon + p}{r} \beta \left[\frac{4\pi G}{c^4} r^2 (\epsilon - p) - 1 + \frac{1}{\beta} - \frac{r\beta'}{2\beta^2} \right] \\
 &= -\frac{G}{c^2} \frac{\epsilon + p}{r} \left[\frac{M(r)}{r} + \frac{4\pi r^2 p}{c^2} \right] \frac{1}{1 - \frac{2GM}{c^2 r}} \\
 &= -\frac{GM\epsilon}{c^2 r^2} \left[1 + \frac{p}{\epsilon} \right] \left[1 + \frac{4\pi r^3 p}{c^2 M} \right] \left[1 - \frac{2GM}{c^2 r} \right]^{-1}.
 \end{aligned} \tag{2.39}$$

Now, this is the TOV-equation that we have been so curious to find. It contains three unknown quantities: ϵ , p and M . In order to constrain all three quantities, we need another two equations. One of them, we already defined. This is the equation for the gravitational mass M

$$M(r) = \int_0^r dr' 4\pi r'^2 \frac{\epsilon(r')}{c^2}. \tag{2.40}$$

The final equation in the system is called an equation of state. This equation describes a relation between the ϵ and p . We will come back to this later. For now, we write it down, so we can see the system of equations together,

$$\epsilon = \epsilon(p). \tag{2.41}$$

These are the equations which constitute the TOV-system of equations.

Although we now have achieved the main results, we have not completely finished treating α and β . The expressions we find here will be put in use later, when we consider the stability of neutron stars. Firstly, we rewrite $\frac{\beta'}{2\beta}$. This can be done by rearranging Eq. (2.32). The rearranging yields

$$\frac{\beta'}{2\beta} = \frac{1}{2r} (1 - \beta) + \frac{4\pi G}{c^4} \epsilon r \beta. \tag{2.42}$$

Next, we tackle α . We have so far not found an expression which determines its behaviour. In order to do this, we look at the linear combination

$$-\frac{r^2 R_{tt}}{2\alpha} - \frac{r^2 R_{rr}}{2\beta} + R_{\theta\theta} = \frac{r\alpha'}{\beta\alpha} + \frac{1}{\beta} - 1. \quad (2.43)$$

If we use Eqs. (2.28), (2.29), and (2.30) for the left hand side and solve for $\frac{\alpha'}{2\alpha}$, we find

$$\frac{\alpha'}{2\alpha} = \frac{4\pi G}{c^4} pr\beta + \frac{1}{2r}(\beta - 1). \quad (2.44)$$

This is equivalent to inserting the Riemann-curvature R expressed in terms of α and β into the rr -component of the Einstein equation. In the time-dependent case, this will give an important constraint on the perturbations. An equivalent, but also useful expression, is to substitute Eq. (2.39) into Eq. (2.37). This procedure yields

$$\frac{\alpha'}{2\alpha} = \frac{c^2 GM + 4\pi r^3 p}{c^2 r(c^2 r - 2GM)} \quad (2.45)$$

We need to determine the integration constant for this differential equation. We require that α is continuous everywhere. Outside the star, $r > R$, we can find an analytic form for both α and β by setting the energy-momentum-tensor to zero. This means that we can take the equations derived above and set $p = \epsilon = 0$. The differential equation for β becomes the same as for the interior derivation, Eq. (2.32), except with the simplification of $\epsilon = 0$. As this is easier than the calculation above, we omit the explicit calculation. We solve the differential equation for β and impose continuity at $r = R$ to arrive at the exterior solution for β

$$\beta = \frac{1}{1 - \frac{2GM}{c^2 r}}, \quad r > R. \quad (2.46)$$

M is no longer r -dependent, but is constant, $M = M(R)$. We want to find the exterior solution for α , so the next natural step is to set $p = 0$ and substitute the exterior solution for β given just above into Eq. (2.44). We find a simple, separable differential equation

$$\frac{d\alpha}{\alpha} = \frac{1}{r} \left(\frac{1}{1 - \frac{2GM}{c^2 r}} - 1 \right) dr = \frac{2GM dr}{c^2 r^2 - 2GM r} = \frac{du}{u(u-1)}, \quad (2.47)$$

where in the last equality we have performed the substitution $u = \frac{c^2 r}{2GM}$. We require that spacetime is flat as we move far away from the spherical star, $r \rightarrow \infty$. This allows us to integrate the left hand side and set the integration constant to zero, while we integrate from u to ∞ on the right hand side

$$\ln(\alpha) = \int_{\infty}^u \frac{du}{u(u-1)} = \int_{\infty}^u \frac{1}{u} - \frac{1}{u-1} = \ln \left(1 - \frac{1}{u} \right). \quad (2.48)$$

Eliminating u in favour for r , we may conclude that α must take the form

$$\alpha = 1 - \frac{2GM}{c^2 r}, \quad r > R. \quad (2.49)$$

Finally, we have obtained the boundary condition for the interior solution for α , namely that

$$\lim_{r \rightarrow R^-} \alpha = 1 - \frac{2GM}{c^2 R}. \quad (2.50)$$

With this condition, we can integrate Eq. (2.45) to find an expression for α inside the star. This will be done numerically in the stability analysis later.

Solution to the TOV-equation for an Incompressible Fluid

The goal in this section is to familiarise ourselves with the TOV-equation. We will do so with a practical example which is analytically solvable. The assumption we must make, is that the star is composed of an incompressible fluid. Along the way, we will make some remarks that are true in general, not only for the specific case we are considering in this section. We will also compare the solution of the TOV-equation to the the solution from Newtonian gravity. We shall see that there are a few important qualitative differences between the two of them. From the previous section, we collect the the important equations we need

$$\frac{dp}{dr} = -\frac{GM(r)\epsilon(r)}{r^2c^2} \left[1 + \frac{p(r)}{\epsilon(r)}\right] \left[1 + \frac{4\pi r^3 p(r)}{M(r)c^2}\right] \left[1 - \frac{2GM(r)}{rc^2}\right]^{-1}, \quad (3.1)$$

$$M(r) = \int_0^r dr' 4\pi r'^2 \rho(r') = \int_0^r dr' \frac{4\pi r'^2 \epsilon(r')}{c^2}, \quad (3.2)$$

$$\epsilon = \epsilon(p). \quad (3.3)$$

Solving this looks like a difficult task, but it turns out to quite manageable once we get our hands dirty.

3.1 TOV-solution for an Incompressible Fluid

The simplest case for solving the TOV-equation is to assume that the fluid of the star is incompressible. This means that its energy density is the same throughout the entire star, no matter how high the pressure becomes. The equation of state reads

$$\epsilon(r) = \epsilon_0. \quad (3.4)$$

This is a quite unreasonable assumption, physically speaking. It means that the matter can withstand any pressure without deforming. The assumption also breaks causality, as the speed of sound becomes infinite. For two events to be related, we know that a signal must have travelled between them. We know that no signal can move faster than the speed of light, c . When we consider the speed of sound in a relativistic fluid [7] (p. 52), we find that it takes the form

$$v_s^2 = c^2 \frac{\partial p}{\partial \epsilon}. \quad (3.5)$$

This equation imposes a restriction on how ϵ can depend on p . We will sometimes refer to it as the causality condition for an equation of state. It reads

$$\frac{\partial \epsilon}{\partial p} > 1. \quad (3.6)$$

This ensures that sound travels slower than light. There exists no signal that travels fast enough to mediate a speed of sound larger than c , and any equation of state breaking Eq. 3.6 will therefore have non-causal sound waves. Due to this, we must refuse any equation of state breaking this inequality. The incompressible equation of state is an extreme example of this, as $\frac{\partial \epsilon}{\partial p} = 0$. Now we see why the speed of sound becomes infinite, and an incompressible star is unphysical. Assuming incompressibility may not be reasonable for a realistic model of a star, but it does serve as a warm-up exercise for solving the TOV-equation. It will also show that general relativity predicts an upper limit of the ratio between the total energy of the star and the radius. This limit does not appear in Newtonian gravity, as we shall see. When we insert Eq. (3.4) into the equation for the gravitational mass, Eq. (3.2), we find

$$M(r) = \frac{4\pi\epsilon_0}{3c^2} r^3. \quad (3.7)$$

Now, this is certainly a simplification of the TOV-system of equations! Two of them are analytically known for every r even before we have treated the TOV-equation. To find $p(r)$, we insert Eqs. (3.4) and (3.7) into Eq. (3.1). We find

$$\frac{dp}{dr} = -\frac{4\pi G\epsilon_0^2}{3c^4} \frac{r}{1 - 2G\frac{4\pi\epsilon_0}{3c^2}r^2} \left[1 + \frac{p}{\epsilon_0}\right] \left[1 + \frac{3p}{\epsilon_0}\right]. \quad (3.8)$$

We are happy to discover that we have reduced the system of equations into one separable first order differential equation. This we can solve with a little work. After we gather every p on the left hand side and every r on the right, the equation reads

$$\epsilon_0^2 \frac{dp}{(\epsilon_0 + p)(\epsilon_0 + 3p)} = -\frac{4\pi G\epsilon_0^2 r dr}{3c^4 - 8\pi G\epsilon_0 r^2}. \quad (3.9)$$

As with any first order differential equation, we need a boundary condition to establish a unique solution. We find this condition from stating that the star ends where the pressure drops to zero. In other words, the radius of the star R is defined from $p(R) = 0$. At zero pressure, there is no force to withstand the pull of gravity, and there can be no more matter outside R for an equilibrium star. Thus, we introduce the lower and upper integration limits for the pressure as $p(r')$ and 0, where $0 < r' < R$. Correspondingly, the lower and upper radius limits are $r = r'$ and $r = R$. For later use, we also define the central pressure $p_c = p(r = 0)$. We start by looking at the left hand side of Eq. (3.9). We integrate this expression with the mentioned limits for p

$$\begin{aligned} \int_{p(r')}^0 \frac{\epsilon_0^2 dp}{(\epsilon_0 + p)(\epsilon_0 + 3p)} &= \frac{\epsilon_0}{2} \int_{p(r')}^0 \frac{3dp}{\epsilon_0 + 3p} - \frac{dp}{\epsilon_0 + p} = \frac{\epsilon_0}{2} \left[\ln \frac{\epsilon_0}{\epsilon_0 + 3p(r')} - \ln \frac{\epsilon_0}{\epsilon_0 + p(r')} \right] \\ &= \frac{\epsilon_0}{2} \ln \left(\frac{\epsilon_0 + p}{\epsilon_0 + 3p} \right). \end{aligned} \quad (3.10)$$

In the first equality, we have used a partial fraction decomposition to make the integrand easy to handle. Next, we tackle the right hand side of Eq. (3.9). By making the substitution $u = 2G\frac{4}{3}\frac{1}{c^4}\pi\epsilon_0 r^2$, the integral becomes quite simple

$$\begin{aligned} - \int_{r'}^R \frac{4\pi G\epsilon_0^2 r dr}{3c^4 - 8\pi G\epsilon_0 r^2} &= -\frac{\epsilon_0}{4} \int_{u(r')}^{u(R)} \frac{du}{1 - u} \\ &= \frac{\epsilon_0}{4} \ln \left(\frac{1 - 2\frac{GM}{c^2 R}}{1 - 2\frac{GM}{c^2 R^3} r'^2} \right). \end{aligned} \quad (3.11)$$

In the last equality, we have introduced the total gravitational mass of the star denoted by M . Explicitly, it reads $M = M(R) = \frac{4\pi\epsilon_0}{3c^2} R^3$. Now, we equate (3.10) to (3.11) and rename r' to r

$$\ln\left(\frac{\epsilon_0 + p(r)}{\epsilon_0 + 3p(r)}\right) = \frac{1}{2} \ln\left(\frac{1 - 2\frac{GM}{c^2 R}}{1 - 2\frac{GM}{c^2 R^3} r^2}\right). \quad (3.12)$$

The rest is just a matter of isolating $p(r)$. When we perform this calculation, we find

$$p(r) = \epsilon_0 \frac{\sqrt{1 - 2MG/c^2 R} - \sqrt{1 - 2MGr^2/c^2 R^3}}{\sqrt{1 - 2MGr^2/c^2 R^3} - 3\sqrt{1 - 2MG/c^2 R}}, \quad r \in [0, R]. \quad (3.13)$$

It is easy to see that the numerator vanishes as $r \rightarrow R$, meaning that $p(R) = 0$ as it should. There is only one more manipulation left before we are satisfied with the solution. It is common to parameterise the star by its central pressure p_c , and thus replace ϵ_0 . Evaluating Eq. (3.13) at $r = 0$, we get

$$p_c = \epsilon_0 \frac{\sqrt{1 - 2MG/c^2 R} - 1}{1 - 3\sqrt{1 - 2MG/c^2 R}}. \quad (3.14)$$

This allows us to eliminate ϵ_0 from Eq. (3.13)

$$p(r) = p_c \frac{1 - 3\sqrt{1 - 2MG/c^2 R}}{\sqrt{1 - 2MG/c^2 R} - 1} \frac{\sqrt{1 - 2MG/c^2 R} - \sqrt{1 - 2MGr^2/c^2 R^3}}{\sqrt{1 - 2MGr^2/c^2 R^3} - 3\sqrt{1 - 2MG/c^2 R}} \quad (3.15)$$

Eq. (3.13) has an interesting property, namely that $p(r)$ can take arbitrarily large values for certain values of M/R . We shall see that in Newtonian gravity, we can choose any M/R , but the relationship is constrained in the GR. The constraint arises from the fact that the denominator in Eq. (3.13) can vanish for $r \in [0, R]$ for large enough M/R . This means that p diverges. Let the divergence of p take place at r_∞ . We set the denominator equal to zero to find

$$\sqrt{1 - 2MGr_\infty^2/c^2 R^3} = 3\sqrt{1 - 2MG/c^2 R}. \quad (3.16)$$

This we can solve for r_∞ . We find

$$r_\infty^2 = 9R^2 - 4\frac{R^3}{MG}. \quad (3.17)$$

To avoid problems with a diverging pressure, one must require that r_∞ does not take any real value. In other words, p_c must be finite and positive, which gives the restriction

$$0 > 1 - 3\sqrt{1 - 2MG/Rc^2} \quad \text{or} \quad \frac{M}{R} < \frac{4c^2}{9G}, \quad (3.18)$$

Here, general relativity predicts an upper limit of the mass-radius ratio. With a bit more work, this limiting mass can be generalised to hold for any equation of state. This is shown in [8] (pp. 129-131). For the incompressible star, the gravitational mass goes as $M(R) \propto R^3$. This means that the mass-radius ratio scales with R^2 , resulting in a maximum radius of $R_{\max} = \frac{c^2}{\sqrt{3\pi G\epsilon_0}}$. The larger the energy density is, the smaller the radius can be.

3.2 Newtonian Gravity and an Incompressible Fluid

In this subsection, we shall derive the differential equation for the hydrostatic pressure in Newtonian gravity for a spherically symmetric star. We shall see that there are some interesting differences between the TOV-equation and the equation obtained by the following derivation.

In hydrostatic equilibrium, we must require that the net force on any volume element must be zero, otherwise the volume element would accelerate, and the system would no longer be static. As we are considering a spherically symmetric geometry, physical quantities can only depend on r . We imagine

an infinitesimal volume element parameterised by the spherical coordinates r, ϕ, θ . For simplicity, and without loss of generality, we choose the coordinates $\theta = \pi/2$ and $\phi = 0$. This is illustrated in Figure 3.1, with exaggerated size of the volume element for readability.

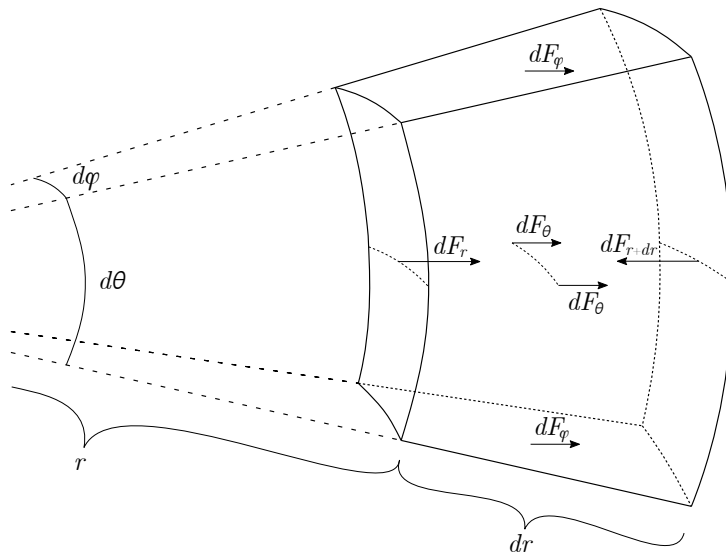


Figure 3.1: Volume element in spherical coordinates situated at a distance r from the centre. The force exerted by the pressure in the radial direction on each face of the volume element is indicated in the figure. The arrow lengths are not to scale, simply showing the direction of the force. The sum of these radially directed forces is equal, but oppositely directed, to the force of gravity acting on the element.

There can be no net force in the θ or ϕ direction, due to the spherical symmetry. Any net force from the pressure must therefore be directed radially. Note that a normal vector on the side surfaces will have a small radial component proportional to $\sin(d\phi/2)$ or $\sin(d\theta/2)$. This is why there is a force contribution marked with dF_ϕ and dF_θ in the figure. We assume that the total magnitude of each force will be the pressure at the centre point of the face multiplied by the area of the face. Any correction to this will be one order higher in dr , which we neglect as it becomes unimportant when we let the volume element be infinitesimal. With these considerations, we find

$$\begin{aligned} dF_r &= p(r)r^2 d\phi d\theta, & dF_{r+dr} &= p(r+dr)(r+dr)^2 d\phi d\theta, \\ dF_\phi &= p(r+dr/2)\sin(d\theta/2)r dr d\phi, & dF_\theta &= p(r+dr/2)\sin(d\phi/2)r dr d\theta. \end{aligned} \quad (3.19)$$

Next, we write the sum of the forces exerted by the pressure as dF_p , and insert the expressions written just above to find

$$\begin{aligned} dF_p &= dF_r + 2dF_\theta + 2dF_\phi - dF_{r+dr} \\ &= p(r)r^2 d\phi d\theta + 2p(r+dr/2)\sin(d\phi/2)r d\theta dr + 2p(r+dr/2)\sin(d\theta/2)r d\phi dr \\ &\quad - p(r+dr)(r+dr)^2 d\phi d\theta \\ &= -[p(r+dr) - p(r)]r^2 d\phi d\theta + 2p(r)\frac{d\phi}{2}r d\theta dr + 2p(r)\frac{d\theta}{2}r d\phi dr - 2p(r+dr)r d\theta d\phi \\ &= -[p(r+dr) - p(r)]r^2 d\phi d\theta = -dp r^2 d\phi d\theta. \end{aligned} \quad (3.20)$$

We have consistently thrown away higher order corrections in the differentials. For instance, in the third equality, $\sin(\dots)$ has been Taylor expanded, and only the first order term is kept. In the last equality, we

have used that $dp = p(r + dr) - p(r)$. The gravitational pull on a volume element with mass density ρ at a distance r from the centre is given by

$$dF_G = \frac{GM(r)dm(r)}{r^2} = \frac{GM(r)\rho(r)}{r^2} r^2 dr d\phi d\theta. \quad (3.21)$$

$M(r)$ is given as before, the gravitational mass. Equating Eq. (3.20) and Eq. (3.21), cancelling equal terms on both sides and gathering the rest of the differentials on one side yields the desired equation

$$\frac{dp}{dr} = -\frac{GM(r)\rho(r)}{r^2} = -\frac{GM(r)\epsilon(r)}{r^2 c^2}, \quad (3.22)$$

where we have substituted the mass density ρ in favour for the energy density ϵ in the last equality, with $\epsilon = \rho c^2$.

From the case of general relativity in Eq. (3.1), one can recover Newtonian gravity. This is done by letting $c \rightarrow \infty$, which reduces Eq. (3.1) to Eq. (3.22), as all the parentheses tend towards unity. For large c we have $p \ll \epsilon$. This we will show is in fact the case later. Besides being more difficult to compute, we can state some qualitative differences of the pressure as described by Eq. (3.1) compared to Eq. (3.22). The pressure p , the energy density ϵ and the gravitational mass inside a radius r , $M(r)$, are all positive. From this we can conclude that the two first parentheses in the TOV-equation are larger than unity. The last parenthesis would also be larger than one as long as $r > 2GM(r)/c^2$. This will always be the case. If we could find r' such that $r' = 2GM(r')/c^2$, the metric of our system would have a divergence in $g_{rr}(r') = -[1 - 2GM(r')/c^2 r']^{-1}$. When this happens for the exterior solution of the spherical star, we are dealing with a black hole. We therefore require that $r > 2GM(r)/c^2$ for a neutron star.

Thus, all the parentheses in Eq. (3.1) are larger than unity. This means that the pressure in the GR description of hydrostatic equilibrium will always drop more rapidly as a function of r than in the Newtonian description. This leads us to conclude that in GR, the pressure is always higher than in Newtonian gravity if we assume the same equation of state and the same radius R .

If we again turn to the incompressible fluid, and substitute Eqs. (3.4) and (3.7) into (3.22), we find

$$\frac{dp}{dr} = -\frac{GM(r)\epsilon(r)}{r^2 c^2} = -\frac{4}{3} G\pi \frac{\epsilon_0^2}{c^4} r. \quad (3.23)$$

This is also a separable first order differential equation, and it is even quite a lot easier to solve than the one we found for the TOV case. We separate it, then we integrate both sides using the boundary condition $p(R) = 0$ to obtain

$$p(r) = \frac{2}{3} G\pi \frac{\epsilon_0^2}{c^4} (R^2 - r^2). \quad (3.24)$$

By making use of the expression for the gravitational mass Eq. (3.7), we can eliminate one power of ϵ_0 . This leads to the expression

$$p(r) = \epsilon_0 \frac{GM}{2c^2 R} \left(1 - \frac{r^2}{R^2}\right). \quad (3.25)$$

Interestingly, and in contrast to the general relativistic case, Eq. (3.24) does not have any divergence in the pressure. The Newtonian theory does therefore not predict any upper bound for the mass-radius ratio. We can eliminate the final ϵ_0 by using $p_c = \epsilon_0 GM/2c^2 R$, which gives

$$p(r) = p_c \left(1 - \frac{r^2}{R^2}\right). \quad (3.26)$$

3.3 Comparing TOV and Newtonian Solution for an Incompressible Fluid

For small $GM/c^2 R$, we expect the solution from general relativity to reduce to the Newtonian one. If we start by fixing p_c , we can investigate the dimensionless quantity p/p_c . For ease of notation, write

$u = 2GM/c^2R$ and $x = r^2/R^2$. Rewriting the Newtonian solution this way, we find

$$\left[\frac{p}{p_c} \right]_{\text{Newton}} = (1 - x), \quad (3.27)$$

where the subscript denotes which hydrostatic equation we have used. We know from Eq. (3.18) that $u = 2GM/c^2R < 8/9$, which means we can Taylor-expand Eq. (3.13). Making use of the expansions to second order

$$\sqrt{1-u} = 1 - \frac{1}{2}u - \frac{1}{8}u^2 + \mathcal{O}(u^3) \quad \text{and} \quad \frac{1}{1-u} = 1 + u + u^2 + \mathcal{O}(u^3), \quad (3.28)$$

we get from Eq. (3.13)

$$\begin{aligned} \left[\frac{p}{p_c} \right]_{\text{TOV}} &= \left[\frac{1 - 3(1 - 1/2u - 1/8u^2)}{1 - 1/2u - 1/8u^2 - 1} \right] \left[\frac{1 - 1/2u - 1/8u^2 - (1 - 1/2ux - 1/8u^2x^2)}{1 - 1/2ux - 1/8u^2x^2 - 3(1 - 1/2u - 1/8u^2)} \right] + \mathcal{O}(u^3) \\ &= \left[\frac{-2 + 3/2u + 3/8u^2}{1 + 1/4u} \right] \left[\frac{(1-x) + 1/4(1-x^2)}{-2 + 1/2u(3-x) + 1/8u^2(3-x^2)} \right] \\ &= (1-x) - \frac{u}{2}(x-x^2). \end{aligned} \quad (3.29)$$

The leading order term is the same in Eq. (3.27) and in Eq. (3.29), which should be the case. Letting $c \rightarrow \infty$, which is equivalent to $u \rightarrow 0$, gives the same solution. The limit $c \rightarrow \infty$ reduces the TOV-equation to the Newtonian hydrostatic equation, as well as the TOV-solution to the Newtonian solution, which shows self-consistency. In addition, we see that the next to leading order term makes the pressure drop more quickly compared to the Newtonian case. This is in accordance with the qualitative discussion of the two equations in section 3.2.

As we have found both solutions analytically, it is easy to generate a plot to showcase the difference between the relativistic and the Newtonian solution. This is done in Fig. 3.2. We see that any ratio $\frac{M}{R}$ in the Newtonian solution gives the same normalized pressure profile, while this is not the case for the TOV-solution. What the normalised pressure profiles fail to show, is the difference in the central pressure for the two distinct solutions for a given ratio $\frac{M}{R}$. For $\frac{MG}{c^2R} = \frac{1}{9}$, the central pressure for the TOV-solution is about 30% larger than for the Newtonian solution. Increasing the ratio further, to $\frac{MG}{c^2R} = \frac{3}{9}$, the TOV-solution is more than three times larger than the Newtonian solution. Despite having quite similar pressure profiles, we see that the GR-approach gives a significantly larger central pressure. The difference only amplifies further. At $\frac{MG}{c^2R} = \frac{399}{900}$, the TOV-solution gives a 300 times larger central pressure than the Newtonian solution! From the pressure profiles, we see clearly that the pressure drops faster with the TOV-equation than the Newtonian hydrostatic equilibrium, as the curve for the Newtonian pressure profile dominates the curves from TOV. This supports the discussion we had earlier, in comparing the equations.

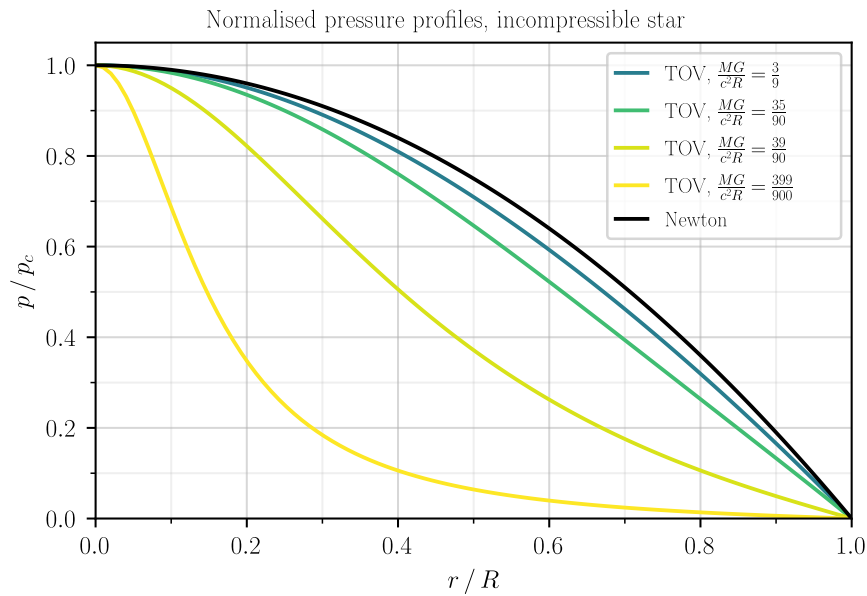


Figure 3.2: Normalised pressure p/p_c as a function of r/R . For a low mass-radius ratio compared to the limiting ratio as given by Eq. (3.18), the relativistic TOV-solution deviates little from the Newtonian solution. Even $MG/c^2R = 3/9$ has a quite similar shape to the Newtonian solution. Closer to the limiting mass-radius ratio, the pressure profiles from the TOV-solution and the Newtonian solution qualitatively deviate from each other. This is clear as we compare the black Newtonian pressure profile to the yellow TOV pressure profile.

Equation of State for an Ideal Fermi Gas

In this section, we are searching for a more realistic equation of state than Eq. (3.7), the incompressible equation of state. We will do so by considering a cold non-interacting neutron gas. This will lead us to the ideal equation of state.

4.1 Fermion Statistics and the Ideal Equation of State

Neutrons are fermions. Therefore, we consider quantum statistical physics for fermions in order to arrive at an equation of state (EoS). Combined with the assumption of non-interacting neutrons, we can write the Hamiltonian for the system of N particles, H , as a sum of Hamiltonians for each individual particle. For a system of free particles with equal mass m , we have

$$H = \sum_{i=1}^N H_i = \sum_{i=1}^N \sqrt{m^2 c^4 + \vec{k}_i^2 c^2}, \quad (4.1)$$

where \vec{k}_i denotes the momentum of the particle (we avoid using the customary \vec{p} to omit ambiguity between pressure and momentum). H_i is a realisation of some energy level E_i . Each energy level E_i can either be occupied by zero or one particle due to the Pauli exclusion principle. Let now $\{\alpha_j\}_{j=1}^N$ denote a set of N unique indices telling us which of the energy states are occupied. Now, we can write the Hamiltonian as a sum of energy levels E_i over all indices in our index set, $i \in \{\alpha_j\}_{j=1}^N$.

$$H_{\{\alpha_j\}_{j=1}^N} = \sum_{i \in \{\alpha_j\}_{j=1}^N} E_i. \quad (4.2)$$

The subscript in $H_{\{\alpha_j\}_{j=1}^N}$ tells precisely which state the Hamiltonian is valid for. Using this, the canonical partition function Z_N for the system reads

$$Z_N = \sum_{\{\alpha_j\}_{j=1}^N} \exp\left[-\beta H_{\{\alpha_j\}_{j=1}^N}\right]. \quad (4.3)$$

The sum in Eq. (4.3) is taken over all possible index sets $\{\alpha_j\}_{j=1}^N$. We say that the sum is constrained, because we limit ourselves to considering N particles. $\beta = 1/k_B T$, where k_B is the Boltzmann constant and T is the temperature, as usual. As this sum is difficult to solve with its restriction of N particles, we make use of the grand partition function Θ . Θ is defined as the sum of Z_N weighted by a factor of

$\exp[\beta\mu N]$ over all particle numbers N

$$\begin{aligned}\Theta &= \sum_{N=0}^{\infty} \exp[\beta\mu N] Z_N = \sum_{N=0}^{\infty} \sum_{\{\alpha_j\}_{j=1}^N} \exp[\beta\mu N] \exp\left[-\beta H_{\{\alpha_j\}_{j=1}^N}\right] \\ &= \sum_{N=0}^{\infty} \sum_{\{\alpha_j\}_{j=1}^N} \exp\left[\sum_{i \in \{\alpha_j\}_{j=1}^N} -\beta(E_i - \mu)\right].\end{aligned}\quad (4.4)$$

Here we have defined μ as the chemical potential, telling us how favourable it is for the system to contain particles. For instance, a positive μ means that the system favours having more particles. The advantage of using the grand canonical formalism is that we sum over all particle numbers N . This means that in total, we sum over all possible configurations. The sum now goes over all states either being occupied or not, independently of the occupancy of other states, that is, the sum becomes unconstrained. Let now an arbitrary configuration be labeled by $\{\alpha\}$. Thus, we can continue from Eq. (4.4) and get

$$\Theta = \sum_{\{\alpha\}} \exp\left[\sum_{i \in \{\alpha\}} -\beta(E_i - \mu)\right] = \prod_{i=1}^{\infty} [1 + \exp[-\beta(E_i - \mu)]].\quad (4.5)$$

From the grand partition function one derives the thermodynamic properties of the system, namely the pressure p , the average particle number $\langle N \rangle$ and the average energy $\langle E \rangle$ as functions of the temperature T and the chemical potential μ

$$\frac{p}{k_B T} = \frac{\ln \Theta}{V},\quad (4.6)$$

$$\langle N \rangle = k_B T \frac{\partial \ln \Theta}{\partial \mu},\quad (4.7)$$

$$\langle E \rangle = \mu \langle N \rangle - \frac{\partial \ln \Theta}{\partial \beta}.\quad (4.8)$$

V denotes the volume of the system. Substituting Eq. (4.5) into Eqs. (4.6), (4.7) and (4.8) we get the desired expression for a fermionic system. Additionally, we eliminate $k_B T$ in favour for β and divide Eqs. (4.7) and (4.8) by V to get the number density $n = \langle N \rangle / V$ and the energy density $\epsilon = \langle E \rangle / V$. Finally, we introduce a degeneracy factor $g = 2$, which takes into account that each fermion has two spin states

$$\beta p = \frac{g}{V} \sum_{i=0}^{\infty} \ln(\exp[-\beta(E_i - \mu)] + 1) = \frac{g}{(2\pi)^3 \hbar^3} \int d^3 k \ln(\exp[-\beta(E(\vec{k}) - \mu)] + 1),\quad (4.9)$$

$$n = \frac{\langle N \rangle}{V} = \frac{g}{\beta V} \sum_{i=0}^{\infty} \frac{\beta}{\exp[\beta(E_i - \mu)] + 1} = \frac{g}{(2\pi)^3 \hbar^3} \int \frac{d^3 k}{\exp[\beta(E(\vec{k}) - \mu)] + 1},\quad (4.10)$$

$$\begin{aligned}\epsilon = \frac{\langle E \rangle}{V} &= \frac{g}{V} \sum_{i=0}^{\infty} \frac{\mu}{\exp[\beta(E_i - \mu)] + 1} - \frac{g}{V} \sum_{i=0}^{\infty} \frac{\mu - E_i}{\exp[\beta(E_i - \mu)] + 1} \\ &= \frac{g}{(2\pi)^3 \hbar^3} \int d^3 k \frac{E(\vec{k})}{\exp[\beta(E(\vec{k}) - \mu)] + 1}.\end{aligned}\quad (4.11)$$

In the final equality in the equations above, we have used that summing over the energies corresponds to summing over the momentum states. In this case, an energy level E_i depends on the momentum \vec{k}_i as it is given in Eq. (4.1). In addition, we know from quantum mechanics that summing over momentum states \vec{k}_i can be approximated by an integral over momentum space and multiplying by a factor of $V/(2\pi)^3 \hbar^3$ when the limit that volume grows towards infinity. We call this the thermodynamic limit. Written explicitly

$$\sum_i f(E_i) = \sum_{\vec{k}} f(E(\vec{k})) \quad \text{and} \quad \sum_{i=0}^{\infty} \rightarrow \frac{V}{(2\pi)^3 \hbar^3} \int d^3 k.\quad (4.12)$$

$f(E_i)$ denotes some function depending on the energy. Eq. (4.9) can be partially differentiated by β , yielding finally:

$$p = \frac{g}{(2\pi)^3 \hbar^3} \int d^3k \frac{\mu - E(\vec{k})}{\exp[\beta(E(\vec{k}) - \mu)] + 1}. \quad (4.13)$$

In all the Eqs. (9.4), (9.6) and (9.3), the expression

$$\frac{1}{\exp[\beta(E(\vec{k}) - \mu)] + 1} \quad (4.14)$$

appears. It is called the Fermi-Dirac distribution. In the expression for the particle density Eq. (9.4) we integrate Eq. (4.14) over all momentum space. This gives it the interpretation of being the probability distribution of particles in terms of their energy and chemical potential. States with energy lower than the chemical potential μ is favoured. Especially for low temperatures, i.e. when β is large, there is a sharp drop in probability for an energy state to be occupied as the energy grows larger than the chemical potential. In the extreme limit $T \rightarrow 0$, the distribution simplifies

$$\lim_{T \rightarrow 0} \frac{1}{\exp[\beta(E(\vec{k}) - \mu)] + 1} = \theta(\mu - E(\vec{k})) = \begin{cases} 1, & \mu - E(\vec{k}) \geq 0 \\ 0, & \mu - E(\vec{k}) < 0. \end{cases} \quad (4.15)$$

In other words, the Fermi-Dirac distribution turns into the Heaviside step function $\theta(\mu - E(\vec{k}))$. The Fermi energy E_F is defined as the energy of the most energetic occupied state at $T = 0$. From this definition, we see that $E_F = \mu$. This allows us to define an upper momentum magnitude over which no states are occupied, the Fermi momentum k_F . Using the energy for free fermion Eq. (4.1), the Fermi momentum reads

$$k_F = \frac{1}{c} \sqrt{\mu^2 - m^2 c^4}. \quad (4.16)$$

We can now calculate the energy density ϵ using Eqs. (9.6) and (4.15). The energy only depends on the magnitude of \vec{k} , so we go to spherical coordinates. Integrating over all angles immediately gives a factor 4π , leaving

$$\begin{aligned} \epsilon &= \frac{4\pi g}{(2\pi)^3 \hbar^3} \int_0^{k_F} dk k^2 \sqrt{m^2 c^4 + k^2 c^2} \\ &= \frac{gm^4 c^5}{2\pi^2 \hbar^3} \int_0^{x_F} dx x^2 \sqrt{1 + x^2} \\ &= \frac{gm^4 c^5}{2\pi^2 \hbar^3} \frac{2x_F^3 \sqrt{1 + x_F^2} + x_F \sqrt{1 + x_F^2} - \operatorname{arcsinh}(x_F)}{8}. \end{aligned} \quad (4.17)$$

From the first to the second line, the substitution $x = k/mc$ was made. To ease the notation a little, we define $\varepsilon_g = \frac{gm^4 c^5}{2\pi^2 \hbar^3}$. g denotes the degeneracy factor. For a spin- $\frac{1}{2}$ particle, we have $g = 2$. We also note that ε_g is a dimensionful quantity corresponding to energy density. As energy density and pressure have the same dimension, this factor will precede both ϵ and p . In turn, we can define the dimensionless energy density $\bar{\epsilon}$ and the dimensionless pressure \bar{p} as $\bar{\epsilon} = \frac{\epsilon}{\varepsilon_g}$ and $\bar{p} = \frac{p}{\varepsilon_g}$. This enables us to analyse the behaviour of ϵ and p without considering a particular unit system. For the case of SI-units and using the neutron mass m_n , the value of ε_g will be

$$\varepsilon_g = 1.65 \times 10^{36} \text{ kg s}^{-2} \text{ m}^{-1}. \quad (4.18)$$

We can follow a similar reasoning for the number density n . Inserting Eq. (4.15) into Eq. (9.4), we get

$$\begin{aligned} n &= \frac{g}{2\pi^2 \hbar^3} \int_0^{k_F} dk k^2 = \frac{gm^3 c^3}{2\pi^2 \hbar^3} \int_0^{x_F} dx x^2 \\ &= \frac{gm^3 c^3}{6\pi^2 \hbar^3} x_F^3 = \frac{\varepsilon_g}{3mc^2} x_F^3. \end{aligned} \quad (4.19)$$

Later, we will eliminate the dimensionless quantity x_F in favour of the number density n in the expressions for ϵ and p . Express x_F in terms of n

$$x_F = \left(\frac{3mc^2}{\epsilon_g} \right)^{\frac{1}{3}} n^{\frac{1}{3}}. \quad (4.20)$$

Finally, we perform the same procedure for p . Insert Eq. (4.15) into Eq. (9.3), eliminate μ with Eq. (4.16) and make the substitution as above

$$\begin{aligned} p &= \frac{g}{2\pi^2\hbar^3} \int_0^{k_F} dk k^2 \left[\sqrt{m^2c^4 + k_F^2c^2} - \sqrt{m^2c^4 + k^2c^2} \right] \\ &= \frac{gm^4c^5}{2\pi^2\hbar^3} \int_0^{x_F} dx x^2 \left[\sqrt{1 + x_F^2} - \sqrt{1 + x^2} \right] \\ &= \epsilon_g \left[\frac{x_F^3\sqrt{1 + x_F^2}}{12} + \frac{\operatorname{arcsinh}(x_F) - x_F\sqrt{1 + x_F^2}}{8} \right]. \end{aligned} \quad (4.21)$$

Note that the dimensionless energy density $\frac{\epsilon}{\epsilon_g}$ and the dimensionless pressure $\frac{p}{\epsilon_g}$ only depends on x_F . As we have found how ϵ and p behaves with respect to x_F , we have found an indirect way of expressing $\epsilon(p)$. This is the ideal equation of state. We will sometimes refer to the the expressions for ϵ and p given by Eqs. (4.17) and (4.21) as the analytic equation of state. By this, we simply mean that we are considering the expression of the analytic solution, and not the expansions in either small or large \bar{p} .

Later, we will be interested in differentiating the pressure with respect to the energy density. As we have already warmed up with calculating ϵ and p , we easily evaluate the derivative with Eqs. (4.17) and (4.21)

$$\frac{dp}{d\epsilon} = \frac{\frac{dp}{dx_F}}{\frac{d\epsilon}{dx_F}} = \frac{\frac{\epsilon_g x_F^4}{3\sqrt{1+x_F^2}}}{\epsilon_g x_F^2 \sqrt{1+x_F^2}} = \frac{x_F^2}{3(1+x_F^2)}. \quad (4.22)$$

Differentiating this once more with respect to the pressure gives

$$\begin{aligned} \frac{d}{dp} \left(\frac{dp}{d\epsilon} \right) &= \frac{dx_F}{dp} \frac{d}{dx_F} \left(\frac{x_F^2}{3(1+x_F^2)} \right) = \frac{3\sqrt{1+x_F^2}}{\epsilon_g x_F^4} \left(\frac{2x_F}{3(1+x_F^2)} - \frac{2x_F^3}{3(1+x_F^2)^2} \right) \\ &= \frac{2}{\epsilon_g x_F^3 \sqrt{1+x_F^2} (1+x_F^2)} = \frac{2}{3(\epsilon+p)(1+x_F^2)}. \end{aligned} \quad (4.23)$$

The last equality is obtained by noticing that $\epsilon + p = \frac{1}{3}\epsilon_g x_F^3 \sqrt{1+x_F^2}$. At the moment, these two last calculations might seem a bit arbitrary, but they will be needed later when we are considering a radially perturbed ideal neutron star.

4.2 Limiting Behavior of the Ideal Equation of State

We now consider two limiting cases: The non-relativistic limit (NR limit) and the ultrarelativistic limit (UR limit). For non-relativistic Fermionic matter, we have $k_F \ll mc$ which implies that the dimensionless substitution variable $x_F \ll 1$. Taylor-expanding the expressions (4.17) and (4.21) allows us to find ϵ and p up to any desired order of x_F . Using the Taylor-expansions

$$\operatorname{arcsinh}(x) = x - \frac{x^3}{6} + \frac{3x^5}{40} - \frac{5x^7}{112} + \mathcal{O}(x^9) \quad \text{and} \quad \sqrt{1+x^2} = 1 + \frac{x^2}{2} - \frac{x^4}{8} + \frac{x^6}{16} + \mathcal{O}(x^6), \quad (4.24)$$

we find the expression for ϵ and p for small x_F

$$\epsilon = \epsilon_g \left[\frac{x_F^3}{3} + \frac{x_F^5}{10} - \frac{x_F^7}{56} \right] + \mathcal{O}(x_F^9), \quad (4.25)$$

$$p = \epsilon_g \left[\frac{x_F^5}{15} - \frac{x_F^7}{42} \right] + \mathcal{O}(x_F^9). \quad (4.26)$$

Define also ϵ_{NR} and p_{NR} as the energy density and the pressure in the non-relativistic limit. The non-relativistic limit means that we keep the first and second leading order terms in the x_F -expansion for ϵ and the first leading order term for p

$$\epsilon_{\text{NR}} = \epsilon_g \left[\frac{x_F^3}{3} + \frac{x_F^5}{10} \right], \quad (4.27)$$

$$p_{\text{NR}} = \epsilon_g \frac{x_F^5}{15}. \quad (4.28)$$

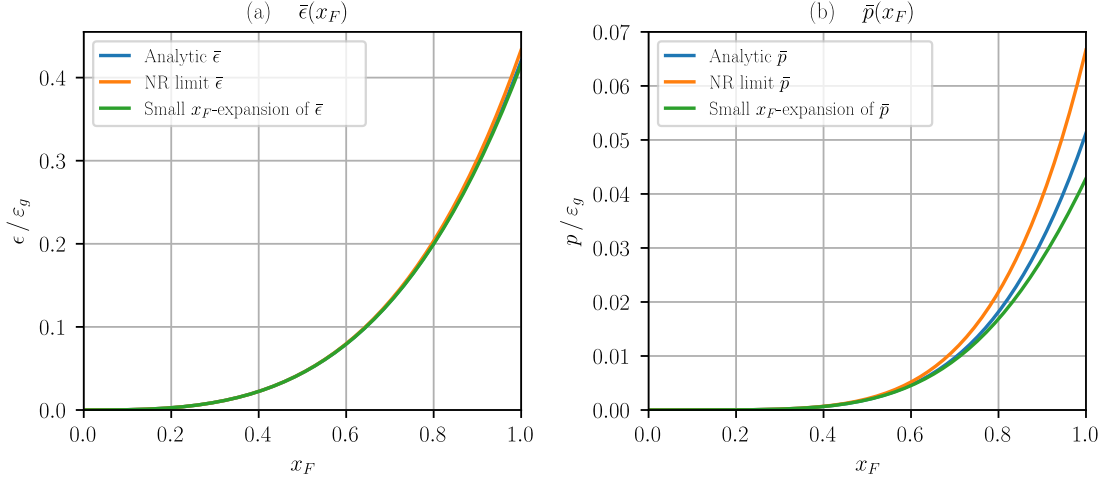


Figure 4.1: (a) displays the dimensionless energy density $\bar{\epsilon} = \frac{\epsilon}{\epsilon_g}$ for $x_F \in [0, 1]$ for a free Fermi gas. The analytic expression is plotted alongside the expansion given in Eq. (4.25) and the non-relativistic limit given in Eq. (4.27). The deviation from the expansion and the analytic solution is small even as $x_F \rightarrow 1$. Similarly, (b) displays the dimensionless pressure $\bar{p} = \frac{p}{\epsilon_g}$. The deviation between the expansion for small x_F as given by Eq. (4.26) is good up to $x_F \sim 0.8$. The non-relativistic limit starts deviating at $x_F \sim 0.6$.

In Section 3.2, we argued that for large c , i.e. the non-relativistic case, $p \ll \epsilon$. We see now that this is correct for a free Fermi gas. The pressure p_{NR} is suppressed by a factor x_F^2 compared to the energy density ϵ_{NR} . We can eliminate x_F in favour of the number density n

$$\epsilon_{\text{NR}} = mc^2 n + \frac{3}{10} \left(\frac{mc^2}{\epsilon_g} \right)^{\frac{2}{3}} mc^2 n^{\frac{5}{3}}, \quad (4.29)$$

$$p_{\text{NR}} = \frac{1}{5} \left(\frac{mc^2}{\epsilon_g} \right)^{\frac{2}{3}} mc^2 n^{\frac{5}{3}}. \quad (4.30)$$

We recognize that the leading order term for ϵ is the rest mass energy density $mc^2 n$. This is the reason we kept also the next to leading order term for the energy density. In non-relativistic physics, we often disregard the rest mass energy density, since it plays no role in the further calculations. The next-to-leading order term represents the first correction to the energy density from the momenta of the particles. Omitting the rest mass energy density, we see that $p = \frac{2}{3}\epsilon$ in the non-relativistic limit.

On the other hand, if the fermionic matter is relativistic at the Fermi energy, we have $x_F \gg 1$. Then we can approximate their expressions by making use of

$$\operatorname{arcsinh}(x_F) = \ln \left(x_F + \sqrt{1 + x_F^2} \right) = \ln(x_F) + \mathcal{O}(1) \quad \text{and} \quad \sqrt{1 + x_F^2} = x_F + \frac{1}{2}x_F^{-1} + \mathcal{O}(x_F^{-3}). \quad (4.31)$$

Inserting Eq. (4.31) into Eqs. (4.17) and (4.21), we find the following

$$\epsilon = \varepsilon_g \left[\frac{x_F^2(x_F^2 + 1)}{4} - \frac{\ln(x_F)}{8} \right] + \mathcal{O}(1), \quad (4.32)$$

$$p = \varepsilon_g \left[\frac{x_F^2(x_F^2 - 1)}{12} + \frac{\ln(x_F)}{8} \right] + \mathcal{O}(1). \quad (4.33)$$

Now we define the ultrarelativistic limit for the energy density ϵ_{UR} and the pressure p_{UR} as the limit where we only keep the leading order term. This gives

$$\epsilon_{\text{UR}} = \varepsilon_g \frac{x_F^4}{4}, \quad (4.34)$$

$$p_{\text{UR}} = \varepsilon_g \frac{x_F^4}{12}. \quad (4.35)$$

In the expressions above, we can see that both ϵ_{UR} and p_{UR} contain x_F^4 as the highest power of x_F . This means that for an ultrarelativistic free Fermi gas the energy density and the pressure are comparably large, $\epsilon \sim p$, unlike the case for the non-relativistic free Fermi gas. In this limit, we get the relation $p = \frac{1}{3}\epsilon$.

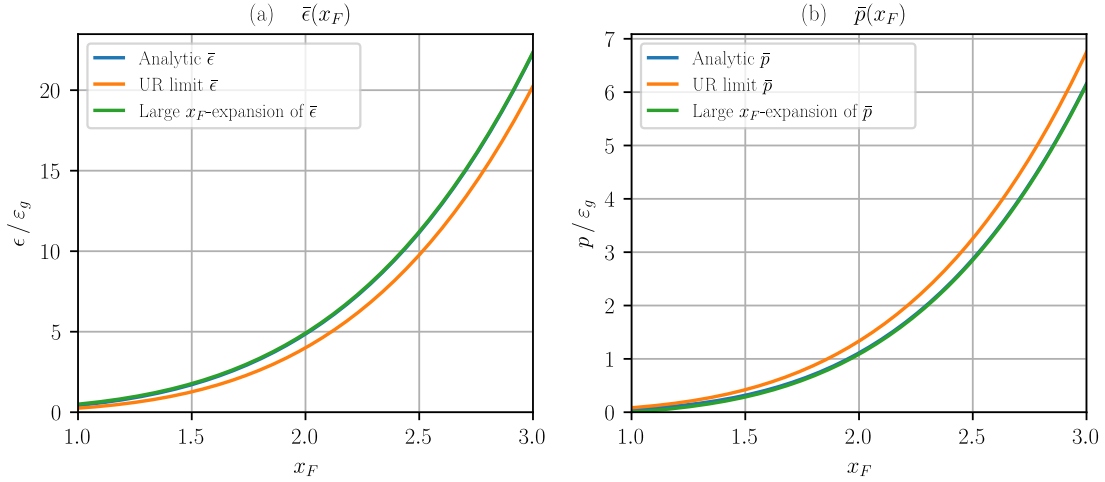


Figure 4.2: (a) shows the dimensionless energy density $\bar{\epsilon} = \frac{\epsilon}{\varepsilon_g}$ as a function of x_F . In this case, the analytic solution and the expansion for large x_F given in Eq. (4.32) coincide, even for values of x_F close to unity. The difference between the ultrarelativistic limit Eq. (4.34) and the analytic solution is increasing with increasing x_F , however, the error relative to the value of $\bar{\epsilon}$ is decreasing with larger x_F . (b) shows the dimensionless pressure $\bar{p} = \frac{p}{\varepsilon_g}$ as a function of x_F . The large x_F -expansion of p given in Eq. (4.33) is again coinciding with the analytic expression. Similarly to the case in (a), the error of the ultrarelativistic limit given in Eq. (4.35) relative to the analytical value of \bar{p} is decreasing with x_F .

Our goal in this section was to find an equation of state $\epsilon = \epsilon(p)$ for the free Fermi gas in order to close the TOV-system of equations, that is, Eqs. (3.1) and (3.2). If we consider the non-relativistic $\epsilon_{\text{NR}} = \epsilon_{\text{NR}}(p)$ and the ultrarelativistic limit $\epsilon_{\text{UR}} = \epsilon_{\text{UR}}(p)$, we get

$$\epsilon_{\text{NR}}(p) = \varepsilon_g^{\frac{2}{3}} \frac{15^{3/5}}{3} p^{\frac{3}{5}} \quad (4.36)$$

$$\epsilon_{\text{UR}}(p) = 3p. \quad (4.37)$$

Analytically expressing $\epsilon = \epsilon(p)$, we will not attempt here. We will, however, do it numerically. That is, for any given value of p , we numerically calculate x_F and then insert this value into $\epsilon(x_F)$. This is possible because Eq. (4.21) is monotonically increasing. In figure 4.3 we compare the this numerically inverted equation of state with the non-relativistic and the ultrarelativistic equations of state.

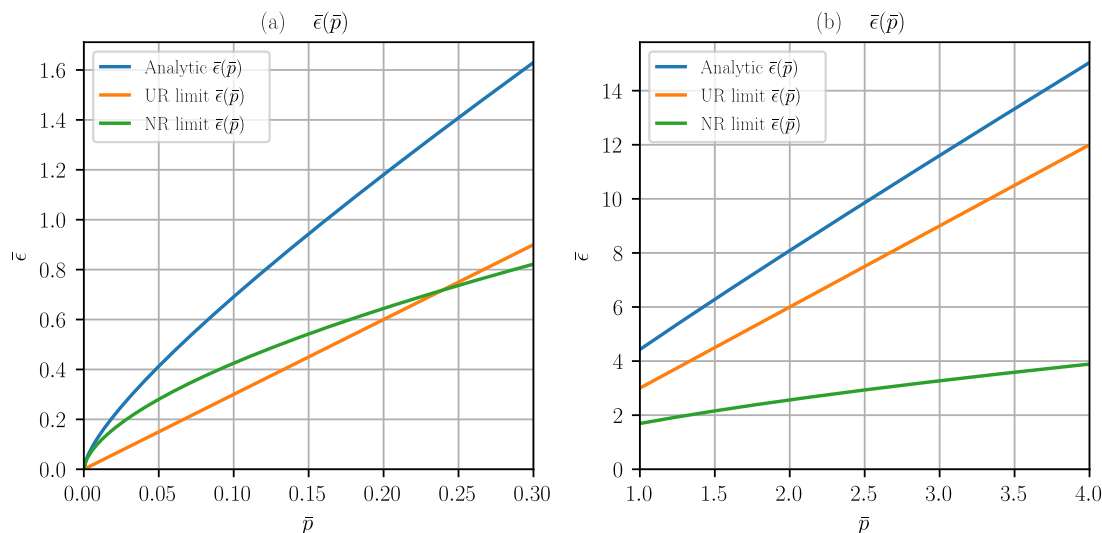


Figure 4.3: (a) depicts the dimensionless energy density $\bar{\epsilon} = \frac{\epsilon}{\epsilon_g}$ as a function of the dimensionless pressure $\bar{p} = \frac{p}{\epsilon_g}$ for small \bar{p} . The blue line shows the equation of state using the analytical expressions Eqs. (4.17) and (4.21). The non-relativistic is only a good approximation for very small \bar{p} . The ultrarelativistic limit is at best a crude approximation for small values of \bar{p} . In (b) the values of \bar{p} range from 1 to 4, which gives an idea of the asymptotic behaviour. It becomes apparent that the NR-limit is a poor approximation in this regime. The error of the UR-limit is increasing, however, the relative error is decreasing. The relative error tends toward 0 asymptotically.

For the small and large x_F expansions, we can consider an additional term in the equation of state $\epsilon(p)$, that is, also taking into account $\mathcal{O}(x_F^5)$ for the small x_F -expansions and $\mathcal{O}(x_F^2)$ for the large x_F -expansions. We arrive at the improved equations of states in the two cases

$$\epsilon = \epsilon_g^{\frac{2}{5}} \frac{15^{3/5}}{3} p^{\frac{3}{5}} + \frac{18}{7} p, \quad (\text{small } x_F) \quad (4.38)$$

$$\epsilon = 3p + \sqrt{3\epsilon_g p}. \quad (\text{large } x_F) \quad (4.39)$$

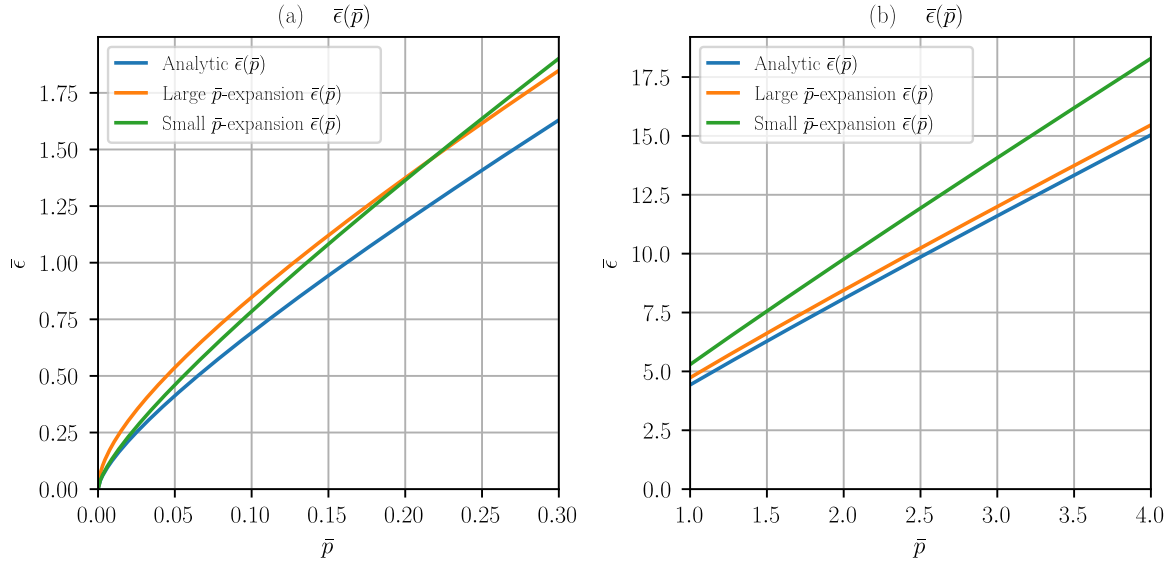


Figure 4.4: (a) shows the dimensionless energy density $\bar{\epsilon} = \frac{\epsilon}{\epsilon_g}$ as a function of the dimensionless pressure $\bar{p} = \frac{p}{\epsilon_g}$ for small \bar{p} . As above, the blue line shows the analytical solution. Both the small and large \bar{p} -expansions approximate the analytic solution better than the limiting approximations in figure 4.3. The small \bar{p} expansion starts deviating around the value 0.05. (b) displays the same plot for larger values of \bar{p} . Here, it is easier to see the asymptotic behaviour, namely that the large \bar{p} -expansion has a small almost constant error. The other expansion has an increasing error, however, it is significantly smaller than for the NR-limit.

TOV-solutions for the free Fermi gas

In this section, we will use the equation of state derived in the previous section in the TOV-system of equations. We will look at the UR-limit, the NR-limit, the large \bar{p} -expansion, the small \bar{p} -expansion as well as for the analytic ϵ and p expressed in terms of x_F .

5.1 TOV Solution for an Ultrarelativistic Equation of State for a Free Fermi Gas

We start by considering the ultrarelativistic equation of state. This is because it is analytically solvable, unlike the others. In order to find the solution, we first make the ansatz

$$p(r) = \kappa r^{-a}, \quad 0 < a < 3. \quad (5.1)$$

Here, κ is some constant. The values of a are limited to the above for the following reasons: A negative a would give rise to a star with a pressure which increases with r . We already know from our discussion of the TOV equation that this cannot be the case. We have already treated the case where $a = 0$, which corresponds to the equation of state where the energy density is constant. Inserting Eqs. (4.37) and (5.1) into Eq. (3.2) with $a \geq 3$, we find that the gravitational mass $M(r)$ diverges for any $r > 0$. We cannot accept an infinite mass. Restricting $0 < a < 3$, we can calculate $M(r)$ with the ansatz and find

$$M(r) = \int_0^r dr' 4\pi r'^2 \frac{\epsilon(r')}{c^2} = \frac{12\pi\kappa r^{3-a}}{(3-a)c^2}. \quad (5.2)$$

Substituting Eq. (5.1) into the left hand side of Eq. (3.1), we find:

$$\frac{dp}{dr} = -\kappa a r^{-(a+1)}. \quad (5.3)$$

Making use of Eqs. (4.37), (5.1), and (5.2), we find for the right hand side of Eq. (3.1)

$$\begin{aligned} \frac{dp}{dr} &= -\frac{GM(r)3p(r)}{r^2 c^2} \left[1 + \frac{1}{3}\right] \left[1 + \frac{4\pi r^3 p(r)}{M(r)c^2}\right] \left[1 - \frac{2GM(r)}{rc^2}\right]^{-1} \\ &= -\frac{36\pi G\kappa^2}{(3-a)c^4} r^{1-2a} \frac{4}{3} \left[1 + \frac{3-a}{3}\right] \left[1 - \frac{24\pi G\kappa}{(3-a)c^4} r^{2-a}\right]^{-1}. \end{aligned} \quad (5.4)$$

We note that the r -dependence drops out in the last bracket if we set $a = 2$. This results in the same total r -dependence above as in Eq. (5.3). Comparing to the left hand side Eq. (5.3), we find that the

ansatz is a solution for a suitably chosen value of κ . Now, we can equate Eq. (5.3) and Eq. (5.4) with $a = 2$ to obtain

$$-2\kappa r^{-3} = -\frac{64\pi G\kappa^2}{c^4 - 24\pi G\kappa} r^{-3}. \quad (5.5)$$

We solve this for κ ,

$$\begin{aligned} \kappa &= \frac{32\pi\kappa^2}{c^4 - 24\pi G\kappa} & \Big| \cdot \frac{c^4 - 24\pi G\kappa}{\kappa} \\ c^4 - 24\pi G\kappa &= 32\pi\kappa \\ \kappa &= \frac{c^4}{56\pi G}. \end{aligned} \quad (5.6)$$

Finally, we insert this back into Eq. (5.1) together with $a = 2$ to find the solution for an ultrarelativistic free Fermi gas as

$$p(r) = \frac{c^4}{56\pi G r^2}. \quad (5.7)$$

This is clearly not a physical solution for a compact star. Firstly, we see that the pressure approaches zero in the limit $r \rightarrow \infty$. From our definition of the radius of a star, $p(R) = 0$, the ultrarelativistic solution gives a star with infinite radius. In addition, the pressure diverges in the limit $r \rightarrow 0$. We can trace the origin of these problems back to our equation of state Eq. (4.37). This equation is only valid when $x_F \gg 1$, which cannot be the case for values of r close enough to R . At some r , matter stops behaving relativistically, and another equation of state must be used.

5.2 Numeric Solution to the TOV-equation for the Free Fermi Gas

We consider the NR limit, the small \bar{p} -expansion, the large \bar{p} -expansion and the analytic equation of state numerically. The procedure is to choose the central pressure p_c as the boundary value for p and integrate the TOV-equation until we find $p(R) = 0$. In this way, we find the stars of mass M and radius R parameterised by different values of p_c .

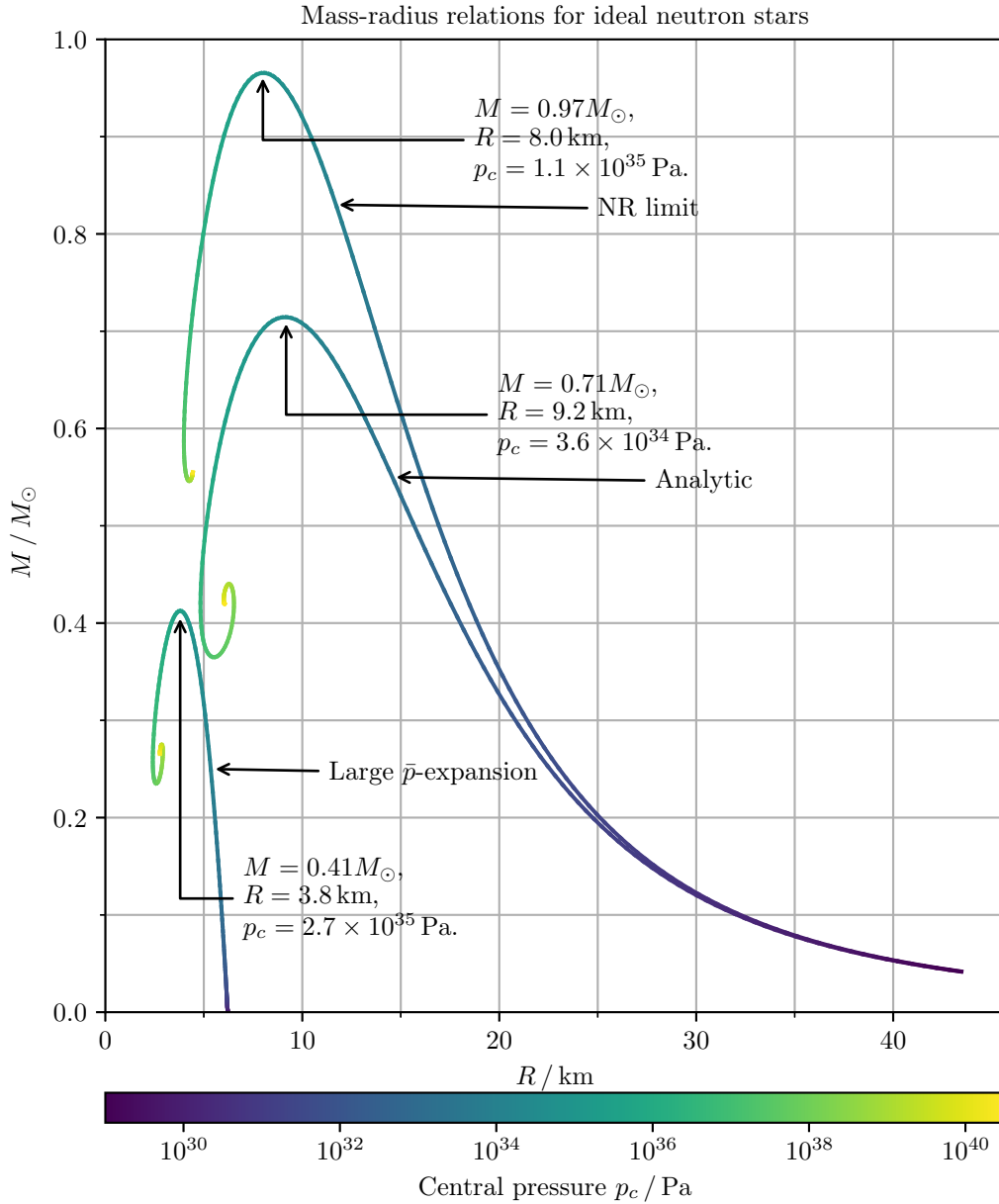


Figure 5.1: Numerical solutions to the TOV-equation with the analytic equation of state, in the NR limit and in the large \bar{p} -expansion. M_{\odot} denotes the solar mass. The respective maxima of the masses M are marked with the corresponding radius R and the parameterising central pressure p_c . The NR limit and the analytic mass-radius curve have a quite similar shape, while the large \bar{p} -expansion equation of state produces a qualitatively different curve.

Figure 5.1 displays these solutions, with the exception of the small \bar{p} -equation of state, which is plotted below, in Figure 5.2. The NR-limit equation of state predicts the most massive stars, of nearly $1M_{\odot}$. The NR-limit results are similar to the analytic results for central pressures p_c up to $p_c \sim 10^{32} \text{ Pa}$, corresponding to $\bar{p} \sim 6 \times 10^{-5}$. In this regime, we certainly have $\bar{p} \ll 1$, as is required for the validity of

the NR-limit equation of state. We can check with figure 4.3 that this is where the NR-limit approximates the analytic solution well. Note that even for the maximal mass $M = 0.97M_\odot$, $\bar{p}_c = 6.5 \times 10^{-2}$ is still quite small. However, at these values, Figure 4.3 shows that both the UR- and the NR-limits are quite poor approximations.

For the analytic equation of state, the upper limit for M is $M_{max} = 0.71M_\odot$. This is the same result as Oppenheimer and Volkoff predicted already in 1939 [9]. Many of the observed neutron star masses are clustered around $1.4M_\odot$ [4] (p. 67). Therefore, we must conclude that assuming an ideal neutron star is not a very good approximation to a physical neutron star. This is not very surprising, as nuclear physics tells us that a non-interacting fermion gas is not very realistic. However, it is interesting that such a simple model gives a prediction which is in the right order of magnitude. Observations from gravitational waves from binary neutron stars have led to a prediction of an absolute limiting mass of $M = 2.3M_\odot$ [10]. Compared to this, the ideal neutron star model is off by about a factor 3. Another point of interest is that solving the TOV-equation sets maximal mass which is quite different from the general upper limit in Eq. (3.18). Converting to SI-units, we find

$$\frac{M_{max}}{R} = 1.5 \times 10^{26} \text{ kg m}^{-1} < \frac{4c^2}{9G} = 6.0 \times 10^{26} \text{ kg m}^{-1}. \quad (5.8)$$

The limiting mass-radius ratio in the analytic case is only about $\frac{1}{4}$ of the absolute upper limit. We also note that $p_c = 3.6 \times 10^{34} \text{ Pa}$ gives a central energy density $\epsilon_c = 3.8 \times 10^{35} \text{ Pa}$, which corresponds to a mass density of $\rho_c = 4.2 \times 10^{18} \text{ kg m}^{-3}$. To compare with a familiar dense metal: This is 14 orders of magnitude larger than the mass density of lead $\rho_{lead} = 1.13 \times 10^4 \text{ kg m}^{-3}$. Another number we can compare this density to, is the nuclear saturation density, $\rho_{sat} = n_0 m_u$, where n_0 is the nuclear saturation number density and m_u is the atomic mass unit. Nuclear saturation number density has been found to be $n_0 = 0.16 \text{ fm}^{-3}$. This is the density that describes matter solely composed of nuclei held together by the strong force. The nuclear saturation density is then $\rho_{sat} = 2.5 \times 10^{17} \text{ kg m}^{-3}$. This is immensely dense! However, it is not as dense as the core of the ideal neutron star of maximum mass. Given that we cannot pack nuclei tighter than the nuclear saturation density, this is a hint we must apply another model to describe the interior of a realistic neutron star.

Another interesting energy density threshold, is the energy density at which deconfinement occurs. By deconfinement, we refer to the breakdown of nuclei into quark constituents. At energy levels lower than the deconfinement threshold, quarks only occur in bound states, such as neutrons. Above this energy density, quarks can exist on their own as free particles. At zero temperature, quarks start to deconfine at baryonic chemical potential, i.e. the chemical potential for neutrons, at $\mu_{quark} = 0.93 \text{ GeV} = 1.49 \times 10^{-10} \text{ J}$ [11]. We calculate the chemical potential inside the maximum mass neutron star by numerically solving Eq. (4.21) for x_F at $p = 3.6 \times 10^{34} \text{ Pa}$. The solution is $x_F = 0.83$. Next, we solve Eq. (4.16) for μ and insert x_F to find $\mu = 1.2 \text{ GeV} = 2.0 \times 10^{-10} \text{ J}$. The chemical potential inside the star is higher than the chemical potential at which deconfinement starts to occur! This means there should be quarks inside the neutron star as well as neutrons, yet again telling us that the ideal neutron star model is too simple.

In contrast to the UR-limit, the large \bar{p} -expansion results in a star of finite radius. However, the mass-radius relation is quite different from the analytic solution. This is due to the fact that it is not approximating the analytic solution for small \bar{p} . As commented on in Section 5.1, the matter of any star will behave non-relativistically close to the edge, as a consequence of the decreasing energy density. Therefore, this approximation will always be poor sufficiently close to the surface.

Note that $\bar{p} \sim 1$ for $p_c \sim 1.7 \times 10^{36} \text{ Pa}$. This means that only central pressures that parameterise stars beyond the maximum mass for will have $\bar{p} > 1$. Thus, it is hardly necessary to make use of the large \bar{p} -expansion, as the stars with a central pressure larger than the value which parameterises the maximum mass will be unstable. This will be discussed in the next section.

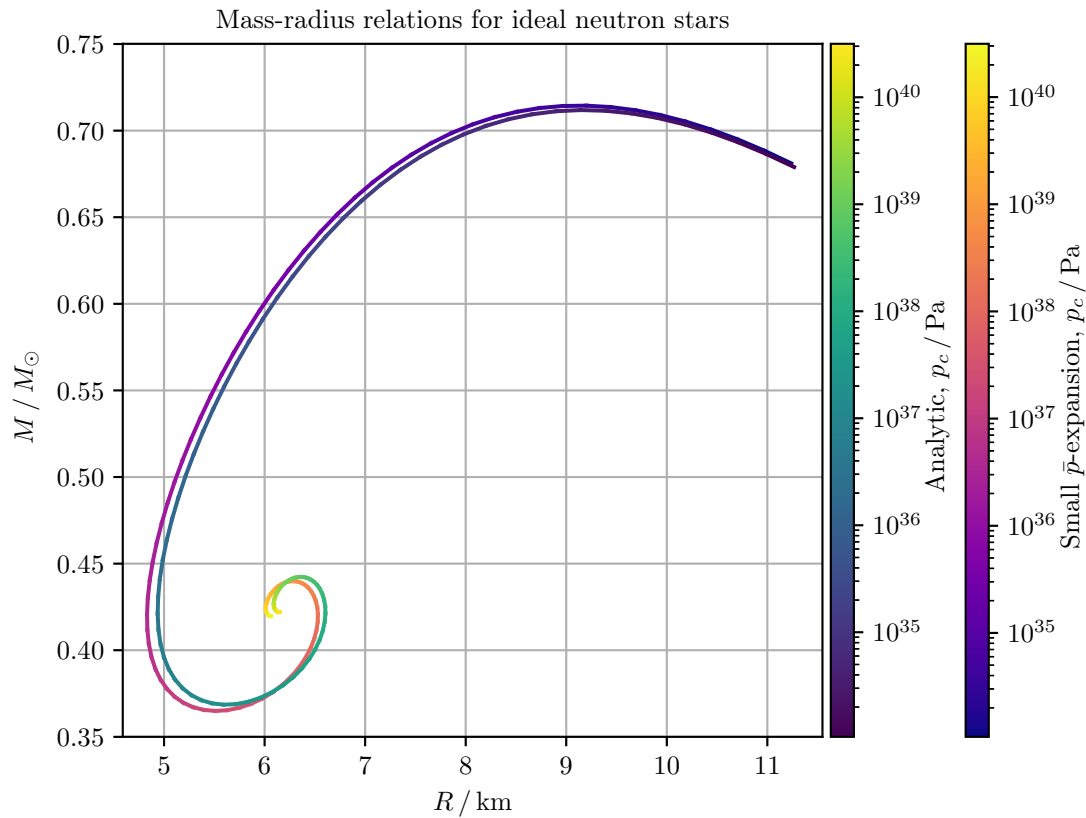


Figure 5.2: Comparison between the analytic and the small \bar{p} -expansion equation of states. The analytic and the approximated case result in similar mass-radius relations. For smaller values of p_c , the curves coincide.

In figure 5.2 we see the mass-radius curves of the analytic equation of state and of the small \bar{p} -expansion, for $p_c \in [10^{34}, 3.2 \times 10^{40}]$ Pa. The expansion equation of state gives a maximum mass of $M = 0.71M_\odot$ with $R = 9.1$ km and $p_c = 3.7 \times 10^{34}$ Pa, quite similar to the values predicted by the analytic one.

Stability of Compact Stars

In our derivation of the TOV-equation, we assumed that there was no time dependence in the metric, i.e. the star is in hydrostatic equilibrium. All the configurations calculated in the previous section are in equilibrium, however, not all these equilibria are stable. For an unstable configuration, a small perturbation would be enough to cause the force exerted by the pressure to win over the inward pull of gravity, and the star would explode. The picture is comparable to a pendulum pointing upwards. One small push, and its configuration will change dramatically. For the star, the other way around is also possible: Some small perturbation could cause the gravitational pull to be greater than the force exerted by the pressure, and the star would collapse. In this section, we aim at finding conditions for when a star is in a stable equilibrium.

6.1 Qualitative Argument for Stability

This subsection is inspired by [4]. Imagine that a neutron star of mass M in equilibrium is perturbed slightly in a way such that its central pressure is increased. The equilibrium configuration to the new internal pressure would be M' . This is illustrated in Fig. 6.1, where M_+ denotes the region where the mass is increasing as a function of p_c , and M_- the region where the mass is decreasing as we increase p_c . The perturbed star would lie in the bend of the arrow between the masses M and M' , marked on the curve. We first consider a mass M where the slope $\frac{dM}{d \log(p_c)} = \frac{dM}{dp_c} \frac{1}{p_c}$ is positive, that is M_+ . This is equivalent to stating $\frac{dM}{dp_c} > 0$. In Fig. 6.1, this is illustrated in the blue part of the plot. The inner pressure would correspond to an equilibrium state of larger mass, i.e. the system is deficit of gravitational pull due to the perturbation. This would cause the star to expand and the inner pressure to decrease. Qualitatively, we have that a perturbation towards larger inner pressure would be counteracted, driving the system back towards its original state. If we, on the other hand, consider a star where the slope $\frac{dM}{d \log(p_c)}$ is negative (equivalent to $\frac{dM}{dp_c} < 0$) and we perturb the equilibrium towards a slightly higher pressure, we find a different behaviour. This behaviour is illustrated in Fig. 6.1 by the green part of the curve. The star of mass M_- now has a central pressure p_c which corresponds to a smaller M'_- . This time, as the mass is in excess, the gravitational pull is stronger than the force exerted by the pressure. The star would start to contract, resulting in an even higher internal pressure. The perturbation would be amplified by the star's contraction, resulting in an internal pressure which corresponds to an even smaller equilibrium mass. The perturbation is self-amplifying. Thus, a slightly perturbed star in this region would start to collapse. From this qualitative discussion, we arrive at the following criterion for stable compact stars

$$\frac{dM}{dp_c} > 0. \tag{6.1}$$

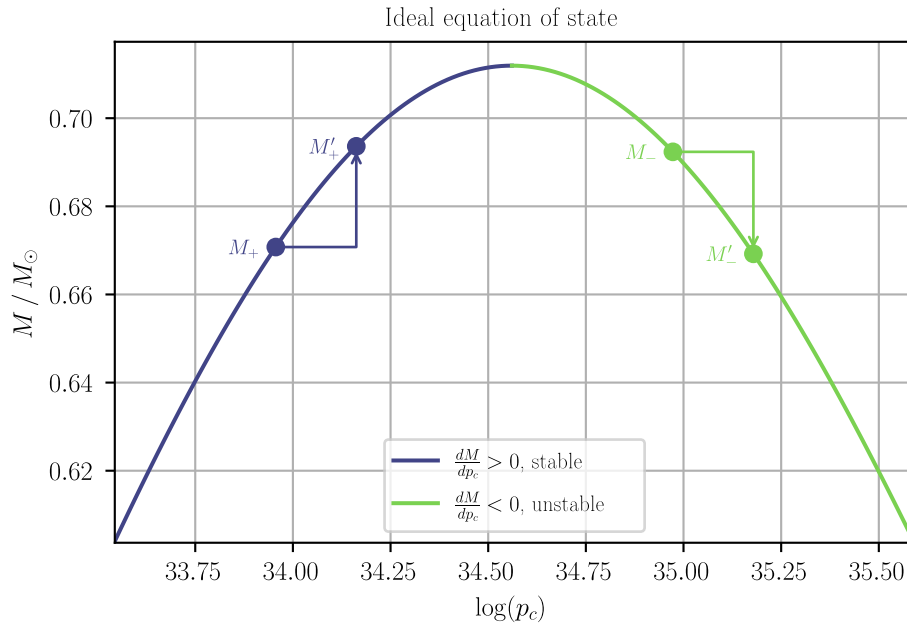


Figure 6.1: The total mass M as a function of $\log(p_c)$ for an ideal EoS. The values chosen are $\log(p_c) \in [33.5, 35.6]$, which are values that parameterise the masses around the maximal mass $M = 0.71M_{\odot}$. Note that $\frac{dM}{d\log(p_c)}$ has the same sign as $\frac{dM}{dp_c}$, since $\frac{d\log(p_c)}{dp_c} = \frac{1}{p_c} > 0$. The graph is divided into a region where the neutron star would be stable, and one region where the neutron star would be unstable.

6.2 Stability Analysis Through Perturbation Theory

After the previous qualitative discussion of stability, let us dive into a more formal approach. We will consider a radially pulsating star in perturbation theory.

6.2.1 Defining the Radial Perturbation

This means that we need a new, time dependent metric to describe the pulsations. We find the Christoffel symbols and Ricci tensor components, which are calculated similarly to the ones for the time independent Schwarzschild metric, in Appendix C. We will follow [5] and [12], and in order to keep a similar notation we now rename the following quantities

$$\alpha \rightarrow \exp(2\nu) \quad \text{and} \quad \beta \rightarrow \exp(2\lambda), \quad (6.2)$$

where λ and ν will be functions of t and r . To be specific, the line element now reads

$$ds^2 = \exp(2\nu)c^2 dt^2 - \exp(2\lambda)dr^2 - r^2 d\Omega^2. \quad (6.3)$$

All the earlier expressions written in terms of α and β can now be expressed in terms of ν and λ by direct substitution. Since we are considering infinitesimal perturbations around the equilibrium solution, let the subscript $_0$ denote the a solution to the unperturbed system as described by the TOV-equations. The perturbed quantities read

$$\begin{aligned} \epsilon(r, t) &= \epsilon_0(r) + \delta\epsilon(r, t), & p(r, t) &= p_0(r) + \delta p(r, t), \\ \nu(r, t) &= \nu_0(r) + \delta\nu(r, t), & \lambda(r, t) &= \lambda_0(r) + \delta\lambda(r, t). \end{aligned}$$

Note that $\exp(2\lambda_0) = \beta$ as it is expressed in Eq. (2.34). Similarly, the conditions we derived for α holds for $\exp(2\nu_0)$. Importantly, we also note that the only time dependent part of the functions above, is the perturbation. This means that applying a partial derivative with respect to time leaves only the perturbation, i.e. $\partial_t \lambda = \dot{\lambda} = \delta\dot{\lambda}$. In addition, we define $\xi(t, r)$ as the radial displacement of a fluid element in the pulsating star compared to a fluid element in the equilibrium star. ξ also counts as one order of the perturbation. This is the only dynamical degree of freedom. $\delta\epsilon$, δp , $\delta\nu$, $\delta\lambda$ and δn will depend on ξ , and we shall find the equations determining their behavior through the Einstein equation and general considerations of relativistic fluids. Having introduced ξ , we write the coordinates of a fluid element the perturbed system

$$x^\mu = (ct, r, \theta, \phi) \rightarrow (ct, r + \xi(t, r), \theta, \phi). \quad (6.4)$$

As we allow for radial motion expressed by ξ , the four-vector velocity obtains a radial component u^r of infinitesimal size

$$u^\mu = (u^t, u^r, 0, 0), \quad (6.5)$$

which is subject to the normalisation condition

$$c^2 = u_\mu u^\mu = \exp(2\nu)(u^t)^2 - \exp(2\lambda)(u^r)^2. \quad (6.6)$$

We wish to express u^r in terms of the displacement $\xi(t, r)$. To this end, we recall from Eq. (2.10) that $u^t = c \frac{dt}{d\tau}$ and $u^r = \frac{d(r+\xi)}{d\tau}$, where the r is kept fixed, as it expresses a radial coordinate in the unperturbed system. Taking their ratio gives

$$\frac{u^r}{u^t} = \frac{\frac{d(r+\xi)}{d\tau}}{c \frac{dt}{d\tau}} = \frac{1}{c} \frac{d(r+\xi)}{dt} = \frac{\dot{\xi}}{c}. \quad (6.7)$$

For our stability analysis, we are only interested in the first order of the perturbations. As ξ is infinitesimal, and hence $\dot{\xi}$ too, we see that u^r is infinitesimal compared to u^t . We now use this fact with the normalisation of the four-velocity in Eq. (6.6) to isolate u^t to the first order of the perturbation.

$$(u^t)^2 = c^2 \exp(-2\nu) + \mathcal{O}(\delta^2), \quad (6.8)$$

where $\mathcal{O}(\delta^2)$ denotes terms of order two and higher in the perturbations. From now on, we omit writing the $\mathcal{O}(\delta^2)$. This means that each "equals" is only valid to the zeroth and first order of the perturbation. Taking the square root of the above equation and neglecting the terms we do not care about, we find u^t . In addition, we use Eq. (6.7) find u^r .

$$u^t = c \exp(-\nu), \quad \text{and} \quad (6.9)$$

$$u^r = \frac{\dot{\xi}}{c} u^t = \dot{\xi} \exp(-\nu). \quad (6.10)$$

We aim at finding the energy momentum tensor $T_{\mu\nu}$ for the perturbed system. After $T_{\mu\nu}$ is found, we consider the Einstein equation (2.16) to constrain the perturbations. After all, the only degree of freedom we have, is the displacement ξ , and all the other perturbations follow. Lowering the indices of u^μ enables us to find $T_{\mu\nu}$ for the perturbed system

$$u_t = g_{t\sigma} u^\sigma = \exp(2\nu) u^t = c \exp(\nu), \quad \text{and} \quad (6.11)$$

$$u_r = g_{r\sigma} u^\sigma = -\exp(2\lambda) u^r = -\dot{\xi} \exp(2\lambda - \nu). \quad (6.12)$$

Now, we recall Eqs. (2.19) and use the expressions for u_t and u_r above in order to obtain $T_{\mu\nu}$. In its full matrix-form glory, it reads

$$\begin{aligned} T_{\mu\nu} &= \begin{pmatrix} \frac{u_t u_t}{c^2} (\epsilon + p) - \exp(-2\nu) p & \frac{u_t u_r}{c^2} (\epsilon + p) & 0 & 0 \\ \frac{u_r u_t}{c^2} (\epsilon + p) & \frac{u_r u_r}{c^2} (\epsilon + p) - \exp(-2\lambda) p & 0 & 0 \\ 0 & 0 & r^2 p & 0 \\ 0 & 0 & 0 & r^2 \sin^2(\theta) \end{pmatrix} \\ &= \begin{pmatrix} \exp(2\nu) \epsilon & -c^{-1} \dot{\xi} \exp(2\lambda) [\epsilon + p] & 0 & 0 \\ -c^{-1} \dot{\xi} \exp(2\lambda) [\epsilon + p] & \exp(2\lambda) p & 0 & 0 \\ 0 & 0 & r^2 p & 0 \\ 0 & 0 & 0 & r^2 \sin^2 \theta p \end{pmatrix}. \end{aligned} \quad (6.13)$$

In the exact same fashion, we find the energy-momentum tensor with upper indices

$$T^{\mu\nu} = \begin{pmatrix} \exp(-2\nu) \epsilon & c^{-1} \dot{\xi} \exp(-2\nu) [\epsilon + p] & 0 & 0 \\ c^{-1} \dot{\xi} \exp(-2\nu) [\epsilon + p] & \exp(-2\lambda) p & 0 & 0 \\ 0 & 0 & r^{-2} p & 0 \\ 0 & 0 & 0 & (r \sin(\theta))^{-2} p \end{pmatrix}. \quad (6.14)$$

An important result we used when we searched for the TOV-equation, was the condition imposed by energy-momentum conservation, namely Eq. (2.36). The energy momentum tensor $T^{\mu\nu}$ has, as we can see above, picked up some new terms as a consequence of the perturbation. Additionally, we found three new Christoffel symbols in Eq. (C.2). Therefore, we investigate how the energy-momentum conservation condition change. To make the substitution of the Christoffel symbols clearer, we write the ones containing α and β with ν and λ

$$\begin{aligned} \Gamma_{tt}^r &= \exp(2\nu - 2\lambda) \nu', & \Gamma_{tt}^t &= \dot{\nu} = \delta \dot{\nu} \\ \Gamma_{rr}^t &= \exp(2\lambda - 2\nu) \dot{\lambda} = \exp(2\lambda - 2\nu) \delta \dot{\lambda}, & \Gamma_{tr}^t &= \nu', \\ \Gamma_{\theta\theta}^r &= -r \exp(-2\lambda), & \Gamma_{rr}^r &= \lambda', \\ \Gamma_{\phi\phi}^r &= -r \sin^2(\theta) \exp(-2\lambda), & \Gamma_{tr}^r &= \dot{\lambda} = \delta \dot{\lambda}. \end{aligned} \quad (6.15)$$

Now we have all the Christoffel symbols and components of the energy-momentum tensor to find an explicit expression from energy-momentum conservation.

$$\begin{aligned} \nabla_\mu T^{\mu r} &= \partial_\mu T^{\mu r} + \Gamma_{\mu\sigma}^\mu T^{\sigma r} + \Gamma_{\mu\sigma}^r T^{\mu\sigma} \\ &= \partial_t T^{tr} + \partial_r T^{rr} + (\Gamma_{tt}^t + \Gamma_{rt}^r) T^{tr} + (\Gamma_{tr}^t + \Gamma_{rr}^r + \Gamma_{\theta r}^\theta + \Gamma_{\phi r}^\phi) T^{rr} + \Gamma_{tt}^r T^{tt} \\ &\quad + \Gamma_{tr}^r T^{tr} + \Gamma_{rt}^r T^{rt} + \Gamma_{rr}^r T^{rr} + \Gamma_{\theta\theta}^r T^{\theta\theta} + \Gamma_{\phi\phi}^r T^{\phi\phi}. \end{aligned} \quad (6.16)$$

We note from Eq. (6.15) that Γ_{tt}^t , Γ_{rr}^r and Γ_{rt}^r are linear in the perturbation. Multiplying these terms with the off-diagonal components of the energy-momentum tensor gives rise to terms that we neglect here. Substituting in the expressions for all components, we find

$$\begin{aligned}
 \nabla_{\mu} T^{\mu r} &= \partial_r T^{rr} + \left(\Gamma_{tr}^t + 2\Gamma_{rr}^r + \Gamma_{\theta r}^{\theta} + \Gamma_{\phi r}^{\phi} \right) T^{rr} + \Gamma_{\theta\theta}^r T^{\theta\theta} + \Gamma_{\phi\phi}^r T^{\phi\phi} + \Gamma_{tt}^r T^{tt} + \frac{1}{c} \partial_t T^{tr} \\
 &= \partial_r (\exp(-2\lambda)p) + \left(\nu' + 2\lambda' + \frac{2}{r} \right) \exp(-2\lambda)p - \frac{2 \exp(-2\lambda)}{r} p \\
 &\quad + \exp(2\nu - 2\mu) \nu' \exp(2\nu) \epsilon + \partial_t \left(\frac{\dot{\xi}}{c^2} \exp(-2\nu_0) (\epsilon_0 + p_0) \right) \\
 &= \exp(-2\lambda) p' + \exp(-2\lambda) \nu' (\epsilon + p) + \frac{\ddot{\xi}}{c^2} \exp(-2\nu_0) (\epsilon_0 + p_0) \\
 &= 0.
 \end{aligned} \tag{6.17}$$

To zeroth order, the above expression is equivalent to what we found for an equilibrium star, Eq. (2.36). This time, however, we consider the linear terms in the perturbation. Multiplying the expression above with $\exp(2\lambda)$, we get the expression into its tidiest form. In this way, energy-momentum conservation gives the constraint

$$\frac{\ddot{\xi}}{c^2} \exp(2\lambda_0 - 2\nu_0) (\epsilon_0 + p_0) = -(\epsilon_0 + p_0) \delta\nu' - \delta p' - \nu_0' (\delta\epsilon + \delta p). \tag{6.18}$$

We have derived the first of five constraints. This equation determines the dynamics of ξ . After we manage to eliminate $\delta\nu'$, $\delta\epsilon$ and δp , this will be the governing equation for how the perturbation ξ evolves. We find the second constraint from considering the rt -component of the Einstein equation. In Appendix C, we calculate R_{rt} , Eq. (C.8), which we can rewrite with λ instead of β . Inserted into the Einstein equation together with T_{rt} from Eq. (6.13), the calculation leads to

$$\frac{-2\delta\lambda}{cr} = -\frac{8\pi G}{c^4} \frac{-\dot{\xi}}{c} \exp(2\lambda_0) (\epsilon_0 + p_0). \tag{6.19}$$

In this equation, we have a time derivative on both sides. To remove the derivative, we integrate both sides, but this comes at the cost of introducing an integration constant. We need to determine this constant. If we set the perturbation ξ to zero, the system should recover its original equilibrium form, i.e. $\delta\lambda = 0$. If we have a non-zero integration constant, this would not be the case. Therefore, we can set the integration constant to zero. Thus, we have found the second constraint on the perturbation

$$\delta\lambda = -\frac{4\pi G}{c^4} \xi r \exp(2\lambda_0) (\epsilon_0 + p_0). \tag{6.20}$$

$\delta\lambda$ will appear in the following constraints, and we will need this expression to substitute away $\delta\lambda$ in favour for ξ . The third constraint is found from Eq. (2.44). In Appendix C we argue that this result is also valid for the time-dependent case. Firstly, we rewrite the equation in terms of ν and λ . This leads to

$$\begin{aligned}
 \nu' &= \frac{4\pi G}{c^4} r p \exp(2\lambda) - \frac{1}{2r} (1 - \exp\{2\lambda\}) \quad | \cdot 2r \exp(-2\lambda) \\
 2r \exp(-2\lambda) \nu' &= \frac{8\pi G}{c^4} r^2 p - \exp(-2\lambda) + 1 \\
 2r \exp(-2\lambda_0) (\nu_0' - 2\nu_0' \delta\lambda + \delta\nu') &= \frac{8\pi G}{c^4} r^2 (p_0 + \delta p) + \exp(-2\lambda_0) (1 - 2\delta\lambda) - 1.
 \end{aligned} \tag{6.21}$$

As before, we look at the terms linear in the perturbation. We isolate $\delta\nu'$ to arrive at the third constraint

$$\delta\nu' = \frac{4\pi G}{c^4} r \exp(2\lambda_0) \delta p + 2\nu_0' \delta\lambda + \frac{\delta\lambda}{r}. \tag{6.22}$$

The two last constraints we find from thermodynamic analysis on relativistic fluid dynamics. This is done in Appendix A. We are going to make use of the energy momentum conservation condition and the expression for the adiabatic index γ

$$u^\mu \nabla_\mu \epsilon = -(\epsilon + p) \nabla_\mu u^\mu, \quad (6.23)$$

$$\gamma = \frac{\epsilon + p}{p} \left(\frac{\partial p}{\partial \epsilon} \right)_s. \quad (6.24)$$

First, let us consider the energy-momentum conservation, Eq. (6.23). We know the expressions of u^μ , ϵ and p , so we can start inserting these quantities. Let us first treat the left hand side of this equation. The result is

$$u^\mu \nabla_\mu \epsilon = \left(\frac{u^t}{c} \partial_t + u^r \partial_r \right) (\epsilon_0 + \delta\epsilon) = \exp(-\nu) \left(\dot{\delta\epsilon} + \epsilon'_0 \dot{\xi} \right). \quad (6.25)$$

The right hand side gives quite a few terms to calculate

$$\begin{aligned} -(\epsilon + p) \nabla_\mu u^\mu &= -(\epsilon + p) \left\{ \frac{\partial_t u^t}{c} + \partial_r u^r + (\Gamma_{tt}^t + \Gamma_{rt}^r) + u^t (\Gamma_{tr}^t + \Gamma_{rr}^r + \Gamma_{\theta r}^\theta + \Gamma_{\phi r}^\phi) u^r \right\} \\ &= -(\epsilon + p) \left\{ -\exp(-\nu) \dot{\nu} + \exp(-\nu) (\dot{\xi}' - \nu' \dot{\xi}) + (\dot{\nu} + \dot{\lambda}) \exp(-\nu) \right. \\ &\quad \left. + \left(\nu' + \lambda' + \frac{2}{r} \right) \dot{\xi} \exp(-\nu) \right\} \\ &= -(\epsilon_0 + p_0) \exp(-\nu) \left\{ \dot{\xi}' + \delta \dot{\lambda} + \lambda'_0 \dot{\xi} + \frac{2}{r} \dot{\xi} \right\}. \end{aligned} \quad (6.26)$$

In the last line, we have noticed that the curly brackets contain only terms that are first order in the perturbation, and we are therefore allowed to include only the zeroth order of the energy density and the pressure, $(\epsilon + p) \rightarrow (\epsilon_0 + p_0)$. We equate Eq. (6.25) and Eq. (6.26) and then multiply both sides with $\exp(\nu)$ to find the relation for $\delta\epsilon$

$$\dot{\delta\epsilon} = -(\epsilon_0 + p_0) \left\{ \dot{\xi}' + \delta \dot{\lambda} + \lambda'_0 \dot{\xi} + \frac{2}{r} \dot{\xi} \right\} - \epsilon'_0 \dot{\xi}. \quad (6.27)$$

This looks promising, and we can even simplify it further. On both sides of the equation, each term has a time derivative acting upon it. Thus, we may integrate in order to remove the time derivatives, at the cost of an integration constant. As in the case for $\delta\lambda$, we set this constant to zero. The reason we can do this, is that the perturbation in ϵ should disappear if we set ξ to zero. From the discussion above, we know that $\delta\lambda$ vanishes as $\xi \rightarrow 0$. With this, we conclude that $\delta\epsilon$ only vanishes if the integration constant is zero. The fourth constraint on the perturbations has finally been derived as

$$\delta\epsilon = -(\epsilon_0 + p_0) \left\{ \xi' + \delta\lambda + \lambda'_0 \xi + \frac{2}{r} \xi \right\} - \epsilon'_0 \xi. \quad (6.28)$$

The only missing piece now is to determine δp . In order to achieve this, we have to evaluate $\frac{\partial p}{\partial \epsilon}$ at constant entropy. To this end, we must discuss what an observer moving along the flow of the fluid would measure. In Eq. (6.4) we define what the perturbations look like for an observer fixed in the coordinate system. This is what we call an Eulerian change. However, this change is not the same as an observer moving along with the perturbed fluid would measure. This observer would experience both the Eulerian perturbation, and a slight change due to the radial displacement ξ . The change an observer moving with the fluid would measure is called a Lagrangian change. To distinguish the two of them, we denote a Lagrangian change by a Δ . The measured energy density for the observer in the rest frame of the fluid element will be $\epsilon = \epsilon_0 + \Delta\epsilon$. In the end, we want to express everything in the terms of the Eulerian change δ . We see how the Eulerian and the Lagrangian change relate to each other if we consider Figure 6.2.

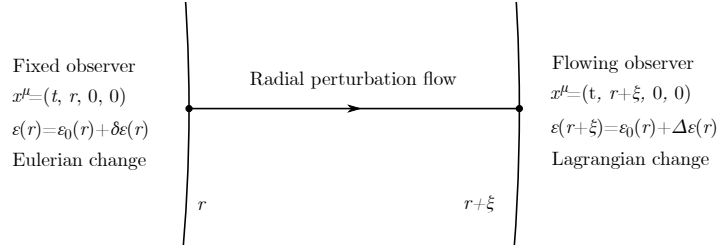


Figure 6.2: An illustration of a fixed observer measuring the Eulerian change and a flowing observer measuring the Lagrangian change in the radially perturbed equilibrium star. When the perturbation ξ is small, we can Taylor-expand $\epsilon(r + \xi)$ around r to obtain a relation between the Eulerian variation δ and the Lagrangian variation Δ .

In the rest frame of a fluid, i.e. for the flowing observer, we must evaluate the energy density ϵ_{rest} at radial coordinate $r + \xi$. We Taylor-expand ϵ around r , and arrive at

$$\begin{aligned} \epsilon_{\text{rest}}(t, r) &= \epsilon(t, r + \xi) = \epsilon_0(r) + \Delta\epsilon(t, r) = \epsilon(r, t) + \partial_r\epsilon(r, t)\xi \\ &= \epsilon_0(r) + \partial_r(\epsilon_0)\xi + \delta\epsilon(r, t). \end{aligned} \quad (6.29)$$

We can now see that the infinitesimal changes are related by an extra term proportional to the radial perturbation ξ .

$$\Delta\epsilon = \delta\epsilon + \epsilon'_0\xi. \quad (6.30)$$

Now that we have considered the relation between a fixed observer with an observer moving with the streamlines, we can evaluate Eq. (6.24) expressed in terms of $\Delta\epsilon$ and Δp , and then in turn express δp . Eq. (6.24) tells us how the change of pressure is related to the change in energy density at constant entropy. This corresponds to Δp over $\Delta\epsilon$, because Δ describes how quantities infinitesimally change along the streamlines, which is exactly what the derivative at constant entropy describes. Therefore, we write

$$\gamma = \frac{\epsilon + p}{p} \frac{\Delta p}{\Delta\epsilon}. \quad (6.31)$$

This allows us to write

$$\begin{aligned} \Delta p &= \gamma \frac{p}{\epsilon + p} \Delta\epsilon \\ \delta p + p'_0\xi &= \gamma \frac{p}{\epsilon + p} (\delta\epsilon + \epsilon'_0\xi). \end{aligned} \quad (6.32)$$

In order to make use of this, we need to evaluate γ to zeroth order, γ_0 . We can do this by simply inserting the equilibrium quantities into Eq. (6.24). This procedure yields

$$\gamma_0 = \frac{\epsilon_0 + p_0}{p_0} \frac{\partial p_0}{\partial \epsilon_0}. \quad (6.33)$$

This is easy to evaluate for a given equation of state. Finally, we have found the fifth and last equation to constrain the perturbations

$$\delta p = \gamma_0 \frac{p_0}{\epsilon_0 + p_0} (\delta\epsilon + \epsilon'_0\xi) - p'_0\xi. \quad (6.34)$$

6.2.2 Constraining the Radial Perturbation

In the previous subsection, we derived five constraints for the perturbations in the radially pulsating star. Here, we shall combine them in order to find a dynamical constraint in the radial perturbation ξ . Since

we only considered the first order in the perturbation, these equations form a set of linear differential equations

$$\frac{\ddot{\xi}}{c^2} \exp(2\lambda_0 - 2\nu_0)(\epsilon_0 + p_0) = -(\epsilon_0 + p_0)\delta\nu' - \delta p' - \nu'_0(\delta\epsilon + \delta p), \quad (6.35)$$

$$\delta\lambda = -\frac{4\pi G}{c^4} \exp(2\lambda_0) r\xi(\epsilon_0 + p_0), \quad (6.36)$$

$$\delta\nu' = \frac{4\pi G}{c^4} \exp(2\lambda_0) r\delta p + 2\nu'_0\delta\lambda + \frac{\delta\lambda}{r}, \quad (6.37)$$

$$\delta\epsilon = -(\epsilon_0 + p_0) \left\{ \xi' + \delta\lambda + \lambda'_0\xi + \frac{2}{r}\xi \right\} - \epsilon'_0\xi, \quad (6.38)$$

$$\delta p = \gamma_0 \frac{p_0}{\epsilon_0 + p_0} (\delta\epsilon + \epsilon'_0\xi) - p'_0\xi. \quad (6.39)$$

In addition, we will need the equilibrium conditions on ν'_0 and λ'_0 . These are easy to read off from Eqs. (2.37), (2.44), and (2.42)

$$\nu'_0 = \frac{-p'_0}{\epsilon_0 + p_0}, \quad (6.40)$$

$$\nu'_0 = \frac{1}{2r} (\exp(2\lambda_0) - 1) + \frac{4\pi G}{c^4} \exp(2\lambda_0) r p_0, \quad (6.41)$$

$$\lambda'_0 = \frac{1}{2r} (1 - \exp(2\lambda_0)) + \frac{4\pi G}{c^4} \exp(2\lambda_0) r \epsilon_0. \quad (6.42)$$

The seek an equation with only ξ and derivatives acting on it, the spatial coordinates and the known equilibrium quantities. The work ahead is frankly looking a little messy. Starting with the good news: $\delta\lambda$ is already expressed solely with ξ , r and unperturbed quantities. In addition, we notice that we can write $\delta\lambda$ in a compact form by utilising Eq. (6.41) and (6.42)

$$\delta\lambda = -\xi \left(\frac{4\pi G}{c^4} \exp(2\lambda_0) r \epsilon_0 + \frac{4\pi G}{c^4} \exp(2\lambda_0) r p_0 \right) = -\xi(\nu'_0 + \lambda'_0). \quad (6.43)$$

The next step is substituting this expression into Eq. (6.38) to make $\delta\epsilon$ independent of perturbations except for ξ .

$$\begin{aligned} \delta\epsilon &= -(\epsilon_0 + p_0) \left\{ \xi' - \xi(\nu'_0 + \lambda'_0) + \lambda'_0\xi + \frac{2}{r}\xi \right\} - \epsilon'_0\xi \\ &= -(\epsilon_0 + p_0) \left\{ \xi' + \frac{2}{r}\xi - \nu'_0\xi \right\} - \epsilon'_0\xi. \end{aligned} \quad (6.44)$$

Now we can substitute $\delta\epsilon$ into Eq. (6.39) to find δp expressed by the desired quantities

$$\begin{aligned} \delta p &= \gamma_0 \frac{p_0}{\epsilon_0 + p_0} \left(-(\epsilon_0 + p_0) \left\{ \xi' + \frac{2}{r}\xi - \nu'_0\xi \right\} - \epsilon'_0\xi + \epsilon'_0\xi \right) - p'_0\xi \\ &= -\gamma_0 p_0 \left\{ \xi' + \frac{2}{r}\xi - \nu'_0\xi \right\} - p'_0\xi. \end{aligned} \quad (6.45)$$

We note that $\delta\epsilon$ and δp have the same dependence of the curly brackets, and hence will also $\delta\nu'$ contain the same bracket, as it can be expressed in terms of δp . In the dynamical constraint on ξ , Eq. (6.35), we see all these quantities appearing in addition to the radial derivative on δp . Therefore, we have ample motivation to write the bracket in a more compact form in order to save a lot of writing,

$$\begin{aligned} \left\{ \xi' + \frac{2}{r}\xi - \nu'_0\xi \right\} &= \frac{(r^2\xi \exp(-\nu_0))'}{r^2 \exp(-\nu_0)} = \frac{\exp(\nu_0)}{r^2} \zeta', \\ &\text{where } \zeta \equiv r^2\xi \exp(-\nu_0). \end{aligned} \quad (6.46)$$

Using ζ instead of ξ to express the radial perturbation simplifies the equations by reducing the amount of terms. Therefore, we find the dynamics of ζ instead of ξ . Anywhere ξ appears, it is an easy task to substitute in ζ . We begin by substituting ζ back into our last expression for δp .

$$\begin{aligned}\delta p &= -\gamma_0 p_0 \frac{\exp(\nu_0)}{r^2} \zeta' - p_0' \frac{\exp(\nu_0)}{r^2} \zeta \\ &= -Z \zeta' - p_0' \frac{\exp(\nu_0)}{r^2} \zeta,\end{aligned}\tag{6.47}$$

$$\text{where } Z \equiv \gamma_0 p_0 \frac{\exp(\nu_0)}{r^2}.\tag{6.48}$$

As mentioned, we are going to evaluate the radial derivative acting on δp , and renaming the prefactor in front of ζ' to Z will simplify this expression. Now we are in a position to express $\delta\epsilon$ in terms of ζ instead of ξ

$$\delta\epsilon = -(\epsilon_0 + p_0) \frac{\exp(\nu_0)}{r^2} \zeta' - \epsilon_0' \frac{\exp(\nu_0)}{r^2} \zeta.\tag{6.49}$$

The last expression we need is $\delta\nu'$. Again we use the equilibrium conditions to find a compact expression, in addition eliminating $\delta\lambda$ and δp by Eqs. (6.43) and (6.47)

$$\begin{aligned}\delta\nu' &= \frac{1}{\epsilon_0 + p_0} (\nu_0' + \lambda_0') \delta p - \left(2\nu_0' + \frac{1}{r}\right) \delta\lambda \\ &= -\frac{\nu_0' + \lambda_0'}{\epsilon_0 + p_0} \{Z\zeta' + p_0' r^{-2} \exp(\nu_0) \zeta\} - (\nu_0' + \lambda_0') \left(2\nu_0' + \frac{1}{r}\right) \frac{\exp(\nu_0)}{r^2} \zeta \\ &= -\frac{\nu_0' + \lambda_0'}{\epsilon_0 + p_0} Z\zeta' - (\nu_0' + \lambda_0') \left(\nu_0' + \frac{1}{r}\right) \frac{\exp(\nu_0)}{r^2} \zeta.\end{aligned}\tag{6.50}$$

In the last line, we have used the condition from equilibrium energy-momentum conservation, Eq. (6.40).

Finally, we are ready to insert everything in the dynamical equation for ξ which we express in terms of ζ . At first we motivate a little as to where we are headed. On the left hand side of Eq. (6.35), we have two time derivatives acting on ξ . This means, that we should be able to write this side of the equation as $X\ddot{\zeta}$, where X is a function we must determine. The right hand side of the same equation contains ζ'' (from the term $-\delta p'$), ζ' and ζ , and it is linear in each of these terms. As a consequence, it should be possible to write the right hand side in the form $A\zeta'' + B\zeta' + C\zeta$, where A, B and C are functions that we must determine. As the terms will be quite long, we handle the left hand side of Eq. (6.35) by itself first

$$\frac{\ddot{\xi}}{c^2} \exp(2\lambda_0 - 2\nu_0) (\epsilon_0 + p) = \frac{\epsilon_0 + p_0}{c^2 r^2} \exp(2\lambda_0 - \nu_0) \ddot{\zeta} = X\ddot{\zeta}.\tag{6.51}$$

Here, we have identified $X = \frac{\epsilon_0 + p_0}{c^2 r^2} \exp(2\lambda_0 - \nu_0)$. It will soon, however, be practical to multiply both sides of the dynamical equation with a factor of $\exp(2\nu_0 + \lambda_0)$. This will soon be justified. For now, let us apply everything we have derived in this section to the right hand side of the dynamical constraint. To be specific, we substitute Eqs. (6.47), (6.49) and (6.50) into Eq. (6.35). This yields a quite large

expression, which fortunately tidies itself up as we collect the terms

$$\begin{aligned}
 X\ddot{\zeta} &= -(\epsilon_0 + p_0)\delta\nu' - \delta p' - \nu'_0(\delta\epsilon + \delta p) \\
 &= (\nu'_0 + \lambda'_0)Z\zeta' + (\epsilon_0 + p_0)(\nu'_0 + \lambda'_0) \left(\nu'_0 + \frac{1}{r} \right) \frac{\exp(\nu_0)}{r^2} \zeta + Z'\zeta' + Z\zeta'' + \left(p'_0 \frac{\exp(\nu_0)}{r^2} \right)' \zeta \\
 &\quad + p'_0 \frac{\exp(\nu_0)}{r^2} \zeta' + \nu'_0 \left[Z\zeta' + p'_0 \frac{\exp(\nu_0)}{r^2} \zeta + (\epsilon_0 + p_0) \frac{\exp(\nu_0)}{r^2} \zeta' + \epsilon'_0 \frac{\exp(\nu_0)}{r^2} \zeta \right] \\
 &= Z\zeta'' + \zeta' \left\{ Z' + (\nu'_0 + \lambda'_0)Z + \nu'_0 Z + p'_0 \frac{\exp(\nu_0)}{r^2} + \nu'_0(\epsilon_0 + p_0) \frac{\exp(\nu_0)}{r^2} \right\} \\
 &\quad + \zeta \frac{\exp(\nu_0)}{r^2} \left[(\epsilon_0 + p_0)(\nu'_0 + \lambda'_0) \left(\nu'_0 + \frac{1}{r} \right) + p''_0 + \nu'_0 p'_0 - p'_0 \frac{2}{r} + \nu'_0(p'_0 + \epsilon'_0) \right] \\
 &= Z\zeta'' + \zeta' \{ Z' + (2\nu'_0 + \lambda'_0)Z \} + \zeta \frac{\exp(\nu_0)}{r^2} (\epsilon_0 + p_0) \left[(\nu'_0 + \lambda'_0) \left(\nu'_0 + \frac{1}{r} \right) - \nu''_0 - (\nu'_0)^2 + \frac{2\nu'_0}{r} \right].
 \end{aligned} \tag{6.52}$$

To obtain the last equality, we have again used the condition from energy-momentum conservation for the equilibrium state. Next, we consider the terms containing ζ'' and ζ' . With a slight rewriting, we may bring the terms with radial derivatives of ζ to the form $[P\zeta']' = P\zeta'' + P'\zeta'$. We are free to multiply both side of the equation with a common factor, meaning that we can chose $P = fZ$, where f is an arbitrary function. Comparing this form of P to the equation above, we get the following requirement

$$[P\zeta']' = P\zeta'' + P'\zeta' = fZ\zeta'' + fZ'\zeta' + f'Z\zeta = fZ\zeta'' + fZ'\zeta' + (3\nu'_0 + \lambda'_0)fZ\zeta. \tag{6.53}$$

The statement just above, is equivalent to the condition $f' = (2\nu_0 + \lambda_0)f$. This simple differential equation has the solution $f = \exp(2\nu_0 + \lambda_0)$. Earlier we stated that we want to multiply both sides of the dynamical equation by $\exp(2\nu_0 + \lambda_0)$, and this is the reason. Doing so, we can write the dynamical constraint on ζ as

$$W\ddot{\zeta} = [P\zeta']' + Q\zeta. \tag{6.54}$$

We have deliberately chosen the same function notation as in [5], in order to make it possible to check that the calculation performed here matches their results. The functions W , P and Q are given by

$$W = \frac{\epsilon_0 + p_0}{c^2 r^2} \exp(\nu_0 + 3\lambda_0), \tag{6.55}$$

$$P = \gamma_0 p_0 \frac{\exp(3\nu_0 + \lambda_0)}{r^2}, \tag{6.56}$$

$$Q = (\epsilon_0 + p_0) \frac{\exp(3\nu_0 + \lambda_0)}{r^2} \left[(\nu'_0 + \lambda'_0) \left(\nu'_0 + \frac{1}{r} \right) - \nu''_0 - (\nu'_0)^2 + \frac{2\nu'_0}{r} \right]. \tag{6.57}$$

Cleaning up the terms for Q is another calculational exercise at the end of this quite long perturbation analysis. Twice we insert identities (with dotted underline) with the intent to find a tidy expression in

the end

$$\begin{aligned}
 -\nu_0'' &= - \left(\frac{1}{2r} (\exp(2\lambda_0) - 1) + \frac{4\pi G}{c^4} \exp(2\lambda_0) r p_0 \right)' \\
 &= \frac{1}{2r^2} (\exp(2\lambda_0) - 1) - 2\lambda_0' \frac{\exp(2\lambda_0)}{2r} - 2\lambda_0' \frac{4\pi G}{c^4} \exp(2\lambda_0) r p_0 + \frac{1}{2r} 2\lambda_0' - \frac{1}{2r} 2\lambda_0' \\
 &\quad - \frac{4\pi G}{c^4} \exp(2\lambda_0) p_0 - \frac{1}{2r^2} (\exp(2\lambda_0) - 1) + \frac{1}{2r^2} (\exp(2\lambda_0) - 1) - \frac{4\pi G}{c^4} \exp(2\lambda_0) r p_0' \\
 &= \frac{1}{r^2} (\exp(2\lambda_0) - 1) - \frac{\lambda_0'}{r} - 2\lambda_0' \left(\frac{1}{2r} (\exp(2\lambda_0) - 1) + \frac{4\pi G}{c^4} \exp(2\lambda_0) r p_0 \right) \\
 &\quad - \frac{1}{r} \left(\frac{1}{2r} (\exp(2\lambda_0) - 1) + \frac{4\pi G}{c^4} \exp(2\lambda_0) r p_0 \right) + \nu_0' \frac{4\pi G}{c^4} \exp(2\lambda_0) r (\epsilon_0 + p_0) \\
 &= \frac{1}{r^2} (\exp(2\lambda_0) - 1) - \frac{\lambda_0'}{r} - 2\lambda_0' \nu_0' - \frac{1}{r} \nu_0' + \nu_0' (\nu_0' + \lambda_0') \\
 &= \frac{1}{r^2} (\exp(2\lambda_0) - 1) + 2(\nu_0')^2 - (\nu_0' + \lambda_0') (\nu_0' + \frac{1}{r}). \tag{6.58}
 \end{aligned}$$

This expression we substitute back into Eq. (6.57). We find

$$\begin{aligned}
 Q &= (\epsilon_0 + p_0) \frac{\exp(3\nu_0 + \lambda_0)}{r^2} \left[(\nu_0')^2 + \frac{2\nu_0'}{r} + \frac{1}{r^2} (\exp(2\lambda_0) - 1) \right] \\
 &= \frac{\exp(3\nu_0 + \lambda_0)}{r^2} \left[\frac{(p_0')^2}{\epsilon_0 + p_0} - \frac{4p_0'}{r} - \frac{8\pi G}{c^4} \exp(2\lambda_0) p_0 (\epsilon_0 + p_0) \right]. \tag{6.59}
 \end{aligned}$$

This is the form it is the easiest for us to evaluate Q , given that we have already found the equilibrium solution.

6.2.3 Finding the Eigenfrequencies of the Radial Perturbation

In this subsection, we treat Eq. (6.54) to show that neutron stars parameterised by central pressures larger than p_c' will be unstable with respect to radial perturbations. To start, we use our favourite technique to solve partial differential equations: Assuming separability. Specifically, we assume that we can write ζ as a product of one time dependent function $T = T(t)$ and one function dependent of the radial coordinate $u = u(r)$

$$\zeta(t, r) = T(t)u(r). \tag{6.60}$$

We substitute this into Eq. (6.54), with the goal of gathering all time dependence on one side of the equation, and all the radial dependence on the other. We find

$$\begin{aligned}
 W\ddot{T}u &= T [Pu']' + TQu \quad | \cdot \frac{1}{WTu} \\
 \frac{\ddot{T}}{T} &= \frac{[Pu']'}{Wu} + \frac{Q}{W} = -\omega^2. \tag{6.61}
 \end{aligned}$$

The last equality follows from the usual separability argument: One side is only dependent on t and the other is only dependent on r , and the equation holds for all t and r . We may conclude that each side is equal to a constant, which we have named $-\omega^2$. For T , this is a very familiar differential equation with the solution

$$T(t) = A_+ \exp(i\omega t) + A_- \exp(-i\omega t), \tag{6.62}$$

where A_+ and A_- are constants. This form of T enforces a constraint on the values of ω . If $-\omega^2 > 0$, ω becomes purely imaginary and T increases unboundedly as we let $t \rightarrow \infty$ and $t \rightarrow -\infty$. At some "largeness" of ζ , the first order perturbation analysis will break down. What happens to the star, we do not know, but we may conclude that the star is sensitive to slight radial perturbations, i.e.

it is unstable. As the differential equation governing ζ is a linear one, we must accept linear combination of solutions. A general perturbation will take the form

$$\zeta = \sum_{n=0}^{\infty} \zeta_n = \sum_{n=0}^{\infty} T_n(t) u_n(r), \quad (6.63)$$

where each T_n corresponds to one ω_n . Any real perturbation will contain contributions from each ζ_n . For a neutron star to be stable, we must therefore require that $-\omega_n^2 < 0$ for each n . Returning to Eq. (6.54) for one particular n , we divide it by T_n and substitute in $\ddot{T}_n/T_n = -\omega_n^2$. The resulting equation is only dependent on the radial coordinate r

$$[P u_n']' + [Q + W \omega_n^2] u_n = 0. \quad (6.64)$$

Equations of this form are called Sturm-Liouville equations, and ω_n^2 is called the eigenvalue of the eigenfunction or normal mode u_n . In order to give the Sturm-Liouville equation a unique solution, we need to impose two boundary conditions. We find the first condition from noting that the perturbations $\delta\epsilon$ and δp should be finite as $r \rightarrow 0$. Considering Eq. (6.38), we see that ξ must approach zero at least linearly for $r \rightarrow 0$ in order to avoid a divergence in $\delta\epsilon$. Thus, we may conclude that ζ , and hence u , must be proportional to r^3 for small r . The second boundary condition stems from the fact that the pressure vanishes where the star ends, at $R + \xi(t, R)$. This condition can be mathematically expressed as $p(R + \xi) = p_0(R) + \Delta p(t, R) = \Delta p(t, R) = 0$. This is equivalent to

$$\Delta p = \delta p + p_0' \frac{\exp(\nu_0)}{r^2} \zeta = -Z \zeta' = 0. \quad (6.65)$$

From these two considerations, we can write the boundary conditions for the Sturm-Liouville equation in terms of the u as

$$u(r) \propto r^3 \quad \text{when } r \rightarrow 0 \quad \text{and} \quad u'(R) = 0. \quad (6.66)$$

Sturm-Liouville problems are well known, and they have some key properties. The most useful to us is the Sturm-Liouville theorem [15], which states that the Eigenvalues come in a discrete sequence

$$\omega_0^2 < \omega_1^2 < \omega_2^2 < \dots, \quad (6.67)$$

each eigenvalue with a corresponding eigenfunction u_0, u_1, u_2, \dots . The eigenvalues do not have an upper bound, however, there exists a lower bound, which is ω_0^2 . An eigenfunction u_n has n zeros, also called nodes. This theorem is important, because we can use it to numerically approximate ω_n^2 and u_n by the help of the shooting method. The idea is to start by letting $u = r^3$ for when $\frac{r}{R}$ is very small. Then we calculate how u evolves by numerically evaluating Eq. (6.64) until we reach $r = R$. Having found a guess for u_n , we can count the number of nodes. If the number of nodes exceed n , we have guessed ω_n^2 to be too large. If the number of nodes are less than or equal to n , the guess for ω_n^2 was too small (or maybe exactly correct, if we are very lucky). Starting with a small ω_n and a large one, we know that the true solution lies in the interval between them. Then we use the bisection method until we have found a sufficiently small interval in which we know the true solution must lie. This is one of the methods for finding ω_n^2 and u_n listed in [13]. The shooting procedure is excellently explained in [1] (p. 165-166). As discussed above, a stable neutron star cannot have any unstable eigenmodes. Therefore, if we guess $\omega_0^2 = 0$, and we find n nodes for the numerically integrated u_0 , we know that there exist n unstable modes for the perturbations.

Next, we massage Eq. (6.54) into a form we can perform numeric calculations upon. We divide by P in

order to isolate u'' . The expression reads

$$\begin{aligned}
 u_n'' &= -\frac{P'}{P}u_n' - \frac{Q}{P}u_n - \omega_n^2 \frac{W}{P}u_n \\
 &= -\left\{ \frac{\gamma_0'}{\gamma_0} + \frac{p_0'}{p_0} + (3\nu_0' + \lambda_0') - \frac{2}{r} \right\} u_n' - \frac{1}{\gamma_0 p_0} \left[\frac{(p_0')^2}{\epsilon_0 + p_0} - \frac{4p_0'}{r} - \frac{8\pi G}{c^4} \exp(2\lambda_0) p_0 (\epsilon_0 + p_0) \right] u_n \\
 &\quad - \frac{\omega_n^2}{c^2} \frac{\epsilon_0 + p_0}{p_0 \gamma_0} \exp(2\lambda_0 - 2\nu_0) u_n \\
 &= -\left\{ \frac{\gamma_0'}{\gamma_0} + \frac{p_0'}{p_0} - \frac{3}{r} + \frac{\exp(2\lambda_0)}{r} + \frac{4\pi G}{c^4} \exp(2\lambda_0) r (3p_0 + \epsilon_0) \right\} u_n' \\
 &\quad - \frac{1}{\gamma_0 p_0} \left[\frac{(p_0')^2}{\epsilon_0 + p_0} - \frac{4p_0'}{r} - \frac{8\pi G}{c^4} \exp(2\lambda_0) p_0 (\epsilon_0 + p_0) \right] u_n - \frac{\omega_n^2}{c^2} \left(\frac{\partial \epsilon_0}{\partial p_0} \right) \exp(2\lambda_0 - 2\nu_0) u_n. \quad (6.68)
 \end{aligned}$$

Everything in the expression above are known quantities, except for the occurrence of γ_0' . We investigate how we can write γ_0' in terms of known expressions

$$\begin{aligned}
 \frac{d\gamma_0}{dr} &= \frac{d}{dr} \left(\frac{\epsilon_0 + p_0}{p_0} \frac{\partial p_0}{\partial \epsilon_0} \right) = \gamma_0 \left(\frac{\epsilon_0' + p_0'}{\epsilon_0 + p_0} - \frac{p_0'}{p_0} + \left(\frac{\partial p_0}{\partial \epsilon_0} \right)' \right) \\
 &= \gamma_0 \left(p_0' \frac{\frac{\partial \epsilon_0}{\partial p_0} + 1}{\epsilon_0 + p_0} - \frac{p_0'}{p_0} + p_0' \frac{\partial}{\partial p_0} \left(\frac{\partial p_0}{\partial \epsilon_0} \right) \frac{\partial \epsilon_0}{\partial p_0} \right), \quad (6.69)
 \end{aligned}$$

where we have used that $\frac{df(p_0)}{dr} = \frac{dp_0}{dr} \frac{\partial f(p_0)}{\partial p_0}$. Now, the rest is just a matter of substituting Eq. (6.69) into (6.68) and calculating $\frac{\partial \epsilon_0}{\partial p_0}$ and $\frac{\partial}{\partial p_0} \left(\frac{\partial p_0}{\partial \epsilon_0} \right)$ from the equation of state.

6.3 Stability of Ideal Neutron Stars

In this subsection, we apply the equations from the stability analysis to an ideal neutron star. In Section 4, we derived the equation of state and the expressions

$$\frac{\partial p_0}{\partial \epsilon_0} = \frac{x_F^2}{3(1 + x_F^2)}, \quad \text{and} \quad \frac{\partial}{\partial p_0} \frac{\partial p_0}{\partial \epsilon_0} = \frac{2}{3(\epsilon_0 + p_0)(1 + x_F^2)}. \quad (6.70)$$

With this we have everything we need to integrate u and count the number of nodes. We calculate the four lowest eigenfrequencies for ideal neutron stars parameterised by central pressures in the range $p_c \in [10^{31}, 10^{41.5}]$ Pa. In this range, we find that all the four lowest frequencies obtain negative values, as seen in Fig. 6.3.

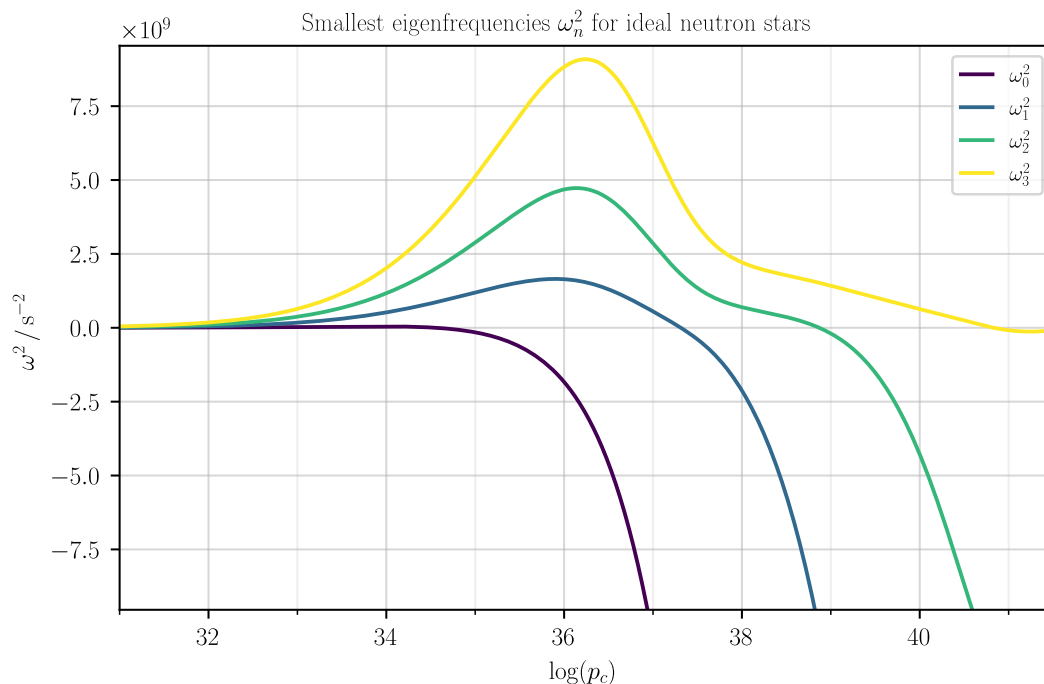


Figure 6.3: A display of the four lowest eigenfrequencies for ideal neutron stars. We see that for large enough central pressures, each frequency becomes negative, resulting in one additional unstable normal mode.

Here we get a rough idea of where the zeros for the eigenfrequencies lie. Next, we use the bisection method to find more accurately which central pressure yields $\omega_n^2 = 0$. For the four frequencies in the plotted in Figure 6.3, we find

- ω_0^2 at $p_c = 3.6 \times 10^{34}$ Pa,
- ω_1^2 at $p_c = 2.1 \times 10^{37}$ Pa,
- ω_2^2 at $p_c = 7.2 \times 10^{38}$ Pa,
- ω_3^2 at $p_c = 4.5 \times 10^{40}$ Pa.

With these values, we can re-plot the mass-radius curve for an ideal neutron star, colouring each segment after how many unstable normal modes which exist. An inspection of Fig. 6.4 reveals that the lowest normal mode becomes unstable at the maximum mass of the neutron star. This is in accordance with the qualitative argument we gave in Section 6.1. With this analysis, however, we get some additional information. From the figure, it seems that every time a new mode becomes unstable, the curve is at a local extremal value. We also see from Fig. 6.3 that for higher pressures, the squared eigenfrequencies which are already negative, drop quickly. This results in an even more unstable star, as the normal mode would grow more quickly as the time-coordinate grows.

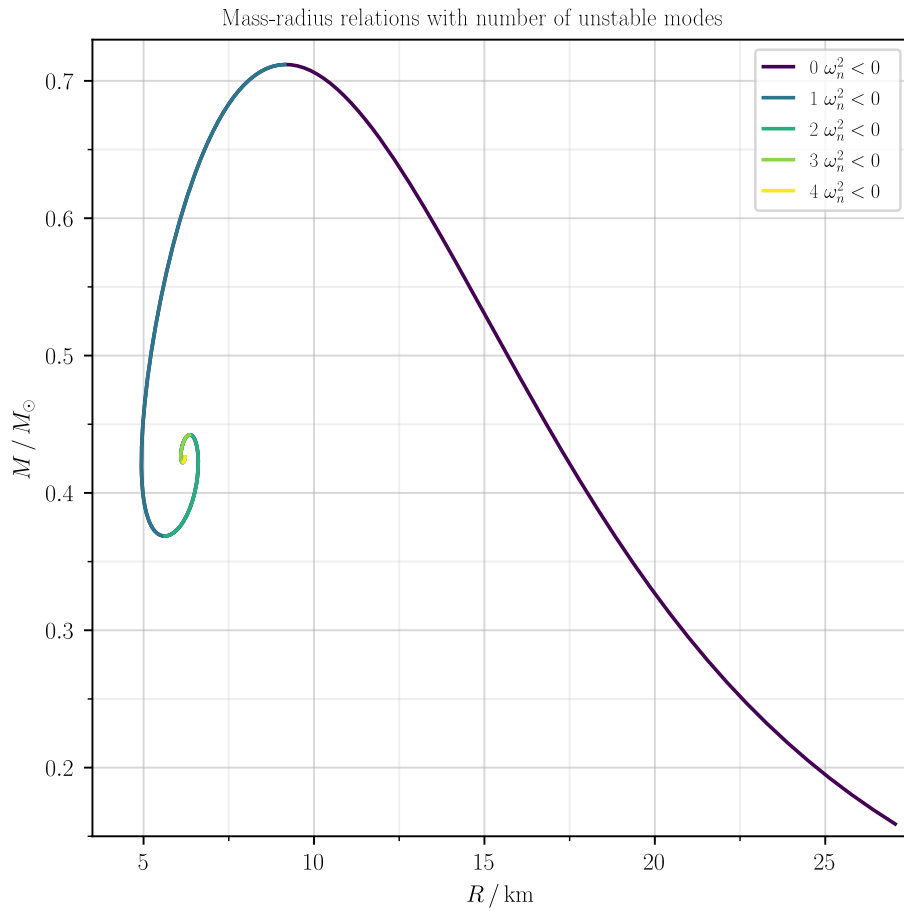


Figure 6.4: A plot of the mass-radius relations for ideal neutron stars in which the number of unstable modes are indicated on the graph. An unstable mode has an eigenfrequency $\omega_n^2 < 0$. As shown in Fig. 5.1, the central pressures increase as we follow the curve from its lower right end towards the spiral.

Summary and outlook

7.1 Summary

In this thesis, we started out from the theory of general relativity and relativistic fluid dynamics to derive the Tolman-Oppenheimer-Volkoff system of equations that governs spherically symmetric equilibrium stars. These three equations are:

- The TOV-equation, which describes the change of pressure with respect to the radial coordinate,
- the gravitational mass equation, which describes the gravitational mass inside a radius r , and
- the equation of state, which provides a relation between the energy density and the pressure.

With these equations, we can parameterise a sequence of stars by the central pressure. We have seen that the TOV-equation predicts an upper bound for the mass-radius ratio $\frac{M}{R} < \frac{4c^2}{9G}$, which is stricter than the limit imposed by the Schwarzschild radius.

To get some hands on experience with the TOV system of equations, we have derived the equation of state for cold non-interacting neutron matter through a statistical physics model for fermions. Although non-interacting, matter resists a gravitational collapse due to the degeneracy pressure. A star composed of such matter is called an ideal neutron star. Having solved the system of equation numerically, we found a maximal mass $M = 0.71M_{\odot}$, with the corresponding radius $R = 9.2\text{km}$. This reproduces the famous result found by Oppenheimer and Volkoff [9] as early as in 1939. To our dismay, astronomers have observed more massive neutron stars, which means that we must turn to another equation of state in hope to realistically describe neutron stars. Our efforts so far have not been in vain, however, as we can use the equations and numerical methods we have developed for the ideal neutron stars for more complex equations of state as well.

The final main topic we have treated in this thesis is stability analysis of neutron stars. Here we followed the idea of Chandrasekhar [12], who originally investigated the stability in 1964. We started by assuming a slight radial perturbation which induces slight perturbations in the energy density, the pressure and the metric functions. Throwing away all terms which were more than linear in the perturbations, we found a dynamic constraint for the radial displacement. Decomposing the radial displacement into normal modes with specific eigenfrequencies, we can find when a neutron star has one or more unstable normal modes. Such stars will be unstable and will not be observed. To apply the analysis to a specific problem, we turned again to the cold, non-interacting neutron model. We found that ideal neutron stars parameterised by central pressures larger than $3.6 \times 10^{34}\text{Pa}$ have at least one unstable normal mode and are unstable. This critical central pressure also parameterises the ideal neutron star of the maximum mass.

7.2 Outlook

We know from the discrepancy between the maximum mass of the ideal neutron star and the measured masses of real neutron stars that we need to improve our model into a more complex one. There are several ways to add more complexity to our model. One of them is to introduce rotation, breaking the spherical symmetry. Some neutron stars rotate rapidly, and this inclusion should be made to describe them realistically. A rotation would add new terms to the metric tensor, and the derivation of the TOV-equation would no longer hold. Solving the rotating system might yield exciting corrections for rotating stars.

We could also modify the non-rotating model by looking at other equations of state, allowing us to keep the TOV-system of equations. This is perhaps even more interesting than adding rotation, as the ideal equation of state suffers from several weaknesses which we can amend in this way. First of all, we know that neutrons undergo a process of inverse β decay through the process

$$n \rightarrow p + e^- + \bar{\nu}_e.$$

Taking this into consideration, we need to add a content of neutrons and electrons to the star. However, this correction actually *decreases* the maximum predicted mass [4] (pp.107-108). Although giving a more correct model, it might not be the correction we are looking for.

Secondly, we know that particles interact with each other, which modifies the relation between the energy density and the pressure. How would interactions quantitatively change the mass-radius relations? An example of how to model interactions is the $\sigma - \omega$ -model, or the Walecka-model [14]. In this model, we add a scalar particle σ and a vector particle ω_μ . These particles mediate the forces between the neutrons

Thirdly, the ideal neutron star model gives hints that there might be other phases of matter in the interior of the neutron star. We have seen that the pressure and energy density inside an ideal neutron star can be immensely large. They can, in fact, be so large that nucleons decompose into their quark constituents, so-called deconfinement. A star consisting of hadronic and quark matter is called a hybrid star. The possibility of deconfinement begs the question: How would a quark phase inside the neutron star affect the mass-radius relations? Another interesting question which arises in this regard is the transition from hadronic matter at the star surface where the energy density is low, to the deconfined quarks closer to the star centre. The simplest model would be a sudden change at some r in the interior of the star. But we could also investigate the possibility of a mixed phase, where hadronic matter coexists with quark matter. Will allowing for a gradual transition significantly change the mass-radius relation as compared to the abrupt transition? Quark deconfinement is another example of introducing more than one particle in the neutron star system.

Finally, we have so far been working with a cold star model, i.e. $T = 0$. After a neutron star is formed, it starts to cool down, as there is no more fusion reactions which produce energy. However, the interior of the star will remain warm for a long time. Will introducing finite temperature significantly modify the maximum mass?

The work done to solve the toy model of the ideal neutron stars paves the road to consider more advanced models of neutron stars. As there exists observational data on neutron stars, we can compare the observed neutron star masses to the predictions of the models we can perform calculations upon. If we predict a maximum mass less than the maximum observed mass, we know that we must modify the model to match observations. As exemplified above, there are several particles we can introduce to the neutron stars system in an attempt of getting better predictions. Adding too many of them will give a very complicated system. Which layers of complexity should we add to our neutron star model to give predictions which are consistent with the observed data? Trying to answer all these questions is a monumental task. In the second part of this document, the Master's thesis, we will look into hybrid stars, trying to figure out how different phase transitions affect the mass-radius relations.

Part II

Quark, Hybrid, and Unified Hybrid Stars with the Quark-Meson Model

Master's Thesis

Spring 2023

Introduction

In this thesis, we will study three types of compact stars: Two-flavour quark stars, hybrid stars, and hybrid stars with a unified equation of state. A quark star consists solely of quark matter, while a hybrid star is composed of a nuclear matter mantle and a quark core, see. Fig 8.1. In order to describe how matter inside these stars behaves, we will dive into quantum field theory at finite chemical potential. After this, we will ascend with an equation of state: An equation which relates the energy density and pressure. In particular, we will use the phenomenological quark-meson model to describe two-flavour quark matter. This will enable us to model quark stars – curious objects consisting only of quark matter, despite the fact that free quarks have never been observed in Nature. From there, we will move on to describe hybrid stars. We will use the Akmal-Pandharipande-Ravenhall equation of state [44] to model the nuclear matter. Approaching the core of the star, the energy density can grow large enough for the nuclear matter to turn into deconfined quarks, enabling us to use the quark-meson model in the hybrid star as well. Furthermore, we will discuss two different methods of bridging the nuclear and quark phases. The first way is to construct an abrupt transition from nuclear to quark matter, referred to as a first-order phase transition, while the latter is to introduce an interpolating phase between the two types of matter, referred to as a unified equation of state.

In the project thesis, we considered ideal neutron stars. We found that the ideal neutron star-description predicts an upper mass-limit of approximately $\sim 0.7M_{\odot}$. This is not large enough to match observational data of neutron stars. The models we discuss in this thesis take into account several particle species and interactions between them, making the models better at predicting neutron star properties. We shall see that the predicted maximum masses will land around $\sim 2M_{\odot}$, which is a large improvement over ideal neutron stars.

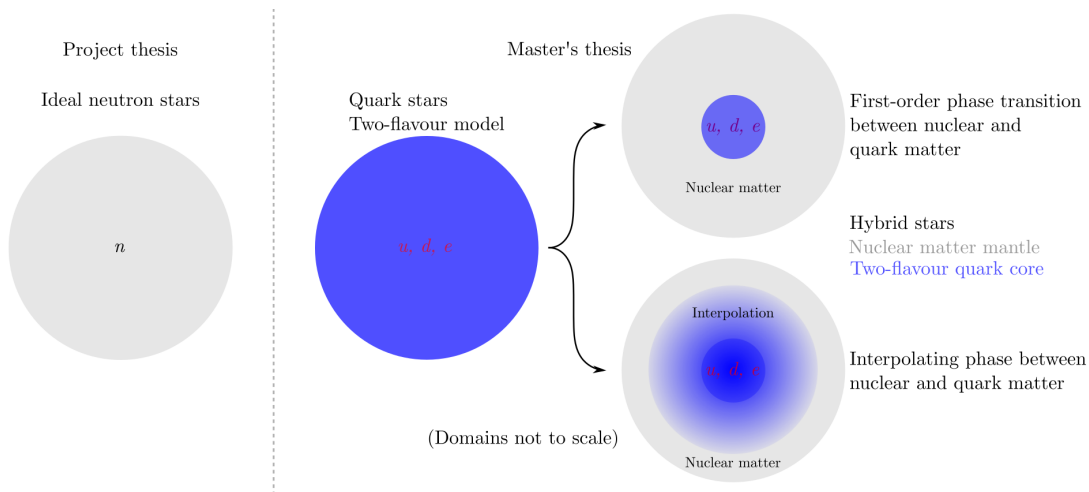


Figure 8.1: A schematic overview of the star models we discuss throughout this thesis. Neutrons are denoted by n , whereas u , d , and e refer to the up quark, down quark, and electron, respectively.

In the beginning, neutron stars were only available to us through theoretical physicists' calculations. Luckily for the astrophysically inclined, this changed after the first observation of a neutron star in 1967 [16]. Today, we have many observations of neutrons stars, and for some of them, we have precise measurements of masses and radii. This gives empirical data for us to test our theoretical models against. According to [17], the neutron stars' masses typically lie in the range $1.17M_{\odot}$ to $2.0M_{\odot}$, with the most common value being about $1.4M_{\odot}$. Observed radii typically lie between 9.9 km and 11.2 km. The observations of neutron stars come from radio, X-ray or gamma radiation from rapidly rotating neutron stars called pulsars. Examples of such observations are provided in Ref. [18]. Of all the observed pulsars, many of them are isolated. For these, we cannot measure the masses. However, some pulsars form binary systems. Based on the orbital motion of binary systems, it is possible to determine the masses of the stars orbiting each other. In particular, we are interested in the heaviest neutron stars, as these pose the strictest constraints on possible equations of state. Among the observations of heavy-weights, we find the massive star with the scientific-sounding name PSR J0348–0432 [19]. The observed mass of this pulsar is $2.01 \pm 0.04M_{\odot}$. This is not a lone outlier – there are other massive pulsars with masses around two solar masses. PSR J1614–2230 [20] is just behind with a mass of $1.97 \pm 0.04M_{\odot}$. Third and last of our heavy pulsar-examples is PSR J0952–0607 [21]. This is the heaviest known neutron star, and it ticks in at a whopping $2.35 \pm 0.17M_{\odot}$. Producing neutron stars as heavy as these three requires a very *stiff* equation of state, which qualitatively means that the matter can support itself from the pull of gravity by producing a large pressure.

To find masses and radii for compact star models, we integrate the TOV-equations, as we discussed in the project thesis. For completion, we re-state the equations with our new unit conventions

$$\frac{dp}{dr} = -\frac{GM(r)\epsilon(r)}{r^2} \left[1 + \frac{p(r)}{\epsilon(r)} \right] \left[1 + \frac{4\pi r^3 p(r)}{M(r)} \right] \left[1 - \frac{2GM(r)}{r} \right]^{-1}, \quad (8.1)$$

$$M(r) = \int_0^r dr' 4\pi r'^2 \rho(r') = \int_0^r dr' 4\pi r'^2 \epsilon(r'), \quad (8.2)$$

$$\epsilon = \epsilon(p). \quad (8.3)$$

The interesting question remains: Will the equations of state we discuss be able to predict maximum masses which lie in the interval of uncertainty for the heavy stars listed in the previous paragraph?

Chapter 9

Quantum Fields at Finite Chemical Potential

The ultimate goal of this thesis is, of course, calculating mass-radius relations for compact stars with the help of the TOV-equations. This chapter will be concerned with the third of them, Eq. (8.3), the equation of state. Specifically, the goal in this chapter is to derive thermodynamical quantities for particles described as fields. In the end, we will have developed a formalism into which we can insert the quark-meson model. In contrast to what we did in the project thesis, the framework we will develop here will be able to handle particle interactions, making it a better tool to find thermodynamical quantities. The strategy will be quite similar: We must identify the grand canonical partition function Θ . Through it, we will find the grand potential, from which we can derive the number density for each particle species, the total energy density, and the total pressure. The procedure we develop here, is what we refer to as quantum field theory (QFT) at finite chemical potential. Textbooks referring to thermal field theory (TFT) handle the same topic, however, we consider cold compact stars, $T = 0$, and are not focusing on the finite temperature corrections. Therefore, we say QFT at finite chemical potential instead of TFT. This chapter will be quite technical, but it does in no way attempt to be rigorous or comprehensive. For the reader who is familiar with this topic or who is only interested in compact stars, this chapter may be perused or skipped. This chapter is inspired by Ref. [22]. For a more thorough walkthrough of the quantum states, see Ref. [23].

9.1 Deriving Thermodynamical Quantities from the Grand Potential

First of all, we recall the relations from statistical physics which we will need. The grand canonical partition function Θ is defined as

$$\Theta = \sum \exp(\beta\mu_i N_i - \beta H), \quad (9.1)$$

where the sum goes over all configurations and all particle numbers N_i . The subscript i enumerates the particle species. In the thermodynamic limit, we find that the grand canonical partition function [24] (p. 119) can be written

$$\Omega V = -k_B T \ln(\Theta) = E - TS - \sum_i \mu_i N_i = -pV. \quad (9.2)$$

Ω denotes the *grand potential*. From the grand potential, or equivalently $\ln(\Theta)$, we can derive all the thermodynamic quantities we are interested in. We note that the grand partition function is a function of the chemical potentials μ_i and the temperature T , namely $\Theta = \Theta(\mu_i, T)$. To find the pressure p , we can simply divide both sides of Eq. (9.2) by V . Secondly, to calculate the particle numbers, N_i , we can perform a partial differentiation with respect to μ_i . Thirdly, we perform a partial differentiation with

respect to T in order to express the entropy, S , in terms of Θ . Written out explicitly, we have

$$p = \frac{k_B T \ln(\Theta)}{V} = \frac{\ln(\Theta)}{\beta V} = -\Omega, \quad (9.3)$$

$$n_i = \frac{N_i}{V} = \frac{k_B T}{V} \frac{\partial \ln(\Theta)}{\partial \mu_i} = \frac{1}{\beta V} \frac{\partial \ln(\Theta)}{\partial \mu_i} = -\frac{\partial \Omega}{\partial \mu_i}, \quad (9.4)$$

$$s = \frac{S}{V} = \frac{1}{V} \frac{\partial (k_B T \ln(\Theta))}{\partial T} = \frac{k_B}{V} \ln(\Theta) + \frac{k_B T}{V} \frac{\partial \ln(\Theta)}{\partial T} = \frac{1}{\beta V} \left(\frac{\ln(\Theta)}{T} + \frac{\partial \ln(\Theta)}{\partial T} \right). \quad (9.5)$$

In all of the lines above, we have introduced $\beta = \frac{1}{k_B T}$. We have also chosen to express the densities instead of the extensive quantities by dividing by the volume. The last line states the entropy volume density s , which we can use to express the energy density $\epsilon = \frac{E}{V}$. We isolate E in Eq. (9.2), divide by V and eliminate s by substituting in Eq. (9.5). This procedure yields

$$\begin{aligned} \epsilon &= -\frac{k_B T}{V} \ln(\Theta) + \frac{k_B T}{V} \left(\ln(\Theta) + T \frac{\partial \ln(\Theta)}{\partial T} \right) + \sum_i \mu_i n_i = \frac{k_B T^2}{V} \frac{\partial \ln(\Theta)}{\partial T} + \sum_i \mu_i n_i \\ &= -\frac{1}{V} \frac{\partial \ln(\Theta)}{\partial \beta} + \sum_i \frac{\mu_i}{\beta V} \frac{\partial \ln(\Theta)}{\partial \mu_i} = \frac{\partial(\beta \Omega)}{\partial \beta} - \sum_i \mu_i \frac{\partial \Omega}{\partial \mu_i}. \end{aligned} \quad (9.6)$$

In the first to the second line, we have eliminated the number densities n_i by substituting in Eq. (9.4). Having expressed both ϵ and p , in terms of the grand potential, the next task is to identify the grand potential.

9.2 The Grand Canonical Partition Function from a Quantum Field Theory Description

We will derive the partition function both for bosons and fermions in terms of a path integral. In the project thesis, we did not explicitly treat the particles as quantum states. The quantum pressure arose from simply imposing the Fermi exclusion principle. Now, we will start from quantum states and physical observables as operators – a proper quantum treatment. We will quickly recapitulate some relations from quantum mechanics before we look at the corresponding relations in a quantum field theory.

From quantum mechanics, we are familiar with promoting observables to operators, and calculating their expectation values. When we perform many experiments, we expect averaging over the measurements to yield the same results as the calculated expectation values. The expectation value of an operator $\hat{\mathcal{O}}$ for a state $|\psi\rangle$ reads

$$\langle \mathcal{O} \rangle_\psi = \langle \psi | \hat{\mathcal{O}} | \psi \rangle. \quad (9.7)$$

We are looking for the grand canonical partition function, which means we wish to calculate the expectation value for $\exp(\mu_i \hat{N}_i - \beta \hat{H})$ over all states, as seen from the classical equivalent in Eq. (9.1). We write

$$\Theta = \text{Tr} [\hat{\Theta}] = \text{Tr} \left[\exp(\beta \mu_i \hat{N}_i - \beta \hat{H}) \right] = \sum_\psi \langle \psi | \exp(\beta \mu_i \hat{N}_i - \beta \hat{H}) | \psi \rangle. \quad (9.8)$$

The sum over ψ goes over all states. Before we can tackle this expression, we need to develop some understanding of quantum fields. We start by looking at some standard quantum mechanics for particles, before we motivate how the theory carries over to fields.

As physical quantities are described by operators and not numbers, their ordering is of great importance as they no longer commutes in general. If we let q_n be the coordinate degrees of freedom in our system described by a Lagrangian $L = L(q_n, \dot{q}_n)$, we know from classical mechanics that we define the canonical momentum p_n as

$$p_n = \frac{\partial L}{\partial \dot{q}_n}. \quad (9.9)$$

After we promote the coordinates and momenta to operators, $q_n \rightarrow \hat{q}_n$ and $p_n \rightarrow \hat{p}_n$, they do no longer commute. Instead we impose the following commutation relations

$$[\hat{q}_n, \hat{q}_m] = [\hat{k}_n, \hat{k}_m] = 0 \quad \text{and} \quad [\hat{q}_n, \hat{k}_m] = i\delta_{nm}, \quad (9.10)$$

where the δ_{nm} is an element of the identity matrix, also called the Kronecker δ . These are called the canonical commutation relations.

The position operators \hat{q}_n and momentum operators \hat{p}_n have eigenstates $|q_1, \dots, q_n, \dots\rangle$ and $|p_1, \dots, p_n, \dots\rangle$, such that

$$\hat{q}_n |q_1, \dots, q_n, \dots\rangle = q_n |q_1, \dots, q_n, \dots\rangle \quad \text{and} \quad \hat{p}_n |p_1, \dots, p_n, \dots\rangle = p_n |p_1, \dots, p_n, \dots\rangle. \quad (9.11)$$

For simplicity, we will now write an eigenstate for a collection of particles with coordinates q_n simply as q , which means that $|q_1, \dots, q_n, \dots\rangle \equiv |q\rangle$. The coordinate eigenstates are orthonormal and form a complete set. Let $|q\rangle$ and $|q'\rangle$ be two coordinate vectors. Orthonormality and completeness can be written as

$$\langle q|q'\rangle = \langle q_1, \dots, q_n, \dots|q'_1, \dots, q'_n, \dots\rangle = \prod_m \delta(q_m - q'_m) \equiv \delta(q - q'), \quad (9.12)$$

$$\mathbb{1} = \int dq |q\rangle\langle q| = \int dq_1 \dots dq_n \dots |dq_1, \dots, dq_n, \dots\rangle\langle dq_1, \dots, dq_n, \dots|. \quad (9.13)$$

$\mathbb{1}$ denotes the identity operator. As the next step towards a path integral description, we must figure out how to calculate the inner product of the canonical coordinates, $\langle q|p\rangle$. This we can do using only the canonical commutation relations given in Eq. (9.10). To do so, we start by acting on a state $|q\rangle$ with the operator $\exp(i\epsilon\hat{p})$ and investigate how $|q\rangle$ changes. When we omit the subscript on \hat{p} , it means that it is acting on every component p_m in $|p\rangle$.

$$\hat{q}_m \exp(i\epsilon\hat{p}) |q\rangle = \hat{q}_m \sum_{n=0}^{\infty} \frac{(i\epsilon\hat{p})^n}{n!} |q\rangle. \quad (9.14)$$

Here, we have simply written the exponential the way it is defined. We know the commutation relation between \hat{q}_n and \hat{p}_i , which means that we can move \hat{q}_m to the right in order for it to act upon the state $|q\rangle$. To make the calculation easy to see, we perform it for one particular $n \geq 1$.

$$\begin{aligned} \hat{q}_m \frac{(i\epsilon\hat{p})^n}{n!} |q\rangle &= \frac{(i\epsilon)^n}{n!} \hat{q}_m \hat{p}^n |q\rangle = \frac{(i\epsilon)^n}{n!} ([\hat{q}_m, \hat{p}] \hat{p}^{n-1} + \hat{p} \hat{q}_m \hat{p}^{n-1}) |q\rangle \\ &= \dots = \frac{(i\epsilon)^n}{n!} (in\hat{p}^{n-1} + q_m \hat{p}^n) |q\rangle = \left(i^2 \epsilon \frac{(i\epsilon\hat{p})^{n-1}}{(n-1)!} + q_m \frac{(i\epsilon\hat{p})^n}{n!} \right) |q\rangle. \end{aligned} \quad (9.15)$$

Above, we have consistently moved \hat{q}_m to the right, until it acts on $|q\rangle$ and produced a scalar q_m . Once for each \hat{p} , we get a term of $i\hat{p}^{n-1}$ due to the canonical commutation relation. In total, n such terms arise. For $n = 1$, we trivially get $\hat{q}_m |q\rangle = q_m |q\rangle$. If we again consider the sum over n , we arrive at

$$\hat{q}_m \exp(i\epsilon\hat{p}) |q\rangle = \sum_{n=0}^{\infty} \left(q_m \frac{(i\epsilon\hat{p})^n}{n!} - \epsilon \frac{(i\epsilon\hat{p})^n}{n!} \right) |q\rangle = (q_m - \epsilon) \exp(i\epsilon\hat{p}) |q\rangle. \quad (9.16)$$

We see that the state $\exp(i\epsilon\hat{p}) |q\rangle$ is an eigenstate of \hat{q}_m , but compared to $|q\rangle$, the eigenvalue is shifted from $q_m \rightarrow q_m - \epsilon$. If we change the sign in the exponential operator, we get a positive shift. These two facts allow us to write

$$\begin{aligned} \exp(-i\epsilon\hat{p}) |q\rangle &= |q + \epsilon\rangle, \quad \text{and thus} \\ \langle q + \epsilon| &= |q + \epsilon\rangle^\dagger = (\exp(-i\epsilon\hat{p}) |q\rangle)^\dagger = \langle q| \exp(i\epsilon\hat{p}). \end{aligned} \quad (9.17)$$

We can remove the dagger from \hat{p} in the last equality, because \hat{p} is an Hermitian operator. Expressing a shift in $|q\rangle$ in this way is very useful, as it allows us to write down a differential equation for the inner product, using the definition of the derivative operator

$$\begin{aligned} \frac{\partial}{\partial q} \langle q|p\rangle &= \lim_{\epsilon \rightarrow 0} \frac{\langle q + \epsilon|p\rangle - \langle q|p\rangle}{\epsilon} = \lim_{\epsilon \rightarrow 0} \frac{\langle q| \exp(i\epsilon\hat{p}) - 1 |p\rangle}{\epsilon} = \lim_{\epsilon \rightarrow 0} \langle q| i\hat{p} + \mathcal{O}(\epsilon) |p\rangle \\ &= ip \langle q|p\rangle. \end{aligned} \quad (9.18)$$

This is a simple differential equation with an exponential solution. We can write

$$\langle q|p\rangle = \exp(ip \cdot q) = \prod_n \exp(ip_n q_n), \quad \text{which implies} \quad (9.19)$$

$$\langle p|q\rangle = \exp(-ip \cdot q) = \prod_n \exp(-ip_n q_n). \quad (9.20)$$

The second line follows from the inner product property $\langle q|p\rangle = \langle p|q\rangle^\dagger$. Next, we can investigate whether we can construct an identity operator from the outer product of $|p\rangle$ states.

$$\int dp |p\rangle\langle p| = \int dq dq' dp |q\rangle \langle q|p\rangle \langle p|q'\rangle \langle q'| = \int dq dq' dp \exp(ip \cdot (q - q')) |q\rangle\langle q'|. \quad (9.21)$$

We recognise the integral over p combined with the exponential as the Fourier representation of the Dirac δ -function. Using this, the expression above takes a simpler form

$$\int dp |p\rangle\langle p| = \int dq dq' 2\pi \delta(q - q') |q\rangle\langle q'| = 2\pi \int dq |q\rangle\langle q| = 2\pi. \quad (9.22)$$

This is a nice result, as it shows us that we can write the identity operator also in the form of an outer product of $|p\rangle$. It reads

$$\mathbb{1} = \int \frac{dp}{2\pi} |p\rangle\langle p|. \quad (9.23)$$

So far, we have been dealing with a collection of coordinates $q = q_1, \dots, q_n, \dots$. An example of such a system which is easy to visualise, is to let each coordinate q_n describe to the displacement of a particle situated at location $n\Delta x$ along a spatial axis x . All the coordinates constitute a string of particles. The mass of the string is distributed among massive point particles. A continuous string would be the corresponding field to this discrete system. Here, the mass of the string is distributed along line segments with a certain mass density. If we imagine adding more coordinates to the collection q while keeping the length and total mass of the string fixed, the massive points of the string will lie closer and closer as well as becoming lighter and lighter. This will make the string resemble a continuous string when the particles lie close enough to each other. Fig. 9.1 illustrates this string system. Naturally, this model is also possible to imagine in dimension $D > 1$. For particles living in space, we imagine this model where q_n is replaced by q_{n_i} , where $i = 1, 2, 3$. A discussion of going to discrete to continuum may be found in Ref. [25], chapter 1, where also the bosonic path integral is derived. Notationally, we can go from the discrete system with coordinates labelled by n to a field by letting the coordinates be denoted by a continuous index, e.g x . We will omit the vector notation \vec{x} , but x may be thought of as a three dimensional vector. We will be explicit about dimension in the measure d^3x . We now also change the notation away from q to distinguish that we are dealing with fields. The results above carries over to the continuous limit

$$\hat{q}_n \rightarrow \hat{\phi}(x) \quad \text{and thus} \quad \hat{\phi}(x) |\phi\rangle = \phi(x) |\phi\rangle, \quad (9.24)$$

$$\hat{p}_n \rightarrow \hat{\pi}(x) \quad \text{and thus} \quad \hat{\pi}(x) |\pi\rangle = \pi(x) |\pi\rangle. \quad (9.25)$$

The commutation relations change only slightly

$$\left[\hat{\phi}(x), \hat{\phi}(y) \right] = \left[\hat{\pi}(x), \hat{\pi}(y) \right] = 0 \quad \text{and} \quad \left[\hat{\phi}(x), \hat{\pi}(y) \right] = i\delta(x - y). \quad (9.26)$$

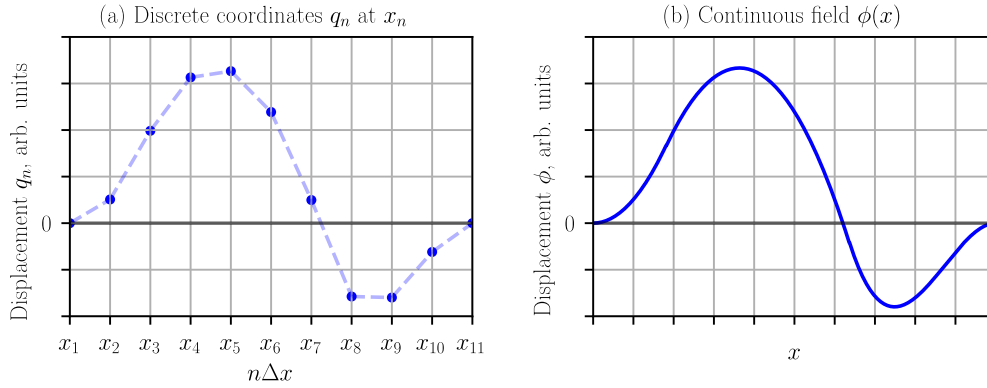


Figure 9.1: (a) illustrates a collection of $N = 11$ particles situated at $x_n = n\Delta x$. Each particle has some displacement, described by q_n . The string of particles has a total length of $L = N\Delta x$ and a total mass $M = mN$, where m is the mass of each particle. Keeping L and M fixed while we let $N \rightarrow \infty$, we can imagine the discrete string assumes the shape of a continuous string, as illustrated in (b). In this case, each line segment has a mass density.

The discrete Kronecker δ_{mn} has turned into its continuous cousin, the Dirac $\delta(x - y)$. In particular, we also have

$$\langle \phi | \pi \rangle = \exp \left(i \int d^3x \phi(x) \pi(x) \right). \quad (9.27)$$

The Lagrangian for fields is calculated as the spatial integral of the Lagrangian density, $\hat{L} = \int d^3x \hat{\mathcal{L}}$. The Hamiltonian is calculated similarly $\hat{H} = \int d^3x \hat{\mathcal{H}}$. The same goes for the particle number \hat{N} . With these notions from going from discrete quantum mechanics to a continuum, we have developed what we need to tackle Eq. (9.8) for fields by the help of the path integral.

9.2.1 Grand Partition Function for Bosons

Particles with spin 0, e.g. the Higgs boson, and with spin 1, e.g. the force mediating particles as photons and gluons, are bosons. This means that when we treat them quantum mechanically, we impose the commutation relations as written down above. Next, we assume that both $\hat{N}_i = \int d^3x \hat{\mathcal{N}}_i$ and $\hat{H} = \int d^3x \hat{\mathcal{H}}$ can be written as functions of field operators and the canonical momenta, namely that

$$\hat{\mathcal{N}}_i = \hat{\mathcal{N}}_i(\hat{\phi}, \hat{\pi}), \quad (9.28)$$

$$\hat{\mathcal{H}} = \hat{\mathcal{H}}(\hat{\phi}, \hat{\pi}). \quad (9.29)$$

In addition, we assume that these operators are ordered in such a way that all the field operators $\hat{\phi}$ stand to the left, and all the momentum operators are to the right. This is called Weyl-ordering. In the classical case, we can choose the ordering of the fields freely. This means that when we quantise, there is an ambiguity to the ordering of the operators. Here, we have made a choice. Thirdly, we let the fields vary with β . By this, we mean that

$$\hat{\phi}(x) |\phi(\beta)\rangle = \phi(x, \beta) |\phi(\beta)\rangle, \quad (9.30)$$

and similarly for $|\pi\rangle$. We allow the states to evolve with β , which corresponds to the Heisenberg picture for time dependent states. Next, we perform a "trick" to calculate Θ as given in Eq. (9.8): We partition β into N pieces

$$\beta = \Delta\beta N = \sum_{n=1}^N \Delta\beta. \quad (9.31)$$

This partitioning of β into a sum of small $\Delta\beta$ is necessary for us to do an expansion of $\exp(\Delta\beta(\mu_i\hat{N}_i - \hat{H}))$ into orders of $\Delta\beta$. This exponential operator will appear quite a few times later, so it is advantageous to give it its own operator symbol. We define

$$\Delta\hat{\Theta} \equiv \exp(\Delta\beta\{\mu_i\hat{N}_i - \hat{H}\}) \quad (9.32)$$

$$= \exp\left(\Delta\beta \int d^3x \{\mu_i\hat{\mathcal{N}}_i - \hat{\mathcal{H}}\}\right) \quad (9.33)$$

$$= 1 + \Delta\beta \int d^3x (\mu_i\hat{\mathcal{N}}_i - \hat{\mathcal{H}}) + \mathcal{O}((\Delta\beta)^2). \quad (9.34)$$

If we keep β fixed and letting $N \rightarrow \infty$, we can throw away higher orders of $\Delta\beta$, as they turn smaller and smaller. To give the above operator some interpretation, we may compare it to the quantum mechanical propagator. In quantum mechanics, we describe how a state $|\psi\rangle$ evolves in time by applying the propagator $\exp(-i\hat{H}t)$. A state at a time $t > t_0$ is calculated by

$$|\psi(t)\rangle = \exp(-i\hat{H}(t - t_0)) |\psi_i(t_0)\rangle. \quad (9.35)$$

Comparing the propagation operator to Eq. (9.32), we may interpret $\Delta\hat{\Theta}$ as a "grand canonical propagator". The Hamiltonian with a negative sign $-H$ is replaced with the $\mu_i N_i - H$, which also takes into account the energy contribution from the particle number. We also have the replacement $it \rightarrow \Delta\beta$. This allows us to think of $\Delta\beta$ as a curious "time step" of imaginary value. Thus, applying $\Delta\hat{\Theta}$ to a position state $|\phi(\beta_i)\rangle$, may be interpreted as evolving the parameter β_i to $\beta_i + \Delta\beta$.

Returning to the expansion of $\Delta\hat{\Theta}$ in Eq. (9.34): The exponential operator simplifies to just two terms: the identity and one term linear in \hat{N}_i and \hat{H} . This, in combination with inserting identities Eqs. (9.13) and (9.23) for the fields and finally the inner product Eq. (9.27), allows us to derive the path integral in thermal field theory. We let $|\psi\rangle$ be some state we sum over in the trace of $\hat{\Theta}$.

$$\begin{aligned} & \langle\psi| \exp\left(\beta \int d^3x \{\mu_i\hat{\mathcal{N}}_i(\hat{\phi}, \hat{\pi}) - \hat{\mathcal{H}}(\hat{\phi}, \hat{\pi})\}\right) |\psi\rangle && \text{(Split } \beta \text{ into } N \text{ pieces of } \Delta\beta) \\ &= \langle\psi| \exp\left(\Delta\beta \int d^3x \{\mu_i\hat{\mathcal{N}}_i - \hat{\mathcal{H}}\} + \dots + \Delta\beta \int d^3x \{\mu_i\hat{\mathcal{N}}_i - \hat{\mathcal{H}}\}\right) |\psi\rangle \\ &= \langle\psi| \exp\left(\Delta\beta \int d^3x \{\mu_i\hat{\mathcal{N}}_i - \hat{\mathcal{H}}\}\right) \dots \exp\left(\Delta\beta \int d^3x \{\mu_i\hat{\mathcal{N}}_i - \hat{\mathcal{H}}\}\right) |\psi\rangle && \text{(apply Eq. (9.33))} \\ &= \langle\psi| \Delta\hat{\Theta} \dots \Delta\hat{\Theta} |\psi\rangle. \end{aligned} \quad (9.36)$$

So far, we have simply written the original exponential operator as a product of the operator $\Delta\hat{\Theta}$. The next step is to start inserting identities between each of the N different $\Delta\hat{\Theta}$ operators. To the left, we insert $\int d\phi |\phi\rangle\langle\phi|$, and to the right, we insert $\int \frac{d\pi}{2\pi} |\pi\rangle\langle\pi|$.

$$\begin{aligned} & \langle\psi| (\Delta\hat{\Theta})^N |\psi\rangle \\ &= \int d\phi_1 \dots d\phi_N \frac{d\pi_1}{2\pi} \dots \frac{d\pi_N}{2\pi} \left\{ \langle\psi|\phi_1\rangle \langle\phi_1| \Delta\hat{\Theta} |\pi_1\rangle \langle\pi_1|\phi_2\rangle \langle\phi_2| \dots |\pi_{N-1}\rangle \langle\pi_{N-1}|\phi_N\rangle \langle\phi_N| \Delta\hat{\Theta} |\pi_N\rangle \langle\pi_N|\psi\rangle \right\}. \end{aligned} \quad (9.37)$$

The line above is quite a beast, but we can treat one term at a time. At first, we notice that we have obtained N terms of inner products between momentum states and field states. These we know from Eq. (9.27).

$$\langle\pi_n|\phi_{n+1}\rangle = \exp\left(-i \int d^3x \pi_n(x)\phi_{n+1}(x)\right). \quad (9.38)$$

In Eq. (9.37) we also find N occurrences of terms on the form $\langle\phi_n| \Delta\hat{\Theta} |\pi_n\rangle$. To express these differently, we make use of the expansion of $\Delta\hat{\Theta}$ in Eq. (9.34). In addition, we need to use the assumptions on Eqs.

(9.28) and (9.29) and the Weyl ordering. With these assumptions, we are allowed to let the operators \hat{N}_i and $\hat{\mathcal{H}}$ act on $\langle\phi_n|$ and $|\pi_n\rangle$. Thus, we may rid ourselves of the operators in favour for their eigenvalues of the fields and the momenta.

$$\begin{aligned}
 \langle\phi_n|\Delta\hat{\Theta}|\pi_n\rangle &= \langle\phi_n|1 + \Delta\beta \int d^3x \left\{ \mu_i \hat{N}_i(\hat{\phi}, \hat{\pi}) - \hat{\mathcal{H}}(\hat{\phi}, \hat{\pi}) \right\} |\pi_n\rangle + \mathcal{O}((\Delta\beta)^2) \\
 &= \langle\phi_n|\pi_n\rangle \left(1 + \Delta\beta \int d^3x \left\{ \mu_i \mathcal{N}_i(\phi_n, \pi_n) - \mathcal{H}(\phi_n, \pi_n) \right\} \right) + \mathcal{O}((\Delta\beta)^2) \\
 &= \exp\left(i \int d^3x \pi_n \phi_n \right) \exp\left(\Delta\beta \int d^3x \left\{ \mu_i \mathcal{N}_i(\phi_n, \pi_n) - \mathcal{H}(\phi_n, \pi_n) \right\} \right) + \mathcal{O}((\Delta\beta)^2) \\
 &= \exp\left(\int d^3x \left\{ i\pi_n \phi_n + \Delta\beta \mu_i \mathcal{N}_i(\phi_n, \pi_n) - \Delta\beta \mathcal{H}(\phi_n, \pi_n) \right\} \right) + \mathcal{O}((\Delta\beta)^2). \tag{9.39}
 \end{aligned}$$

In going from the second to the third equality, we have used Eqs. (9.27) and (9.34) to rewrite the multiple terms as one exponential. This only introduces an error on the order of $\mathcal{O}((\Delta\beta)^2)$. From now on we will omit writing $\mathcal{O}((\Delta\beta)^2)$ as we will let $N \rightarrow \infty$ in the end, rendering those terms unimportant. The last terms we need to calculate are $\langle\psi|\phi_1\rangle$ and $\langle\pi_N|\psi\rangle$. In calculating Θ , we are interested in taking the trace over $\hat{\Theta}$. This means that we sum over all external states, which in the case for fields means that we introduce an integral over ψ . If now rename $\psi \rightarrow \phi_{N+1}$, we see that we may write the curly brackets of Eq. (9.37) as one product from $n = 1$ to $n = N$. Using these relations, the calculation proceeds as

$$\begin{aligned}
 &\int d\phi_{N+1} \langle\phi_{N+1}|(\Delta\hat{\Theta})^N|\phi_{N+1}\rangle \\
 &= \int d\phi_{N+1} \prod_{n=1}^N \left[d\phi_n \left(\frac{d\pi_n}{2\pi} \right) \right] \langle\phi_{N+1}|\phi_1\rangle \prod_{n=1}^N \left(\langle\phi_n|\Delta\hat{\Theta}|\pi_n\rangle \langle\pi_n|\phi_{n+1}\rangle \right) \\
 &= \int d\phi_{N+1} \delta(\phi_{N+1} - \phi_1) \prod_{n=1}^N \left\{ \left[d\phi_n \left(\frac{d\pi_n}{2\pi} \right) \right] \exp\left(\int d^3x i\pi_n \phi_n + \Delta\beta [\mu_i \mathcal{N}_i(\phi_n, \pi_n) - \mathcal{H}(\phi_n, \pi_n)] \right) \right. \\
 &\quad \left. \exp\left(- \int d^3x i\pi_n \phi_{n+1} \right) \right\} \\
 &= \int_{\phi_{N+1}=\phi_1} \prod_{n=1}^N \left\{ \left[d\phi_n \left(\frac{d\pi_n}{2\pi} \right) \right] \exp\left(\Delta\beta \int d^3x \mu_i \mathcal{N}_i(\phi_n, \pi_n) - i\pi_n \frac{\phi_{n+1} - \phi_n}{\Delta\beta} - \mathcal{H}(\phi_n, \pi_n) \right) \right\} \\
 &= \int_{\phi_{N+1}=\phi_1} \left[\prod_{n=1}^N d\phi_n \left(\frac{d\pi_n}{2\pi} \right) \right] \exp\left(\Delta \sum_{n=1}^N \beta \int d^3x \mu_i \mathcal{N}_i(\phi_n, \pi_n) - i\pi_n \frac{\phi_{n+1} - \phi_n}{\Delta\beta} - \mathcal{H}(\phi_n, \pi_n) \right). \tag{9.40}
 \end{aligned}$$

Quite a few things happened in the lines above. Notably, we used the field equivalent of Eq. (9.12) to obtain the δ -function. Integrating this out identifies ϕ_{N+1} to ϕ_1 , which we have indicated by the subscript under the integral sign. This is the same as imposing *periodic boundary conditions*. This is important: The bosonic path integral in thermal field theory is periodic. Keeping β fixed and letting $N \rightarrow \infty$ we also let $\Delta\beta \rightarrow 0$, which sends the error $\mathcal{O}((\Delta\beta)^2) \rightarrow 0$. We also see that we can rewrite the middle term in the exponential

$$\lim_{\Delta\beta \rightarrow 0} -i\pi_n \frac{\phi_{n+1} - \phi_n}{\Delta\beta} = i\pi_n \dot{\phi}_n. \tag{9.41}$$

The dot over $\dot{\phi}$ now denotes the derivative with respect to β . Note that the sign changes in the last equality, as β increases with smaller n . Had we reversed the numbering of the identities we inserted, we would not have changed the sign. Now we are at the point when things get really interesting. We take

the continuum limit, and find

$$\prod_{n=1}^{\infty} d\phi_n \xrightarrow{\text{continuum}} \mathcal{D}\phi, \quad (9.42)$$

$$\prod_{n=1}^{\infty} \frac{d\pi_n}{2\pi} = \prod_{n=1}^{\infty} \bar{d}\pi_n \xrightarrow{\text{continuum}} \mathcal{D}\pi, \quad (9.43)$$

$$\exp\left(\Delta\beta \sum_{n=1}^N \int d^3x \left\{ \dots \right\}\right) \xrightarrow{\text{continuum}} \exp\left(\int_0^\beta d\beta \int d^3x \left\{ \dots \right\}\right). \quad (9.44)$$

Two remarks about the above limits are in order. Firstly, we have introduced a slash-notation in the differential, i.e. $\bar{d}, \bar{\mathcal{D}}$. By this, we simply mean that we absorbed a factor of $\frac{1}{2\pi}$ into each degree of freedom, saving us some writing. Sometimes, the bar in \bar{d} is difficult to spot. If there is suspicion of whether factors of $\frac{1}{2\pi}$ are missing, have an extra look at the differentials! Secondly, had we used the substitution $\tau = -i/\beta$, we get exactly the shape of the path integral in QFT, with the exception that we are integrating imaginary time. Combining our result so far, we may compactly write

$$\begin{aligned} \Theta &= \text{Tr}(\hat{\Theta}) \\ &= \oint \mathcal{D}\phi \bar{\mathcal{D}}\pi \exp\left(\int_0^\beta d\beta \int d^3x \mu_i \mathcal{N}_i(\phi, \pi) + i\pi\dot{\phi} - \mathcal{H}(\phi, \pi)\right) \end{aligned} \quad (9.45)$$

This is a path integral. Now ϕ does no longer denote a single ϕ_n -state, but it denotes all the degrees of freedom, which in the countable case corresponds to the collection $\{\phi_n\}_{n=1}^{\infty}$. Taking this to the continuous limit, it means that $\phi = \{\phi_\beta\}$, where β varies continuously. The same goes for π . We have also indicated that this is a closed loop integral, as a consequence of the periodic boundary.

A path integral is a quite lofty concept, so how may one think of it? Qualitatively, we have a field in some start configuration, and as β evolves, the field configuration changes. In the end, we find with the same configuration we started with, due to the periodic boundary condition we stated earlier. For one particular evolution of $\phi(\beta)$ and $\pi(\beta)$, the exponential in Eq. (9.45) returns a weight for that particular configuration. The path integral returns us the sum of all these weights. When we integrate, we sum over all the different paths ϕ and π may take as we evolve the parameter β . We have illustrated a discrete partitioning of an interval β and their continuous equivalent in Fig. 9.2, to try to visualise the continuum transition.

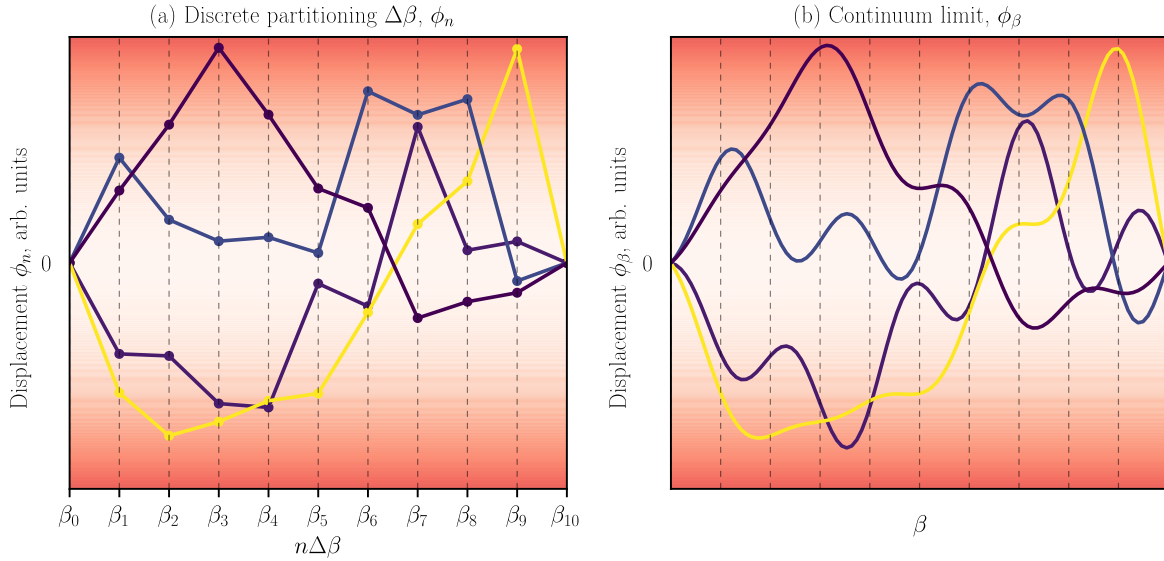


Figure 9.2: (a) is an illustration of four configurations of a discretely partitioned β . Before we take the continuum limit, we may think of these as what the field looks like. Integrating one ϕ_n sums over all values the point at β_n can have. Instead of thinking of β as a generic coordinate, it can be instructive to think of it as a time parameter. In this case, the "string" represents how one massive particles moves around at different time steps. (b) shows how the discrete strings may look in the continuum limit. In principle, everything works the same way: One field configuration may be thought of as how one particle moves around with time. In the continuum case, however, the space of all configurations is vastly larger than for the discrete string.

To highlight the similarity to the QFT path integral, we now eliminate β in favour of $\tau = -i\beta$. To avoid having to write two integrals, we may adopt a new measure d^4x_e . The "e" stands for Euclidean, as introducing an imaginary time gives back the four-dimensional Euclidian metric, as opposed to the Minkowski metric. Keep also in mind that we integrate the time-component from 0 to $-i\beta$. Using this formalism, we write the path integral as

$$\oint \mathcal{D}\phi \mathcal{D}\pi \exp\left(i \int d^4x_e \mu_i \mathcal{N}_i(\phi, \pi) + \pi \dot{\phi} - \mathcal{H}(\phi, \pi)\right), \quad (9.46)$$

which is certainly similar to the standard version from QFT. The dot now denotes a derivative with respect to τ .

Having derived the path integral is well and all, however, it is of little use to us if we cannot use it for calculation. We would not like to leave this problem unattended, and in Appendix E, we look at the procedure of calculating Gaussian path integral as the continuum limit of an N -dimensional Gaussian integral.

9.3 Grand Partition Function for Fermions

In this section, we seek to develop a path integral formalism also for fermionic particles. Paul Dirac famously described relativistic fermions with the Dirac equation [26], which we can derive from the free fermion Lagrangian density

$$\mathcal{L} = \bar{\Psi}(i\gamma^\mu \partial_\mu - m)\Psi \quad (9.47)$$

Here, a fermion field Ψ can be visualised as a complex 4-component vector. $\bar{\Psi}$ denotes $\Psi^\dagger \gamma^0$. As usual, we calculate the canonical momentum

$$\pi = \frac{\partial \mathcal{L}}{\partial(\partial_t \Psi)} = i\Psi^\dagger \gamma^0 \gamma^0 = i\Psi^\dagger \quad (9.48)$$

This relations will be useful again at the end of this subchapter. When we quantise the fermions, we assign operators to the fields as for bosons. These fermionic operators anti-commute, in contrast to the bosonic operators and their commutation. This is the reason why we could not just use the derivation of the path integral for bosons for both types of particles. The derivation relied upon the commutation relation of the field operator $\hat{\phi}$ and its canonical momentum $\hat{\pi}$. The new derivation will rather rely on the soon-to-be-introduced anti-commutation relations. First of all, we must define the anti-commutator of two operators. For operators \hat{A} and \hat{B} , we write the anti-commutator.

$$\{\hat{A}, \hat{B}\} = \hat{A}\hat{B} + \hat{B}\hat{A}. \quad (9.49)$$

From this definition, we see that when the anti-commutator is equal to zero, we can swap the ordering of the operators at the cost of adding a negative sign. Thus, two adjacent equal anti-commuting operators yields zero. We quantise the fermionic field operator and its canonical momentum in the ordinary way, except now we use the anti-commutator. For a discretely labeled fermionic operator, we impose

$$\{\hat{\Psi}_i, \hat{\Psi}_j^\dagger\} = \delta_{ij}, \quad (9.50)$$

where δ_{ij} is the Kronecker delta. Going from a discrete pair of labels i and j to a continuous pair x and y (recall that we omit the vector notation \vec{x} , \vec{y}), the anti-commutation changes slightly

$$\{\hat{\Psi}(x), \hat{\Psi}^\dagger(y)\} = \delta(x - y). \quad (9.51)$$

Just as in the commutation relations for the bosons, Eq. (9.10), the other anti-commutators give zero. This is equivalent to

$$\{\hat{\Psi}(x), \hat{\Psi}(y)\} = \{\hat{\Psi}^\dagger(x), \hat{\Psi}^\dagger(y)\} = 0. \quad (9.52)$$

So far, the new commutator relations seem harmless. However, a problem arises once we let the anti-commutator between $\hat{\Psi}(x)$ and $\hat{\Psi}(x)$ act upon an eigenstate of the field operator $|\Psi\rangle$. We will describe this eigenstate $|\Psi\rangle$ more later, but for now, we just allow it to produce eigenvalues from the operators $\hat{\Psi}$.

$$0 = \{\hat{\Psi}(x), \hat{\Psi}(y)\} |\Psi\rangle = (\Psi(x)\Psi(y) + \Psi(y)\Psi(x)) |\Psi\rangle. \quad (9.53)$$

After we have let the operator $\hat{\Psi}(x)$ act upon its eigenstate, it produces a "number" $\Psi(x)$. Above, we assumed that the eigenvalue commutes with the operator. However, when we have imposed the anti-commutation relations as given in Eq. (9.52), we see that the "numbers" $\Psi(x)$ and $\Psi(y)$ cannot behave like ordinary scalars. For the anti-commutation relations to make sense, we must require that the eigenvalue "numbers" the operators produce also anti-commute. Such "numbers" are called *Grassmann numbers*. We will need to develop an understanding of how the Grassmann numbers behave in order to derive the fermion path integral.

9.3.1 Grassmann Numbers

In this subchapter, we will develop the notions we need about Grassmann numbers to perform calculations on fermion states. There are several good textbooks which also explain Grassmann numbers, see e.g. [27], chapter 9. First of all, two Grassmann numbers ξ_1 and ξ_2 are anti-commuting

$$\{\xi_1, \xi_2\} = 0 \quad \text{which means} \quad \xi_1 \xi_2 = -\xi_2 \xi_1. \quad (9.54)$$

Notably, we have that a Grassmann number squared is equal to zero. This also holds for sums of Grassmann numbers. We can write it mathematically as

$$\left(\sum_{i=1}^N \xi_i\right)^n = 0, \quad \text{for any } n \geq 2. \quad (9.55)$$

In addition, ordinary numbers commute with Grassmann numbers. In addition, Grassmann numbers anti-commute with fermion operators, in order for Eq. (9.53) to be consistent. Finally, we make a mental remark that *pairs* of Grassmann numbers commute. The take-home message is that pairs of Grassmann numbers behaves like ordinary numbers. In the following, we will denote Grassmann numbers with greek letters, while ordinary numbers will be denoted by latin letters. With the notion of Grassmann numbers, we can develop an understanding of Grassmannian functions and integration. We define a function of a Grassmann variable in terms of its power expansion. For a function of one Grassmann variable, this means that we can write

$$f(\xi) = \sum_{n=0}^{\infty} a_n \frac{\xi^n}{n!} = a_0 + a_1 \xi. \quad (9.56)$$

Any higher order of the expansion will disappear due to the anti-commutation of equal Grassmann numbers. A function of several Grassmann numbers will have more terms. Let $\boldsymbol{\xi}$ denote a collection of N single Grassmann numbers ξ_i . We may write f as

$$f(\boldsymbol{\xi}) = a_0 + \sum_{i=1}^N a_i \xi_i + \sum_{i,j=0}^N b_{ij} \xi_i \xi_j + \dots + c_N \xi_N \xi_{N-1} \dots \xi_{i_1}. \quad (9.57)$$

Note that for the final term, we define the number c_N for when the Grassmann variables are *decreasing*. We also note to ourselves that in the continuum limit, we exchange the discrete indices, n , with a continuous one, x , specifically $\xi_n \rightarrow \xi(x)$. Grassmann numbers may be complex, too. In that case, we treat ξ and its complex conjugate ξ^* as two independent numbers. We define the complex conjugation of Grassmann numbers

$$(\xi_1 \xi_2)^* = \xi_2^* \xi_1^*. \quad (9.58)$$

We shall see why this is sensible later on. One particularly important function is the exponential function. At first we might be discouraged to find that

$$\exp(\xi) \exp(\eta) = (1 + \xi)(1 + \eta) = 1 + \xi + \eta + \xi\eta \neq 1 + \xi + \eta = \exp(\xi + \eta). \quad (9.59)$$

Does this mean that all the nice properties of the exponential function are ruined? Partially, yes. However, we remember that pairs of Grassmann numbers commute, i.e. behaves like ordinary numbers. Therefore, we may use the customary property of the exponential as long as at least one of the exponentials contains solely Grassmannian pairs. For example, we have

$$\begin{aligned} \exp\left(\sum_{i=1}^M \xi_i + \sum_{i=1}^N \zeta_i \eta_i\right) &= 1 + \sum_{k=1}^{\infty} \frac{1}{k!} \left\{ \sum_{i=1}^M \xi_i + \sum_{i=1}^N \zeta_i \eta_i \right\}^k \\ &= 1 + \sum_{k=1}^{\infty} \frac{1}{k!} \left\{ \left(\sum_{i=1}^N \zeta_i \eta_i\right)^k + k \sum_{i=1}^M \xi_i \left(\sum_{j=1}^N \zeta_j \eta_j\right)^{k-1} \right\} \\ &= \left(1 + \sum_{i=1}^M \xi_i\right) \left(1 + \sum_{k=1}^{\infty} \frac{1}{k!} \left\{ \sum_{i=1}^N \zeta_i \eta_i \right\}^k\right) = \exp\left(\sum_{i=1}^M \xi_i\right) \exp\left(\sum_{i=1}^N \zeta_i \eta_i\right), \end{aligned} \quad (9.60)$$

which is the desired property. To reach the second line, we have made use of Eq. (9.55). After we have eliminated any higher power of the sum over ξ_i , we move all ξ_i terms to the right. Had both exponentials only contained Grassmannian pairs, we would be able to treat both of them as ordinary exponentials.

Next, we define the derivative. We define the derivative through the expansion

$$\begin{aligned} f(\xi + d\xi) &= f(\xi) + \frac{d}{d\xi} f(\xi) d\xi \\ a_0 + a_1(\xi + d\xi) &= a_0 + a_1\xi + \frac{d}{d\xi} f(\xi) d\xi. \end{aligned} \quad (9.61)$$

Note that above, we have made a choice to set $d\xi$ to the right of $f'(\xi)$. Had we chosen set $d\xi$ to the left and let f depend on another Grassmann number ξ_2 , the difference between the left and right choice is a minus-sign in the terms containing an odd number of Grassmann variables. From the above, we may conclude that the derivative reads

$$\frac{df(\xi)}{d\xi} = a_1 \quad (9.62)$$

The definition is readily generalisable to a function of N Grassmann numbers, but we must be careful about the signs and our definition of the derivative in the case of several variables. We are nearly at the end of definitions for Grassmann numbers, but before we can stop, we need to know integration over Grassmann numbers. We want the integral to be linear and that the integral over total derivatives disappear. For a function of one Grassmann variable, the integral must read

$$\begin{aligned} 0 &= \int d\xi \frac{d}{d\xi} f(\xi) = \int d\xi a_1 \\ &= a_1 \int d\xi 1. \end{aligned} \quad (9.63)$$

The Grassmann integral over an ordinary number is zero. We also define

$$\int d\xi \xi \equiv 1. \quad (9.64)$$

In the end, we are interested in integrals over all ξ_n and exponential functions. At first we notice that when we integrate a function over all Grassmann variables ξ_i , we find

$$\begin{aligned} \int d\xi^N f(\xi) &= \int d\xi_1 \dots d\xi_N f(\xi) \\ &\stackrel{(9.57)}{=} \int d\xi_1 \dots d\xi_N \left\{ a_0 + \sum_{i=1}^N a_i \xi_i + \dots + c_N \xi_N \dots \xi_1 \right\} \\ &\stackrel{(9.63)}{=} c_N \int d\xi_1 \dots d\xi_N \xi_N \dots \xi_1 \stackrel{(9.64)}{=} c_N \end{aligned} \quad (9.65)$$

Now we see why we chose to order ξ_i in a decreasing order in the index, such that we would not have to anti-commute them around in order to perform each integration. Now we only lack one final piece before we know everything we need to know about Grassmann integration: Performing linear transformations. If we let $\xi' = A\xi$, where A is an $N \times N$ -matrix with components a_{ij} . With this we can write the integral

$$\begin{aligned} \int d\xi^N f(\xi') &= \int d\xi_1 \dots d\xi_N c_N (a_{11}\xi_1 + \dots + a_{1N}\xi_N) \dots (a_{N1}\xi_1 + \dots + a_{NN}\xi_N) \\ &= c_N \int d\xi_1 \dots d\xi_N \sum_{\sigma \in S_N} (-1)^\sigma a_{1\sigma(1)} \xi_{\sigma(1)} \dots a_{N\sigma(N)} \xi_{\sigma(N)} \\ &= c_N \det(A) \end{aligned} \quad (9.66)$$

In the first equality, we have simply inserted the linear transform $\xi' = A\xi$ and only taken into account non-zero contributions. The second equality is a bit harder to see. At first, we must take into consideration that only terms containing all ξ_n will give a non-zero integration. When we consider all such terms, we find that these terms are all the permutations of the N indices. This is what we indicate with the sum.

σ is a permutation of N elements, or in other words, σ is an element of the permutation group S_N . By (-1^σ) , we mean -1 if σ is an odd permutation or 1 if σ is an even permutation. This factor stems from the fact that we must order the Grassmann numbers before we can integrate. Why did we perform all of this rewriting? As it turns out, this is exactly how we calculate the determinant of a matrix. Thus, arrive at the last equality.

In calculating ordinary integrals, we are often helped by the appearance of Dirac δ -functions. Therefore, we are motivated to explore what the δ -function looks like for Grassmann integrals. For a one-dimensional integral it is quite easy to see that

$$\int d\xi (\xi - \eta) f(\xi) = \int d\xi (\xi - \eta)(a_0 + a_1 \xi) = \int d\xi (\xi a_0 + a_1 \xi \eta) = a_0 + a_1 \eta = f(\eta). \quad (9.67)$$

9.3.2 Path Integral Tools for Fermions

Now we are ready to tackle fermionic operators and states, now that we know how the eigenvalues behaves. At first, we will need to define the so-called coherent fermion states, or the eigenstates of the fermion field operator $\hat{\Psi}(x)$. Earlier in Eq. (9.53), we shamelessly used such an eigenstate without asking ourselves what it may look like. Here, we will justify the eigenstate's existence. To do so, we introduce the normalised ground state as $|0\rangle$. It satisfies the following relations

$$\hat{\Psi}(x) |0\rangle = 0 \quad \text{and therefore} \quad \langle 0 | \hat{\Psi}^\dagger(x) = 0, \quad (9.68)$$

$$\langle 0 | 0 \rangle = 1 \quad (9.69)$$

for all x . To see how the fermi exclusion principle arises from the anti-commutation relations and the vacuum state, we consider the simplest fermionic operator, without any index. We can now see what states we can build from the vacuum, letting *only* one fermionic $\hat{\Psi}^\dagger$ act on it. There are not many states to build from only $\hat{\Psi}^\dagger$. We write

$$\hat{\Psi}^\dagger |0\rangle = |1\rangle \quad \text{and} \quad \hat{\Psi}^\dagger \hat{\Psi}^\dagger |0\rangle = 0. \quad (9.70)$$

For only one fermion state, the only states are the vacuum and the state with one "fermionic occupant". This fact enforces the Pauli principle. However, things get a little more involved and interesting when we add Grassmann numbers into the mix. We now wish to construct the coherent state by letting an operator act on the ground state. We ask ourselves what the operator to create such a state must look like, when we consider that we will apply one operator $\hat{\Psi}(x)$ on it. The operator creating the coherent state should contain $\hat{\Psi}^\dagger(y)$ to stop us from being able to commute $\hat{\Psi}(x)$ straight past. It needs to integrate over every spatial coordinate y in order not to be bypassed by any x . In addition, it needs to be an infinite sum of increasing orders of $\hat{\Psi}^\dagger$ as the anti-commutation removes one order of $\hat{\Psi}^\dagger$. Our favourite way to construct such a sequence, is using the exponential, so let us try

$$|\xi\rangle = \exp\left(-\int d^3y \xi(y) \hat{\Psi}^\dagger(y)\right) |0\rangle \quad (\text{continuum}) \quad (9.71)$$

$$|\xi\rangle = \exp\left(-\sum_{i=1}^N \xi_i \hat{\Psi}_i^\dagger\right) |0\rangle = \prod_{i=1}^N (1 - \xi_i \hat{\Psi}_i^\dagger). \quad (\text{discrete}) \quad (9.72)$$

$\xi(x)$ is a Grassmann number, and we hope for it to be the "eigen-Grassmann-value" of the fermionic field operator $\hat{\Psi}(x)$, or $\hat{\Psi}_i$ for the discrete case. In the last equality of the second line, we have expanded the exponential. We have foreseeingly added a negative sign to cancel a sign from anti-commutation. We apply the field operator to Eq. (9.71) and find

$$\begin{aligned} \hat{\Psi}(x) |\xi\rangle &= \hat{\Psi}(x) \exp\left(-\int d^3y \xi(y) \hat{\Psi}^\dagger(y)\right) |0\rangle \\ &= \hat{\Psi}(x) \left(1 - \int d^3y \xi(y) \hat{\Psi}^\dagger(y) + \dots + \frac{(-1)^n}{n!} \int d^3y_1 \dots d^3y_n \xi(y_1) \hat{\Psi}^\dagger(y_1) \dots \xi(y_n) \hat{\Psi}^\dagger(y_n) + \dots\right) |0\rangle \end{aligned} \quad (9.73)$$

To solve this, we must move $\hat{\Psi}(x)$ past every term in the expansion of $\exp(\dots)$. To do so, we handle the n -th term, where $n \geq 1$.

$$\begin{aligned}
 & \hat{\Psi}(x) \frac{(-1)^n}{n!} \int d^3 y_1 \dots d^3 y_n \xi(y_1) \hat{\Psi}^\dagger(y_1) \dots \xi(y_n) \hat{\Psi}^\dagger(y_n) |0\rangle \\
 &= \frac{(-1)^{n-1}}{n!} \int d^3 y_1 \dots d^3 y_n \xi(y_1) \left(\left\{ \hat{\Psi}(x), \hat{\Psi}^\dagger(y_1) \right\} - \hat{\Psi}^\dagger(y_1) \hat{\Psi}(x) \right) \dots \xi(y_n) \hat{\Psi}^\dagger(y_n) |0\rangle \\
 &= \frac{(-1)^{n-1}}{n!} \xi(x) \int d^3 y_2 \dots d^3 y_n \xi(y_2) \hat{\Psi}^\dagger(y_2) \dots \xi(y_n) \hat{\Psi}^\dagger(y_n) |0\rangle \\
 & \quad + \frac{(-1)^n}{n!} \int d^3 y_1 \dots d^3 y_n \xi(y_1) \hat{\Psi}^\dagger(y_1) \hat{\Psi}(x) \xi(y_2) \hat{\Psi}^\dagger(y_2) \dots \xi(y_n) \hat{\Psi}^\dagger(y_n) |0\rangle \\
 &= \dots = \frac{(-1)^{n-1}}{(n-1)!} \xi(x) \int d^3 y_1 \dots d^3 y_{n-1} \xi(y_1) \hat{\Psi}^\dagger(y_1) \dots \xi(y_{n-1}) \hat{\Psi}^\dagger(y_{n-1}) |0\rangle. \tag{9.74}
 \end{aligned}$$

In the first equality, we have simply anti-commuted $\hat{\Psi}(x)$ and $\hat{\Psi}^\dagger(y_1)$, as well as having picked up a sign from the anti-commutation of $\xi(y_1)$. In the second equality, we have used Eq. (9.51) and integrated out the δ -function. We are left with one term of $n-1$ integrations over $\xi(y_i) \hat{\Psi}^\dagger(y_i)$, and one term equal to what we started with, except that $\hat{\Psi}(x)$ has been moved one step closer to $|0\rangle$. Every $\xi(y_i)$ that turns into $\xi(x)$ after integrating out the δ -function can be commuted past the even number of terms until it is outside the integral. Thus, no sign is picked up from moving it outside the integral. Continuing the anti-commutation procedure yields n equal terms after we rename the integration variables. In the end, we see that we end up with the $\xi(x)$ multiplied by the $n-1$ -th term of the expansion of the exponential. Performing this for every n , and summing up all the terms, we find that

$$\begin{aligned}
 \hat{\Psi}(x) |\xi\rangle &= \hat{\Psi}(x) \exp\left(-\int d^3 y \xi(y) \hat{\Psi}^\dagger(y)\right) |0\rangle = \xi(x) \exp\left(-\int d^3 y \xi(y) \hat{\Psi}^\dagger(y)\right) |0\rangle \\
 &= \xi(x) |\xi\rangle. \tag{9.75}
 \end{aligned}$$

Our state $|\xi\rangle$ was in fact the coherent state! From the calculation above, we also see that

$$\langle \xi | = \langle 0 | \exp\left(-\int d^3 y \hat{\Psi}(y) \xi^*(y)\right) \quad \text{where} \quad \langle \xi | \hat{\Psi}^\dagger(x) = \langle \xi | \xi^*(x). \tag{9.76}$$

Above, we have used that the dagger operator exchange positions of a Grassmann number and a fermionic operator ($\xi \hat{\Psi}^\dagger$) $^\dagger = \hat{\Psi} \xi^*$. This is why we defined complex conjugation as interchanging the ordering of two Grassmann numbers in Eq. (9.58). For the discrete case, the state reads

$$\langle \xi | = \langle 0 | \exp\left(-\sum_{i=1}^N \hat{\Psi}_i \xi_i^*\right) = \langle 0 | \prod_{i=1}^N (1 - \hat{\Psi}_i \xi_i^*). \tag{9.77}$$

In the derivation of the path integral for bosons, we inserted many identities. We need to know how to express the identity operator also in the fermionic case. With this goal in mind, we first calculate the inner product between two coherent fermion states $|\zeta\rangle$ and $|\xi\rangle$

$$\begin{aligned}
 \langle \zeta | \xi \rangle &= \langle 0 | \exp\left(-\int d^3 x \hat{\Psi}(x) \zeta^*(x)\right) \exp\left(-\int d^3 y \xi(y) \hat{\Psi}^\dagger(y)\right) |0\rangle \\
 &= \langle 0 | \left(1 - \int d^3 x \hat{\Psi}(x) \zeta^*(x) + \dots\right) \left(1 - \int d^3 y \xi(y) \hat{\Psi}^\dagger(y) \dots\right) |0\rangle. \tag{9.78}
 \end{aligned}$$

Before we move on, we note that only terms containing an *equal* number of $\hat{\Psi}$ and $\hat{\Psi}^\dagger$ will survive. If there is more of one or the other, we will always end up with either $\hat{\Psi}$ acting on $|0\rangle$ or $\hat{\Psi}^\dagger$ acting on $\langle 0|$ after we have done all the anti-commuting. The only terms we are interested in are thus of the n -th order

in both ξ and ζ^* . We consider one such term, and we are glad we can reuse the calculation done in Eq. (9.74). We can merge the prefactors $\frac{(-1)^n}{n!}$ from each term and write the total expression as

$$\begin{aligned}
 & \langle 0 | \frac{1}{(n!)^2} \int d^3x_1 d^3y_1 \dots d^3x_n d^3y_n \hat{\Psi}(x_1) \zeta^*(x_1) \dots \hat{\Psi}(x_n) \zeta^*(x_n) \xi(y_1) \hat{\Psi}^\dagger(y_1) \dots \xi(y_n) \hat{\Psi}^\dagger(y_n) | 0 \rangle \\
 &= \langle 0 | \frac{n}{(n!)^2} \int d^3x_1 d^3y_1 \dots d^3x_{n-1} d^3y_{n-1} d^3x_n \\
 & \quad \left\{ \hat{\Psi}(x_1) \zeta^*(x_1) \dots \hat{\Psi}(x_{n-1}) \zeta^*(x_{n-1}) \zeta^*(x_n) \xi(x_n) \xi(y_1) \hat{\Psi}^\dagger(y_1) \dots \xi(y_{n-1}) \hat{\Psi}^\dagger(y_{n-1}) \right\} | 0 \rangle \\
 &= \dots = \langle 0 | \frac{n!}{(n!)^2} \int d^3x_1 \dots d^3x_n \zeta^*(x_1) \xi(x_1) \dots \zeta^*(x_n) \xi(x_n) | 0 \rangle \\
 &= \frac{1}{n!} \int d^3x_1 \dots d^3x_n \zeta^*(x_1) \xi(x_1) \dots \zeta^*(x_n) \xi(x_n). \tag{9.79}
 \end{aligned}$$

from the first to the second line, we have moved $\hat{\Psi}(x_n)$ past $\zeta^*(x_n)$, picking up a minus sign. Next, we recognise that the left part of the integral is exactly what we calculated in Eq. (9.74), which we then substitute in directly. We have obtained a factor n , removed the n -th pair of $\hat{\Psi}$ and $\hat{\Psi}^\dagger$, and picked up another negative sign, cancelling the first. One integration over d^3x_n survives. Repeating this procedure until we have eliminated all operators, we can make the ground states meet. We must also keep track of all the signs which appear from anti-commutation. Doing everything carefully, we see that the last expression is the n -th term of an exponential. Thus, we can puzzle together all terms to find

$$\langle \zeta | \xi \rangle = \exp \left(\int d^3x \zeta^*(x) \xi(x) \right). \tag{9.80}$$

We now see that the naive guess of an identity operator as $\int d\xi |\xi\rangle\langle\xi|$ would not work for fermion states. To resolve the apparent problem, we must add a term to counteract the exponential and in return give us a δ -function. We suggest the following operator to be the identity, and prove that it is in fact the case.

$$\mathbb{1}_{\text{Grass}} = \int d\xi^*(x) d\xi(x) |\xi\rangle \exp \left(\int d^3x \xi(x) \xi^*(x) \right) \langle \xi | \tag{9.81}$$

Notice the ordering of the differentials, which is important for this relation to hold. Proving that this is the identity operator is perhaps easiest to do with a discrete index n running from 1 to N , and then understand the relation above as the continuum limit. We know that this operator is the identity if it sends any state $|\eta\rangle$ to $|\eta\rangle$. So, let us apply our proposed identity operator $\mathbb{1}_{\text{Grass}}$ to $|\eta\rangle$ and see what happens

$$\begin{aligned}
 \mathbb{1}_{\text{Grass}} |\eta\rangle &= \int \left(\prod_{n=1}^N d\xi_n^* d\xi_n \right) |\xi\rangle \exp \left(\sum_{n=1}^N \xi_n \xi_n^* \right) \langle \xi | \zeta \rangle \\
 &= \int \left(\prod_{n=1}^N d\xi_n^* d\xi_n \right) |\xi\rangle \exp \left(\sum_{n=1}^N (\xi_n - \eta_n) \xi_n^* \right) \\
 &= \int \left(\prod_{n=1}^N d\xi_n^* d\xi_n \right) \exp \left(\sum_{n=1}^N (\xi_n - \eta_n) \xi_n^* \right) \exp \left(- \sum_{n=1}^N \xi_n \Psi_n^\dagger \right) | 0 \rangle. \tag{9.82}
 \end{aligned}$$

From the first to the second line, we have applied Eq. (9.80) for a case of N Grassmann variables, and commuted η_n and ξ_n^* in the second exponential giving a sign change. In addition, we have merged the two exponentials together. From the second to the third, we have commuted the exponential past the $|\xi\rangle$ state, and written the state in terms of an operator acting on the vacuum. The exponential actually acts

as a $\delta(\xi_n - \eta_n)$. Continuing from above, we can write the exponentials as products on the following form

$$\begin{aligned}
 \mathbb{1}_{\text{Grass}} |\eta\rangle &= \int \left(\prod_{n=1}^N d\xi_n^* d\xi_n \right) \prod_{j=1}^N (1 + \xi_j \xi_j^* - \eta_j \xi_j^*) \prod_{i=1}^N (1 - \xi_i \Psi_i^\dagger) |0\rangle \\
 &= \int \left(\prod_{n=1}^N d\xi_n^* d\xi_n \right) (1 + \xi_1 \xi_1^* - \eta_1 \xi_1^*) (1 - \xi_1 \Psi_1^\dagger) \prod_{j=2}^N (1 + \xi_j \xi_j^* - \eta_j \xi_j^*) \prod_{i=2}^N (1 - \xi_i \Psi_i^\dagger) |0\rangle \\
 &= \int \left(\prod_{n=2}^N d\xi_n^* d\xi_n \right) (1 - \eta_1 \Psi_1^\dagger) \prod_{j=2}^N (1 + \xi_j \xi_j^* - \eta_j \xi_j^*) \prod_{i=2}^N (1 - \xi_i \Psi_i^\dagger) |0\rangle \\
 &= \dots = \prod_{i=1}^N (1 - \eta_i \Psi_i^\dagger) |0\rangle = \exp\left(-\sum_{i=1}^N \eta_i \Psi_i^\dagger\right) |0\rangle = |\eta\rangle.
 \end{aligned} \tag{9.83}$$

Of course, this holds for any $|\eta\rangle$. This concludes the proof that we indeed stated the identity operator for Grassmann states in Eq. (9.81). Going to the second line, we pulled the first term in each product to the front. This we can do, because all terms only contains pairs of Grassmann variables (in this case, the fermionic operator behaves just like a Grassmann number). Then we integrate, and only two of the in total six combinations gives non-zero contributions, leading us to the third line. Keep in mind that we need the right ordering before integration, giving a negative sign in front of $\eta_1 \Psi_1^\dagger$. This procedure we can perform until we have exhausted the products, as indicated by \dots . At last, we recognise the remaining product as a new exponential, creating a $|\eta\rangle$ -state.

Next, we need to know how to take the trace. Taking the trace, we want to "sandwich" an operator \hat{O} between equal states, and then sum over every state. As an example, for the single fermion state, the trace reads $\text{Tr}(\hat{O}) = \langle 0 | \hat{O} | 0 \rangle + \langle 1 | \hat{O} | 1 \rangle$. To express the trace in terms of an integral over Grassmann numbers and coherent state, we cannot just use the most naive guess. In finding the trace, it is perhaps easiest to consider a discrete amount of Grassmann coordinates, as for the identity operator. So far, we have been dragging along many Grassmann numbers. Let us for the sake of variety also just include *two* grassmann numbers, making us able to write out every term. Maybe it will also shed some light on the more involved calculations with N Grassmann numbers. We can produce a state from this Grassmann number just like before. We imagine we have some operator \hat{O} , and we consider the expression

$$\begin{aligned}
 &\int d\xi_1^* d\xi_1 d\xi_2^* d\xi_2 \exp(\xi_1 \xi_1^* + \xi_2 \xi_2^*) \langle -\xi_1, -\xi_2 | \hat{O} | \xi_1, \xi_2 \rangle \quad (\text{use (9.72) + (9.77)}) \\
 &= \int d\xi_1^* d\xi_1 d\xi_2^* d\xi_2 (1 + \xi_1 \xi_1^*)(1 + \xi_2 \xi_2^*) \langle 0, 0 | (1 + \hat{\Psi}_1 \xi_1^*)(1 + \hat{\Psi}_2 \xi_2^*) \hat{O} \\
 &\quad (1 - \xi_1 \hat{\Psi}_1^\dagger)(1 - \xi_2 \hat{\Psi}_2^\dagger) | 0, 0 \rangle
 \end{aligned} \tag{9.84}$$

In the expression above, we search for the terms where all of the Grassmann numbers ξ_i and ξ_i^* appear. The others vanish under integration. There are four non-vanishing terms in total. Where we can integrate immediately, we do so. Continuing the calculation above, we are left with

$$\begin{aligned}
 &\langle 0, 0 | \hat{O} | 0, 0 \rangle - \int d\xi_2^* d\xi_2 \langle 0, 0 | \hat{\Psi}_2 \xi_2^* \hat{O} \xi_2 \hat{\Psi}_2^\dagger | 0, 0 \rangle - \int d\xi_1^* d\xi_1 \langle 0, 0 | \hat{\Psi}_1 \xi_1^* \hat{O} \xi_1 \hat{\Psi}_1^\dagger | 0, 0 \rangle \\
 &+ \int d\xi_1^* d\xi_1 d\xi_2^* d\xi_2 \langle 0, 0 | \hat{\Psi}_1 \xi_1^* \hat{\Psi}_2 \xi_2^* \hat{O} \xi_1 \hat{\Psi}_1^\dagger \xi_2 \hat{\Psi}_2^\dagger | 0, 0 \rangle \\
 &= \langle 0, 0 | \hat{O} | 0, 0 \rangle + \langle 0, 1 | \hat{O} | 0, 1 \rangle \langle 1, 0 | \hat{O} | 1, 0 \rangle + \langle 1, 1 | \hat{O} | 1, 1 \rangle \\
 &= \sum_{n_1=0}^1 \sum_{n_2=0}^1 \langle n_1, n_2 | \hat{O} | n_1, n_2 \rangle = \text{Tr}(\hat{O}).
 \end{aligned} \tag{9.85}$$

To arrive at the equality, we move the Grassmann numbers past the fermionic operators. In the two terms with the negative signs in front, we see that the anti-commutations in total cancel these signs.

Note that we have tacitly assumed that the operator $\hat{\mathcal{O}}$ only contains terms where fermionic operators occur in pairs. Otherwise, $\hat{\mathcal{O}}$ picks up signs in some terms, which is certainly undesired behaviour, and ruins the trace. This shows that the expression we introduced in the beginning of Eq. (9.84) is, in fact, the trace! Note in particular the minus sign we introduced in the $\langle -\xi_1, -\xi_2 |$. It is discrete, but very important: It leads an anti-periodic boundary. This will be important later, and it is a key difference between the bosonic and the fermionic path integral.

Finally, we have developed every tool we need in order for the path integral derivation. The derivation goes along a quite similar fashion to the bosonic path integral: We start by splitting the β into smaller pieces and then separate $\hat{\Theta}$ into pieces of $\Delta\hat{\Theta}$. Remember that for the bosonic case, we assume Weyl-ordering. This time, we choose the opposite convention, namely that in $\hat{\mathcal{N}}(\hat{\Psi}^\dagger, \hat{\Psi})$ and $\hat{\mathcal{H}}(\hat{\Psi}^\dagger, \hat{\Psi})$, all the $\hat{\Psi}$ are standing to the right, while all the $\hat{\Psi}^\dagger$ operators are standing to the left. Using this ordering scheme, we may replace the operators with Grassmann numbers.

$$\begin{aligned} \Theta &= \text{Tr}\{\hat{\Theta}\} = \int d\xi_0^* d\xi_0 \exp\left(-\int d^3x \xi_0^* \xi_0\right) \langle -\xi_0 | (\Delta\hat{\Theta})^{N+1} | \xi_0 \rangle \\ &= \int d\xi_0^* d\xi_0 \left(\prod_{i=1}^N d\xi_i^* d\xi_i \right) \exp\left(-\int d^3x \xi_0^* \xi_0\right) \langle -\xi_0 | \Delta\hat{\Theta} | \xi_N \rangle \left(\prod_{j=N}^1 \exp\left(-\int d^3x \xi_j^* \xi_j\right) \langle \xi_j | \Delta\hat{\Theta} | \xi_{j-1} \rangle \right). \end{aligned} \quad (9.86)$$

To arrive at the second line, we have inserted N identities, Eq. (9.81), just like we did for the bosonic case. We have then moved all the differentials to the left. They come in pairs, so we may freely do so without picking up any signs in the end. In the last expression, we have some inner products we must calculate. Take the n -th one, where $1 \leq n < N$

$$\begin{aligned} &\exp\left(-\int d^3x \xi_n^* \xi_n\right) \langle \xi_n | \Delta\hat{\Theta} | \xi_{n-1} \rangle \\ &= \exp\left(-\int d^3x \xi_n^* \xi_n\right) \langle \xi_n | \exp\left(\Delta\beta \int d^3x \mu_i \hat{\mathcal{N}}_i(\hat{\Psi}^\dagger, \hat{\Psi}) - \hat{\mathcal{H}}(\hat{\Psi}^\dagger, \hat{\Psi})\right) | \xi_{n-1} \rangle \\ &= \exp\left(-\int d^3x \xi_n^* \xi_n - \xi_n^* \xi_{n-1}\right) \exp\left(\Delta\beta \int d^3x \mu_i \mathcal{N}_i(\xi_n^*, \xi_{n-1}) - \mathcal{H}(\xi_n^*, \xi_{n-1})\right) + \mathcal{O}((\Delta\beta)^2) \\ &= \exp\left(\Delta\beta \int d^3x \mu_i \mathcal{N}_i(\xi_n^*, \xi_{n-1}) - \xi_n^* \frac{\xi_n - \xi_{n-1}}{\Delta\beta} - \mathcal{H}(\xi_n^*, \xi_{n-1})\right) + \mathcal{O}((\Delta\beta)^2). \end{aligned} \quad (9.87)$$

From the first to the second line, we simply inserted the expression for $\Delta\hat{\Theta}$. Then, we expanded the exponential to linear order in $\Delta\beta$, let the operators act, and written it as an exponential again. This picks up an error of $(\Delta\beta)^2$. The states meet after the operators have done their job, and we use Eq. (9.80). Now we are at the second to last line. Finally, we just write everything in one exponential. We need to pay a little extra attention for $n = N$. If we write $-\xi_0 = \xi_{N+1}$ and $-\xi_0^* = \xi_{N+1}^*$, we may include also the $j = N + 1$ in the sum. Continuing, we neglect the higher order terms in $\Delta\beta$ and insert the remaining expression into Eq. (9.86). We continue directly from the final expression in order to find

$$\begin{aligned} &\int \prod_{i=0}^N (d\xi_i^* d\xi_i) \left(\prod_{j=N+1}^1 \exp\left(-\int d^3x \xi_j^* \xi_j\right) \langle \xi_j | \Delta\hat{\Theta} | \xi_{j-1} \rangle \right) \Bigg|_{\substack{\xi_{N+1} = -\xi_0 \\ \xi_{N+1}^* = -\xi_0^*}} \\ &= \int \prod_{i=0}^N (d\xi_i^* d\xi_i) \exp\left(\Delta\beta \sum_{j=N+1}^1 \int d^3x \mu_i \mathcal{N}_i(\xi_j^*, \xi_{j-1}) - \xi_j^* \frac{\xi_j - \xi_{j-1}}{\Delta\beta} - \mathcal{H}(\xi_j^*, \xi_{j-1})\right) \Bigg|_{\substack{\xi_{N+1} = -\xi_0 \\ \xi_{N+1}^* = -\xi_0^*}}. \end{aligned} \quad (9.88)$$

Now we are nearly at the end. Taking the continuum limit, the sum goes to an integral, and the difference goes to a derivative. In addition, we have been a little sloppy with $*$ and \dagger . In the previous derivation, the

Grassmann numbers were single numbers. However, fermions are described by four component vectors – we therefore upgrade the Grassmann numbers to occur in vectors of four, which we indicate by $\ast \rightarrow \dagger$. We also add a minus sign-subscript to the integral to remind ourselves of the anti-periodic boundary

$$\Theta = \oint_{-} \mathcal{D}\xi \mathcal{D}\xi^{\dagger} \exp\left(\int_0^{\beta} d\beta \int d^3x \mu_i \mathcal{N}_i(\xi^{\dagger}, \xi) - \xi^{\dagger} \dot{\xi} - \mathcal{H}(\xi^{\dagger}, \xi) \right). \quad (9.89)$$

This looks remarkably similar to the bosonic case. If we take into consideration the free fermion Lagrangian and its canonical momentum we find $\psi^{\dagger} = -i\pi$, making the similarity complete.

As commented at the end of the derivation of the bosonic path integral, we are not much impressed by deriving equations we cannot use. Therefore, we have also included a way of understanding Gaussian fermionic path integral as the continuum limit of the N -dimensional Grassmannian Gaussian integral in Appendix E.2. As a peak ahead, we will later also calculate the path integral for quarks in the quark-meson model using Matsubara frequency summation. Stay tuned for subchapter 11.1.1.

9.4 The Number Density Operator $\hat{\mathcal{N}}$

Up until now, we have not discussed the term of $\mu_i \hat{\mathcal{N}}_i$. We are already familiar with the Hamiltonian and the Lagrangian, but how do we implement the number density? In QFT, a chemical potential μ_i is associated with a conserved charge Q_i . Such conserved charges are found from conserved currents, j^μ . The conserved currents stem from continuous symmetries of the Lagrangian, as stated by Noether's theorem (for a brief discussion, see Appendix F). In terms of equations, we write a conserved charge Q_i if there is a conserved current j^μ such that

$$\partial_\mu j_i^\mu = 0, \quad \text{which implies a charge} \quad Q_i = \int d^3x j_i^0 \quad \text{with} \quad \frac{dQ}{dt} = 0. \quad (9.90)$$

We have seen conserved charges before in quantum mechanics, when an operator commutes with the Hamiltonian. In some sense, this is the field-theoretical equivalent. When we construct a Lagrangian, we couple conserved currents to gauge fields. For instance, in quantum electrodynamics the electrons couple to the photon fields through an interaction term that we can write as $A_\mu j^\mu$, where A_μ is the (gauge) photon field and j^μ is the conserved current from the U(1) symmetry, i.e. $\Psi \rightarrow \exp(i\theta)\Psi$. If we identify Q_i with N_i , we see that

$$\mu_i N_i = \int d^3x \mu_i \mathcal{N}_i = \int d^3x \mu_i j_i^0. \quad (9.91)$$

The chemical potential couples to the zeroth component of a conserved current, and therefore, we may interpret it as the zeroth component of a gauge field. Later, we will consider Lagrangians with a fermionic sector $\Psi^\dagger(i\not{\partial} - m)\Psi$. For Lagrangians where Ψ^\dagger appears together with Ψ , we always have the global symmetry transformation $\Psi \rightarrow \exp(i\theta)\Psi$, just like in quantum electrodynamics. Noether's theorem gives from this (as calculated in Appendix F)

$$j_f^0 = \frac{\partial \mathcal{L}}{\partial(\partial_0 \Psi_f)} i\Psi_f = -\Psi_f^\dagger \Psi_f. \quad (9.92)$$

This look a bit like a mass term, but it is in fact not. Notice that the mass term is $m\bar{\Psi}\Psi = m\Psi^\dagger\gamma^0\Psi$, whereas the current has no γ^0 between the fermions.

Two-Flavour Quark-Meson Model

In this chapter, we will discuss the quark-meson model (QM model) as an effective model of quantum chromodynamics (QCD). We will see how the same symmetries and symmetry breaking patterns occur in both QCD and in the QM model. Noteworthy, the QM model is a phenomenological model which tries to capture the behaviour of QCD, for instance in the mapping of the QCD phase diagram, see e.g. [28] or [29].

10.1 From QCD to the Quark-Meson Model

We have spent some time developing the path integral formalism. Now it is time to put it into practical use. To do so, we must define the Lagrangian density we are going to work with. In the rest of this thesis, we will be interested in the two-flavour quark-meson model (QM model). This model is a so-called *effective* model of quarks. The full theory of quarks goes under the name of quantum chromodynamics (QCD), which is a complicated theory. Being an effective model means that the QM model tries to capture certain aspects of QCD, without necessarily having to deal with all the calculations and difficulties of a full theory of quarks. The philosophy of developing an effective field theory/model is described in Ref. [30]. The overall goal in this chapter is to prepare us to find the equation of state from the QM model, which ties all the field theory we have gone through to the TOV-equations. The reason we write the QM model and not the QM theory, is that the QM model is phenomenological in nature, and not a systematic expansion like e.g. chiral perturbation theory [31]. We save the explicit expression for the QM model for the next subchapter.

Before starting with the QM model, we must consider the theory it tries to describe, QCD. It is defined by the QCD Lagrangian. There are several good textbooks containing chapters on QCD, so we will just rush through. For instance, Refs. [27] chapters 15 and 16, and [32] chapter 26 discuss the QCD Lagrangian and its properties at length. We will just qualitatively and briefly summarise some of its main properties. As a side remark, the mentioned chiral perturbation theory is also an effective description of QCD which has proved particularly important. In its full glory, the QCD Lagrangian reads

$$\mathcal{L}_{\text{QCD}} = \bar{q}_a^f \left(i\gamma^\mu D_{\mu,ab} \delta^{ff'} - M_{ff'} \delta_{ab} \right) q_b^{f'} - \frac{1}{4} \mathcal{G}_{\mu\nu}^A \mathcal{G}^{\mu\nu,A}, \quad \text{where} \quad (10.1)$$

$$\mathcal{G}_{\mu\nu}^A = \partial_\mu A_\nu^A - \partial_\nu A_\mu^A + ig f^{ABC} A_\mu^B A_\nu^C, \quad \text{and} \quad D_{\mu,ab} = \delta_{ab} \partial_\mu - ig A_\mu^A T_{ab}^A. \quad (10.2)$$

This surely needs a proper explanation for all the new symbols and indices. The fermions here are the quarks, described by q_a^f . The quarks come in different flavours, denoted by the **flavour index** f . For our purposes, the three lightest quarks are the most relevant, namely the *up*, *down* and *strange*. This means that $f, f' \in \{u, d, s\}$. $M_{ff'}$ denotes the mass matrix, which is diagonal, with the masses of the quark

flavours along its diagonal. The subscript a is the **color index**. This means that in addition to flavour, each quark comes in three colours, meaning that $a, b \in \{1, 2, 3\}$. We may think of the three colours as three versions of each quark. They interact with one another and a gluon through the T^A matrices, which are in general not diagonal. The T^A matrices are the generators of the gauge group $SU(3)$, and are called the Gell-Mann matrices. There are eight of them, i.e. $A \in \{1, \dots, 8\}$. The generators of $SU(3)$ constitute the Lie-algebra $su(3)$ ¹, which brings us on to the structure constants f^{ABC} . These constants describe the algebra and are defined from the commutator (Lie-bracket) between two algebra elements $[T^A, T^B]$ as

$$[T^A, T^B] = if^{ABC}T^C. \quad (10.3)$$

A_μ^A denotes the vector boson mediating the force between the fermions, in other words, the gluons. $\mathcal{G}_{\mu\nu}^A$ is the gluon field strength tensor. As we can see from Eq. (10.2), the field strength tensor contains a term which is quadratic in the gluon field A_μ^A . When we contract the field strength tensor with itself in the Lagrangian density, we will have gluon self-interactions. This fact makes QCD-calculations very complicated. Therefore, we have ample motivation to try to introduce a simpler theory which reflects the properties of this theory. Another very important remark which arises from renormalising this Lagrangian, is that the coupling constant between the fermions and the gluons g grows larger at lower energies, while at high energies, g decreases. This property is famously known as asymptotic freedom [32]. We will discuss renormalising later, in the context of the QM model. Asymptotic freedom means that for very large energies, perturbative QCD calculations will not need to take into account many perturbative terms in order to obtain good results. It also means that for smaller energies, perturbative calculations break down as g grows large. Later, we will be working with energies which are too low QCD to be practical, and therefore we need the QM model. The large coupling at low energy is also the reason why we never observe free quarks. The coupling between them is so strong that they bind to form hadrons, e.g. nucleons and mesons.

Many of the defining characteristics of a Lagrangian come from its symmetries, so the symmetries of the QCD-Lagrangian are essential. The first symmetry group we mention is the $SU(3)_c$ -gauge transformation-symmetry. This symmetry acts on the colour indices, and therefore we call it $SU(3)_c$. The Lagrangian in Eq. (10.1) is in fact constructed to be $SU(3)_c$ -symmetric. In a sense, enforcing a $SU(3)_c$ -gauge symmetry fixes the interaction terms of the theory. In this case, the interactions refer to the quark-gluon interaction and the gluon-gluon interactions. The word *gauge* means that the transformation is x -dependent, or local. For convenience in expressing the transformation, we define the 3×3 -matrix $\mathbf{A}_\mu = A_\mu^A T^A$. A general $SU(3)_c$ -gauge transformation may be written in terms of a matrix $U(x) = \exp(i\alpha(x)^A T^A)$. The eight x -dependent $\alpha^A(x)$ parameterise the transformation. With these definitions, the quark and gluon fields transform like

$$q_a^f \xrightarrow{SU(3)_c\text{-gauge}} U_{ab}(x)q_b^f, \quad (10.4)$$

$$\mathbf{A}_{\mu, ab} \xrightarrow{SU(3)_c\text{-gauge}} U_{ac}(x)\mathbf{A}_{\mu, cd}U_{db}^\dagger(x) - \frac{i}{g}[\partial_\mu U_{ac}(x)]U_{cb}^\dagger(x). \quad (10.5)$$

In the QM-model, we avoid the difficulties the gluons bring with their self interactions. The QM-model is colour neutral: The colours only contribute to a factor of $N_c = 3$ as we sum over the colour indices. This means that the $SU(3)_c$ -gauge transformation does not carry over to the QM-model, as this is where a lot of the calculational difficulties lie.

Next, we look at *global* symmetries, meaning that they are not x -dependent. Ref. [32], chapter 28 goes more in depth into this global symmetry-topic. The first one we call the *vector* symmetry. It is a global $U(1)$ -symmetry which we will denote by $U(1)_V$. Under the vector symmetry, the quark fields transform as

$$q_a^f \xrightarrow{U(1)_V} \exp(i\alpha)q_a^f, \quad (10.6)$$

where the x -independent α is a constant parameterising the specific transformation. It is quite easy to see that this transformation is a symmetry by simple insertion into Eq. (10.1). In fact, if we assume that

¹Symmetry groups and Lie-algebras are worthwhile studying themselves, but such a discussion is certainly outside the scope of this thesis. For Lie-algebras, definitions and clarifying examples may be found in Ref. [33].

the quark masses are equal, we may promote $U(1)_V \rightarrow U(N_f)_V = SU(N_f)_V \times U(1)_V$. To parameterise an element from the $SU(N_f)_V$ -group, we add the generators for the $SU(N_f)$ to the exponential, e.g. $U = \exp(i\alpha^A T^A) \in SU(3)$. Assuming that the quarks are massless, $M_{ff'} = 0$, we also have an *axial* symmetry, denoted by $U(1)_A$ (the A must not be confused with the generator index). From now on, we will assume that the quarks are massless. Under it, the quarks transform like

$$q_a^f \xrightarrow{U(1)_A} \exp(i\alpha\gamma^5) q_a^f. \quad (10.7)$$

Recalling that the γ^5 matrix commutes with all γ^μ and that $\bar{q}_a^f = (q_a^f)^\dagger \gamma^0$, we see that this is also a symmetry when the mass matrix vanishes. This symmetry may also be promoted $1 \rightarrow N_f$. When the Lagrangian is symmetric under both vector and axial transformations, we write that it is symmetric under $U(1)_V \times U(1)_A$. Having defined the vector and axial symmetries, we can define the *chiral* symmetries. For this we need the right and left handed projection operator, $P_{R/L}$.

$$P_{R/L} = \frac{1}{2} (1 \pm \gamma^5) \quad \text{and} \quad q_{R/L} = P_{R/L} q. \quad (10.8)$$

The projection operator has several important properties, which are easy to show using Eq. (0.8). One finds that

$$P_{R/L}^2 = \frac{1}{4} (1 \pm \gamma^5) (1 \pm \gamma^5) = \frac{1}{4} (2 \pm 2\gamma^5) = P_{R/L} \quad (\text{projection property}), \quad (10.9)$$

$$P_{R/L} P_{L/R} = \frac{1}{4} (1 \pm \gamma^5) (1 \mp \gamma^5) = 0 \quad (\text{orthogonal projections}), \quad (10.10)$$

$$P_{R/L} \gamma^\mu = \frac{1}{2} (1 \pm \gamma^5) \gamma^\mu = \gamma^\mu \frac{1}{2} (1 \mp \gamma^5) = \gamma^\mu P_{L/R} \quad (\text{commutation property}), \quad (10.11)$$

$$P_R + P_L = 1, \quad \text{and} \quad P_R - P_L = \gamma^5. \quad (10.12)$$

If we write $q = (P_L + P_R)q = q_L + q_R$, we can split the Lagrangian into one part containing only the right handed quarks, q_R , and the other one containing only left handed quarks, q_L . The cross terms, e.g. containing \bar{q}_R and q_L vanish due to orthogonality property of the projection operators. Furthermore, we may write an infinitesimal symmetry transformation from $U(1)_V \times U(1)_A$ as

$$\underbrace{\exp(i\alpha_V)}_{\in U(1)_V} \underbrace{\exp(i\alpha_A \gamma^5)}_{\in U(1)_A} = (1 + i\alpha_V)(1 + i\alpha_A \gamma^5) = 1 + i(\alpha_V + \alpha_A \gamma^5) \\ \stackrel{(10.12)}{=} P_R + P_L + i\alpha_V(P_R + P_L) + i\alpha_A(P_R - P_L) \quad (10.13)$$

$$= (1 + i[\alpha_V + \alpha_A])P_R + (1 + i[\alpha_V - \alpha_A])P_L \\ = \exp(\alpha_R)P_R + \exp(\alpha_L)P_L. \quad (10.14)$$

In the last equality, we defined $\alpha_R = \alpha_V + \alpha_A$ and $\alpha_L = \alpha_V - \alpha_A$. The calculation above shows that we may write a vector-axial symmetry-transformation as a sum of two transformations, each transformation acting only on either the left or right handed quark. From this, we see that a $U(1)_V \times U(1)_A$ -symmetry is equivalent to a $U(1)_R \times U(1)_L$ -symmetry where the $U(1)_R$ acts only on q_R and $U(1)_L$ acts on q_L . The left- and right-handed symmetries can be promoted from $U(1) \rightarrow U(N_f)$. As we are interested in the two-flavour QM model, we set $N_f = 2$. The global symmetries can be written

$$U(2)_L \times U(2)_R \cong SU(2)_L \times SU(2)_R \times U(1)_L \times U(1)_R. \quad (10.15)$$

In QCD, the ground state has a non-zero expectation-value

$$0 \neq \langle \bar{q}q \rangle = \langle (q^\dagger (P_L + P_R) \gamma^0 (P_L + P_R) q) \rangle = \langle q^\dagger P_L \gamma^0 P_R q + q^\dagger P_R \gamma^0 P_L q \rangle = \langle \bar{q}_R q_L \rangle + \langle \bar{q}_L q_R \rangle. \quad (10.16)$$

This expression is not invariant under $SU_R(2) \times SU_L(2)$. When the vacuum breaks the symmetry in this way, we say that the symmetry is *spontaneously broken*. If $L \in SU(2)_L$ and $R \in SU(2)_R$, then we must require $L = R$ for the vacuum to remain unaffected by a transformation, which is the same as a

$SU(2)_V$ -transformation. Therefore, we say that only the vector symmetry $SU(2)_V$ is conserved in the vacuum. This is what is known as *chiral symmetry breaking*. Chiral perturbation theory is built around this symmetry-breaking pattern. In the same way, the QM model must have an inherent chiral symmetry breaking. The magnitude of the symmetry breaking, i.e. the vacuum expectation value, will be used to fix the symmetry breaking parameter in the QM model, linking QCD to the effective model. In addition to spontaneous symmetry breaking, there is *explicit symmetry breaking*. This happens when we have a term in the Lagrangian density which violates a symmetry. For example, introducing a mass matrix where the elements along the diagonal are equal explicitly breaks the $SU(2)_A$ -symmetry. Similarly, as the quark masses are not exactly the same, a mass matrix with different masses along the diagonal is an example of an explicit symmetry breaking of $U(2)_V$ down to a $U(1)_V$.

Of course, a quark-meson model will in the end yield an equation of state where matter consists of quarks and mesons. This means that we will in fact describe a *quark star*. As previously mentioned, we never actually observe free quarks, so trying to describe a compact star composed by them does certainly seem strange at first glance. To justify spending time on quarks through the QM model, we present two arguments. The first one regards the *strange matter hypothesis*, which is discussed in Refs. [35] and [34]. The idea is that nucleons may not be the most stable form of matter. In particular, quark matter with up, down, and strange quarks might actually form matter with less energy per baryon than nuclear matter. It is the addition of strange quarks which gives the hypothesis its name. Quark matter consisting of only up and down quarks must be less stable than nuclear matter. Accepting the strange matter hypothesis, there might exist strange compact stars, making a quark star model-study worthwhile. To formulate a quantitative version of the strange matter hypothesis, we let ϵ_{3q} and $n_{B,3q}$ denote the energy density and baryonic number density of three flavour quark matter ($q \in \{u, d, s\}$), respectively. We let ϵ_{2q} and $n_{B,2q}$ denote the same two quantities for two flavour quark matter ($q \in \{u, d\}$). Then, the strange matter hypothesis reads

$$\frac{\epsilon_{3q}}{n_{B,3q}} < 931 \text{ MeV} < \frac{\epsilon_{2q}}{n_{B,2q}}. \quad (10.17)$$

The energy densities are to be evaluated at zero pressure. Sandwiched between the quark matter energy densities per baryon, is the energy per baryon in the most stable nuclear matter, Fe^{56} [4].

The second and perhaps more convincing argument as to why the QM model is useful to us, is the concept of a hybrid star. Inside a compact star, the energy densities may be very large, as illustrated in the project thesis in the discussion about ideal neutron stars. Therefore, there might be quark matter in the core of the compact star. When the energy density grows large enough, the quarks will deconfine as a result of asymptotic freedom. The relevant degrees of freedom in the large-energy density core of a star will therefore be quarks, not nucleons. Towards the end of this thesis, we will discuss two hybrid star models in which we use the QM model to describe the quark core.

In Table 10.1 we list the masses and baryon numbers of the up and down quark. Particularly, we see that the baryon numbers are $\frac{1}{3}$. This is why we introduce this factor when we start discussing baryonic number densities.

Flavour	Mass [MeV]	Baryon number
u	2.2	$\frac{1}{3}$
d	4.7	$\frac{1}{3}$

Table 10.1: Masses and baryon numbers of the quarks we consider. Baryon numbers are from [4]. The masses are listed in Ref. [36], p. 32.

The masses we refer to here, are the lone masses. This means that it is the mass of a quark without the contribution from the gluons. When the quarks are bound in a hadron, much of the hadron mass comes from the gluon contribution. The the up and down quark masses are quite small, and they are therefore often assumed to be zero.

10.2 The Two-Flavour Quark-Meson Lagrangian

We will now look explicitly at the two-flavour quark-meson model. It contains the two quarks, denoted by q_f , three pseudo-scalar pions, which will be denoted by a three-component vector $\boldsymbol{\pi}$, and one scalar particle σ [37]. We will suppress the flavour and colour indices in the following. The pions and the scalar are the so-called mesons. The Lagrangian density reads

$$\mathcal{L}_{\text{QM}} = \bar{q} [i\not{\partial} + \mu\gamma^0 - g(\sigma + i\boldsymbol{\gamma}^5 \boldsymbol{\tau} \cdot \boldsymbol{\pi})] q + \frac{1}{2} (\partial_\mu \sigma \partial^\mu \sigma + \partial_\mu \boldsymbol{\pi} \partial^\mu \boldsymbol{\pi}) - \frac{\lambda}{4} (\sigma^2 + \boldsymbol{\pi}^2 - v^2)^2 + h\sigma. \quad (10.18)$$

The vector $\boldsymbol{\tau} = (\tau_1, \tau_2, \tau_3)$ are the generators of the $SU(2)$ -group, the familiar Pauli-matrices. Note also that the mesonic potential $\mathcal{V}(\sigma, \boldsymbol{\pi})$ is the negative of the last parenthesis and the negative of the last, linear term $-h\sigma$. Isolated, it reads

$$\mathcal{V}(\sigma, \boldsymbol{\pi}) = \frac{\lambda}{4} (\sigma^2 + \boldsymbol{\pi}^2 - v^2)^2 - h\sigma. \quad (10.19)$$

In the previous subsection, we argued that an effective model must contain the symmetries and the symmetry breaking patterns of the full theory. How does chiral symmetry breaking appear here? The derivation is discussed in Ref. [38], and we will follow along the same lines here. At first we must impose chiral symmetry. The quarks transform as in the previous section. To find the transformation property of the mesons, we start by a little rewriting of the quark-meson interaction term using the projection operator

$$\begin{aligned} \bar{q}(\sigma + i\boldsymbol{\gamma}^5 \boldsymbol{\tau} \cdot \boldsymbol{\pi})q &= \bar{q}([P_L + P_R]\sigma + [P_R - P_L]i\boldsymbol{\tau} \cdot \boldsymbol{\pi})q \\ &= \bar{q}(P_R[\sigma + i\boldsymbol{\tau} \cdot \boldsymbol{\pi}] + P_L[\sigma - i\boldsymbol{\tau} \cdot \boldsymbol{\pi}])q \\ &= \bar{q}(P_R\Sigma + P_L\Sigma^\dagger)q = \bar{q}(P_R\Sigma P_R + P_L\Sigma^\dagger P_L)q \\ &= \bar{q}_L \Sigma q_R + \bar{q}_R \Sigma^\dagger q_L. \end{aligned} \quad (10.20)$$

In the second to third line, we have defined the 2×2 -flavour space matrix

$$\Sigma \equiv \mathbb{1}_{2 \times 2} \sigma + i\boldsymbol{\tau} \cdot \boldsymbol{\pi} = \begin{pmatrix} \sigma + i\pi_3 & i\pi_1 + \pi_2 \\ i\pi_1 - \pi_2 & \sigma - i\pi_3 \end{pmatrix}. \quad (10.21)$$

Let now a chiral $SU(2)_R$ -transformation be denoted by R and a chiral $SU(2)_L$ -transformation be denoted by L . A chiral transformation will change the interaction terms as

$$\bar{q}_L \Sigma q_R + \bar{q}_R \Sigma^\dagger q_L \xrightarrow{SU(2)_L \times SU(2)_R} \bar{q}_L L^\dagger \Sigma' R q_R + \bar{q}_R R^\dagger (\Sigma')^\dagger L q_L \quad \text{which imposes } \Sigma' = L \Sigma R^\dagger. \quad (10.22)$$

This yields chirally symmetric quark-meson interaction terms. We must check that these transformation properties give a chirally symmetric mesonic sector as well. In order to do so, the next task is expressing the potential in terms Σ .

$$\frac{1}{2} \text{Tr}[\Sigma^\dagger \Sigma] = \frac{1}{2} \text{Tr}[(\mathbb{1}_{2 \times 2} \sigma - i\boldsymbol{\tau} \cdot \boldsymbol{\pi})(\mathbb{1}_{2 \times 2} \sigma + i\boldsymbol{\tau} \cdot \boldsymbol{\pi})] = \frac{1}{2} \text{Tr}[\mathbb{1}_{2 \times 2} \sigma^2 + (\boldsymbol{\tau} \cdot \boldsymbol{\pi})^2] \stackrel{(0.11)}{=} (\sigma^2 + \boldsymbol{\pi}^2). \quad (10.23)$$

Apart from the linear term in the mesonic potential, we can write \mathcal{V} in terms of $\frac{1}{2} \text{Tr}(\Sigma^\dagger \Sigma)$. In exactly the same fashion, one can show that the kinetic terms are possible to write as $\frac{1}{2} \text{Tr}(\partial_\mu \Sigma^\dagger \partial^\mu \Sigma)$. The trace is invariant under the imposed transformation in Eq. (10.22)

$$\text{Tr}[\Sigma^\dagger \Sigma] \xrightarrow{SU(2)_R \times SU(2)_L} \text{Tr}[(L \Sigma R^\dagger)^\dagger L \Sigma R^\dagger] = \text{Tr}[R \Sigma^\dagger L^\dagger L \Sigma R^\dagger] = \text{Tr}[\Sigma^\dagger \Sigma]. \quad (10.24)$$

In the last equality above, we have used the cyclic property of the trace, $\text{Tr}(AB) = \text{Tr}(BA)$ to make R and R^\dagger meet and cancel. This shows that the Lagrangian density is symmetric under chiral transformation,

apart from the linear term $h\sigma$, which is clearly *not* invariant. The fact that we can accept $h \neq 0$ is related to the fact that also QCD had explicit symmetry breaking terms.

Having discussed the chiral symmetry transformations, we turn to chiral symmetry breaking. Importantly, the mesonic potential is not minimised for $\sigma = \pi_i = 0$. This means that we will find vacuum expectation values $\langle\sigma\rangle$ and $\langle\boldsymbol{\pi}\rangle$ which are generally non-zero. Due to this, we write σ and $\boldsymbol{\pi}$ as the vacuum expectation value and the fluctuations around the minimum

$$\sigma = \langle\sigma\rangle + \sigma_1, \quad \boldsymbol{\pi} = \langle\boldsymbol{\pi}\rangle + \boldsymbol{\pi}_1. \quad (10.25)$$

We let σ_1 and $\boldsymbol{\pi}_1$ denote the fluctuations. As the vacuum corresponds to no fluctuations, we note that the fluctuations describe the particle content, namely that σ_1 and $\boldsymbol{\pi}_1$ are the particles of the model. To find $\langle\sigma\rangle$ and $\langle\boldsymbol{\pi}\rangle$ which minimise the potential, we calculate

$$\left. \frac{\partial\mathcal{V}(\sigma, \boldsymbol{\pi})}{\partial\sigma} \right|_{\substack{\sigma=\langle\sigma\rangle \\ \boldsymbol{\pi}=\langle\boldsymbol{\pi}\rangle}} = 0 \quad \text{and} \quad \left. \frac{\partial\mathcal{V}(\sigma, \boldsymbol{\pi})}{\partial\boldsymbol{\pi}} \right|_{\substack{\sigma=\langle\sigma\rangle \\ \boldsymbol{\pi}=\langle\boldsymbol{\pi}\rangle}} = 0. \quad (10.26)$$

Starting from the conditions for π_i

$$\lambda\langle\pi_i\rangle (\langle\sigma\rangle^2 + \langle\boldsymbol{\pi}\rangle^2 - v^2) = 0 \quad \text{which enforces} \quad \langle\pi_i\rangle = 0 \quad \text{or} \quad (\langle\sigma\rangle^2 + \langle\boldsymbol{\pi}\rangle^2 - v^2) = 0. \quad (10.27)$$

Looking at the condition for σ ,

$$\lambda\langle\sigma\rangle (\langle\sigma\rangle^2 + \langle\boldsymbol{\pi}\rangle^2 - v^2) - h = 0, \quad (10.28)$$

we see that for $h = 0$, $\langle\sigma\rangle = 0$ is a solution. However, this represents a maximum, not a minimum. The minima lie at $\langle\sigma\rangle^2 + \langle\boldsymbol{\pi}\rangle^2 - v^2 = 0$. This is the famous Mexican hat-potential. An illustration of the potential is given in Fig. 10.1. The black point marks the solution where $\langle\sigma\rangle = \langle\boldsymbol{\pi}\rangle = 0$, and it is very clear that these are local maxima. In the case of $h = 0$, the minima lies on a ring, a "vacuum circle".

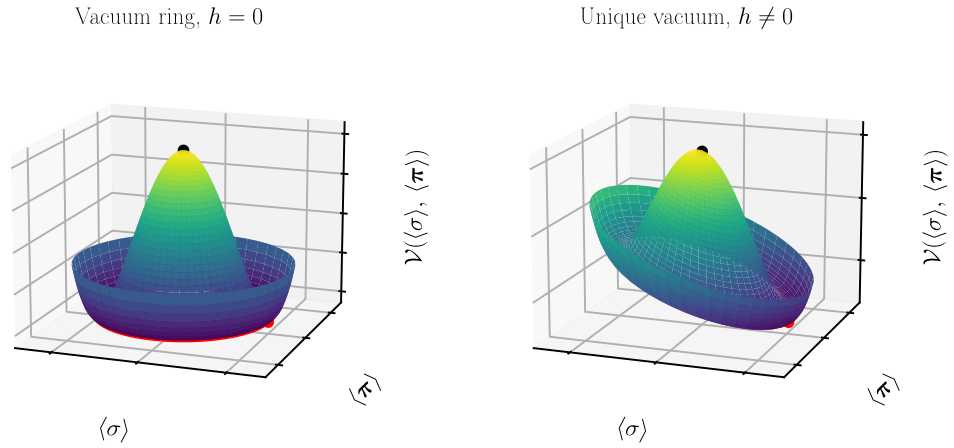


Figure 10.1: The mexican hat potential with and without a linear term $h\langle\sigma\rangle$. We see that the addition of a linear term fixes a unique vacuum, while $h = 0$ gives a whole ring of minima.

This "vacuum circle" is invariant under the symmetry transformations. However, when we pick a particular vacuum, which we may chose to be whatever point along the vacuum circle, the $SU(2)_R \times SU(2)_L$ -symmetry is broken into $SU(2)_V$ -symmetry. In the figure, we indicate by the red dot that we choose

$$\langle\sigma\rangle \neq 0 \quad \text{and} \quad \langle\pi_i\rangle = 0, \quad (10.29)$$

to be the vacuum configuration. In the case of $h \neq 0$, we no longer have the option: It must be this way. To verify our symmetry breaking claim, we write σ in terms of Σ and apply a chiral transformation.

$$\sigma = \frac{1}{4} \text{Tr} [\Sigma + \Sigma^\dagger] \xrightarrow{SU(2)_R \times SU(2)_L} \frac{1}{4} \text{Tr} [L\Sigma R^\dagger + R\Sigma^\dagger L^\dagger] = \frac{1}{4} \text{Tr} [\Sigma R^\dagger L + \Sigma^\dagger L^\dagger R]. \quad (10.30)$$

The above transformation is a symmetry if $L = R$, as the unitary transformations would then cancel. This is exactly the vector transformations, $SU(2)_V$. This shows that the chiral symmetry is spontaneously broken in the QM model. This serves to justify the Lagrangian in Eq. (10.18) as an effective model of quarks.

Inserting Eq. (10.25) with a non-zero $\langle\sigma\rangle$ back into the mesonic potential we generate new interaction terms, and modify the already existing square terms.

$$\begin{aligned} \mathcal{V}(\sigma_1, \boldsymbol{\pi}_1) &= \underbrace{\frac{\lambda}{4}(\sigma_1^4 + (\boldsymbol{\pi}^2)^2 + \sigma_1^2 \boldsymbol{\pi}^2)}_{\mathcal{L}_{\text{int}}(\sigma_1, \boldsymbol{\pi})} + \lambda \langle\sigma\rangle (\sigma_1^3 + \sigma_1 \boldsymbol{\pi}^2) + \frac{1}{2} \underbrace{\lambda(3\langle\sigma\rangle^2 - v^2)}_{m_\sigma^2} \sigma_1^2 + \frac{1}{2} \underbrace{\lambda(\langle\sigma\rangle^2 - v^2)}_{m_\pi^2} \boldsymbol{\pi}^2 \\ &\quad + (\lambda \langle\sigma\rangle - h) \sigma_1 + \frac{\lambda}{4} (\langle\sigma\rangle^2 - v^2)^2 - h \langle\sigma\rangle \\ &= \mathcal{L}_{\text{int}}(\sigma_1, \boldsymbol{\pi}) + \frac{m_\sigma^2}{2} \sigma_1^2 + \frac{m_\pi^2}{2} \boldsymbol{\pi}^2 + h' \sigma_1 + \frac{\lambda}{4} (\langle\sigma\rangle^2 - v^2)^2 - h \langle\sigma\rangle. \end{aligned} \quad (10.31)$$

Above, we have defined the masses m_σ^2 and m_π^2 , in addition to a $h' = \lambda \langle\sigma\rangle - h$. In order to produce any physical results from this Lagrangian density, we must of course find a value for the constants we have introduced, e.g. $\langle\sigma\rangle$. This is a task we will deal with later.

The simplest approximation we can make to proceed, is the *mean-field* approximation for the mesonic sector. By the mean-field approximation, we mean that we neglect any fluctuations in the fields – we only consider the mean-field value, $\langle\sigma\rangle$. In practise, this means that the mesonic sector of the Lagrangian density only contributes with the potential

$$\mathcal{V}(0, 0; \langle\sigma\rangle, \lambda, v^2, h) \equiv \mathcal{V}(\langle\sigma\rangle) = \frac{\lambda}{4} \langle\sigma\rangle^4 + \frac{m^2}{2} \langle\sigma\rangle^2 - h \langle\sigma\rangle + \frac{\lambda v^4}{4}, \quad (10.32)$$

where we defined $m^2 = -\lambda v^2$. In addition, the couplings between the mesons and quarks turn into a dynamic mass term, proportional to $\langle\sigma\rangle$.

Quark Stars with the QM-model

With the mean-field approximation for the mesonic sector, we will calculate the grand potential for the two-flavour QM model. Going from there, we find expressions for the energy density, pressure, and number density. These quantities are all we need to find an equation of state. With the QM model equation of state, we will calculate mass-radius relations for two-flavour quark stars: Our first compact star-results in this thesis.

11.1 The Grand Potential in the Mean-Field Approximation

The first interesting property of the non-vanishing mean field value $\langle\sigma\rangle \neq 0$, is that it effectively gives a mass term to the quarks, $m_q = g\langle\sigma\rangle$. This mass term is called a dynamic mass, as it changes with $\langle\sigma\rangle$, making it quite a lot more interesting than a fixed mass, as we shall see. Neglecting the fluctuations, we may write the full Lagrangian density as

$$\mathcal{L}_{\text{QM}} = \mathcal{L}_{\Psi} - \mathcal{V}(\langle\sigma\rangle) = \mathcal{L}_{\Psi} - \frac{\lambda}{4}\langle\sigma\rangle^4 + \frac{m^2}{2}\langle\sigma\rangle^2 + h\langle\sigma\rangle. \quad (11.1)$$

Writing out the Lagrangian density concerning the fermions, \mathcal{L}_{Ψ} , we find

$$\mathcal{L}_{\Psi} = \bar{\Psi}_q(i\cancel{\partial} - \mu\gamma^0 - g\langle\sigma\rangle)\Psi_q = \bar{\Psi}_q(i\gamma^0\partial_0 + i\gamma^i\partial_i - \mu\gamma^0 - g\langle\sigma\rangle)\Psi_q. \quad (11.2)$$

We have reinstated the notation of Ψ in order to make the notation compatible to the Chapter 9.3. To remember that we are dealing with quarks we have added the subscript q which denotes which fermion we take into account, namely the up and down quark, in each of their colours. For ease of notation, we omit the summation over colours $\sum_{n=1}^{N_c=3}$, as adding a colour index only further clutter the notation. \mathcal{L} is independent of the colour indices, and in the end the sum will only contribute with a factor N_c . Thus we may write the Hamiltonian density

$$\mathcal{H}_{\Psi} = \pi_q\partial_0\Psi_q - \mathcal{L}_{\Psi} = \bar{\Psi}_q(-i\gamma^i\partial_i + \mu\gamma^0 + g\langle\sigma\rangle)\Psi_q, \quad \text{with} \quad \pi_q = i\Psi_q^{\dagger}. \quad (11.3)$$

This Hamiltonian density we can plug back into Eq. (9.89). We find that we must calculate the following Grand partition function

$$\begin{aligned} \Theta &= \oint_{-} \mathcal{D}\Psi_q^{\dagger}\mathcal{D}\Psi_q \exp\left(\int_0^{\beta} d\tau \int d^3x \bar{\Psi}_q(-\gamma^0\partial_{\tau} + i\gamma^i\partial_i - \mu\gamma^0 - g\langle\sigma\rangle)\Psi_q - \mathcal{V}(\langle\sigma\rangle, 0)\right) \\ &= \exp\left(-\beta\mathcal{V}(\langle\sigma\rangle) \int d^3x\right) \oint_{-} \mathcal{D}\Psi_q^{\dagger}\mathcal{D}\Psi_q \exp\left(\int_0^{\beta} d\tau \int d^3x \bar{\Psi}_q(-\gamma^0\partial_{\tau} + i\gamma^i\partial_i - \mu\gamma^0 - g\langle\sigma\rangle)\Psi_q\right) \end{aligned} \quad (11.4)$$

Above we have used that $\mathcal{V}(\langle\sigma\rangle)$ is independent of space and τ , so we may replace the integral over τ with a factor β and pull \mathcal{V} outside the spatial integral. We see that we can factor Θ into a product of simpler terms. Therefore, we name $\Theta_{\langle\sigma\rangle} = \exp(-\beta\mathcal{V}(\langle\sigma\rangle) \int d^3x)$. Next, we turn to the fermionic path integral. We will also consider just one fermion species, omitting the subscript q . Each fermion species contributes with one Θ_q .

As we know from Chapter 9.3 and our minus-subscript by the integral, the fermionic fields are anti-periodic in β . Due to this, we know that we can decompose the function into its Fourier modes in τ -space which are anti-periodic, i.e.

$$\Psi(\mathbf{x}, \tau) = \frac{1}{\sqrt{\beta}} \sum_{n=-\infty}^{\infty} \psi_n(\mathbf{x}) \exp\left(\frac{2\pi i\tau}{\beta} \left\{n + \frac{1}{2}\right\}\right). \quad (11.5)$$

In space, we do not have periodicity, but there is a nifty trick we can use, namely **box quantisation**. By this, we mean that we put the field inside a box of volume $V = L^3$ and impose anti-periodic boundary conditions. Since the system is not actually in a box, the idea is to let the volume $V \rightarrow \infty$, that is, taking the thermodynamic limit. The box allows us to write

$$\Theta_{\langle\sigma\rangle} \xrightarrow{\text{box}} \Theta_{\langle\sigma\rangle, V} = \exp\left(-\beta V \mathcal{V}(\langle\sigma\rangle)\right). \quad (11.6)$$

More importantly, the box allows us to decompose $\psi_n(\mathbf{x})$ as well, yielding a full decomposition

$$\Psi(\mathbf{x}, \tau) = \frac{1}{\sqrt{\beta V}} \sum_{n=-\infty}^{\infty} \sum_{\mathbf{k}} \tilde{\psi}_n(\mathbf{k}) \exp(i\mathbf{x} \cdot \mathbf{k}) \exp\left(\frac{2\pi i\tau}{\beta} \left\{n + \frac{1}{2}\right\}\right), \quad (11.7)$$

$$\Psi^\dagger(\mathbf{x}, \tau) = \frac{1}{\sqrt{\beta V}} \sum_{n=-\infty}^{\infty} \sum_{\mathbf{k}} \tilde{\psi}_n^\dagger(\mathbf{k}) \exp(-i\mathbf{x} \cdot \mathbf{k}) \exp\left(-\frac{2\pi i\tau}{\beta} \left\{n + \frac{1}{2}\right\}\right). \quad (11.8)$$

In the equation above, we have introduced a sum over $\mathbf{k} = (\frac{2\pi n_i}{L}, \frac{2\pi n_j}{L}, \frac{2\pi n_k}{L})$, where n_i , n_j and n_k are integers. Keep in mind that $\tilde{\psi}_n^\dagger$ and $\tilde{\psi}_n$ are still four component vectors. The periodic boundary restricts the number of modes to a countable amount. In sending the volume to infinity, we must let the sum go to an integral. The sum is dimensionless, but the integral comes with a measure d^3k . We must therefore add a constant in the transition between sum and integration. We realise that the volume of the boxes we sum over, are of the size $\Delta V = (\frac{2\pi}{L})^3$, meaning that

$$\sum_{\mathbf{k}} \rightarrow \int \frac{d^3k}{(\frac{2\pi}{L})^3} = V \int d^3k. \quad (11.9)$$

The advantage of box quantisation, is that we may work with a discrete sum over \mathbf{k} instead of a continuous integral. When we integrate over all functions, we are thus back to integrating over all values $\tilde{\psi}_n(\mathbf{k})$ may take. With discrete \mathbf{k} this allows us to write

$$\mathcal{D}\Psi = \prod_{\mathbf{k}, n} d\tilde{\psi}_n(\mathbf{k}) \quad \text{and} \quad \mathcal{D}\Psi^\dagger = \prod_{\mathbf{k}, n} d\tilde{\psi}_n^\dagger(\mathbf{k}). \quad (11.10)$$

The anti-periodic boundary conditions are now encoded in the decomposition of Ψ and Ψ^\dagger . We now

consider the contents of the exponent, to see how it behaves under our rewriting of the fields

$$\begin{aligned}
 & \int_0^\beta d\tau \int_{-\frac{\beta}{2}}^{\frac{\beta}{2}} d^3x \Psi^\dagger (-\partial_\tau + i\gamma^0 \gamma^i \partial_i - \mu - \gamma^0 g\langle\sigma\rangle) \Psi \\
 &= \int_0^\beta d\tau \int_{-\frac{\beta}{2}}^{\frac{\beta}{2}} d^3x \frac{1}{\sqrt{\beta V}} \sum_{n'=-\infty}^{\infty} \sum_{\mathbf{k}'} \tilde{\psi}_{n'}^\dagger(\mathbf{k}') \exp\left(-\frac{2\pi i\tau}{\beta} \left\{n' + \frac{1}{2}\right\} - i\mathbf{x} \cdot \mathbf{k}'\right) (-\partial_\tau + i\gamma^0 \gamma^i \partial_i - \mu - \gamma^0 g\langle\sigma\rangle) \\
 & \quad \frac{1}{\sqrt{\beta V}} \sum_{n=-\infty}^{\infty} \sum_{\mathbf{k}} \tilde{\psi}_n(\mathbf{k}) \exp\left(\frac{2\pi i\tau}{\beta} \left\{n + \frac{1}{2}\right\} + i\mathbf{x} \cdot \mathbf{k}\right) \\
 &= \frac{1}{\beta V} \sum_{n,n'} \sum_{\mathbf{k},\mathbf{k}'} \tilde{\psi}_{n'}^\dagger(\mathbf{k}') \left(\frac{-2\pi i}{\beta} \left\{n + \frac{1}{2}\right\} - \gamma^0 \gamma^i k_i - \mu - \gamma^0 g\langle\sigma\rangle\right) \tilde{\psi}_n(\mathbf{k}) \\
 & \quad \underbrace{\int_0^\beta d\tau \exp\left(\frac{2\pi i\tau}{\beta} \{n - n'\}\right)}_{=\beta\delta_{n,n'}} \underbrace{\int_{-\frac{\beta}{2}}^{\frac{\beta}{2}} d^3x \exp(i\mathbf{x} \cdot (\mathbf{k} - \mathbf{k}'))}_{=V\delta_{\mathbf{k},\mathbf{k}'}} \\
 &= - \sum_{n=-\infty}^{\infty} \sum_{\mathbf{k}} \tilde{\psi}_n^\dagger(\mathbf{k}) \left(\frac{2\pi i}{\beta} \left\{n + \frac{1}{2}\right\} + \gamma^0 \gamma^i k_i + \mu + \gamma^0 g\langle\sigma\rangle\right) \tilde{\psi}_n(\mathbf{k}) = \sum_{n=-\infty}^{\infty} \sum_{\mathbf{k}} \tilde{\psi}_{n,\alpha}^\dagger(\mathbf{k}) A_{\alpha\beta}(\mathbf{k}, n) \tilde{\psi}_{n,\beta}(\mathbf{k}). \tag{11.11}
 \end{aligned}$$

Notice that we absorbed the negative sign into our definition of A . To abbreviate the expression a little, we rename $\omega_n = \frac{2\pi}{\beta} \left\{n + \frac{1}{2}\right\}$. To proceed the calculation, we need to use what we know about the γ -matrices. We listed them in the beginning of this document, in the Notations section. After a straightforward substitution of Eq. (0.6) into Eq. (11.11), we find that the matrix A between the four-component Fourier modes reads

$$\begin{aligned}
 -A(\mathbf{k}, n) &= i\omega_n + \gamma^0 \gamma^i k_i + \mu + \gamma^0 g\langle\sigma\rangle \\
 &= \begin{pmatrix} i\omega_n + \mu + g\langle\sigma\rangle & 0 & k_3 & k_1 - ik_2 \\ 0 & i\omega_n + \mu + g\langle\sigma\rangle & k_1 + ik_2 & -k_3 \\ k_3 & k_1 - ik_2 & i\omega_n + \mu - g\langle\sigma\rangle & 0 \\ k_1 + ik_2 & -k_3 & 0 & i\omega_n + \mu - g\langle\sigma\rangle \end{pmatrix}. \tag{11.12}
 \end{aligned}$$

Now we just need to combine the results from Eqs. (11.10) and (11.11) to find the grand partition function for a system with one fermion of flavour f and one colour c inside a quantisation volume V . We denote it $\Theta_V^{f,c}$. The partition function the whole system with box quantisation, Θ_V , is simply the product of $\Theta_V^{f,c}$ and $\Theta_{\langle\sigma\rangle, V}$. In total, it reads

$$\begin{aligned}
 \Theta_V &= \Theta_{\langle\sigma\rangle, V} \prod_{f,c} \Theta_V^{f,c} \\
 &= \Theta_{\langle\sigma\rangle, V} \prod_{f,c} \int \prod_{\substack{\mathbf{k},\mathbf{k}' \\ n,n'}} d\tilde{\psi}_n(\mathbf{k}) d\tilde{\psi}_{n'}^\dagger(\mathbf{k}') \exp\left(-\sum_{\substack{n,n' \\ =-\infty}}^{\infty} \sum_{\mathbf{k},\mathbf{k}'} \tilde{\psi}_{n',\alpha}^\dagger(\mathbf{k}') \delta_{\mathbf{k},\mathbf{k}'} \delta_{n,n'} A_{\alpha\beta}(\mathbf{k}, n) \tilde{\psi}_{n,\beta}(\mathbf{k})\right). \tag{11.13}
 \end{aligned}$$

We know just how to solve this type of integral! We derive it in Appendix E.2, and it turns out to be the determinant of the matrix between the Grassmannian numbers $\tilde{\psi}_{n',\alpha}^\dagger(\mathbf{k}')$ and $\tilde{\psi}_{n,\beta}(\mathbf{k})$. This is expressed in Eq. (E.23). The matrix is already diagonal in n, n' and \mathbf{k}, \mathbf{k}' which means that the determinant over those indices just returns a product over n and \mathbf{k} . However, $A_{\alpha\beta}$ is not a diagonal matrix, and hence we must find its determinant. This is precisely why we calculated $-A$ explicitly in Eq. (11.12). We need not consider the sign in the determinant, as A is a 4×4 matrix, and pulling out the minus sign of A yields a factor $(-1)^4 = 1$.

$$\Theta_V = \exp(-\beta V \mathcal{V}) \prod_{q,c} \prod_{\mathbf{k},n} \det [A(\mathbf{k}, n)]. \tag{11.14}$$

Remembering way back to Eqs. (9.3) and (9.6), we see that we are in fact only interested in the logarithm of the grand partition function divided by V . Taking the limit $V \rightarrow \infty$ changes the sum over \mathbf{k} to an integral and introduces a factor V , which cancels the division. This removes the problem of dealing with a diverging volume factor. Taking the logarithm now is convenient, as it turns the product into a sum. We divide by β too, which allows us to identify that we are in fact calculating the negative grand potential, $-\Omega$.

$$\begin{aligned}
 -\Omega &= \frac{\ln[\Theta_V]}{\beta V} = -\mathcal{V} + \frac{1}{\beta V} \sum_{f,c} \sum_{n=-\infty}^{\infty} \sum_{\mathbf{k}} \ln [\det (A(\mathbf{k}, n))] \\
 &\xrightarrow{V \rightarrow \infty} -\mathcal{V} + \frac{N_c}{\beta} \sum_f \sum_{n=-\infty}^{\infty} \int d^3k \ln [\det (A(\mathbf{k}, n))], \tag{11.15}
 \end{aligned}$$

where we used Eq. (11.9). We have also used that A is independent of colour, and replaced that sum with N_c . We are now taking into account that the different fermions may not have the same chemical potential μ_f . In order to avoid a very cluttered notation, we will suppress the subscript f as there are already quite a few sub- and superscripts to take into account. But we will keep the summation, reminding us that we do in fact have different μ_f . The more faint of heart might use a computer program to proceed, but we try our luck at this 4×4 -determinant calculation. But first, we define $D_n^\pm = i\omega_n + \mu \pm g\langle\sigma\rangle$ (D for diagonal) and $k_\pm = k_1 \pm ik_2$, with $k_+k_- = k_1^2 + k_2^2$. This implies that $\mathbf{k}^2 = k_+k_- + k_3^2$. Armed with this simplifying rewriting, we find

$$\begin{aligned}
 \begin{vmatrix} D_n^+ & 0 & k_3 & k_- \\ 0 & D_n^+ & k_+ & -k_3 \\ k_3 & k_- & D_n^- & 0 \\ k_+ & -k_3 & 0 & D_n^- \end{vmatrix} &= D_n^+ \begin{vmatrix} D_n^+ & k_+ & -k_3 \\ k_- & D_n^- & 0 \\ -k_3 & 0 & D_n^- \end{vmatrix} + k_3 \begin{vmatrix} 0 & D_n^+ & -k_3 \\ k_3 & k_- & 0 \\ k_+ & -k_3 & D_n^- \end{vmatrix} - k_- \begin{vmatrix} 0 & D_n^+ & k_+ \\ k_3 & k_- & D_n^- \\ k_+ & -k_3 & 0 \end{vmatrix} \\
 &= D_n^+ D_n^- (D_n^+ D_n^- - k_3^2 - k_+k_-) - k_3^2 (D_n^+ D_n^- - k_3^2 - k_+k_-) \\
 &\quad - k_+k_- (D_n^+ D_n^- - k_3^2 - k_+k_-) \\
 &= (D_n^+ D_n^-)^2 - 2D_n^+ D_n^- \mathbf{k}^2 + \mathbf{k}^2 \mathbf{k}^2 = (D_n^+ D_n^- - \mathbf{k}^2)^2 \tag{11.16}
 \end{aligned}$$

Luckily, that determinant turned out to simplify quite a lot. Plugging Eq. (11.16) back into Eq. (11.15), we find that we must calculate

$$\begin{aligned}
 \frac{\ln[\Theta]}{\beta V} + \mathcal{V} &= \frac{2N_c}{\beta} \sum_f \int d^3k \sum_{n=-\infty}^{\infty} \ln [D_n^+ D_n^- - \mathbf{k}^2] \\
 &= \frac{2N_c}{\beta} \sum_f \int d^3k \sum_{n=-\infty}^{\infty} \ln [(i\omega_n + \mu)^2 - g^2\langle\sigma\rangle^2 - \mathbf{k}^2] \\
 &= \frac{2N_c}{\beta} \sum_f \int d^3k \sum_{n=-\infty}^{\infty} \ln [(i\omega_n + \mu)^2 - E_{\mathbf{k}}^2] \tag{11.17}
 \end{aligned}$$

The term $(i\omega_n + \mu)^2$ contains all dependencies of n , and $E_{\mathbf{k}} = \sqrt{g^2\langle\sigma\rangle^2 + \mathbf{k}^2}$, which contains all dependencies of \mathbf{k} . $E_{\mathbf{k}}$ has the same form as the relativistic energy, $E = \sqrt{m^2 + \mathbf{p}^2}$. To proceed from here, we need some clever tricks. The first one is to split the expression above into two sums. Then we reorder the second sum, such that it runs in a decreasing fashion, from ∞ to $-\infty$. Thirdly, we notice that $\omega_n = \frac{2\pi}{\beta} \{n + \frac{1}{2}\} = -\frac{2\pi}{\beta} \{-(n+1) + \frac{1}{2}\} = -\omega_{-n-1}$. The index shift does not matter, as the sum goes over all integers. Finally, we can merge the two sums together again and use the logarithm multiplication

property to obtain

$$\begin{aligned}
 2 \sum_{n=-\infty}^{\infty} \ln [(i\omega_n + \mu)^2 - E_{\mathbf{k}}^2] &= \sum_{n=-\infty}^{\infty} \ln [(i\omega_n + \mu)^2 - E_{\mathbf{k}}^2] + \sum_{n'=-\infty}^{\infty} \ln [(i\omega'_{n'} + \mu)^2 - E_{\mathbf{k}}^2] \\
 &= \sum_{n=-\infty}^{\infty} \ln [(i\omega_n + \mu)^2 - E_{\mathbf{k}}^2] + \sum_{n'=\infty}^{-\infty} \ln [(-i\omega_{-n'-1} + \mu)^2 - E_{\mathbf{k}}^2] \\
 (\text{let } n = -n' - 1 \text{ in the second term}) &= \sum_{n=-\infty}^{\infty} \ln [(i\omega_n + \mu)^2 - E_{\mathbf{k}}^2] + \sum_{n=-\infty}^{\infty} \ln [(-i\omega_n + \mu)^2 - E_{\mathbf{k}}^2] \\
 &= \sum_{n=-\infty}^{\infty} \ln [\{(i\omega_n + \mu)^2 - E_{\mathbf{k}}^2\} \{(-i\omega_n + \mu)^2 - E_{\mathbf{k}}^2\}].
 \end{aligned} \tag{11.18}$$

Now, the game is simply to multiply out the parentheses. We perform the calculation to find

$$\begin{aligned}
 \{(i\omega_n + \mu)^2 - E_{\mathbf{k}}^2\} \{(-i\omega_n + \mu)^2 - E_{\mathbf{k}}^2\} &= \underbrace{(i\omega_n + \mu + E_{\mathbf{k}})}_{\dots\dots\dots} \underbrace{(i\omega_n + \mu - E_{\mathbf{k}})}_{\dots\dots\dots} \underbrace{(-i\omega_n + \mu + E_{\mathbf{k}})}_{\dots\dots\dots} \underbrace{(-i\omega_n + \mu - E_{\mathbf{k}})}_{\dots\dots\dots} \\
 &= \underbrace{\{(\mu + E_{\mathbf{k}})^2 - (i\omega_n)^2\}}_{\dots\dots\dots} \underbrace{\{(\mu - E_{\mathbf{k}})^2 - (i\omega_n)^2\}}_{\dots\dots\dots} \\
 &= \{(\mu + E_{\mathbf{k}})^2 + \omega_n^2\} \{(\mu - E_{\mathbf{k}})^2 + \omega_n^2\}.
 \end{aligned} \tag{11.19}$$

The dotted underline indicates which parentheses we have multiplied together. In the end, we have managed to isolate the ω_n to only appear squared. The next trick is write the logarithm in terms of an integral. Note that we neglect whatever integration constant which may appear, as adding a constant to the logarithm of the partition function Θ does not change any of the thermodynamic properties. We now define $E_{\mathbf{k}}^{\pm} = E_{\mathbf{k}} \pm \mu$ to find

$$\begin{aligned}
 \frac{\ln[\Theta]}{\beta V} &= -\mathcal{V} + \frac{N_c}{\beta} \sum_f \int d^3k \sum_{n=-\infty}^{\infty} (\ln [E_{\mathbf{k}}^{+2} + \omega_n^2] + \ln [E_{\mathbf{k}}^{-2} + \omega_n^2]) \\
 &= -\mathcal{V} + \frac{N_c}{\beta} \sum_f \int d^3k \sum_{n=-\infty}^{\infty} \left(\int dE_{\mathbf{k}}^{+2} \frac{1}{E_{\mathbf{k}}^{+2} + \omega_n^2} + \int dE_{\mathbf{k}}^{-2} \frac{1}{E_{\mathbf{k}}^{-2} + \omega_n^2} \right) \\
 &= -\mathcal{V} + \frac{N_c}{\beta} \sum_f \int d^3k \sum_{n=-\infty}^{\infty} \left(\int dE_{\mathbf{k}}^+ \frac{2E_{\mathbf{k}}^+}{E_{\mathbf{k}}^{+2} + \omega_n^2} + \int dE_{\mathbf{k}}^- \frac{2E_{\mathbf{k}}^-}{E_{\mathbf{k}}^{-2} + \omega_n^2} \right).
 \end{aligned} \tag{11.20}$$

As a notational clarification here: The integral over momentum \mathbf{k} goes over all possible momenta $k_1, k_2, k_3 \in (-\infty, \infty)$, while the integral over $E_{\mathbf{k}}^{\pm}$ is an indefinite integral, which we introduced out of calculational convenience to remove the logarithms.

11.1.1 Matsubara Frequency Summation

So far, we have done a lot of manipulations in order to get the grand fermionic partition function to a calculable form. The next step is called Matsubara frequency summation. At first we exchange the ordering of taking the sum over n and the integral over $E_{\mathbf{k}}^{\pm}$ in Eq. (11.20). The problem at hand is to calculate the infinite sum over all n . In this section, we assume familiarity with complex analysis, specifically familiarity with residue calculation.

The idea is to write the sum as a complex contour integral. We are therefore going to use Cauchy's theorem the other way than it is ordinarily used – we are going from a sum to a closed contour in the complex plane. It may seem that we in this way are making the problem more convoluted. However, translating the problem into a complex integral actually allows us to reduce the number of summands from infinitely many to only two! We shall shortly see how this is the case. At first, our task is to find a

complex function $g(\omega)$ such that

$$\sum_{n=-\infty}^{\infty} \frac{1}{E_{\mathbf{k}}^{\pm 2} + \omega_n^2} = 2\pi i \sum_{n=-\infty}^{\infty} \operatorname{Res}_{\omega=\omega_n} g(\omega) = \oint_{\mathcal{C}} d\omega g(\omega). \quad (11.21)$$

The curve we integrate along in the complex plane needs to contain infinitely many poles in order for this strategy to work. As we sum over $\omega_n = \frac{2\pi}{\beta} \{n + \frac{1}{2}\}$, we look for a function which has poles at $p_n = \frac{2\pi}{\beta} \{n + \frac{1}{2}\}$, or alternatively at $p_n = \frac{2\pi i}{\beta} \{n + \frac{1}{2}\}$ for every n . By thinking a while of functions with such a periodic pole behaviour, we may suggest

$$f(\omega) = \frac{1}{1 + \exp(\beta\omega)}, \quad \omega \in \mathbb{C}. \quad (11.22)$$

We notice how the denominator approaches zero whenever ω approaches $\frac{2\pi i}{\beta} \{n + \frac{1}{2}\}$, just like we wanted. Everywhere else, $f(\omega)$ is analytic. Now we need to find the residue of this function around one particular pole p_n . From complex analysis, we know that the residue is the coefficient in front of the $\frac{1}{\omega}$ in the Laurent-expansion. Therefore, we investigate how $f(\omega)$ behaves close to a pole, that is at $\omega = \frac{2\pi i}{\beta} \{n + \frac{1}{2}\} + \epsilon$

$$\begin{aligned} f\left(\frac{2\pi i}{\beta} \{n + \frac{1}{2}\} + \epsilon\right) &= \frac{1}{1 + \exp(2\pi i \{n + \frac{1}{2}\} + \beta\epsilon)} = \frac{1}{1 + \exp(2\pi i n) \exp(i\pi) \exp(\beta\epsilon)} \\ &= \frac{1}{1 - (1 + \beta\epsilon + \mathcal{O}(\beta^2\epsilon^2))} = \frac{1}{\beta\epsilon} \frac{1}{1 + \mathcal{O}(\beta\epsilon)} = \frac{1}{\beta\epsilon} h(\beta\epsilon), \end{aligned} \quad (11.23)$$

where $h(\beta\epsilon) \xrightarrow{\epsilon \rightarrow 0} 1$. We may conclude that $f(\omega)$ has simple poles at p_n , with the coefficient $\frac{1}{\beta}$. If we now let \mathcal{C}_n denote a closed curve containing *one* pole p_n and that the curve is oriented counter-clockwise, we find from Cauchy's integral formula that

$$\operatorname{Res}_{\omega=\omega_n} f(\omega) = \frac{1}{2\pi i} \oint_{\mathcal{C}_n} d\omega f(\omega) = \lim_{\epsilon \rightarrow 0} \frac{1}{\beta} h(\beta\epsilon) = \frac{1}{\beta}. \quad (11.24)$$

With our $f(\omega)$, we have found a complex function with poles which are situated where we want them, but the values of the residues are not what we want. However, if we modify $f(\omega)$ with an extra term which is analytic close to the imaginary axis, we may get the residues we seek. We take

$$g(\omega) = \frac{\beta}{E_{\mathbf{k}}^{\pm 2} - \omega^2} \frac{f(\omega)}{2\pi i}. \quad (11.25)$$

We see that $g(\omega)$ now has two new poles along the real axis, in $r_{\pm} = \pm E_{\mathbf{k}}^{\pm}$. Do not confuse the superscript \pm in $E_{\mathbf{k}}^{\pm}$ to be related to the sign in front of the pole! When we evaluate the residue of a pole along the imaginary axis p_n , we find

$$\oint_{\mathcal{C}_n} d\omega g(\omega) = 2\pi i \operatorname{Res}_{\omega=\omega_n} g(\omega) = \frac{2\pi i \beta}{E_{\mathbf{k}}^{\pm} + \omega_n^2} \frac{1}{2\pi i \beta} = \frac{1}{E_{\mathbf{k}}^{\pm} + \omega_n^2}. \quad (11.26)$$

We have found just the function $g(\omega)$ we were looking for. $g(\omega)$ has another key property, namely that it vanishes at infinity at least as quickly as $\frac{1}{|\omega^2|}$. The integral along a half-circle where we send $r \rightarrow \infty$ therefore vanishes. It also implies the convergence of the sum over n , which we tacitly assumed when we changed the ordering of sums and integrals. Summing over all n corresponds to taking a contour containing all the poles along the imaginary axis. In Fig. 11.1 we illustrate how contours \mathcal{C}_n around each pole correspond to one contour containing all. Finally, we show an equivalent contour $\mathcal{C}' = \mathcal{C}'_1 + \mathcal{C}'_2$. This alternative contour contains only the two simple poles due to the factor $\frac{1}{E_{\mathbf{k}} - \omega^2}$.

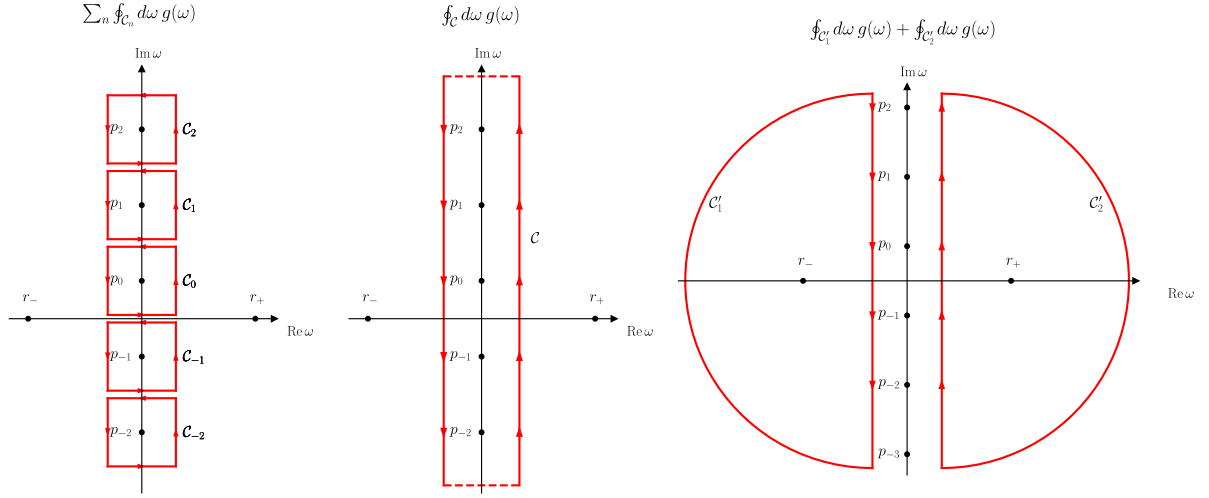


Figure 11.1: The figure shows a portion of the complex plane with some of the poles of $g(\omega)$ as given in Eq. (11.25). The poles appear equidistantly along the imaginary axis towards both positive and negative infinity. There are also two poles on the real axis, labelled r_- and r_+ . These are the only poles not lying on the imaginary axis. To the right, we have illustrated contours which only contain *one* pole each. We calculate the integral along one such loop in Eq. (11.26). In the middle, we have plotted one single contour, which is equivalent to summing up all the loops containing only one pole. This contour integral is equal to the sum we seek to calculate given in Eq. (11.21). Instead of calculating the sum over residues of an infinite number of poles, we may deform our contour into containing only the two poles lying in the real axis. This task is a lot easier than calculating the infinite sum.

Now, calculating the residue of two simple poles is certainly a problem we are able to solve. In total, we may summarise the whole procedure mathematically as

$$\begin{aligned}
 \sum_{n=-\infty}^{\infty} \frac{1}{E_{\mathbf{k}}^{\pm 2} + \omega_n^2} &= 2\pi i \sum_{n=-\infty}^{\infty} \operatorname{Res}_{\omega=\omega_n} g(\omega) = \sum_{n=-\infty}^{\infty} \oint_{C_n} d\omega g(\omega) = \oint_C d\omega g(\omega) \\
 &= \oint_{C'_1} d\omega g(\omega) + \oint_{C'_2} d\omega g(\omega) = 2\pi i \operatorname{Res}_{\omega=r_-} g(\omega) + 2\pi i \operatorname{Res}_{\omega=r_+} g(\omega) \\
 &= 2\pi i \lim_{\omega \rightarrow -E_{\mathbf{k}}^{\pm}} (\omega + E_{\mathbf{k}}^{\pm}) \frac{\beta}{(E_{\mathbf{k}}^{\pm} + \omega)(E_{\mathbf{k}}^{\pm} - \omega)} \frac{1}{1 + \exp(\beta\omega)} \frac{1}{2\pi i} \\
 &\quad 2\pi i \lim_{\omega \rightarrow E_{\mathbf{k}}^{\pm}} (\omega - E_{\mathbf{k}}^{\pm}) \frac{\beta}{(E_{\mathbf{k}}^{\pm} + \omega)(E_{\mathbf{k}}^{\pm} - \omega)} \frac{1}{1 + \exp(\beta\omega)} \frac{1}{2\pi i} \\
 &= \frac{\beta}{2E_{\mathbf{k}}^{\pm}} \frac{1}{1 + \exp(-\beta E_{\mathbf{k}}^{\pm})} - \frac{\beta}{2E_{\mathbf{k}}^{\pm}} \frac{1}{1 + \exp(\beta E_{\mathbf{k}}^{\pm})} \\
 &= \frac{\beta}{2E_{\mathbf{k}}^{\pm}} \left(1 - \frac{2}{1 + \exp(\beta E_{\mathbf{k}}^{\pm})} \right). \tag{11.27}
 \end{aligned}$$

From the second to the third line above, we have simply used the formula for calculating residues of simple poles. After tidying up, we arrive at a compact expression for the infinite sum we wished to evaluate. Armed with this result, we are ready to continue the calculation of $\ln[\Theta]$ in Eq. (11.20).

11.2 Divergence in the Quark-Meson Model in the Mean Field Approximation

Without further ado, we substitute Eq. (11.27) into Eq. (11.20).

$$\begin{aligned}
 \frac{\ln[\Theta]}{\beta V} &= -\mathcal{V} + \frac{N_c}{\beta} \sum_f \int d^3k \left[\int dE_{\mathbf{k}}^+ \frac{2E_{\mathbf{k}}^+ \beta}{2E_{\mathbf{k}}^+} \left(1 - \frac{2}{1 + \exp(\beta E_{\mathbf{k}}^+)} \right) + \int dE_{\mathbf{k}}^- \frac{2E_{\mathbf{k}}^- \beta}{2E_{\mathbf{k}}^-} \left(1 - \frac{2}{1 + \exp(\beta E_{\mathbf{k}}^-)} \right) \right] \\
 &= -\mathcal{V} + \frac{N_c}{\beta} \sum_f \int d^3k \left[\beta E_{\mathbf{k}}^+ + \beta E_{\mathbf{k}}^- + 2 \ln [1 + \exp(-\beta E_{\mathbf{k}}^+)] + 2 \ln [1 + \exp(-\beta E_{\mathbf{k}}^-)] \right] \\
 &= -\mathcal{V} + \frac{2N_c}{\beta} \sum_f \int d^3k \left[\beta E_{\mathbf{k}} + \ln [1 + \exp(-\beta E_{\mathbf{k}} - \beta \mu_q)] + \ln [1 + \exp(-\beta E_{\mathbf{k}} + \beta \mu_f)] \right]. \quad (11.28)
 \end{aligned}$$

Here, we have calculated the indefinite integral and remembered how we defined $E_{\mathbf{k}}^{\pm} = E_{\mathbf{k}} \pm \mu_f$ (earlier, we suppressed the flavour index). To check that we performed the indefinite integral correctly, we calculate the derivative

$$\frac{d}{dE_{\mathbf{k}}^{\pm}} \left(\ln [1 + \exp(-\beta E_{\mathbf{k}}^{\pm})] \right) = -\beta \frac{\exp(-\beta E_{\mathbf{k}}^{\pm})}{1 + \exp(-\beta E_{\mathbf{k}}^{\pm})} = \frac{-\beta}{1 + \exp(\beta E_{\mathbf{k}}^{\pm})}, \quad (11.29)$$

which is the verification we wanted. Additionally, we notice that the first term of the integrand, $E_{\mathbf{k}}$, is clearly divergent. We shall fix this divergence in the standard way, namely that we regularise the integral and remove the divergent part through renormalisation. We use dimensional regularisation, which we discuss in Appendix H. Notice that in Appendix H, we dimensionally regularised an integral with measure $d^d k$, while we here have a factor of $(2\pi)^{-d}$ absorbed in the measure, as denoted by the bar in $\bar{d}^3 k$. We must remember to include this factor in Eq. (H.24) with $d = 3$, $a = \frac{1}{2}$. We also recall $\Delta = g^2 \langle \sigma \rangle^2$.

$$\begin{aligned}
 \int \bar{d}^3 E_{\mathbf{k}} \xrightarrow{\text{dim.reg.}} \mu^{2\epsilon} \int d^{3-2\epsilon} k E_{\mathbf{k}} & \quad (\text{Eq. (H.24)}) \\
 &= \mu^{2\epsilon} \frac{\pi^{\frac{3}{2}-\epsilon}}{(2\pi)^{3-2\epsilon}} \frac{\Gamma(-2+\epsilon)}{\Gamma(-\frac{1}{2})} \Delta^{2-\epsilon} = \frac{\Delta^2}{(4\pi)^{\frac{3}{2}}} \left(\frac{4\pi\mu^2}{\Delta} \right)^{\epsilon} \frac{\Gamma(-2+\epsilon)}{\Gamma(-1+\frac{1}{2})} \\
 &= \frac{\Delta^2}{(4\pi)^{\frac{3}{2}}} \left[1 + \epsilon \ln \left(\frac{4\pi\mu^2}{\Delta} \right) \right] \frac{\Gamma(-2+\epsilon)}{\Gamma(-1+\frac{1}{2})}. \quad (11.30)
 \end{aligned}$$

In Appendix H, we also briefly reviewed the Γ -function. To re-express the Γ s above we need property (2) from Eq. (H.7), specifically $\Gamma(1+x) = x\Gamma(x)$. Using $-1+x$ instead of x we can write

$$\Gamma(-2+\epsilon) = \frac{\Gamma(-1+\epsilon)}{-2+\epsilon} = \frac{\Gamma(\epsilon)}{(-1+\epsilon)(-2+\epsilon)} = \frac{\frac{1}{\epsilon} - \gamma_E + \mathcal{O}(\epsilon)}{2-3\epsilon+\epsilon^2} = \frac{1}{2} \left(\frac{1}{\epsilon} + \frac{3}{2} - \gamma_E \right) + \mathcal{O}(\epsilon), \quad (11.31)$$

$$\Gamma(-1+\frac{1}{2}) = \frac{\Gamma(\frac{1}{2})}{-1+\frac{1}{2}} = -2\sqrt{\pi}. \quad (11.32)$$

This allows us to continue Eq. (11.30). Naturally, we neglect any term $\mathcal{O}(\epsilon)$ which appears.

$$\begin{aligned}
 2N_c \sum_q \int \bar{d}^3 k E_{\mathbf{k}} &= -N_f N_c \frac{\Delta^2}{16\pi^2} \left[1 + \epsilon \ln \left(\frac{4\pi\mu^2}{\Delta} \right) \right] \left(\frac{1}{\epsilon} + \frac{3}{2} - \gamma_E \right) \\
 &= -N_f N_c \frac{g^4 \langle \sigma \rangle^4}{16\pi^2} \left[\frac{1}{\epsilon} + \frac{3}{2} + \ln \left(\frac{\tilde{\mu}^2}{g^2 \langle \sigma \rangle^2} \right) \right]. \quad (11.33)
 \end{aligned}$$

In the last line, we defined a new dimensionful scale $\tilde{\mu}^2 = 4\pi \exp(-\gamma_E) \mu^2$, which we will soon comment. In the regularised integral, we find that there is no dependence of quark flavour, and we are allowed to replace the sum with a factor N_f . Had we considered different masses, m_q , for the different quarks, we

would simply keep the sum and noted that m_q varies with flavour f . Of course, we would like to remove the divergent term. This procedure is called *renormalisation*. The idea is that we redefine our Lagrangian density such that it no longer causes divergences. To do so, we include so-called counterterms, which are designed to cancel the divergences. The original Lagrangian we now rename \mathcal{L}_0 , and call it the *bare* Lagrangian. We may write the new Lagrangian density as

$$\mathcal{L} = \underbrace{\mathcal{L}_0}_{\text{bare } \mathcal{L}} + \underbrace{\delta\mathcal{L}}_{\text{counterterm } \mathcal{L}}. \quad (11.34)$$

This has to be done whenever we encounter divergent integrals in field theory. To make the procedure a bit more tangible, we consider the Lagrangian we are working with in this section. We have one divergence which is proportional to $g^4\langle\sigma\rangle^4$

$$\begin{aligned} \mathcal{L}_0 + \delta\mathcal{L} &= \bar{\Psi}(i\cancel{\partial} - \mu\gamma^0 - m)\Psi - \mathcal{V}(\langle\sigma\rangle) + \delta\mathcal{L} \\ &= \bar{\Psi}(i\cancel{\partial} - \mu\gamma^0 - m)\Psi - (\lambda + \delta\lambda)\frac{\langle\sigma\rangle^4}{4} + \frac{m^2}{2}\langle\sigma\rangle^2 + h\langle\sigma\rangle. \end{aligned} \quad (11.35)$$

In our specific case, we can remove the divergence by adding a counterterm to the coupling constant $\lambda \rightarrow \lambda + \delta\lambda$. Equivalently, we identify the counterterm Lagrangian density $\delta\mathcal{L} = -\delta\lambda\frac{\langle\sigma\rangle^4}{4}$. To remove the divergent $\frac{1}{\epsilon}$ -term, we may set

$$\delta\lambda = -N_f N_c \frac{g^4}{4\pi^2} \frac{1}{\epsilon}. \quad (11.36)$$

An important note on renormalisation is that there are several schemes to choose from. In Eq. (11.33) we absorbed two factors, $\ln(4\pi)$ and $-\gamma_E$, into a new scale $\tilde{\mu}$. Removing the divergence with a counterterm and defining the scale in this way is called the modified minimal subtraction scheme, denoted $\overline{\text{MS}}$. Had we not redefined the scale this way, and simply counteracted the divergent $\frac{1}{\epsilon}$ -term, the regularisation procedure would have contributed with two more terms, $\ln(4\pi)$ and $-\gamma_E$ to the new Lagrangian. This, we call the minimal subtraction scheme, denoted MS.

We have illustrated how to remove a divergence by introducing a counterterm to the Lagrangian. However, we have only done so for the fermions. For instance, had we not started off with the mean-field approximation, we would have found divergences from the mesonic sector as well. Renormalising the mesonic sector would have given other finite term, just as in the case for the fermionic renormalisation. These finite terms would have acted as corrections to the masses and couplings to the theory. When we substitute the parameters of the theory with measured values, these corrections influence the substitutions. Thus, not renormalising the full theory is in one way inconsistent.

A full renormalisation requires *a lot* of calculation. Luckily, there exists one simplifying "limit" we can consider in order to save many steps. This is called the **large N_c -limit**. We know that $N_c = 3$, however, we could pretend that $N_c \rightarrow \infty$. If we draw up and start to calculate all the one loop-diagrams, we find that some of them are $\mathcal{O}(N_c^1)$, while others are only $\mathcal{O}(N_c^0)$. In the large N_c -limit, we can justify only taking into account the diagrams that are $\mathcal{O}(N_c^1)$. Thus, we are systematic in going to one loop *and* disregarding diagrams which give contributions of $\mathcal{O}(N_c^0)$. This treatment is arguably a consistent one. We know that N_c is in fact not very large, but the diagrams we are neglecting are at least suppressed by a factor of $\frac{1}{3}$ as compared to the ones we take into account.

11.3 Pressure and Energy Density in the Quark-Meson Model at Zero Temperature

Now that we have commented on the difficult, divergent part of the integral, we turn to the well-behaved terms. By typing these sorts of integrals into an integral solver, we find that the solutions are the so-called polylogarithmic functions. However, if we are interested in *cold* neutron stars, we take the limit $T \rightarrow 0$, or equivalently, $\beta \rightarrow \infty$. This allows us to express $\frac{\ln[\Theta]}{\beta V}$ in terms of familiar functions. To see how the

integral simplifies, we consider the two last terms of the exponentials in Eq. (11.28) for $\beta \gg E_{\mathbf{k}}, \mu$

$$\ln[1 + \exp(-\beta\{E_{\mathbf{k}} \pm \mu_q\})] = \begin{cases} -\beta(E_{\mathbf{k}} - \mu_q) + \mathcal{O}[\exp(-\beta\{\mu_q - E_{\mathbf{k}}\})], & \text{when } E_{\mathbf{k}} - \mu_q < 0, \\ 0 + \mathcal{O}[\exp(-\beta\{E_{\mathbf{k}} \pm \mu_q\})], & \text{otherwise.} \end{cases} \quad (11.37)$$

Since we know that $E_{\mathbf{k}} = \sqrt{k^2 + m_q^2} > 0$, and we assume that we are dealing with positive chemical potentials μ_q , we immediately see that choosing $E_{\mathbf{k}} + \mu_q$ gives a small exponential term. Remember that $m_q = g\langle\sigma\rangle$. Similarly, the exponential term will be very small if the difference $E_{\mathbf{k}} - \mu$ is positive. On the other hand, if the difference $E_{\mathbf{k}} - \mu$ is negative, then the act of letting β be large leaves us one term proportional to β which we certainly are not allowed to neglect. If we like, we could perform an expansion and calculate the results up to some desired order of $\exp(-n\beta(E_{\mathbf{k}} \pm \mu))$. More interestingly for us: Choosing β large enough allows us to neglect all $\mathcal{O}(\dots)$. In the following, we will do this, and it is called the zero temperature limit. We note that the condition $E_k - \mu < 0$ is equivalent to $k^2 < \mu^2 - m_q^2$. From the two finite terms in Eq. (11.28), the zero-temperature limit allows us to only consider

$$\begin{aligned} \frac{2N_c}{\beta} \int d^3k \ln[1 + \exp(-\beta(E_{\mathbf{k}} - \mu_f))] &\stackrel{\beta \rightarrow \infty}{=} \frac{8\pi N_c}{(2\pi)^3} \int_0^{\sqrt{\mu_f^2 - m_q^2}} dk k^2 (\mu_f - \sqrt{k^2 + m_q^2}) \\ &= \frac{m_q^4 N_c}{\pi^2} \left(\frac{x_{F,f}^3 \sqrt{1 + x_{F,q}^2}}{12} + \frac{\operatorname{arcsinh}(x_{F,f}) - x_{F,f} \sqrt{1 + x_{F,f}^2}}{8} \right) \\ &= \frac{m_q^4 N_c}{\pi^2} \mathcal{F}(x_{F,f}), \end{aligned} \quad (11.38)$$

where $x_{F,f}$ is the dimensionless Fermi-momentum for quark-flavour f . For the up and down quark, it reads

$$x_{F,u} = \sqrt{\frac{\mu_u^2}{g^2\langle\sigma\rangle^2} - 1} \quad x_{F,d} = \sqrt{\frac{\mu_d^2}{g^2\langle\sigma\rangle^2} - 1}. \quad (11.39)$$

In Eq. (11.38), we have skipped quite a few steps from the first to the second line. This is because we have encountered exactly this type of integrals before! This happened back in the section about ideal neutron stars. Apart from some constants, we perform the calculation in Eq. (4.21). Since the parenthesis appears in a few of the following calculations, we give it its own name, $\mathcal{F}(x_{F,f})$. Its derivative will also be important. It reads

$$\frac{d\mathcal{F}(x_{F,f})}{dx_{F,f}} = \frac{1}{3} \frac{x_{F,f}^4}{\sqrt{x_{F,f}^2 + 1}}, \quad (11.40)$$

We are now in a position to write the grand potential for a system with two quark flavours as

$$\Omega = \underbrace{\mathcal{V} + \frac{N_f N_c g^4 \langle\sigma\rangle^4}{16\pi^2} \left[\frac{3}{2} + \ln\left(\frac{\tilde{\mu}^2}{g^2\langle\sigma\rangle^2}\right) \right]}_{\Omega_0} - \frac{g^4 \langle\sigma\rangle^4 N_c}{\pi^2} [\mathcal{F}(x_{F,u}) + \mathcal{F}(x_{F,d})]. \quad (11.41)$$

In addition to two quark flavours, we expect to find electrons inside the neutron star. Adding free electrons is a simple exercise: We just get a contribution as though there were one more quark, except that the mass and chemical potential are different. In short, we add $\Omega_e = -\frac{m_e^4}{\pi^2} \mathcal{F}(x_{F,e})$. We introduce N_i , which is unity for the electron and N_c for the quarks, in order to write everything in one sum over i . In terms of the chemical potentials and the particle masses, p reads in its full glory

$$\begin{aligned} p = -\Omega &= -\Omega_0 + \frac{g^4 \langle\sigma\rangle^4 N_c}{\pi^2} [\mathcal{F}(x_{F,u}) + \mathcal{F}(x_{F,d})] + \frac{m_e^4}{\pi^2} \mathcal{F}(x_{F,e}) \\ &= -\mathcal{V} - \frac{N_f N_c m_q^4}{16\pi^2} \left[\frac{3}{2} + \ln\left(\frac{\tilde{\mu}^2}{m_q^2}\right) \right] \\ &\quad + \sum_{i \in \{u, d, e\}} \frac{N_i}{4\pi^2} \left[\frac{1}{3} (\mu_i^2 - m_i^2)^{\frac{3}{2}} \mu_i + \frac{m_i^4}{2} \ln\left(\sqrt{\frac{\mu_i^2}{m_i^2} - 1} + \frac{\mu_i}{m_i}\right) - \frac{m_i^2}{2} \sqrt{\mu_i^2 - m_i^2} \mu_i \right]. \end{aligned} \quad (11.42)$$

In the beginning, we recalled Eq. (9.3) to realise that we have actually calculated the pressure when we found $-\Omega$. Additionally, we have expressed $\operatorname{arcsinh}(x)$ in terms of $\ln(x)$. The last two lines of the expression above arise from having a positive chemical potential. In other words, setting the chemical potentials $\mu_u = \mu_d = \mu_e = 0$ leaves us with only the first line of the second equality. This is also a good time to be satisfied about finding similar results to the simpler statistical physics model. Had we only introduced one massive non-interacting fermion, as we did in the case for the ideal neutron star, we would have found the same p and ϵ , apart from the Ω_0 . What we have managed to capture by using the path integral formalism, is that an interaction with a constant background field will give a dynamic mass to the particles. This mass will change as μ_u and μ_d changes, as we shall see later.

We also notice from the expression for p that even with no particles present, the mesonic potential will give a contribution to the pressure. This background pressure has some curious implications. In a sense, it acts as though there existed a force which pushes the particles apart (when positive) or pulls them together (when negative). In fact, this is how the MIT bag model implements a way to model quark confinement [39]. In this model, we choose a bag parameter B which acts as a negative pressure in the vacuum. A bound hadronic state is in the bag model three quarks "held together" by the external pressure in a bag. Later, we will shift the pressure in the vacuum, which is equivalent to choosing such a bag parameter. The bag constant is added to the grand potential, which means that the pressure and energy density change like

$$p \xrightarrow{\text{bag shift}} p - B, \quad \text{and} \quad \epsilon \xrightarrow{\text{bag shift}} \epsilon + B. \quad (11.43)$$

This bag shift will be important later, however, we will leave the pressure and energy density unshifted for now.

We would also like to find the energy density, ϵ . For this, we use Eq. (9.6) and our results for the evaluation of Eq. (11.28).

$$\begin{aligned} \epsilon &= -\frac{1}{V} \frac{\partial \ln[\Theta]}{\partial \beta} + \sum_{i \in \{u, d, e\}} \frac{\mu_i}{\beta V} \frac{\partial \ln[\Theta]}{\partial \mu_i} = -\frac{1}{V} \frac{\partial(\beta V \Omega)}{\partial \beta} + \sum_i \mu_i \frac{\partial x_{F,i}}{\partial \mu_i} \frac{\partial \Omega}{x_{F,i}} \\ &= -p + \sum_i \frac{N_i m_i^4}{3} \frac{x_{F,i}^3}{\pi^2} \sqrt{x_{F,i}^2 + 1} \\ &= \Omega_0 + \sum_i N_i \frac{m_i^4}{\pi^2} \left[\frac{x_{F,i}^3 \sqrt{x_{F,i}^2 + 1}}{4} + \frac{x_{F,i} \sqrt{x_{F,i}^2 + 1} - \ln(x_{F,i} + \sqrt{x_{F,i}^2 + 1})}{8} \right] \\ &= \mathcal{V} + \frac{N_f N_c m_q^4}{16\pi^2} \left[\frac{3}{2} + \ln\left(\frac{\tilde{\mu}^2}{m_q^2}\right) \right] \\ &\quad + \sum_{i \in \{u, d, e\}} \frac{N_i}{4\pi^2} \left[(\mu_i^2 - m_i^2)^{\frac{3}{2}} \mu_i + \frac{m_i^2}{2} \sqrt{\mu_i^2 - m_i^2} \mu_i - \frac{m_i^4}{2} \ln\left(\sqrt{\frac{\mu_i^2}{m_i^2} - 1} + \frac{\mu_i}{m_i}\right) \right]. \end{aligned} \quad (11.44)$$

In the zero-temperature limit, Ω is independent of β , and therefore the derivative with respect to β becomes simple in the first line. Despite being quite long expressions, p and ϵ are only consisting of well-known functions, which we soon will use numerically.

Lastly, the expression for the number densities will come in handy. Let now q denote one of the two quark flavours. Combining Eqs. (9.4) and (11.41) with the addition of electrons, we find

$$\begin{aligned} n_q &= -\frac{\partial \Omega}{\partial \mu_q} = \frac{g^4 \langle \sigma \rangle^4 N_c}{\pi^2} \frac{\partial x_{F,q}}{\partial \mu_q} \frac{\partial \mathcal{F}(\mathcal{F},)}{\partial x_{F,q}} = \frac{g^3 \langle \sigma \rangle^3 N_c}{3\pi^2} x_{F,q}^3 = \frac{N_c}{3\pi^2} (\mu_q^2 - g^2 \langle \sigma \rangle^2)^{\frac{3}{2}}, \\ n_e &= \frac{1}{3\pi^2} (\mu_e^2 - m_e^2)^{\frac{3}{2}}. \end{aligned} \quad (11.45)$$

11.4 Parameter Fit at Tree Level

Before we can let a numerical integrator tear away at the TOV-equations with the newly acquired expressions for p and ϵ , we need to constrain the host of parameters that we have introduced along the way. The parameters are

- μ_f , three chemical potentials,
- $\langle\sigma\rangle$, the mean field value of the σ -meson,
- g , the coupling between σ and the quarks,
- λ , the interaction coupling for the mesons,
- h , the linear, chiral symmetry breaking coupling,
- v^2 , which appears in the mass terms,
- $\tilde{\mu}^2$, the renormalisation scale.

As a first approximation, we will simply take the masses and couplings appearing in the Lagrangian as they stand. This is called the tree-level masses and couplings. We keep in mind that a proper renormalising of the theory will give corrections to these terms. In truth, it is the shifted, renormalised values for the masses and couplings which may be substituted with physical measurements. Nevertheless, the computation is instructive, and it resembles the one we shall perform for the properly renormalised theory. We will call the tree-level substitution for the inconsistently renormalised QM model.

So, what physical values shall substitute the parameters of our theory? In Eq. (10.31), we recognise the masses of the σ -particle and the pions. The Particle Data Group (PDG) have extensive data on measurements of different particle masses, and the σ -particle and the pions are among them. Everything is contained in Ref. [36]. As this paper is *immensely* long, we help narrow down the search: The pion masses are listed on p. 38, while the scalar σ goes under the name of $f_0(500)$, and is found on p. 860, in (64.4). We use the average value of the three pions, rounded up.

In the fermionic sector of the Lagrangian density, we have also a quark mass term for the up and down quark. It is tempting to use the masses for the quarks listed by PDG directly. These are called the bare masses, and they are not directly accessible through experiments, as quarks are never observed on their own. For our model, however, we are interested in the quark *constituent* mass. Loosely speaking, this is the mass each quark contributes with in a bound state, as discussed in Ref. [40], pp. 121–122. There, the quark constituent mass of the u and d are reported to be ~ 363 MeV when the quarks are bound in hadrons. We are, however, warned that the numbers are both "speculative" and "model-dependent". Using a bag model for confinement, it makes sense to use the constituent quark masses. A hadron is, as mentioned, three quarks held together by a bag pressure. The mass of the total system should be the masses of the constituents and the binding energy from the bag constant B . Lastly, we have a non-zero mean-field value $\langle\sigma\rangle$. This is the symmetry breaking term – which, in the vacuum, is related to the pion decay constant, $f_\pi = 93$ MeV, Ref. [27], p. 670 (Note that there are different conventions, shifting the pion decay constant by factors of $\sqrt{2}$, see e.g. Ref. [41]). We list the parameter values we use in Table 11.1.

Physical quantity	Measured/modelled value [MeV]	Relation to QM model at tree level
m_q	300	$m_q = g\langle\sigma\rangle$
m_π	139	$m_\pi^2 = \lambda(\langle\sigma\rangle^2 - v^2)$
m_σ	400-550	$m_\sigma^2 = \lambda(3\langle\sigma\rangle^2 - v^2)$
f_π	93	$f_\pi = \langle\sigma\rangle$

Table 11.1: Physical quantities which links the parameters of the quark-meson model to measurements. The measurements of m_π and f_π are precise. The measured value of m_σ , however, has large uncertainty. m_q is the constituent quark mass which is model dependent. We opted for the same value as in Ref. [1], to make comparison easy.

With the relations and values listed in Table 11.1, we can express both λ and v^2 solely in terms of m_π ,

m_σ and f_π . To determine h , we use that $\langle\sigma\rangle = f_\pi$ minimises the mesonic potential \mathcal{V} , which gives the expression Eq. (10.28). Apart from the chemical potentials, we only need to restrain the renormalisation scale, $\tilde{\mu}$. To do this, we turn our attention to the grand potential when the fermionic chemical potentials are all vanishing, which we have named Ω_0 . From looking at Eq. (11.41), we find that it reads

$$\Omega_0(\langle\sigma\rangle) = \mathcal{V}(\langle\sigma\rangle) + \frac{N_f N_c g^4 \langle\sigma\rangle^4}{16\pi^2} \left[\frac{3}{2} + \ln \left(\frac{\tilde{\mu}^2}{g^2 \langle\sigma\rangle^2} \right) \right]. \quad (11.46)$$

We impose the constraint that Ω_0 has an extremal value when $\langle\sigma\rangle = f_\pi$.

$$0 = \frac{\partial\Omega_0}{\partial\langle\sigma\rangle} \Big|_{\langle\sigma\rangle=f_\pi} = \frac{\partial\mathcal{V}}{\partial\langle\sigma\rangle} \Big|_{\langle\sigma\rangle=f_\pi} + \frac{\partial}{\partial\langle\sigma\rangle} \left(\frac{N_f N_c g^4 \langle\sigma\rangle^4}{16\pi^2} \left[\frac{3}{2} + \ln \left(\frac{\tilde{\mu}^2}{g^2 \langle\sigma\rangle^2} \right) \right] \right) \Big|_{\langle\sigma\rangle=f_\pi}. \quad (11.47)$$

By assumption, we already know that the mesonic potential \mathcal{V} is at its minimum at $\langle\sigma\rangle = f_\pi$, allowing us to set the first term to zero. The relation above thus forces the second derivative to be zero, or more specifically that

$$\tilde{\mu}^2 = m_q^2 \exp(-1). \quad (11.48)$$

At this point, we have constrained all the parameters of the mesonic sector of the quark-meson model. Combining these together, we get the tree-level relations for the vacuum

$$\begin{aligned} \langle\sigma\rangle = f_\pi = 93 \text{ MeV}, \quad g = \frac{m_q}{f_\pi} = 3.23, \quad h = m_\pi^2 f_\pi = (122 \text{ MeV})^3, \\ \lambda = \frac{m_\sigma^2 - m_\pi^2}{2f_\pi^2}, \quad v^2 = f_\pi^2 \frac{m_\sigma^2 - 3m_\pi^2}{m_\sigma^2 - m_\pi^2}, \quad \text{and} \quad \tilde{\mu} = m_q \exp(-\frac{1}{2}) = 182 \text{ MeV}. \end{aligned} \quad (11.49)$$

We have not yet assigned a value to the parameters that depend on m_σ . This is because we 'will use different values of m_σ as "half free" model parameter. In our tree-level treatment of the QM model, we may in fact just barely choose a m_σ within the range of the measured values. To see why, we consider the grand potential for zero chemical potential as a function of $\langle\sigma\rangle$ for different values of m_σ . Note that we keep *all* other parameters fixed as given in Eq. (11.49). In this way, we have chosen the parameters such that the derivative of the grand potential will be zero at $\langle\sigma\rangle = f_\pi$, but we are not guaranteed to find a minimum. We can calculate the curvature of Ω_0 with respect to $\langle\sigma\rangle$, and require it to be larger than zero to ensure a grand potential minimum. The calculation (doubly differentiation Eq. (10.32) and the terms from the inconsistent renormalisation) yields the constraint

$$m_\sigma > \frac{\sqrt{3}}{\pi} \frac{m_q^2}{f_\pi} \approx 533 \text{ MeV}. \quad (11.50)$$

As we see, this mass lies in the very upper end of the measured values of m_σ . We illustrate this by plotting the grand potential given in Eq. (10.32) with different values for $\langle\sigma\rangle$ in Fig. 11.2. For larger and larger m_σ , the minimum becomes more and more pronounced. We also note that the background pressure is also negative, as though there was a force pulling the particles together.

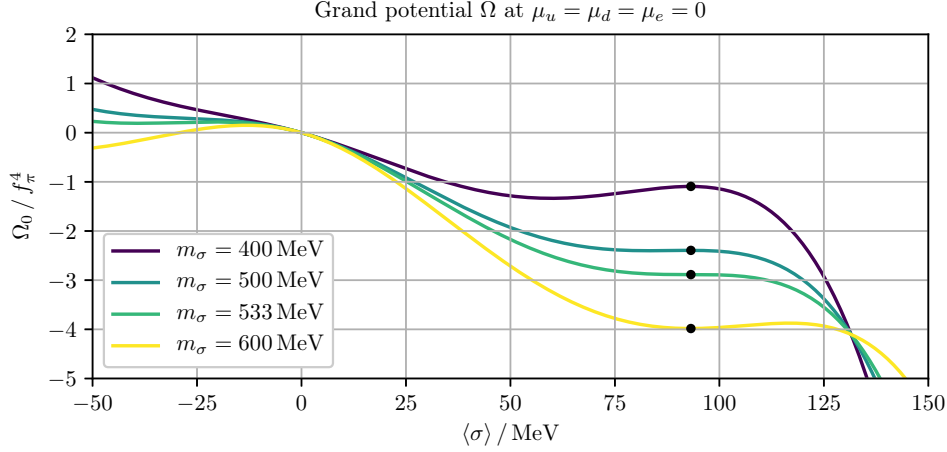


Figure 11.2: The grand potential at zero chemical potential, Ω_0 , as a function of the mean field value $\langle \sigma \rangle$ for different values of m_σ . The parameters of the model is fixed such that when $\langle \sigma \rangle = f_\pi$, Ω_0 has a stationary point. These points coincide with the black dots on the graphs. However, only some values of m_σ lead to a local minimum at the stationary point. For a minimum to occur, we must choose $m_\sigma > 533 \text{ MeV}$.

When our theory is no longer in vacuum, we have four free parameters, namely $\langle \sigma \rangle$, μ_u , μ_d and μ_e . The next task is to determine three of these parameters, such that only one of them is free to parameterise the energy density and the pressure. We will prefer to determine the chemical potentials, leaving $\langle \sigma \rangle$ free. The first constraint may be found by assuming charge neutrality. In Ref. [4], p. 82 it is argued why the total charge is negligible. The total charge of the star may be found by integrating the number density multiplied by the electric charge of each particle. If we let the charged particle species be indexed by i , the expression for the total charge reads

$$Q = \sum_i q_i \int_0^R dr 4\pi r^2 n_i(r), \quad (11.51)$$

where q_i denotes the electrical charge of fermion species i . Similarly, $n_i(r)$ denotes the number density of fermion species i at radius r . Charge neutrality means setting $Q = 0$. With this condition, there still exists a lot of freedom regarding how the charged fermions distribute themselves in the neutron star. To make things simpler for us, we rather require the stricter condition of *local* charge neutrality. Local charge neutrality means that

$$\begin{aligned} 0 &= \sum_i q_i n_i(r) = - \sum_i q_i \frac{\partial \Omega}{\partial \mu_i} \\ &= \frac{N_c m_u^4}{\pi^2} \frac{q_u x_{F,u}^3}{3m_u} + \frac{N_c m_d^4}{\pi^2} \frac{q_d x_{F,d}^3}{3m_d} + \frac{m_e^4}{\pi^2} \frac{q_e x_{F,e}^3}{3m_e} \\ &= \frac{e}{\pi^2} \left[\frac{2}{3} (\mu_u^2 - m_u^2)^{\frac{3}{2}} - \frac{1}{3} (\mu_d^2 - m_d^2)^{\frac{3}{2}} - \frac{1}{3} (\mu_e^2 - m_e^2)^{\frac{3}{2}} \right]. \end{aligned} \quad (11.52)$$

Here, e denotes the electron charge. In the first line, we use Eq. (9.4) to express the number density in terms of a derivative on the grand potential, $n_i = -\frac{\partial \Omega}{\partial \mu_i}$. The calculation is perhaps easiest expressed in terms of $x_{F,i}$, and then using $m_i x_{F,i} = \sqrt{\mu_i^2 - m_i^2}$. In the last line above, we have used that $q_u = \frac{2}{3}e$, $q_d = -\frac{1}{3}e$ and $q_e = -e$, together with $N_c = 3$ [36]. For the next constraint on the chemical potentials, we introduce a reaction process in which quarks and electrons react and emit a neutrino. These processes are known as Urca processes, and they are particularly important for the cooling of neutron stars and

white dwarfs. The process we consider, is the one where one up quark and one electron turns into a down quark and neutrino, and it reads

$$u + e^- \longleftrightarrow d + \nu_e. \quad (11.53)$$

This process is only in equilibrium when the sum of the chemical potentials on each side is equal. As we assume the neutrinos escape the neutron star, we may take μ_{ν_e} to be vanishing. This gives us a simple constraint for μ_e

$$\mu_u + \mu_e = \mu_d, \quad (11.54)$$

$$x_{F,e} = \sqrt{\frac{(\mu_d - \mu_u)^2}{m_e^2} - 1}. \quad (11.55)$$

This one is easy to use to eliminate μ_e in Eq. (11.52). The combined condition of local charge neutrality and Urca process equilibrium is then equivalent to

$$0 = \frac{2}{3}(\mu_u^2 - g^2\langle\sigma\rangle^2)^{\frac{3}{2}} - \frac{1}{3}(\mu_d^2 - g^2\langle\sigma\rangle^2)^{\frac{3}{2}} - \frac{1}{3}\left[(\mu_d - \mu_u)^2 - m_e^2\right]^{\frac{3}{2}}. \quad (11.56)$$

Thirdly, we still require that the grand potential is minimised. Now that we have non-zero chemical potentials, we find the constraint

$$0 = \frac{\partial\Omega}{\partial\langle\sigma\rangle} = \frac{\partial}{\partial\langle\sigma\rangle}\left(\Omega_0 - \frac{g^4\langle\sigma\rangle^4 N_c}{\pi^2}\mathcal{F}(x_{F,u}) - \frac{g^4\langle\sigma\rangle^4 N_c}{\pi^2}\mathcal{F}(x_{F,d}) - \frac{m_e^4}{\pi^2}\mathcal{F}(x_{F,e})\right). \quad (11.57)$$

We are already familiar with Ω_0 , so the new terms we need to consider are the ones stemming from the derivative acting upon $\mathcal{F}(x_{F,u})$ and $\mathcal{F}(x_{F,d})$ and $\mathcal{F}(x_{F,e})$. The last term does not explicitly depend on $\langle\sigma\rangle$, as seen from Eq. (11.55), and vanishes under the derivative. Upon closer inspection, we find

$$\begin{aligned} \frac{\partial\Omega_0}{\partial\langle\sigma\rangle} &= \frac{\partial}{\partial\langle\sigma\rangle} \sum_{f \in \{u, d\}} \frac{g^4\langle\sigma\rangle^4 N_c}{\pi^2} \mathcal{F}(x_{F,f}) \\ &= \sum_{f \in \{u, d\}} \left[4 \frac{g^4\langle\sigma\rangle^3 N_c}{\pi^2} \mathcal{F}(x_{F,f}) + \frac{g^4\langle\sigma\rangle^4 N_c}{\pi^2} \frac{\partial x_{F,f}}{\partial\langle\sigma\rangle} \frac{\partial \mathcal{F}(x_{F,f})}{\partial x_{F,f}} \right] \\ &= 4 \frac{g^4\langle\sigma\rangle^3 N_c}{\pi^2} \left[\mathcal{F}(x_{F,u}) + \mathcal{F}(x_{F,d}) - \frac{x_{F,u}^3 \sqrt{x_{F,u}^2 + 1}}{12} - \frac{x_{F,d}^3 \sqrt{x_{F,d}^2 + 1}}{12} \right]. \end{aligned} \quad (11.58)$$

Looking at \mathcal{F} in Eq. (11.38), we see that there is a cancellation on the left hand side. If we also insert the expression for the derivative of Ω_0 , we find that Eq. (11.57) is equivalent to

$$\begin{aligned} 0 &= \lambda\langle\sigma\rangle^3 - \lambda v^2\langle\sigma\rangle - h + \frac{N_f N_c g^4\langle\sigma\rangle^3}{4\pi^2} \left[1 + \ln\left(\frac{\tilde{\mu}^2}{g^2\langle\sigma\rangle^2}\right) \right] \\ &\quad - \frac{g^4\langle\sigma\rangle^3 N_c}{2\pi^2} \left\{ \ln(x_{F,u} + \sqrt{x_{F,u}^2 + 1}) + \ln(x_{F,d} + \sqrt{x_{F,d}^2 + 1}) - x_{F,u} \sqrt{x_{F,u}^2 + 1} - x_{F,d} \sqrt{x_{F,d}^2 + 1} \right\} \\ &= \lambda\langle\sigma\rangle^3 - \lambda v^2\langle\sigma\rangle - h + \frac{N_f N_c g^4\langle\sigma\rangle^3}{4\pi^2} \left[1 + \ln\left(\frac{\tilde{\mu}^2}{g^2\langle\sigma\rangle^2}\right) \right] + \frac{g^4\langle\sigma\rangle^3 N_c}{2\pi^2} \mathcal{G}(x_{F,u}, x_{F,d}), \end{aligned} \quad (11.59)$$

where we defined $\mathcal{G}(x_{F,u}, x_{F,d})$ as the curly bracket multiplied by -1 in the second line above. Now we have enough to eliminate the chemical potentials and use $\langle\sigma\rangle$ as our free parameter. This system of equation we can readily solve numerically. Now we note that these equations are a lot more interesting with a dynamic quark constituent mass than if the quarks had a fixed mass.

Having solved the system of equations for a given m_σ , we may plot μ_u and μ_d as a function of $\langle\sigma\rangle$ as done in Fig 11.3. We notice that for small enough m_σ , μ_u may take the same value for two different $\langle\sigma\rangle$. This will again cause the pressure, for instance, to take two values for one μ_u .

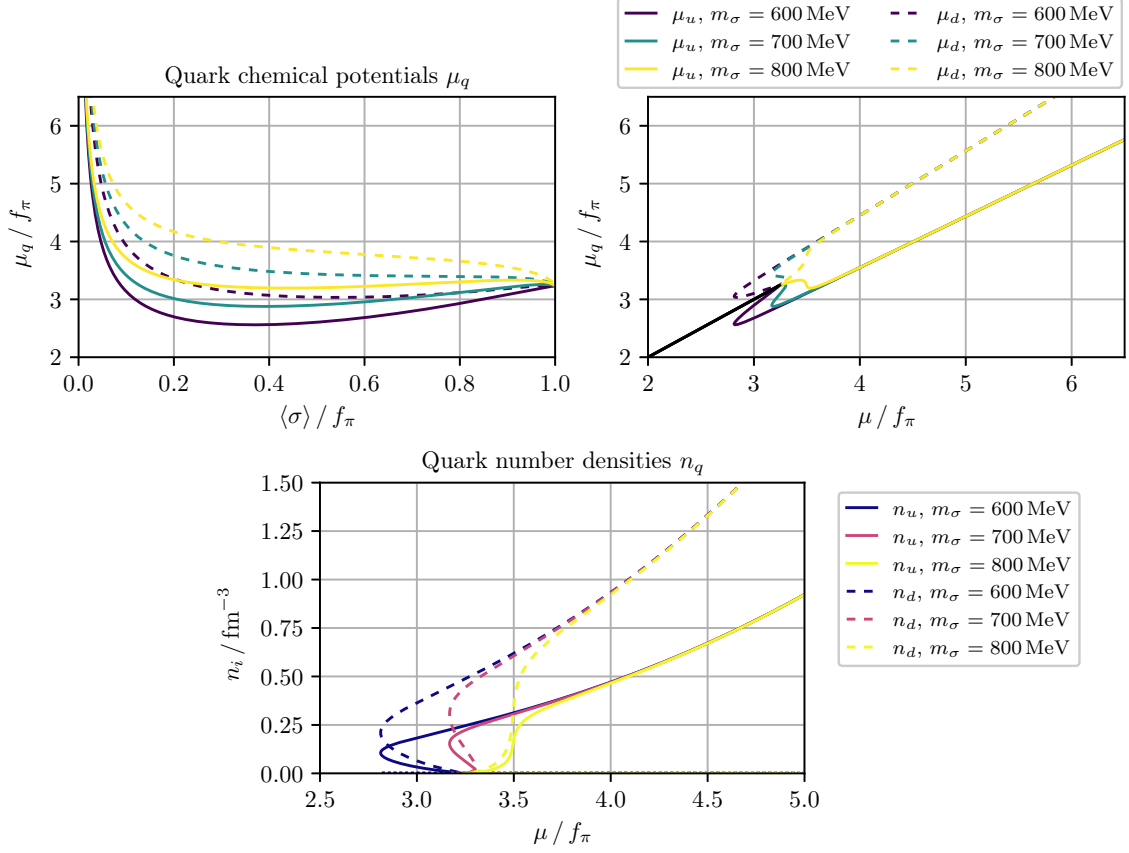


Figure 11.3: The upper left panel shows the profiles of μ_u and μ_d as a function of $\langle\sigma\rangle$, consistent with Eqs. (11.56) and (11.59). The upper right panel shows μ_u and μ_d plotted against their average, μ . The black line illustrates their value *before* their values have reached gf_π , i.e. in the vacuum. Having calculated μ_u and μ_d , we can evaluate the number densities n_q and n_e , Eq. (11.45), which we have done in the lower panel.

The behaviour of the chemical potentials displays some interesting properties. Firstly, we notice that as $\langle\sigma\rangle$ goes toward zero, the chemical potentials diverge. Secondly, where we have plotted μ_u and μ_d against their average, $\mu = (\mu_u + \mu_d)/2$, we see that they start behaving quite linearly. When the linear behaviour has begun, μ_d grows faster than μ_u , though not by much. We see that changing the value of m_σ will mainly play a role for $\mu < 4$, as the solutions converge toward each other for larger μ . Finally, a reader with exceptional eyesight will discover that there are some faint dots along the μ -axis in the number densities plot. These dots represent the electron number density. Compared to n_u and n_d , n_e is vanishing, however, it is not zero. The main importance of the electrons is to balance the charge neutrality conditions, allowing the quark chemical potentials to grow apart.

Now we are ready to look at the pressure and energy density. Before we start plotting, we shift the pressure such that it is zero whenever we are in vacuum. Recalling our brief discussion on the bag shift, we know that adding the value of the pressure in the vacuum to the grand potential achieves this. If we let B_0 (subtly hinting that we will perform another bag shift with B later) denote the grand potential shift to have 0 pressure in the vacuum, the pressure and energy density change like

$$p \rightarrow p - B_0, \quad \text{and} \quad \epsilon \rightarrow \epsilon + B_0, \quad (11.60)$$

where we identify $B_0 = \Omega_0(\langle\sigma\rangle = 1)$. For $m_\sigma \in \{600, 700, 800\}$ MeV, we get the following values for the

shift

$$\begin{aligned}
 m_\sigma = 600 \text{ MeV} & \text{ gives a shift of } B_0 = (131.4 \text{ MeV})^4, \\
 m_\sigma = 700 \text{ MeV} & \text{ gives a shift of } B_0 = (144.7 \text{ MeV})^4, \text{ and} \\
 m_\sigma = 800 \text{ MeV} & \text{ gives a shift of } B_0 = (156.5 \text{ MeV})^4.
 \end{aligned}$$

Now we are ready to visualise the pressure and energy density as functions of the chemical potential μ , see Fig. 11.4.

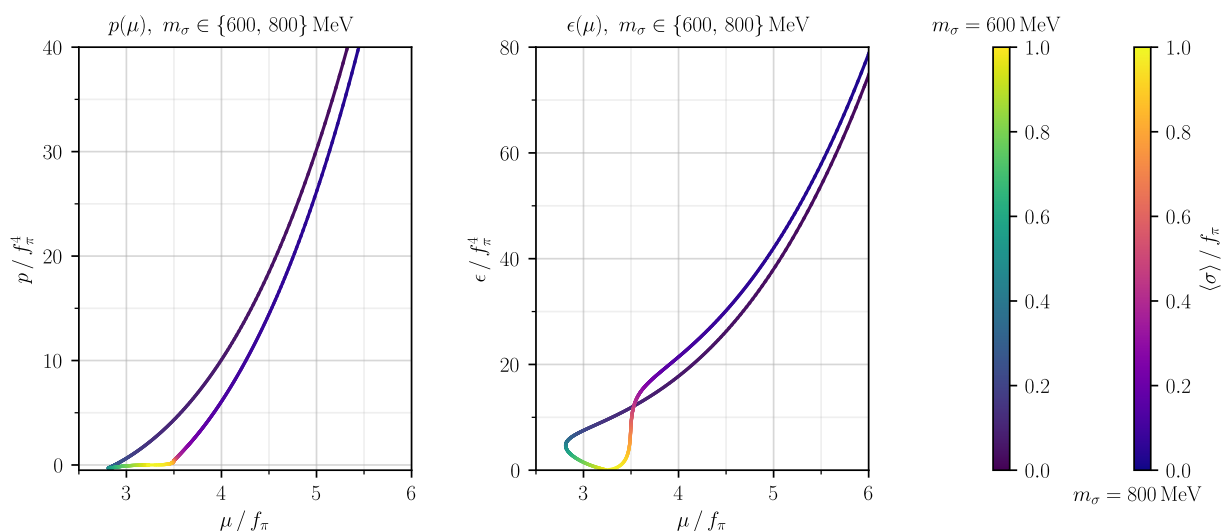


Figure 11.4: The pressure and energy density as a function of $\mu = (\mu_u + \mu_d)/2$. We have shifted the pressure and the energy density according to Eq. (11.60). We see that for $m_\sigma = 600 \text{ MeV}$, the pressure drops below zero. In comparison, the pressure for $m_\sigma = 800 \text{ MeV}$ is more well behaved. The colours of the graph indicate the $\langle \sigma \rangle$ which parameterise the value of μ .

In Fig. 11.4 we have plotted the pressure and the energy density. Interestingly, we see that for $m_\sigma = 600 \text{ MeV}$, the pressure falls below zero for a certain range of μ , before it starts to grow monotonically. Meanwhile, the curves for the heavier σ -particle, $m_\sigma = 800 \text{ MeV}$ behave more intuitively, with monotonically rising pressure and energy density. We are now ready to match one value for p and one for ϵ to each parameterising $\langle \sigma \rangle$. However, the result will not be a function for $m_\sigma = 600 \text{ MeV}$, as p is initially decreasing before it starts to increase. This means that there will be at least two values of p which correspond to one ϵ . To handle this ambiguity we will perform a Maxwell construction. In fact, we have a phase transition at our hands. The Maxwell construction is explained in [42], pp. 55–57. Finally, we present the equation of state in Fig. 11.5. Note that in this plot, we have reinstated units, i.e. we have *not* taken $\hbar = c = 1$. Using the conversion in Eq. (0.12), we may relate the units in Fig. 11.4 to SI-units.

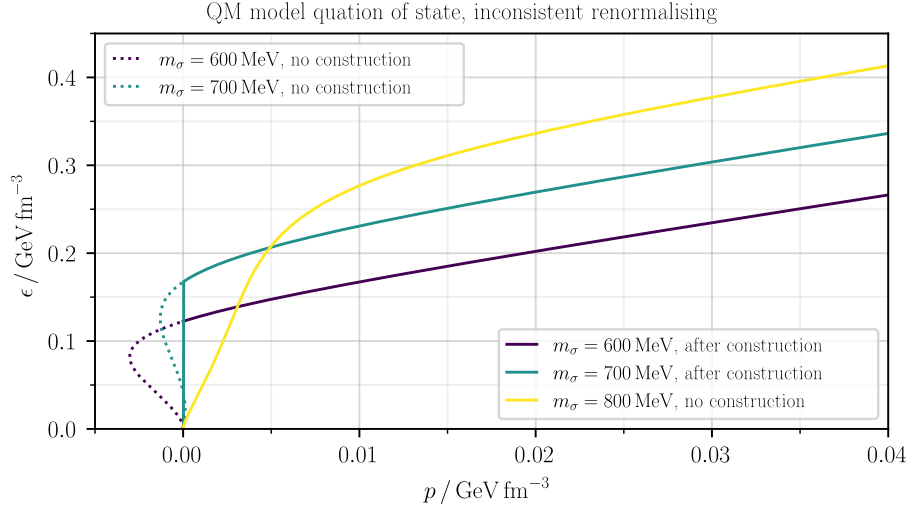


Figure 11.5: Equation of state for the inconsistently renormalised Quark-Meson model. The numerical solution for $\epsilon(p)$ yields a curve where several ϵ may be found at the same p . To address this ambiguity, we have performed a Maxwell construction to distinguish the physically attainable ϵ . The dotted line indicates where the original curves was, before the construction was performed.

We see that in the right part of the plot, the curves start behaving quite linearly. This is the relativistic area, where the slope $\epsilon = 3p$, just as we found for the ideal neutron stars. However, in the lower left corner of the plot, we see that the quark matter behaves quite differently than ideal neutrons.

Earlier, we shifted the pressure such that the vacuum had zero pressure, which seemed a natural choice. However, we must elaborate upon the shift of the vacuum pressure before we may start to calculate mass-radius relations, because such shifts significantly influence the equation of state.

11.4.1 Determining the Bag Constant

To arrive at the model above, we shifted the pressure in the vacuum, namely that we added the constant $\Omega_0(\langle\sigma\rangle = 1)$ to the grand potential. It seems sensible to let the vacuum state have zero pressure, however, this is problematic. If we do not shift the vacuum pressure, we will in fact observe quark stars with very large radii for $m_\sigma = 800$ MeV. The physical interpretation of allowing non-zero vacuum pressures is that it models confinement of quarks. In this subsection, we wish to illustrate how we can find a bound on what values the bag constant B may take. Note that we define the bag constant B as the shift in p that we perform *in addition* to B_0 .

When we introduced the quark stars of the QM model, we mentioned the strange matter hypothesis to justify our study of quark stars. In this hypothesis, we postulated that the nucleon matter is more stable than two-flavour quark matter. Put differently, we know that the energy per baryon must be larger for two-flavour quark matter than for normal nucleon matter, stated mathematically in right part of Eq. (10.17). Had we included the strange quark to our model, we could have used the strange matter hypothesis to include another bound, giving us a window of allowed B . In the two-flavour model, however, we have to accept only one bound, which we recall to be

$$\frac{\epsilon_q}{n_B}(p=0) > 931\text{MeV} = e_{\text{nuc}}, \quad (11.61)$$

where we let ϵ_q denote the sum of the energy density contributions from the quarks and e_{nuc} denote the energy density per baryon for stable iron nuclei. This is the same as the total energy density without

the electron contribution. n_B denotes the baryonic number density. The up and down quark both have baryon number $\frac{1}{3}$, which means that $n_B = \frac{1}{3}(n_u + n_d)$. Since we know how to calculate both ϵ_q and n_B , we may evaluate them at zero pressure. Then we can vary B , and find how their fraction changes. We must choose B such that Eq. (11.61) is barely satisfied to find its limiting value. We illustrate how this looks for $m_\sigma = 800$ MeV in Fig. 11.6.

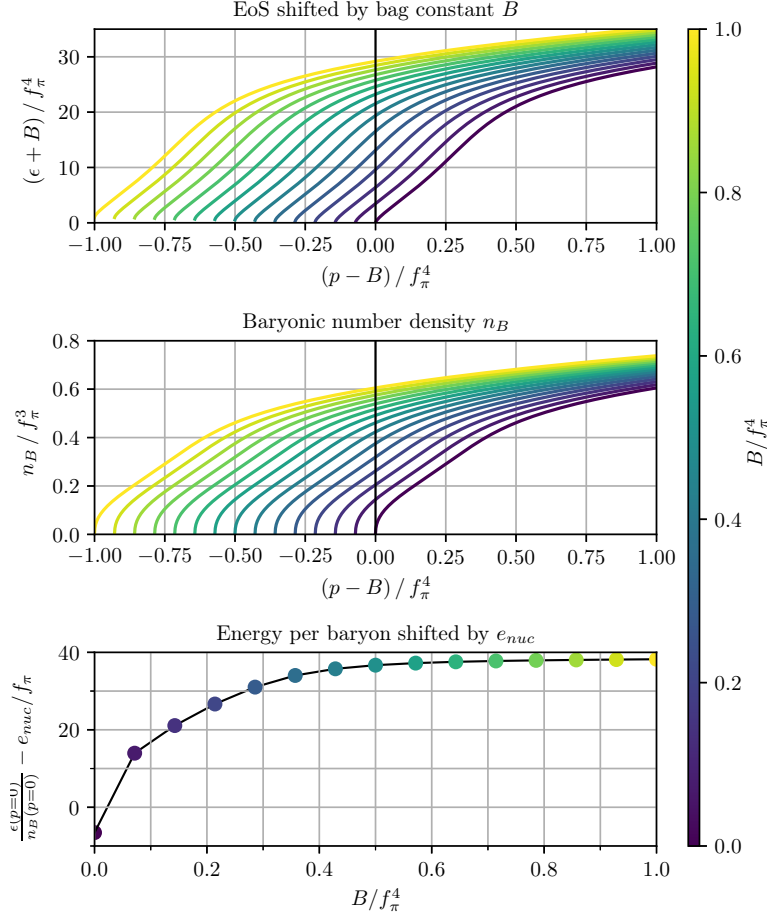


Figure 11.6: For different values of B , we see that $\epsilon(p = 0)$ takes different values. When we in addition calculate the baryonic density $n_B = 1/3(n_u + n_d)$ at zero pressure, we may compare the energy density per baryon in the QM-model to the energy density per baryon in the iron nucleus, e_{nuc} . We may only choose a bag constant which allows us to find that iron nuclei is more stable than quark matter. The points in the scatter plot correspond to where the curves in the two upper plots cross $p - B = 0$.

We see that increasing the bag constant shifts the equation of state to the left and slightly up. This moves the energy density at zero pressure, as we can see from where the equation of state crosses the black line in the upper plot. The same is true for the baryonic number density: Adding a bag constant gives potentially large values of n_B at zero pressure. If we imagine a neutron star in a universe with a very large B , the neutron star ends in a high energy density surface (remember: we defined the end of a neutron star as where $p = 0$). A visual interpolation allows us to discern that we must introduce a small bag constant for $m_\sigma = 800$ MeV in order to produce quark stars in accordance to the strange matter hypothesis. Larger bag constants are allowed. The limiting bag constant does not take a very significant value for the largest m_σ . It does, however, take significant values for both of the other two values of m_σ which we are interested in. Solving Eq. (11.61) numerically for limiting B , we determine the bounding

bag constants

$$\begin{aligned}
 m_\sigma = 600 \text{ MeV} & \text{ gives a minimum bag shift } B = (110.9 \text{ MeV})^4, \\
 m_\sigma = 700 \text{ MeV} & \text{ gives a minimum bag shift } B = (69.1 \text{ MeV})^4, \text{ and} \\
 m_\sigma = 800 \text{ MeV} & \text{ gives a minimum bag shift } B = (27.5 \text{ MeV})^4.
 \end{aligned}$$

We see that for the smallest m_σ , the limiting bag constant is certainly an important correction to the zero-shift B_0 . For $m_\sigma = 700 \text{ MeV}$, the limiting value is less important, but still noticeable compared to B_0 .

We may now plot mass-radius relations for the different values of m_σ with bag constants in accordance with the strange matter hypothesis. In Fig. 11.7, we show three different mass-radius relation for quark stars with the middle value of m_σ . This serves to illustrate how the mass radius-relations change when we vary the bag pressure. As is made clear in the figure, the smallest bag value gives the largest and heaviest star. Therefore, we restrict our attention to the smallest possible bag value for future plotting.

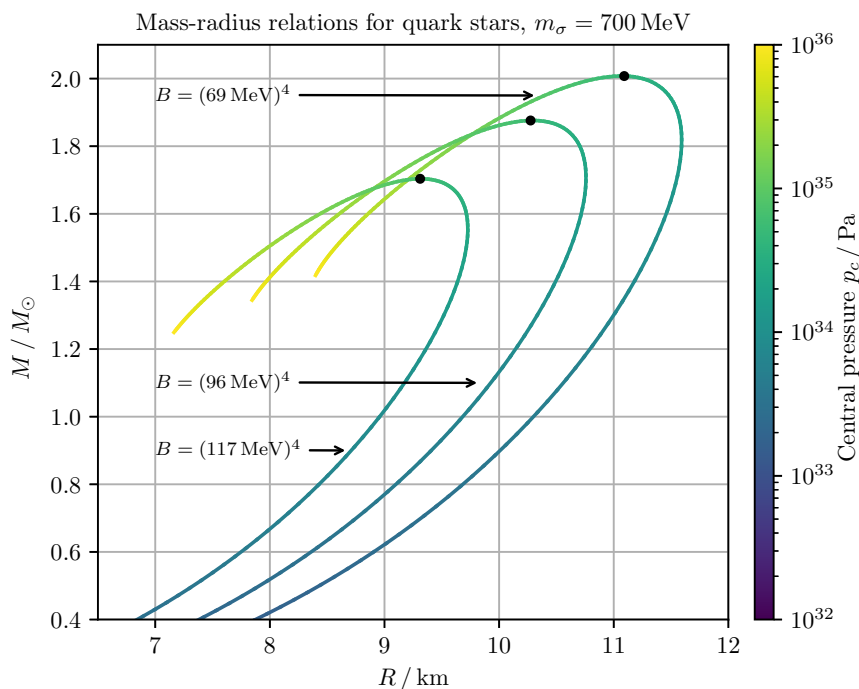


Figure 11.7: Mass-radius relations for $m_\sigma = 700 \text{ MeV}$ for different bag shifts. The smallest bag shift yields the largest maximum mass. The mass maxima are marked by the black dots.

We would also like to see how the mass radius relations change as we vary the mass of m_σ . This is displayed in Fig. 11.8.

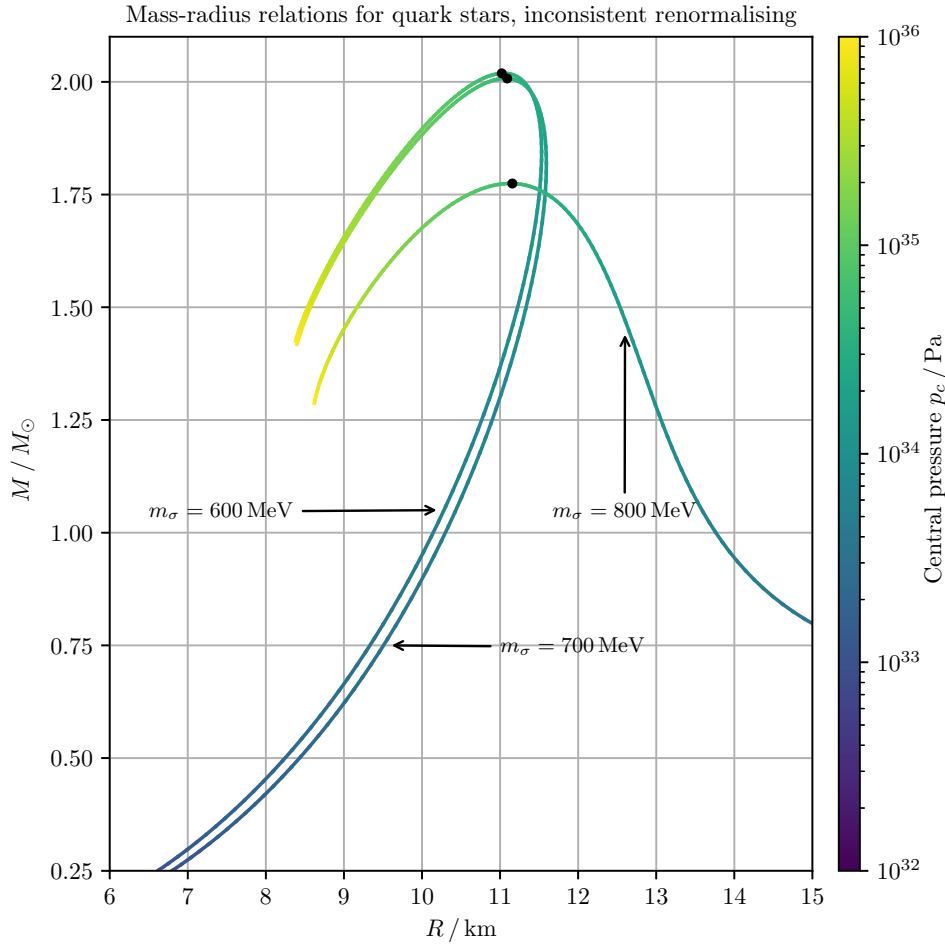


Figure 11.8: The mass radius relation for $m_\sigma \in \{600, 700, 800\}$ MeV.

Now is also a good time to recall the qualitative stability argument we presented in Section 6.1: In a region where the mass falls as we increase the pressure, the star is unstable. All points at a higher pressure than the maximum mass on one of the mass-radius curves in Fig. 11.8 represent unstable stars. The numerical values for the mass maxima are presented in Table 11.2.

m_σ	$M [M_\odot]$	R [km]	p_c [Pa]
600	2.02	11.0	4.7×10^{34}
700	2.00	11.1	4.5×10^{34}
800	1.77	11.2	5.7×10^{34}

Table 11.2: The mass maxima and the corresponding radii and central pressures for the different values of m_σ .

We save the discussion of the maxima until we have handled the consistently renormalised QM model.

11.5 Consistent Renormalising of the Quark-Meson model

The results from the previous chapter are based on the assumption that the tree level parameters directly correspond to physical quantities. However, this is inconsistent. In particular, we know that quantum

fluctuations will renormalise the parameters of the theory. This means that when we eliminate the masses and couplings of the QM model with the quark mass, the pion decay constant and the pion mass, we are eliminating the parameters of the QM model incorrectly. To determine the parameters of the model consistently, we need to do a proper renormalisation, as mentioned at the end of Section 11.2. Therefore, we turn our attention to the Feynman diagrams of the quark-meson model to one-loop order in the large N_c -limit. In short, we need to consider the renormalisation of all diagrams which contain one fermion loop, as these loops are $\mathcal{O}(N_c)$. In the large N_c -limit, there are four diagrams we must take into account from the mesonic sector

$$\begin{aligned}
 & \text{Diagram 1: } \sigma \text{ line with a loop} = L_\sigma^1, & \text{Diagram 2: } \pi_i \text{ line with a loop} = L_{\pi_i}^1, \\
 & \text{Diagram 3: } \sigma \text{ line with a tadpole loop} = L_\sigma^2, & \text{Diagram 4: } \pi_i \text{ line with a tadpole loop} = L_{\pi_i}^2.
 \end{aligned} \tag{11.62}$$

In addition come the counterterm diagrams. The path to a usable expression for the grand potential is quite long computationally. We have added the calculation of one of these diagrams in Appendix G, to illustrate what these diagrams represent. At first, we must regularise and calculate these diagrams according to the Feynman rules. After this is done, we find the equations for how the couplings run with the renormalisation scale, the renormalisation group equations. These constitute a coupled set of differential equation. In the end, we may plug everything back into what we call a consistently renormalised grand potential for the QM model, Ω . This calculation is done in [29], and we use their result. The final expression is quite long, but there is good news. The only part of Ω that has changed compared to the inconsistently renormalised theory, is the mesonic contribution, Ω_0 . The explicit expression reads

$$\begin{aligned}
 \Omega = & \Omega_q + \Omega_e + \frac{3m_\pi^2 f_\pi^2}{4} \left[1 - \frac{4m_q^2 N_c}{16\pi^2 f_\pi^2} G(m_\pi^2) \right] \frac{\Delta^2}{m_q^2} \\
 & - \frac{m_\sigma^2 f_\pi^2}{4} \left[1 + \frac{4m_q^2 N_c}{16\pi^2 f_\pi^2} \left\{ \left(1 - \frac{4m_q^2}{m_\sigma^2} \right) F(m_\sigma^2) + \frac{4m_q^2}{m_\sigma^2} - F(m_\pi^2) - G(m_\pi^2) \right\} \right] \frac{\Delta^2}{m_q^2} \\
 & + \frac{m_\sigma^2 f_\pi^2}{8} \left[1 - \frac{4m_q^2 N_c}{16\pi^2 f_\pi^2} \left\{ \frac{4m_q^2}{m_\sigma^2} \left[\ln \left(\frac{\Delta^2}{m_q^2} \right) - \frac{3}{2} \right] - \left(1 - \frac{4m_q^2}{m_\sigma^2} \right) F(m_\sigma^2) + F(m_\pi^2) + G(m_\pi^2) \right\} \right] \frac{\Delta^4}{m_q^4} \\
 & - \frac{m_\pi^2 f_\pi^2}{8} \left[1 - \frac{4m_q^2 N_c}{16\pi^2 f_\pi^2} G(m_\pi^2) \right] \frac{\Delta^4}{m_q^4} - m_\pi^2 f_\pi^2 \left[1 - \frac{4m_q^2 N_c}{16\pi^2 f_\pi^2} G(m_\pi^2) \right] \frac{\Delta}{m_q}.
 \end{aligned} \tag{11.63}$$

Above, we have introduced two dimensionless functions, F and G , which are defined as follows

$$F(m^2) = 2 - 2 \left[\frac{4m_q^2}{m^2} - 1 \right]^{\frac{1}{2}} \arctan \left(\left[\frac{4m_q^2}{m^2} - 1 \right]^{-\frac{1}{2}} \right), \tag{11.64}$$

$$G(m^2) = \frac{4m_q^2 m_\pi^2}{m^4} \left[\frac{4m_q^2}{m^2} - 1 \right]^{-\frac{1}{2}} \arctan \left(\left[\frac{4m_q^2}{m^2} - 1 \right]^{-\frac{1}{2}} \right) - \frac{m_\pi^2}{m^2}. \tag{11.65}$$

Note that we have defined the function G slightly differently than F' in [29]. Ω_q and Ω_e are defined just as for the inconsistently renormalised theory. In Eq. (11.63), we have also introduced $\Delta = g\langle\sigma\rangle$, the

quark mass as a function of the symmetry breaking parameter $\langle\sigma\rangle$, which we earlier denoted m_q . Now, we let m_q denote the *vacuum* quark mass, i.e. $m_q = gf_\pi$. The new Ω may seem a lot more complex compared to before, however, it is mostly in appearances. Plotting the grand potential in vacuum for different $\langle\sigma\rangle$, we see that there are only slight adjustments, as illustrated in Fig. 11.9.

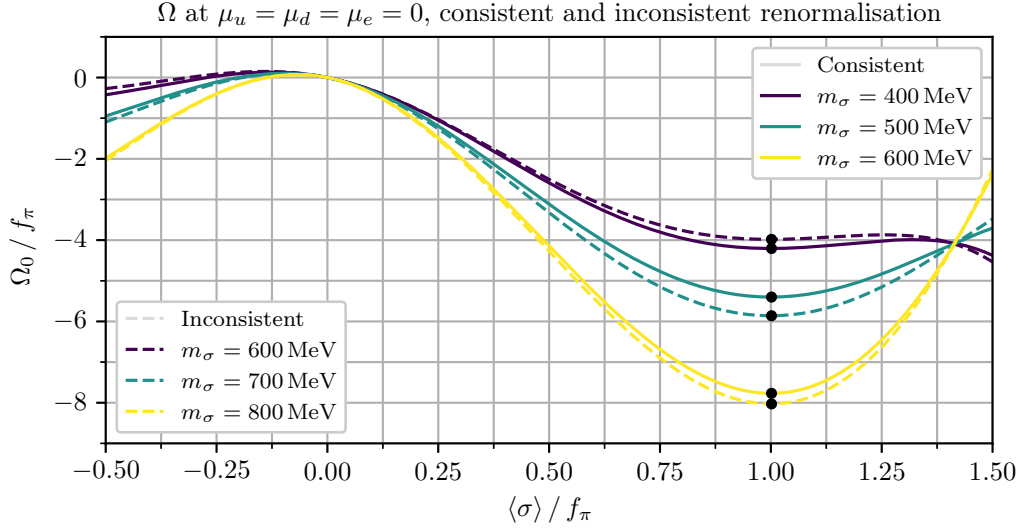


Figure 11.9: A comparison between the grand potential at zero chemical potential for the inconsistently and consistently renormalised QM model given by Eq. (11.41) and Eq. (11.63), respectively. As we can see, the differences are small with the exception that the masses we use for m_σ has been reduced significantly.

The most important difference is that we now may use smaller values for m_σ . Luckily, the values of m_σ now lie within the experimental range. This is certainly good news, as it lends more credibility to the QM model. The model now works for physically reasonable values of m_σ . To proceed, we go through the same steps as we did for the inconsistently renormalised theory. The only thing that has changed, is that requiring the grand potential to be extremised now takes a slightly different form. We still require

$$\frac{\partial\Omega}{\partial\langle\sigma\rangle} = 0. \quad (11.66)$$

Numerically, this will look a little different. In Appendix I, we write it out explicitly. Highlighting the similarities once more, we may have a look at the equation of state.

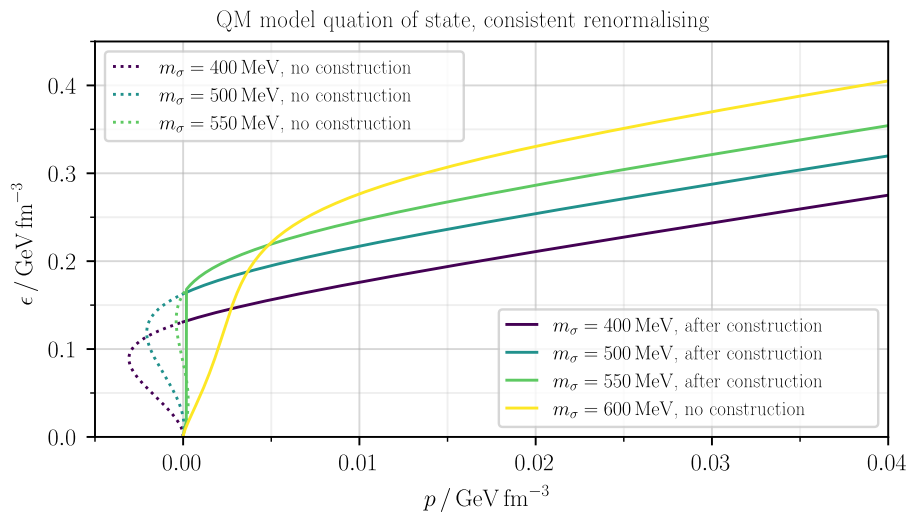


Figure 11.10: The equation of state for the consistently renormalised QM model. Comparing to Fig. 11.5, we see that the equations of state have not changed by much, with the exception of shifting $m_\sigma \rightarrow m_\sigma - 200$ MeV.

We also calculate the bag constant lower bounds, as given by Eq. (11.61). They are not very different either.

$$\begin{aligned}
 m_\sigma = 400 \text{ MeV} & \text{ gives a minimum bag shift } B = (107.7 \text{ MeV})^4, \\
 m_\sigma = 500 \text{ MeV} & \text{ gives a minimum bag shift } B = (84.7 \text{ MeV})^4, \\
 m_\sigma = 550 \text{ MeV} & \text{ gives a minimum bag shift } B = (30.7 \text{ MeV})^4, \text{ and} \\
 m_\sigma = 600 \text{ MeV} & \text{ gives a minimum bag shift } B = (27.9 \text{ MeV})^4.
 \end{aligned}$$

At last, we may also plot the mass-radius relation for the consistently renormalised QM model. The results are plotted in Fig. 11.11.

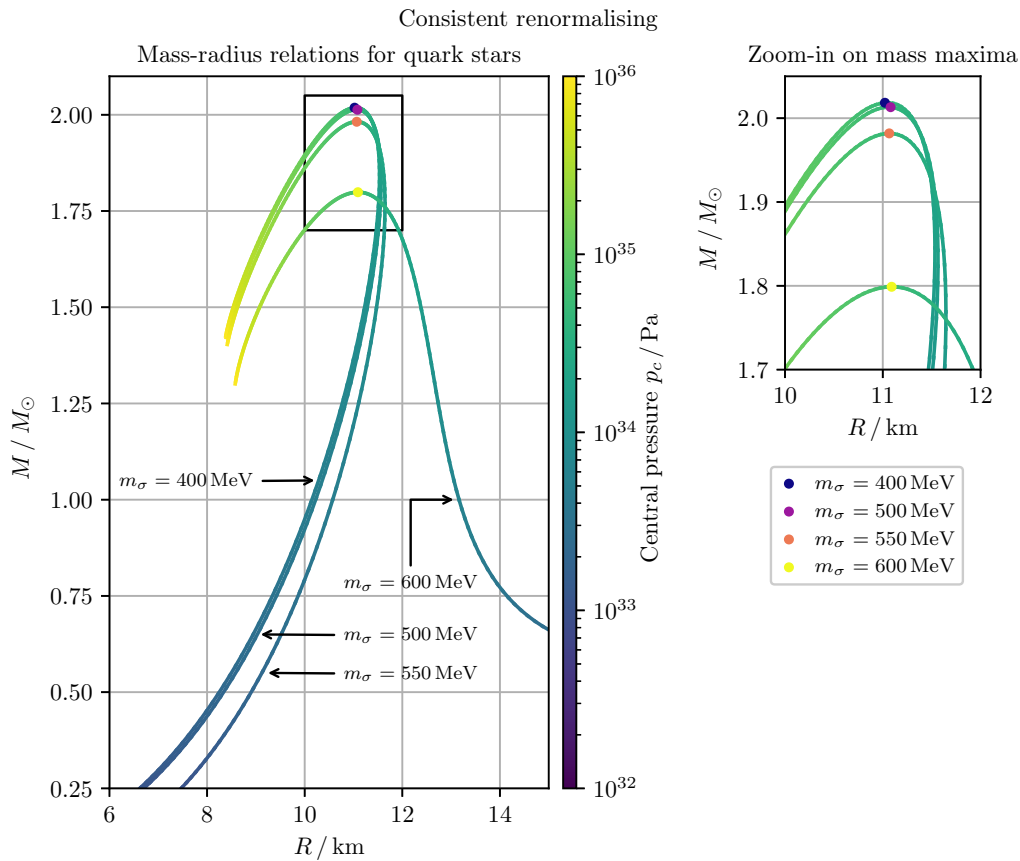


Figure 11.11: Mass-radius relations for QM model quark stars with a consistent renormalisation. The resemblance to the mass-radius relations in Fig. 11.8 is striking.

We added $m_\sigma = 550$ MeV to cover the whole range of possible values of m_σ . However, not much new information is gained – it seems that values in the range [400, 550] MeV yield approximately the same mass-radius relation curves. As for the inconsistently renormalised QM-model, we supply the mass maxima values in each case, see Table 11.3.

m_σ	$M [M_\odot]$	R [km]	p_c [Pa]
400	2.02	11.0	4.7×10^{34}
500	2.01	11.1	4.5×10^{34}
550	1.98	11.1	4.7×10^{34}
600	1.80	11.1	5.7×10^{34}

Table 11.3: The mass maxima and the corresponding radii and central pressures for the different values of m_σ , this time for the consistently renormalised QM model.

This is also a good time to consider the *stiffness* of the equations of state. The larger the pressure for a given energy density, the stiffer the equation of state, as discussed in Ref. [43], where there is stiffness is also elaborated upon graphically. We are now in the position to look at both the equations of state and the mass-radius relations. Fixing an energy density $\epsilon^* > 2.3 \text{ GeV fm}^{-3}$, it is easy to see from Fig 11.10 that the $m_\sigma = 600$ MeV is the curve with the lowest pressure. In other words, this value of m_σ yields the softest equation of state apart from in the lower left part of the plot. This is reflected in the fact that it also has the smallest maximum mass. The equation of state for $m_\sigma = 400$ MeV is the stiffest

equation of state. The reason the mass maximum is almost identical to $m_\sigma = 500$ MeV is due to the fact that we require a larger minimum bag shift. Considering what a bag shift does in Eq. (11.43), we see that adding a B shifts the graph in the up and to the left. This increases the pressure at a given energy density yielding a softer equation of state. In Fig. 11.7, it is very clear that increasing the bag pressure, i.e. softening the equation of state, gives smaller maximum masses.

One thing to keep in mind after this quark star discussion, is that we only included the two lightest quarks. A more complete quark star model should also include the s -quark, upgrading to the three-flavour quark-meson model. At this point, we choose to press on and tackle hybrid stars, instead of dwelling on the quark stars. However, Ref. [1], chapter 9, investigates the addition of the s -quark. In the end, the resulting mass-radius relations look similar in shape to two-flavour quark stars, although the maximum masses have shrunk by roughly $0.2M_\odot$ for each value of m_σ .

Hybrid Stars

Now we turn our attention to the so-called hybrid stars, which in some sense is the culmination of this thesis. These are stars which consist of both nuclear matter and quark matter, and they are arguably the most realistic compact stars we discuss. The ideal neutron star model suffered from the fact that it excluded all sorts of interactions and particle varieties which occur in Nature. The quark star model captures particle interactions, however, it assumes the existence of quark matter at low energy densities, on the contrary to what QCD tells about quark confinement. The hybrid star will include both interactions between particles and nuclear matter at low densities.

A hybrid star consists of a quark core and a nuclear matter mantle and crust. The outer layers, the crust and the mantle, consist of matter at *relatively* low energy densities compared to the core. Here, we expect the quarks to be confined in hadrons, as dictated by QCD. If the energy densities reach high enough values in the interior of the star, we expect quarks to be deconfined. In order to describe a hybrid star, we therefore need an equation of state for both nucleon matter and quark matter. For the deconfined quark phase, we may use the quark-meson model we developed in the previous chapters. To describe the crust and the mantle, we will use an equation of state describing *interacting* nuclear matter, as opposed to our approach for the ideal neutron stars. Finally, we need to describe the transition between the nuclear phase and the quark phase. A review on the topic of hybrid stars can be found in [43], an article which has inspired this section.

12.1 The Akmal-Pandharipande-Ravenhall Equation of State

At first we look into the nucleon matter equation of state. We would like to use a more realistic equation of state than the ideal equation of state, one which includes several particle species and interactions. Therefore, we will use Akmal-Pandharipande-Ravenhall (APR) equation of state, described in [44]. This is an equation of state for interacting nucleon matter. The specific calculations for the data we use, also rest on the works [45] and [46]. We do not go into any details of the calculation, however, we may mention that the final data takes into account an outer nucleonic crust, an inner nucleonic crust and a nucleonic interior. The data points are collected from CompOSE, whose description is given in [47]. To get a feel for how this matter behaves, we may look at Fig. 12.1.

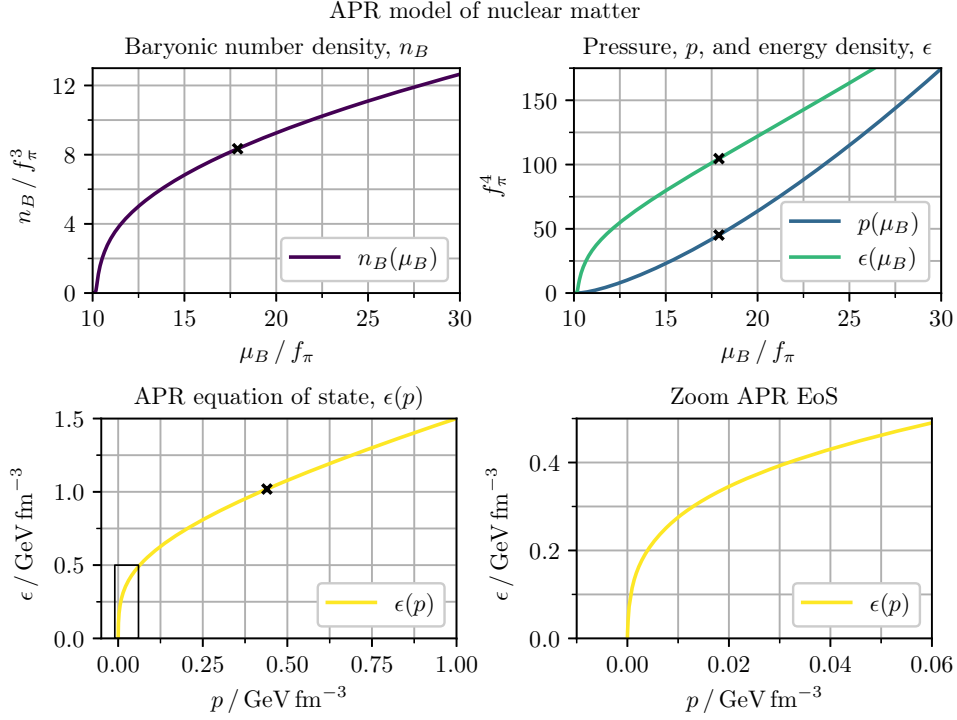


Figure 12.1: The panels display some of the properties of dense nucleon matter in the APR equation of state. We have used the same units as in Figs. 11.4, 11.5 and 11.10 to make comparison easier. The lower right plot displays a magnification of the black box in the lower left plot. The magnification is chosen to approximately match Figs. 11.5 and 11.10. The black crosses mark where APR matter becomes non-causal, $\frac{\partial \epsilon}{\partial p} < 1$. The part of the graph which lies higher than the x is non-causal.

As we are dealing with nucleon matter, the natural chemical potential to consider is the baryonic, μ_B . In the modelling of the APR-equation of state, the neutron mass takes the value

$$m_n = 939.6 \text{ MeV}. \quad (12.1)$$

We can see this in Fig. 12.1, as when the baryonic chemical potential reaches m_n , n_B , p and ϵ start taking non-zero values (remember that $f_\pi = 93 \text{ MeV}$). Note that the baryonic chemical potential relates to the average quark chemical potential μ through

$$-\frac{\partial \Omega}{\partial \mu_B} = n_B = \frac{1}{3}(n_u + n_d) = -\frac{1}{3} \left(\frac{\partial \Omega}{\partial \mu_u} + \frac{\partial \Omega}{\partial \mu_d} \right) = -\frac{1}{3} \frac{\partial \Omega}{\partial \mu}, \quad \text{giving}$$

$$\mu_B = 3\mu = \frac{3}{2}(\mu_u + \mu_d), \quad (12.2)$$

which is useful when we would like to compare the upper right panel to Fig. 11.4. At first we notice how *stiff* this equation of state is. We recall that a stiff equation of state has a higher pressure at a given energy density than a soft equation of state. The stiffer the equation of state is, the more massive the stars may be. From the lower left plot in Fig. 12.1, we see that for large pressures, the energy density behaves very roughly like $\epsilon \sim 0.7p$, which is a lot stiffer than the relativistic matter equation of state $\epsilon \sim 3p$. When we remember back to Eq. (3.6), we realise that this is in fact so stiff that the speed of sound in APR nucleon matter will *exceed* the speed of light! For a causal neutron star, we cannot accept this to happen. In the panels of Fig. 12.1, we have marked the points where the speed of sound is equal to the speed of light. This means that for number densities, pressures and energy densities above these marks, APR matter cannot be accepted. Quantitatively, the transition from causal to non-causal

happens at

$$n = 0.87 \text{ fm}^{-3}, \quad p = 7.0 \times 10^{34} \text{ Pa} \quad \text{and} \quad \epsilon = 1.0 \text{ GeV fm}^{-3}. \quad (12.3)$$

Due to the stiffness, we expect an APR-modelled neutron star to be massive, however, we may only treat it only as a theoretical upper bound after the speed of sound exceeds the speed of light.

12.2 First-Order Transition Between Nucleon Matter and Quark Matter

Since we now have both equation of states we need, we require a way to "patch" them together. The simplest way to achieve this, is to introduce an abrupt transition from nucleon matter to quark matter. As a guiding principle, we used that the grand potential is minimised, or equivalently, and perhaps more intuitively, that the pressure is maximised. By imposing this condition again, we can determine when the transition from nucleon to quark matter take place as a function of the baryonic potential. We simply choose the equation of state which yields the higher pressure at a given μ_B . To write it mathematically, we first add a subscript to the nucleon energy density $\epsilon_N(\mu_B)$ and one for the pressure $p_N(\mu_B)$ to distinguish the nucleon and quark phases. Similarly, we denote the quark energy density $\epsilon_q(\mu_B)$ and quark phase pressure $p_q(\mu_B)$. Now, we may write the total equation of state as

$$\epsilon(p) = \begin{cases} \epsilon_N(p_N), & p_N(\mu_B) > p_q(\mu_B), \\ \epsilon_q(p_q), & p_N(\mu_B) < p_q(\mu_B). \end{cases} \quad (12.4)$$

There is one caveat to keep in mind, namely that the quark pressure should be lowest for small enough μ_B . Otherwise, the star would simply be a quark star, and the introduction of nucleon matter has achieved nothing. We note that $p_q(\mu_B)$ is dependent on both the mass m_σ and the bag constant B . As minimising the bag constant yields the heaviest stars, we will focus mainly on the minimal bag constants. In addition, since the properly renormalised QM model is the most convincing, we will focus on this version. We will, however, take into account the different values of m_σ . In general, there is a "kink" where $p_N(\mu_B) = p_q(\mu_B)$, which implies that the derivative of p with respect to μ_B is discontinuous at this point. As the energy density contains terms $\frac{\partial \Omega}{\partial \mu_i}$, we expect that this construction will produce a discontinuous equation of state, a first order phase transition.

There is one inconsistency between the APR-data and our modelling so far. The APR data use a neutron mass as given in Eq. 12.1, and we use a "quark constituent mass" in the vacuum of $m_q = 300 \text{ MeV}$. This means that three quarks together constitute one neutron of mass less than the APR neutron mass. For the "patching" to work, we would need either to change m_q or pretend that the neutron mass is smaller. The alternative would force us to choose large additions to the bag shift to even have a crossing. This forced crossing would also happen at relatively small μ_B , most likely overextending the quark phase. To be consistent throughout this thesis, we take the freedom to use the APR-data with our "modified" neutron mass. In this section, and until we explicitly mention the neutron mass shift again, we will take

$$m_n = 900 \text{ MeV}. \quad (12.5)$$

This shift results in another pressure at which the APR equation of state becomes non-causal. The non-causal values from Eq. (12.3) for the shifted neutron mass become

$$n = 0.84 \text{ fm}^{-3}, \quad p = 6.3 \times 10^{34} \text{ Pa}, \quad \text{and} \quad \epsilon = 0.93 \text{ GeV fm}^{-3}. \quad (12.6)$$

After the neutron mass shift, the resulting equations of state are displayed in Fig. 12.2.

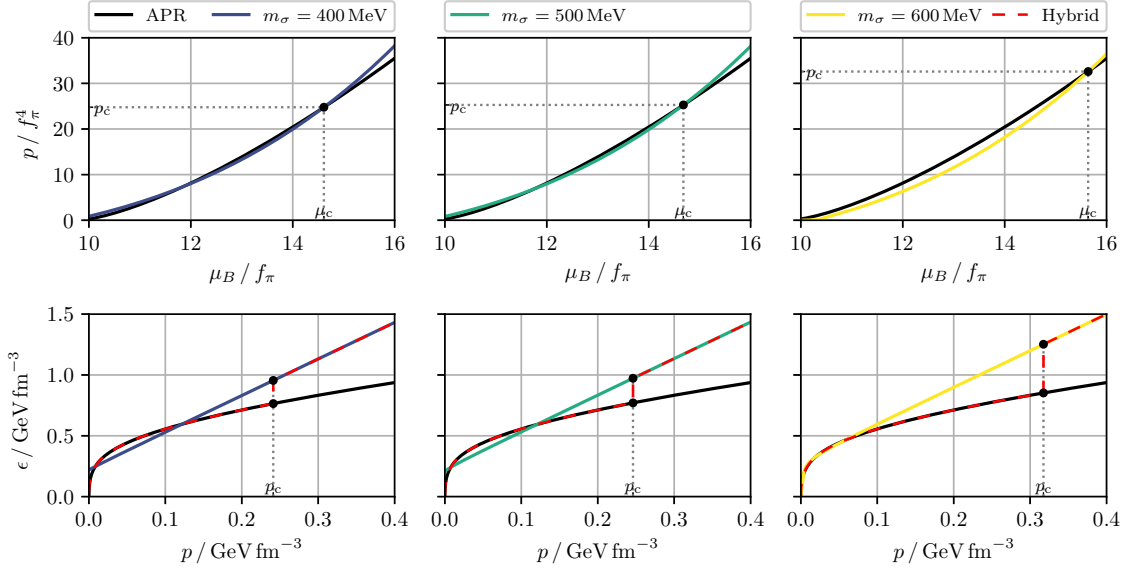


Figure 12.2: The upper panels show $p_N(\mu_B)$ in black and $p_q(\mu_B)$ for $m_\sigma \in \{400, 500, 600\}$ MeV in different colours. The last crossing point, where p_q grows larger than p_N , is marked by a black dot in each panel. Its value (denoted p_c in the panels, not to be confused with the central pressure of a star) is projected onto the p -axis, visualised by the horizontal dotted line. The critical chemical potential μ_c is also indicated by the vertical dotted lines. The lower panels display the equations of state for the above mentioned values of m_σ and for APR nuclear matter. The critical pressure is in each case indicated by the vertical dotted black line. The red, dashed graph indicate what we call the hybrid equation of state.

The observant reader will notice that for $m_\sigma \in \{400, 500\}$ MeV there are not only one, but several crossings between $p_N(\mu_B)$ and $p_q(\mu_B)$. Perhaps stranger still, for the smallest values of μ_B which are greater than m_n , we see that $p_q > p_N$. Following the argument that the system favours the phase which has the larger pressure at a given μ_B , this should result in a hybrid star with more than one phase transition. It would also result in quark matter at the exterior of the star. This is precisely the issue we wanted to solve: We do not expect quark matter to be present at relatively low energy densities. In the equation of state-panels above, we have only included the innermost phase transition, favouring the nuclear matter at lower energy densities. This might seem inconsistent – we have earlier relied upon minimising the grand potential. On the other hand, it is compelling to remain sceptical about quark matter at small densities. We could argue that we *must* throw away the quark matter equation of state at small energy densities due to confinement. Another way out of trouble, is to view the re-introduction of quark matter as an argument why we must increase the bag constant. Such an increase would simply lower the pressure curves in the upper panels. A large enough increase would resolve the issue. On the other hand, this would also raise the critical pressure as the curves would intersect at a larger μ_B .

In each of the three cases above, the critical pressure p_{crit} is large. This means that only heavy stars will contain quark matter at their core. The critical number densities, $n_{B, \text{crit}}$, are also large. In Table 12.1 we present our numerical findings.

m_σ [MeV]	APR $n_{B, \text{crit}}$ [fm^{-3}]	Quark $n_{B, \text{crit}}$ [fm^{-3}]	p_{crit} [Pa]
400	0.73	0.85	3.9×10^{34}
500	0.73	0.86	3.9×10^{34}
600	0.79	1.0	5.1×10^{34}

Table 12.1: Number densities at critical pressures for nucleon and quark phase. For reference, the nuclear saturation density is $n_0 = 0.16 \text{ fm}^{-3}$.

Even for the earliest phase transition, we see that the nucleonic number density reaches $n_{B, \text{crit}} \approx 4.6n_0$. This is certainly a large number density! This begs the question: Is the APR equation of state trustworthy at such large number densities? Luckily, and at the very least, the critical values do not reach into the regime of non-causal APR matter for any of the three values of m_σ when we compare with Eq. (12.6).

Momentarily throwing away all doubts about quarks reappearing at small pressures and the validity of APR nucleon matter at $n_B \sim 4.6n_0$, we may churn the new hybrid equations of state through a numerical integration together with the rest of the TOV-equations. We find the mass-radius relations presented in Fig. 12.3.

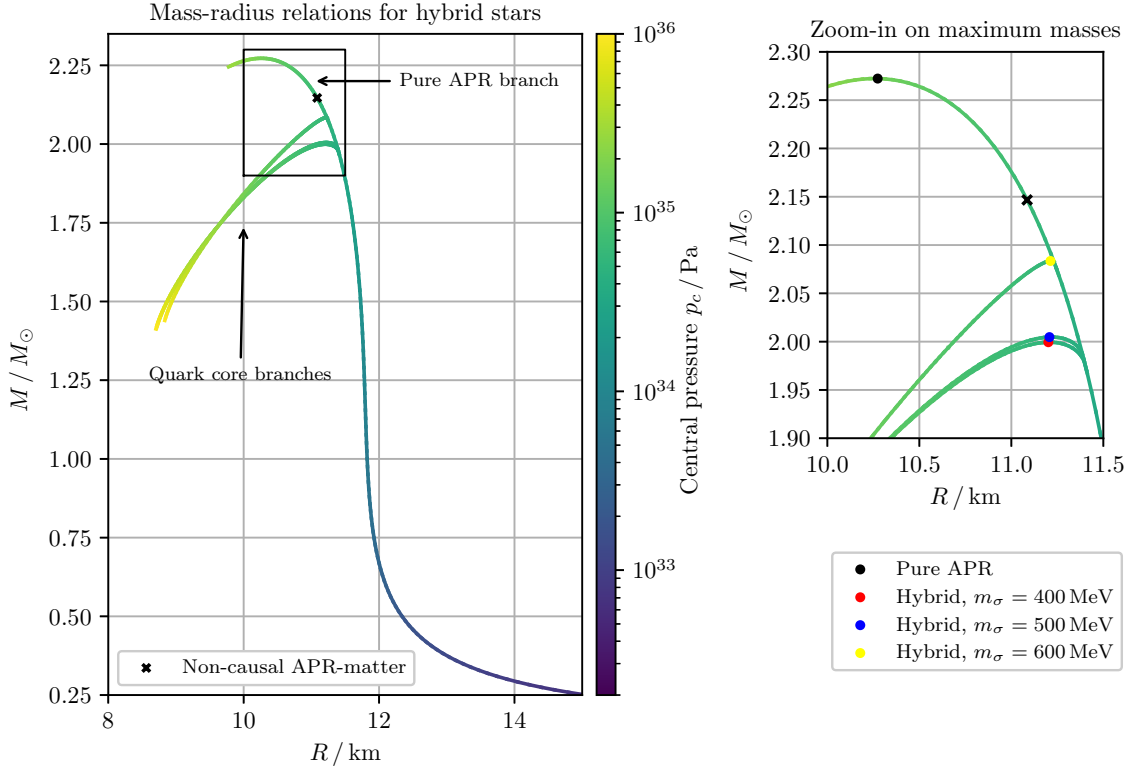


Figure 12.3: The mass-radius relations for hybrid stars in the cases of $m_\sigma \in \{400, 500, 600\} \text{ MeV}$. For comparison, the mass-radius relations for a pure APR-matter star has been added, as indicated by the top annotation. When the central pressure is beyond the transition point to quark matter, the star has a quark core, which in turn gives the branching off the APR-matter curve. The two smallest m_σ -values give almost coinciding branches.

In the panel displaying the zoom-in on the maximal masses, we have marked the points on the mass-radius relations where the maximum masses occur. Their numerical values are listed in Table 12.2.

m_σ	$M [M_\odot]$	R [km]	p_c [Pa]
400	2.00	11.2	5.1×10^{34}
500	2.00	11.2	5.1×10^{34}
600	2.08	11.2	5.3×10^{34}

Table 12.2: The values for the maximum mass-hybrid star for each of the three values of m_σ . As seen from Fig. 12.3, the $m_\sigma = 400$ MeV-maximum is not exactly at the same point as for $m_\sigma = 500$ MeV, but the difference is certainly small.

The maximum mass for a pure APR star is $2.27M_\odot$ with the corresponding radius of 10.3 km at a central pressure of $p_c = 1.6 \times 10^{35}$ Pa, as marked by the black dot on the zoom-in in Fig. 12.3. Comparing to the stars with a quark core, this is quite a large increase in maximum mass. However, we see that the central pressure is past the pressure where the APR equation of state becomes non-causal, stated in Eq. (12.6). If we instead take the maximum mass to be where the central pressure reaches the limit of causality, we find a new maximum mass and radius of

$$M = 2.15M_\odot, \quad \text{and} \quad R = 11.1 \text{ km.} \quad (12.7)$$

We notice from Fig. 12.3 that the quark-core branches quickly bend downwards for larger pressures. Following our qualitative stability argument in Section 6.1, this means that the quark core stars quickly become unstable. This is particularly true for $m_\sigma = 600$ MeV. Nevertheless, we find a small region where they are stable for each of the three values of m_σ .

12.3 Interpolating Between the Nucleonic Phase and the Quark Phase

The second way to bridge the two phases of matter which is outlined in [43], is the so-called unified equation of state. Instead of introducing an abrupt transition at $\mu_{B, \text{crit}}$, we rather construct an interpolating equation of state between the two phases. We will refer to this type of "patching" as a *unified equation of state*, as opposed to a hybrid equation of state from the previous section. Note that a unified equation of state still describes a hybrid star – it is just a name to differentiate between the two techniques. Naturally, the mass-radius results will depend on how we construct the interpolation, which might not seem very promising: We would not like the final results to depend heavily on a somewhat arbitrarily chosen interpolating function. However, there exists a good argument why this approach still might be better than the first-order phase transition. We should be sceptical of the nucleonic equation of state when the energy density becomes too large. A description of what goes wrong can be found in [43]. Typically, the calculations become less trustworthy for a baryonic number density around $n_B \gtrsim 2n_0$, where n_0 is as usual the nuclear saturation density. For quarks, it is the other way around. Ref. [43] uses a lower limit for the quark equation of state where $n_B \gtrsim (4 - 7)n_0$. For the upper limit of the APR domain, we can find $\mu_{B, l}$ (l for lower limit of the interpolation) and for the lower limit of the quark domain, we can find $\mu_{B, u}$ (u for upper limit of the interpolation). In the interpolation regime, $\mu_{B, l} < \mu_B < \mu_{B, u}$, it is very hard to find a good descriptive model, as hadrons begin to overlap, but the interactions between the constituents are still too strong for any perturbative treatment to be accurate. This is even true in the core, which is why we introduced the QM model instead of using perturbative QCD in the first place. Instead of looking for a description, we will simply try to find a function which interpolates between the APR-matter endpoint to where quark matter begins.

The interpolating function $p(\mu_B)$ will be used to find both n_i and ϵ_i through $n_i = \frac{\partial p}{\partial \mu_B}$ and $\epsilon_i = -p + \mu_B n_B$. We note that these relations do not hold for the quark phase, e.g. the energy density is $\epsilon_q = -p + \sum_j \mu_j n_j \neq -p + \mu_B n_B$. Due to the fact that we have no actual description of which particles are present in the unifying phase, we may not express ϵ as the sum over particles we have for the quark phase. However, if $-\mu_B \frac{d\Omega}{d\mu_B} \approx \sum_j \mu_j n_j$ in the quark phase, we will find that the equation of state from the interpolating $p(\mu_B)$ will be quite similar to ϵ_q at $\mu_{B, u}$. For the quark phase, we consider the

expression

$$\mu_B \frac{d\Omega}{d\mu_B} = \mu_B \left(\frac{\partial\Omega}{\partial\mu_u} \frac{d\mu_u}{d\mu_B} + \frac{\partial\Omega}{\partial\mu_d} \frac{d\mu_d}{d\mu_B} + \frac{\partial\Omega}{\partial\mu_e} \frac{d\mu_e}{d\mu_B} \right). \quad (12.8)$$

Recalling Eqs. (11.54) and (12.2), we can evaluate the different derivatives of the chemical potentials as

$$\begin{aligned} \frac{d\mu_u}{d\mu_B} &= \left(\frac{d\mu_B}{d\mu_u} \right)^{-1} = \left(\frac{\partial\mu_B}{\partial\mu_u} \frac{d\mu_u}{d\mu_u} + \frac{\partial\mu_B}{\partial\mu_d} \frac{d\mu_d}{d\mu_u} \right)^{-1} \stackrel{(12.2)}{=} \left(\frac{3}{2} + \frac{3}{2} \frac{d\mu_d}{d\mu_u} \right)^{-1} = \frac{2}{3} \frac{1}{1 + \frac{d\mu_d}{d\mu_u}}, \\ \frac{d\mu_d}{d\mu_B} &= \frac{2}{3} \frac{1}{1 + \frac{d\mu_u}{d\mu_d}}, \\ \frac{d\mu_e}{d\mu_B} &\stackrel{(11.54)}{=} \frac{d\mu_d}{d\mu_B} - \frac{d\mu_u}{d\mu_B} = \frac{2}{3} \frac{\frac{d\mu_d}{d\mu_u} - \frac{d\mu_u}{d\mu_d}}{2 + \frac{d\mu_d}{d\mu_u} + \frac{d\mu_u}{d\mu_d}}. \end{aligned} \quad (12.9)$$

Directly substituting this back into Eq. (12.8) is not too instructive. We do not have an analytic expression for μ_d and μ_u , but we know their behaviour from Fig. 11.3. We see that for $\mu \gtrsim 4f_\pi$, which corresponds to $\mu_B \gtrsim 6f_\pi$, $\mu_u(\mu)$ and $\mu_d(\mu)$ behave linearly. Since they are both linear with slightly different slopes, we may assume that μ_d is a linear function of μ_u in this regime. Of course, this is a poor approximation for smaller μ , but as we set the lower limit for quark matter $\mu_{B,u}$ large enough, the assumption holds. As we will soon see, the baryonic chemical potential at which the quark phase reappears is $\mu_{B,u} = 13.3f_\pi$, which is large enough for the linear phase to have begun. As a result of this, we write

$$\mu_d = a\mu_u = (1 + \Delta)\mu_u, \quad \text{where} \quad 0 < \Delta < 1. \quad (12.10)$$

Using this expression for μ_d together with the expressions for the derivatives of the chemical potentials and expanding to first order of Δ , we find

$$\begin{aligned} \mu_B \frac{d\Omega}{d\mu_B} &= \frac{3}{2} [\mu_u + (1 + \Delta)\mu_u] \left[\frac{2}{3} \frac{\partial\Omega}{\partial\mu_u} \frac{1}{1 + (1 + \Delta)} + \frac{2}{3} \frac{\partial\Omega}{\partial\mu_d} \frac{1}{1 + \frac{1}{1 + \Delta}} + \frac{2}{3} \frac{\partial\Omega}{\partial\mu_e} \frac{(1 + \Delta) - \frac{1}{1 + \Delta}}{2 + (1 + \Delta) + \frac{1}{1 + \Delta}} \right] \\ &= \mu_u(2 + \Delta) \left[\frac{\partial\Omega}{\partial\mu_u} \left(\frac{1}{2} - \frac{\Delta}{4} \right) + \frac{\partial\Omega}{\partial\mu_d} \left(\frac{1}{2} + \frac{\Delta}{4} \right) + \frac{\partial\Omega}{\partial\mu_e} \left(\frac{\Delta}{2} \right) \right] + \mathcal{O}(\Delta^2) \\ &= \frac{\partial\Omega}{\partial\mu_u} \mu_u + \frac{\partial\Omega}{\partial\mu_d} \mu_u(1 + \Delta) + \frac{\partial\Omega}{\partial\mu_e} \Delta\mu_u + \mathcal{O}(\Delta^2) = \sum_{i \in \{u, d, e\}} \mu_i \frac{\partial\Omega}{\partial\mu_i} + \mathcal{O}(\Delta^2). \end{aligned} \quad (12.11)$$

So, as long as Δ is small, the approximation $\sum_i \mu_i n_i \approx \mu_B n_B$ holds. Asymptotically, we find that

$$\mu_d \approx 1.26\mu_u, \quad \text{which yields} \quad \Delta = 0.26. \quad (12.12)$$

This is small enough for the expansion in Δ in Eq. (12.11) to be reasonable, however, the $\mathcal{O}(\Delta^2)$ -term is not rendered entirely insignificant.

To construct the interpolating function for $p(\mu_B)$, we used two third-degree polynomials. The two polynomials are constructed such that both $p(\mu_B)$ and $n(\mu_B)$ are continuous. We have included the details about the interpolating procedure in Appendix I.2. The results are displayed in Fig. 12.4.

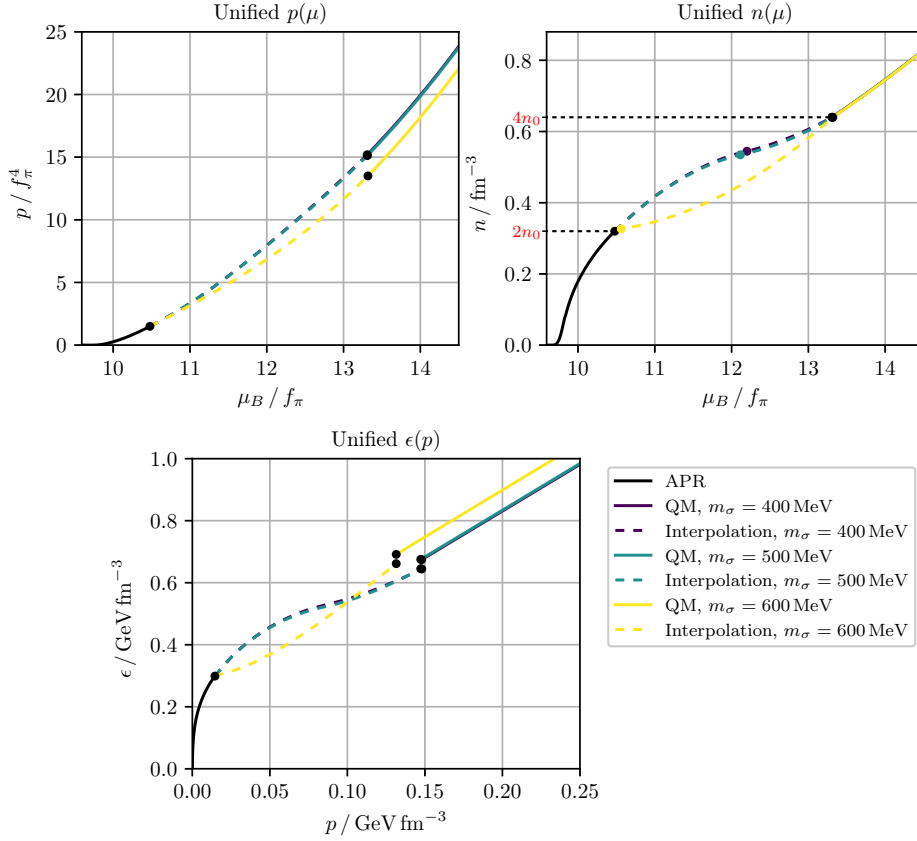


Figure 12.4: The upper left panel displays the two third degree polynomials which interpolate between the APR $p(\mu_B)$ and the QM-model $p(\mu_B)$ for each of the three values of m_σ we consider. The upper right panel displays the derivative of $p(\mu_B)$, which is the number density $n(\mu_B)$. Here, we have indicated the limiting number density for the APR-phase (lower black) and the limiting number density for the quark phase (upper, full lines). The lower plot displays the resulting equation of state. For $m_\sigma = 400$ MeV and $m_\sigma = 500$ MeV, the curves are almost coinciding.

At first we notice the small gap in the unified equation of state. This is a result of the $\mathcal{O}(\Delta^2)$ -terms in Eq. (12.11). The observant reader will also notice the coloured dots in the upper right plot. These are the points where we have forced the interpolating polynomials to run through in order to fix all degrees of freedom, as discussed in Appendix I.2. With our choice of boundary conditions, the interpolating curve for $m_\sigma = 600$ MeV is probably the least satisfactory, intuitively. We claim this due to the fact that it quite quickly takes a different shape than the continuation of the APR curve in the equation of state. In the beginning of the interpolation, the equation of state is even stiffer than the one for APR matter, which is one of the properties of the APR equation of state we were sceptical about.

To compare the equations of state we have discussed so far, we plot them together in Fig. 12.5. Note that the quark phase takes over earlier with the unified construction as compared to the hybrid equations of state. In units of Pascal, the earliest transition to the quark phase lands at $p(\mu_{B,u}) = 2.1 \times 10^{34}$ Pa, while the latest transition happens at $p(\mu_{B,u}) = 2.4 \times 10^{34}$ Pa. In all the cases, we stop trusting the APR equation of state at $p(\mu_{B,l}) = 2.3 \times 10^{33}$ Pa. Due to the QM equation of state being softer, we expect the maximal hybrid star mass to be smaller than in the case of an abrupt transition from APR to quark matter.

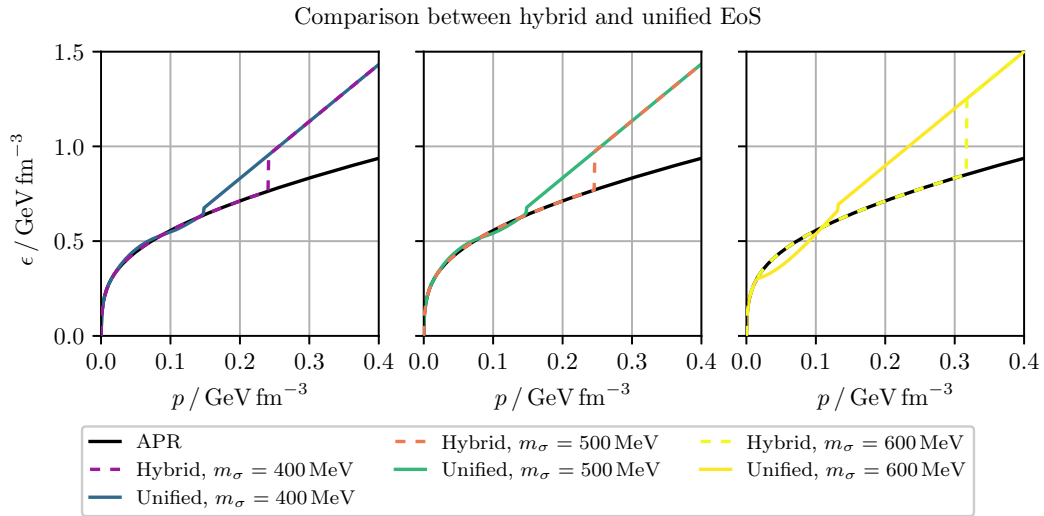


Figure 12.5: Comparison between the hybrid and unified equations of state for $m_\sigma \in \{400, 500, 600\}$ MeV. The unified equations of state start behaving like quark matter at a smaller p than in the case of the hybrid equation of state.

There turns out to be a few qualitative changes. The branching into quark-hybrid stars happens at a lower pressure and at a significantly lower mass. If we again invoke the qualitative stability argument from Section 6.1, we may conclude that the stability regime for the unified hybrid star is larger than for the hybrid stars. This is illustrated in Fig. 12.6.

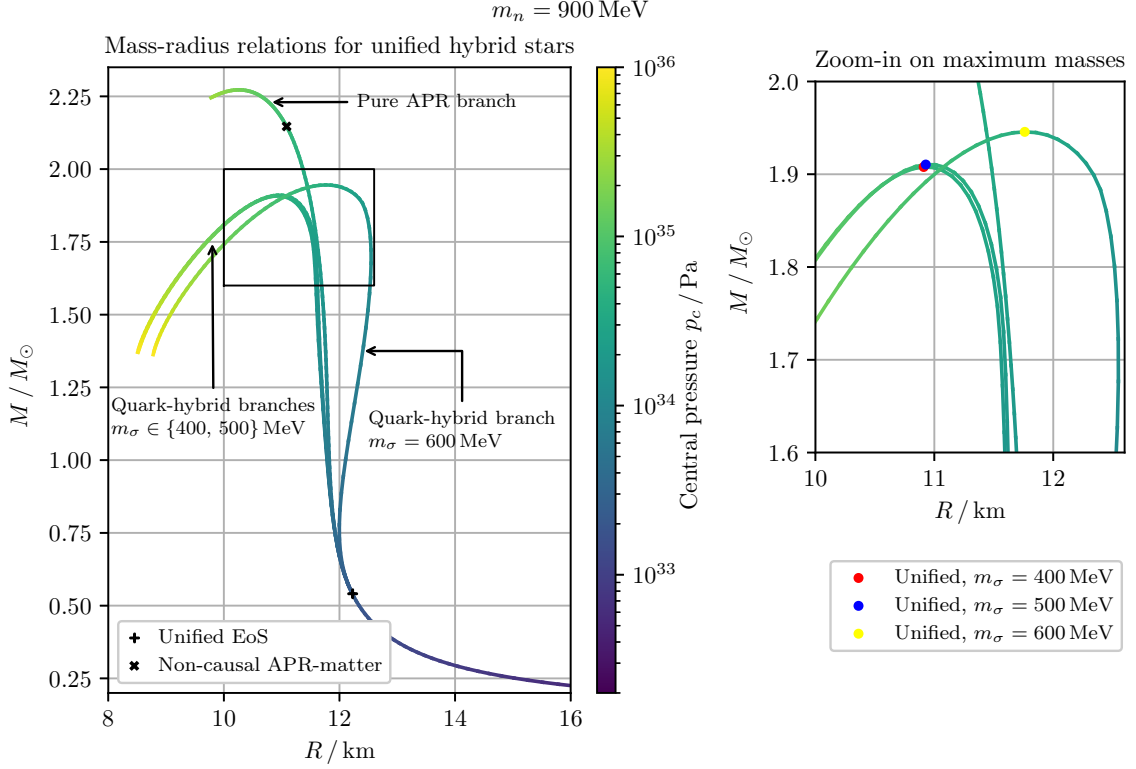


Figure 12.6: The mass-radius relations for hybrid stars with unified equations of state for $m_\sigma \in \{400, 500, 600\}$ MeV. As for the case of the first-order transition into quark matter, we have added the pure APR-matter mass-radius curve for reference. The branching happens at smaller central pressures. The branching point is marked with $+$. Due to the unified equations of state for $m_\sigma \in \{400, 500\}$ MeV being very similar to the APR equation of state in the beginning of the interpolation, the branchings for these curves only become apparent at larger central pressures.

The maximum mass-values M , R and p_c are listed in Table 12.3. Compared to the first-order transition hybrid stars, we see that the unified hybrid equations of state give slightly lighter stars. None of the values for m_σ breaks the $2M_\odot$ -benchmark.

m_σ [MeV]	M [M_\odot]	R [km]	p_c [Pa]
400	1.91	10.9	5.7×10^{34}
500	1.91	10.9	5.7×10^{34}
600	1.95	11.7	4.1×10^{34}

Table 12.3: The maximum mass-values for a unified equation of state. These values correspond to the points marked in the zoom-in panel of Fig. 12.6.

The advantage of interpolating between the equations of state, is that we do not need to require the neutron mass $m_n = 900$ MeV to obtain satisfactory results. For the hybrid equation of state, it was almost a prerequisite to shift the neutron mass down to find proper equation of state. To illustrate this, we close this section about unified hybrid stars by looking at what happens when we shift the neutron mass value back to its measured value, as given in Eq. (12.1). In addition, we turn up our scepticism towards the quark matter and trust the QM model at an even later stage, at $n(\mu_{B,u}) = 6n_0$. The results are displayed in Fig. 12.7, and the interpolating functions look reasonably smooth.

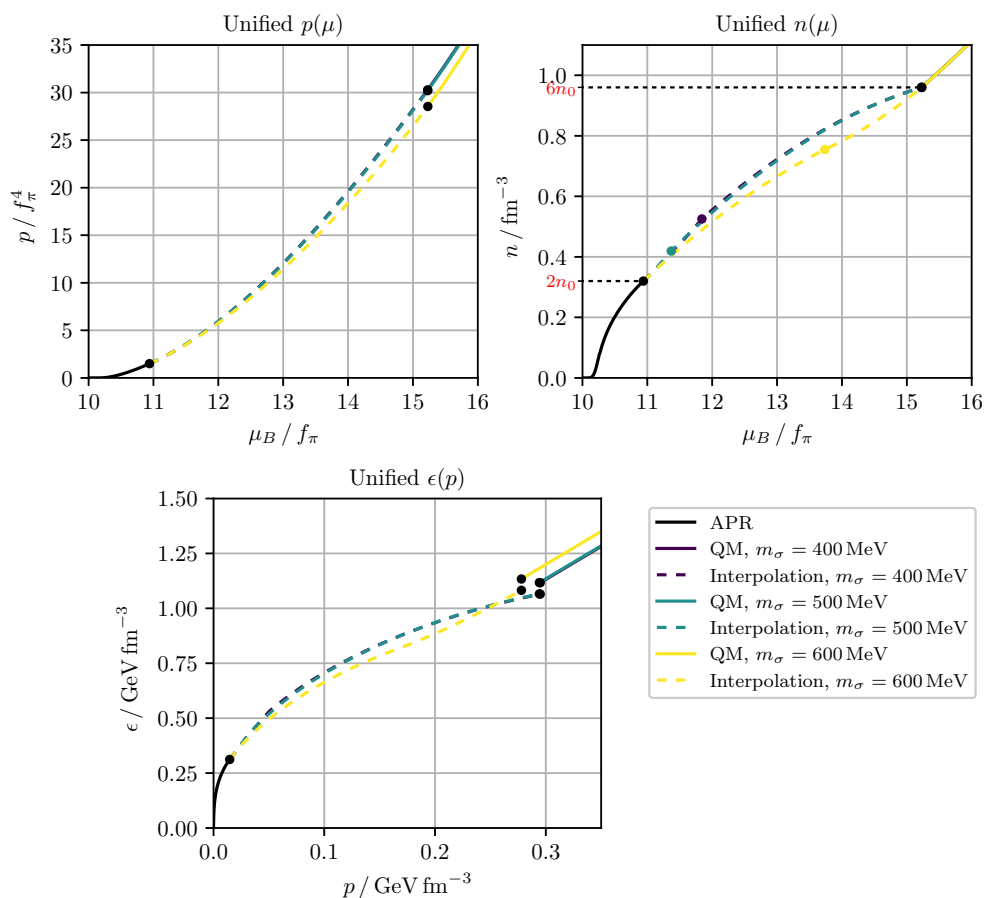


Figure 12.7: Unified $p(\mu_B)$, $n(\mu_B)$ and equation of state, just like in Fig. 12.4. We have changed the lower number density limit for the quarks from $4n_0$ up to $6n_0$. In addition, we changed the value of the neutron star from the shifted value of, $m_n = 900 \text{ MeV}$, back to the value used in the APR-calculations, $m_n = 939.6 \text{ MeV}$.

These equations of state seem a little softer than the ones displayed in the lower panel of Fig. 12.4, as there seems to be slightly higher energy density at most values of the pressure in the interpolating phase. As a consequence, our guess is that the maximum masses will be somewhat smaller. We plot the mass-radius relations in order to verify our statement, as seen in Fig. 12.8.

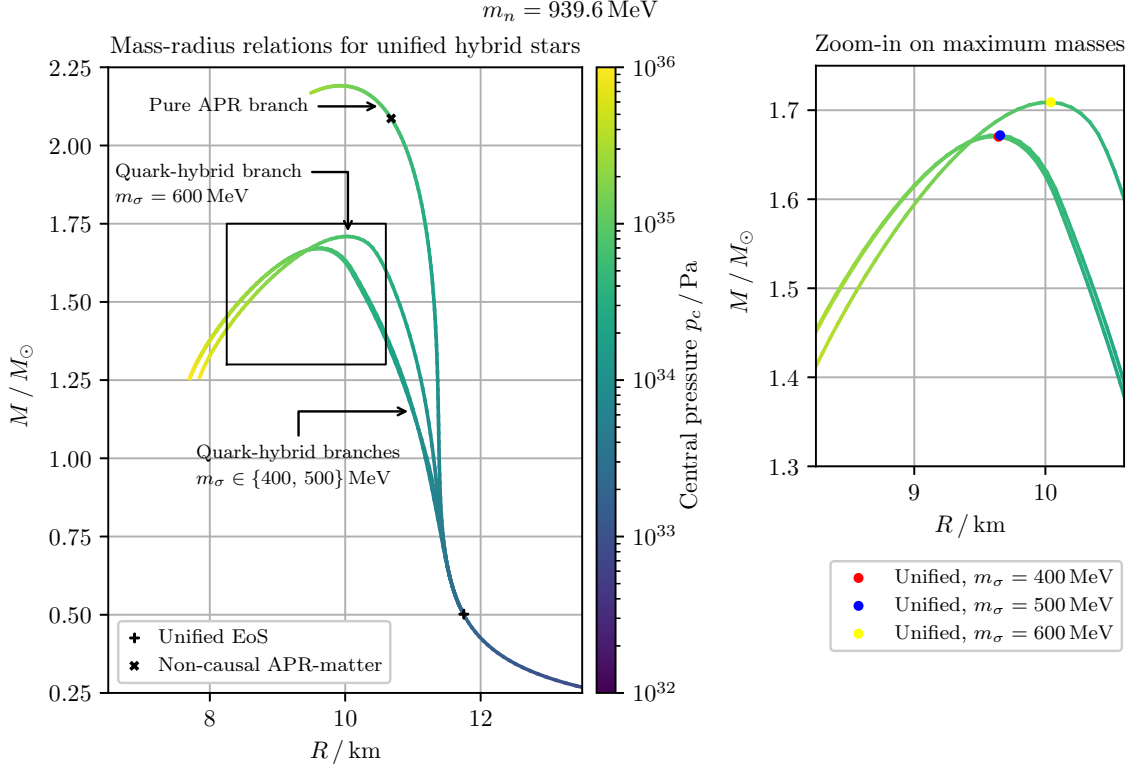


Figure 12.8: A similar plot to Fig. 12.6, with two exceptions. Firstly, we have used the unshifted value for the neutron mass, as stated in the figure title. Secondly, we have chosen to trust the quark matter equation of state at an even later stage, when the baryonic number density reaches $6n_0$.

There are a couple of noteworthy changes compared to Figs. 12.3 and 12.6. As guessed, the maxima for the masses are smaller than seen in Fig. 12.6, and significantly so. This also holds for the corresponding radii of the mass maxima, which have decreased by more than 1 km in each case. Their numerical values are shown in Table 12.4.

m_σ [MeV]	M [M_\odot]	R [km]	p_c [Pa]
400	1.67	9.64	7.9×10^{34}
500	1.67	9.66	7.9×10^{34}
600	1.71	10.0	7.0×10^{34}

Table 12.4: The maximum mass-values for unified equations of state. The unification is in the domain when the baryonic number density is between $2n_0$ and $6n_0$. The neutron mass is taken to be $m_n = 939.6 \text{ MeV}$.

Not only the hybrid stars have changed their mass-radius-profiles in Fig. 12.8, the pure APR-matter stars have changed as well. The curve has been translated towards lower radii. We see that the point where the curves branch off has been moved from a little over 12 km, to a little below 12 km. This translation is also reflected in the previously mentioned fact that all of the radii for the maximum mass-stars are smaller. This time, the barely causal, pure APR matter star has a mass and radius of

$$M = 2.08M_\odot \quad \text{and} \quad R = 10.7 \text{ km.} \quad (12.13)$$

12.4 Comparing the Quark and Hybrid Stars to Observed Neutron Stars

In the introduction, we mentioned three measurements of heavy neutron stars. We list them in Table 12.5.

Name	Our name	$M [M_{\odot}]$
PSR J1614–2230	Star ₁	1.97 ± 0.04
PSR J0348–0432	Star ₂	2.01 ± 0.04
PSR J0952–0607	Star ₃	2.35 ± 0.17

Table 12.5: Three observed neutron stars with particularly large masses, Refs. [20], [19] and [21]. We have also given the stars our own names just for this discussion, as their scientific names are just a bit *too scientific* for readability. The subscript colours match the boundaries in Fig. 13.1.

Firstly, and somewhat disappointingly, we notice that none of our models produce a large enough upper bound for the mass to accommodate for Star₃ within the limits of causality. In fact, the super-stiff pure APR-matter for the shifted neutron mass is the only equation of state which predicts a large enough maximum mass to fall inside the interval of uncertainty. However, this type of pure APR-star stops being causal at a mass of $2.15M_{\odot}$, just slightly below the interval of uncertainty. Even worse, when we take the unshifted neutron mass, the maximum mass in Eq. (12.13) for a barely causal star is clearly below the mass range of Star₃. The mass of Star₃ certainly poses a strict condition on the equation of state – even an equation of state so stiff that it violates causality is not stiff enough to predict that large a mass. An equation of state which is stiffer at smaller energy densities might, however, predict such a massive star.

The hybrid star model’s mass maxima fall within the uncertainty ranges of both Star₁ and Star₂, for all three values of m_{σ} . The maximum mass of the unified hybrid star model with m_{σ} taken to be 600 MeV falls within the range solely of Star₁, while the unified hybrid star with unshifted neutron mass produce mass maxima far away from the all of the heavy star-measurements. This suggests that we need to find equations of state which are stiffer than the ones these models produce, in particular for lower pressures, as the high density domain of pure APR matter is very stiff indeed.

Chapter 13

Summary & Outlook

13.1 Summary

At the beginning of this thesis, we set ourselves the goal to develop more realistic compact star models than ideal neutron stars, motivated by the fact that ideal neutron stars only reach a maximum mass of $\sim 0.7M_{\odot}$. A realistic model cannot contain non-interacting particles only, which require us to turn to quantum field theories at finite chemical potential with interaction terms. In chapter 9, we develop the tools we need to calculate thermodynamic quantities from a given Lagrangian density, specifically calculating the grand potential. In the following chapter, we proceed to discuss the two-flavour quark-meson model, described by \mathcal{L}_{QM} . This is a model of two free¹ quarks which interact with four mesons. Using the mean-field approximation in the mesonic sector, i.e. neglecting the mesonic fluctuations, we find that the quarks obtained a dynamic mass depending on the mean-field value of the scalar particle, which is one of the mesons. At first, we constrain the parameters of the model in an inconsistent renormalisation. The mass of the scalar meson, m_{σ} , remain a parameter of the model. Therefore, we consider three different values. This is due to the fact that the mass measurement of the scalar particle is uncertain, and its value lies in a quite broad range. From here, we are able to calculate the energy density ϵ , the pressure p , and the number density n as a function of the chemical potentials and the expectation value for the scalar particle. Constraining these with Urca-process equilibrium, local charge neutrality, and requiring that the grand potential is extremised, we manage to find ϵ , p , and n in terms of only one common chemical potential, before we finally arrive at an equation of state for quark matter.

By applying the numerical machinery we developed in the project thesis, we calculate the mass-radius relations for quark stars. It is a simple task to perform the same calculation for a consistent large N_c -limit renormalisation once we borrow the result for the properly renormalised grand potential. We find similar results with the two different renormalisations, with the exception of shifting the value of m_{σ} .

Moving on from the two-flavour quark stars, we consider hybrid stars. We model these stars with a nuclear-matter mantle using the APR equation of state, and, if the central pressures are large enough, the core using the quark-matter equation of state. At first, we discuss a sudden transition from nuclear matter to quark matter. To find credible results, we have to take the liberty to use a modified, slightly smaller, neutron mass. In the mass-radius relations, the abrupt transition gives sudden branching off an APR-matter curve at the pressure where the quark core appears. So far, we reproduce the results of Ref. [1], but moving over to unified hybrid stars, we enter uncharted (or at least *less* charted) territory. For a unified hybrid star model, we begin by determining a number density where we no longer trust the APR equation of state and a larger energy density where we start trusting the the QM equation of

¹In the sense that they are deconfined.

state. To bridge the two regions, we introduce an interpolating equation of state. The mass-radius curves for the unified equation of state branch off the APR mass-radius curve at a smaller pressure, and the branchings are less abrupt than for the sudden crossover. We test the interpolating equation of state for two different number densities at which we begin to trust the quark phase. We see what happens when we shift the neutron mass back, as the interpolating procedure can handle both values of the neutron mass well. Changing the interpolation limits and the neutron mass had a quite large impact on the predicted maximum mass. The difference was about a quarter of a solar mass. Fig. 13.1 summarises the mass-radius results for the different star models. In the figure, we have indicated the mass-ranges of the heavy neutron star measurements given in Table 12.5. For a slightly less crammed plot, we include only the consistently renormalised quark stars, and we restrict ourselves to the two largest values of m_σ .

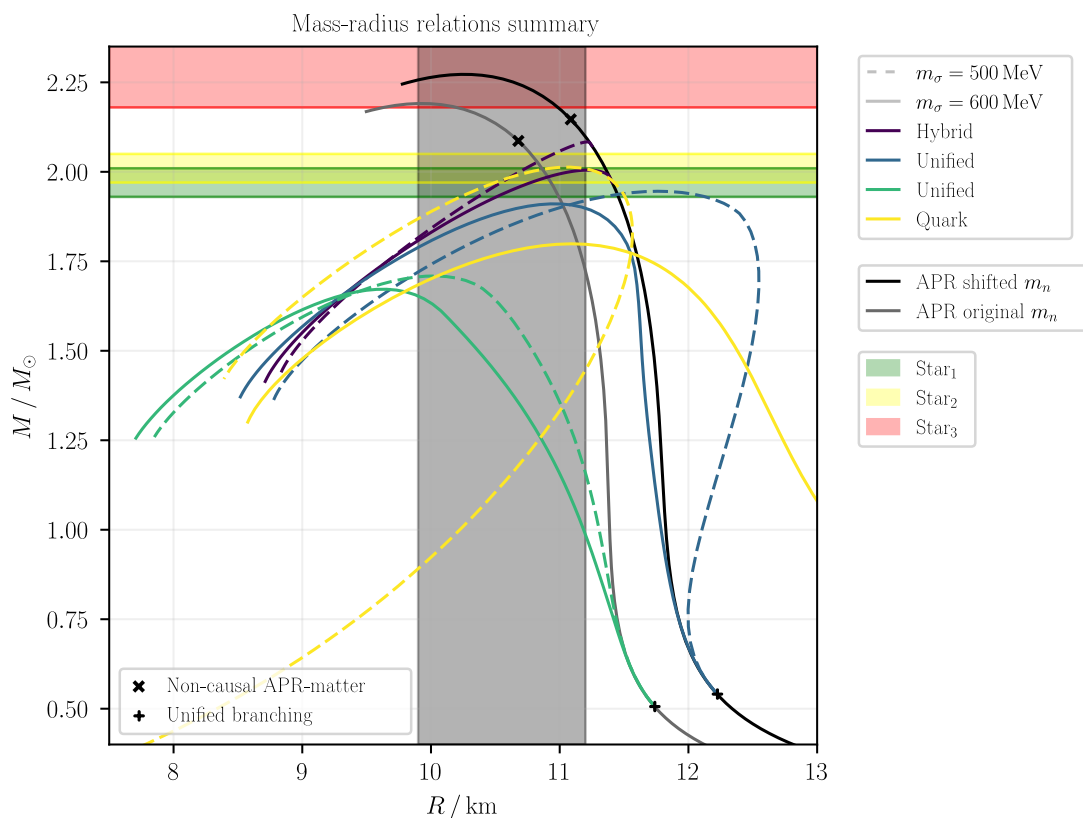


Figure 13.1: A display of most of the mass-radius relations we have found throughout this thesis. The bluer of the curves marked "Unified" are the curves for the shifted neutron mass. The coloured horizontal bands are the ranges in which the masses of three particularly heavy neutron stars lie. The grey vertical band marks a range of common radii of observed neutron stars.

In Fig. 13.1, we are happy to see that several of the discussed models reach into the interval of uncertainty for Star₁ and Star₂. Two of the heavy-weights may have been explained by the quark and hybrid models. We also see that the grey band of common star radii lies approximately in the region where most of the mass-radius curves correspond to stable stars. Lastly, we see that only the non-causal segments of the pure APR-matter stars (above the black x on the black and grey curves) reach into the mass interval of Star₃. Finding a causal equation of state which reaches into the red band is a challenge for future work. For the quark and hybrid stars, the mass-limits fall short of Star₃. In total, we have managed to move the mass threshold of our models up to the $2M_\odot$ -benchmark. The final challenge of predicting a maximum mass which reaches into the range of Star₃ contribute to keeping neutron stars a fascinating topic. The existence of the heaviest observed neutron star implies that there is still more neutron star-physics to be

uncovered, whetting our appetite for further studies of dense matter.

13.2 Outlook

This section presents what we consider to be particularly interesting future work in the continuation of this thesis. By future work, we refer both to tying up loose ends and considering new questions which arise in light of our results.

Firstly, we left an unresolved issue in the unified star models. In the equation of state for the unified stars, we accepted that there was a slight discontinuity in the energy density at the point where the interpolating phase ends and the quark phase begins, for example seen in Fig. 12.4. In the interpolating phase, we know the pressure, the baryonic chemical potential, and the baryonic number density. We must find the energy density from these quantities. However, the expression for the energy density in the quark phase does not explicitly depend on the baryonic chemical potential and the baryonic number density, but rather the chemical potentials and number densities of the quarks and the electron. Eq. (12.11) tells us that the gap is small. We find that this is true when we compare it to the gap in the first-order transition seen in Fig. 12.2. Nevertheless, an interpolation with a continuous equation of state does seem the more realistic case, making it worthwhile having a look into methods to remove the gap.

Our results also leave unanswered questions. Of particular importance is how to find an upper mass-bound to accommodate for Star₃, PSR J0952–0607. Answering this question might include broader, more general improvements to work on. As also mentioned in the project thesis, one approach is studying rotating neutron stars. In the introduction, we mentioned that the observational data of compact stars consist of radiation from pulsars, rapidly rotating compact stars. Therefore, it would be only natural to look into whether including rotations significantly impacts the mass-radius relations of different star models. This would require going back to general relativity, and finding an updated, rotation compatible TOV-equation.

Additionally, including the s -quark to QM model is in order. Ref. [40] reports that the strange quark has a constituent mass in baryons at a little over 500 MeV. The chemical potential relevant for the quark core grows larger than the strange quark mass. For example, when we started trusting the QM model equation of state at a number density of $4n_0$, we find $\mu = 8.9f_\pi \approx 820$ MeV where the quark phase takes over. This indicates that strange quarks can significantly affect the equation of state. Sorting by weight, the next quark is the charm quark, with a constituent mass of around 1.5 GeV. Therefore, the heavier quarks are likely to contribute little, and stopping at the strange quark is probably sufficient.

Relativistic Thermo- and Fluid Dynamics

In this appendix, we will derive several important results for relativistic fluids. We will refer to these results in the main chapter of this thesis. The following sections are inspired by [5] and [7].

A.1 Energy-momentum Tensor for Ideal Fluid

To begin, we would like to find the energy-momentum tensor for an ideal or perfect fluid. We do this in SR, and then generalise to GR through the general covariance principle. To define such a fluid, we imagine a fluid whose flow is described by a velocity field u^μ . An observer moving with the flow, will see the surrounding fluid to be isotropic, i.e. equal in any direction. Put differently, being in the rest frame of a fluid element, gives us local spherical symmetry. This is what we mean whenever we refer to an ideal fluid. In the rest frame of a fluid element, we can measure an energy density ϵ and a pressure p which is the same in all directions. In this particular frame in a Cartesian coordinate system, the fluid will be described by the following energy momentum tensor

$$T_{\mu\nu} = \begin{pmatrix} \epsilon & 0 & 0 & 0 \\ 0 & p & 0 & 0 \\ 0 & 0 & p & 0 \\ 0 & 0 & 0 & p \end{pmatrix}. \quad (\text{A.1})$$

We want to see how a Lorentz boost would change the energy momentum tensor. For simplicity, we take to boost of velocity v to be along the x -direction. From SR, we know that the coordinate transform is described by

$$\Lambda_\mu^\nu = \begin{pmatrix} \frac{1}{\sqrt{1-\frac{v^2}{c^2}}} & \frac{v}{c} \frac{1}{\sqrt{1-\frac{v^2}{c^2}}} & 0 & 0 \\ \frac{v}{c} \frac{1}{\sqrt{1-\frac{v^2}{c^2}}} & \frac{1}{\sqrt{1-\frac{v^2}{c^2}}} & 0 & 0 \\ 0 & 0 & 1 & 0 \\ 0 & 0 & 0 & 1 \end{pmatrix}. \quad (\text{A.2})$$

Now we can write down the boosted form of the energy-momentum tensor $T'_{\mu\nu}$

$$T'_{\mu\nu} = \Lambda_\mu^\alpha \Lambda_\nu^\beta T_{\alpha\beta} = \begin{pmatrix} \frac{\epsilon + \frac{v^2}{c^2} p}{1 - \frac{v^2}{c^2}} & \frac{v}{c} \frac{1}{\sqrt{1-\frac{v^2}{c^2}}} (\epsilon + p) & 0 & 0 \\ \frac{v}{c} \frac{1}{\sqrt{1-\frac{v^2}{c^2}}} (\epsilon + p) & \frac{p + \frac{v^2}{c^2} \epsilon}{1 - \frac{v^2}{c^2}} & 0 & 0 \\ 0 & 0 & p & 0 \\ 0 & 0 & 0 & p \end{pmatrix}. \quad (\text{A.3})$$

In the unboosted frame, take a four-velocity vector of zero spatial velocity $u_\mu = (c, 0, 0, 0)$. In the boosted frame, the same velocity takes form $u'_\mu = \Lambda_\mu{}^\nu u_\nu = (c/\sqrt{1-v^2/c^2}, v/\sqrt{1-v^2/c^2}, 0, 0)$. From looking at Eqs. (A.1) and (A.2), we notice that we can express $T_{\mu\nu}$ in any Lorentz frame in terms of the four-velocity and the Minkowski metric. In component form, we write

$$T_{\mu\nu} = \frac{u_\mu u_\nu}{c^2}(\epsilon + p) - \eta_{\mu\nu}p. \quad (\text{A.4})$$

Using the principle of general covariance, we let $\eta_{\mu\nu} \rightarrow g_{\mu\nu}$ and have thus found the energy-momentum tensor we were looking for.

A.2 Thermodynamics for an Ideal Fluid

Here we consider basic thermodynamic quantities, with the end goal of finding thermodynamic conservation laws for ideal fluids. These will be used in the stability analysis of compact stars. The relevant quantities are

- n = Baryon number density,
- ϵ = Energy density,
- p = Pressure,
- T = Temperature,
- s = Entropy per baryon, and
- μ_B = Baryonic chemical potential.

A fundamental law in physics, is the law of baryon conservation. It states that in any reaction, the baryon number N is conserved. If we let V denote a volume where there is no baryon transport over the boundary, we have that $nV = N$ is a constant. We formulate the conservation law as a derivative on nV

$$0 = \frac{d(nV)}{d\tau} = V u^\mu \nabla_\mu n + n \frac{dV}{d\tau}. \quad (\text{A.5})$$

We do not wish to have an explicit dependence of V , so we need to figure out how to rid ourselves of $\frac{dV}{d\tau}$. To do so, we imagine an infinitesimal box-volume moving along a streamline x^μ . As we know from the section on GR, we can always find a locally flat coordinate system at any point, that is, space is described by the Minkowski metric $\eta_{\mu\nu}$. We work in the coordinate system which is locally flat in the box centre.

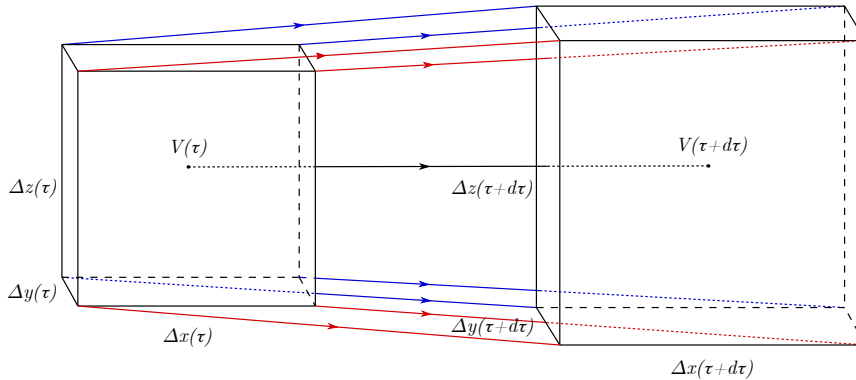


Figure A.1: An illustration of how a box-shaped fluid element with side lengths Δx , Δy and Δz evolves. Imagine that we erect a coordinate system which is flat around the box centre, which is marked by a black dot. The centre point follows the streamline coloured black. Each of the corners follow different, slightly separated streamlines. The red streamlines in the figure show the flow of the front corners, and the blue lines the corners in the back. In general, the side lengths change as τ evolves, resulting in a change of the total volume. We can describe the evolution of the side lengths if we know the fluid flow $u^\mu(x)$.

Let the side lengths of the box be $\Delta x(\tau)$, $\Delta y(\tau)$ and $\Delta z(\tau)$ as measured by an observer in the box centre. The box-volume is equal to their product. The corners of the box will follow neighbouring streamlines, which will take slightly different paths as τ evolves for the observer in the centre of the box. This is illustrated in Figure A.1 by the red and blue streamlines. For instance, $\Delta x(\tau) = x_2(\tau) - x_1(\tau)$, where x_2 is the x -coordinate of the right side of the box and x_1 the left. For each of the corners, we can find the four-vector velocity component by differentiating with respect to τ , e.g. $\frac{dx_1}{d\tau} = u_1^x$. We see that the length will be distorted and the volume will in general change. We express the rate of change of the box size as

$$\begin{aligned} \frac{dV}{d\tau} &= \Delta y \Delta z \frac{d\Delta x}{d\tau} + \Delta x \Delta z \frac{d\Delta y}{d\tau} + \Delta x \Delta y \frac{d\Delta z}{d\tau} \\ &= \Delta y \Delta z (u_2^x - u_1^x) + \Delta x \Delta z (u_2^y - u_1^y) + \Delta x \Delta y (u_2^z - u_1^z) \\ &= V \left(\frac{u_2^x - u_1^x}{\Delta x} + \frac{u_2^y - u_1^y}{\Delta y} + \frac{u_2^z - u_1^z}{\Delta z} \right) \\ &= V (\partial_x u^x + \partial_y u^y + \partial_z u^z). \end{aligned} \quad (\text{A.6})$$

In the last line, we used that $u_2^x - u_1^x = \partial_x u^x \Delta x$ for infinitesimally separated points x_1 and x_2 . u^x is the four-velocity x -component for an observer located at the centre of the volume. Note that in this rest frame, u^x is equal to zero, but the rate of change as we move one of the spatial direction does not necessarily vanish. The same procedure is also done for y and z . The parenthesis is looking very similar to the divergence $\partial_\mu u^\mu$, so we take a look at the missing piece, namely $\partial_t u^t$. If we go to the rest frame of the observer in the fluid-box element again, we find that $\frac{dt}{d\tau} = 1$, and this implies that $\partial_t u^t = 0$. With this argument, we can safely add $\partial_t u^t$ term to Eq. (A.6) and express the rate of change with the divergence of the four vector velocity of the box centre as

$$\frac{dV}{d\tau} = V (\partial_t u^t + \partial_x u^x + \partial_y u^y + \partial_z u^z) = V \partial_\mu u^\mu. \quad (\text{A.7})$$

Finally, we can use the principle of general covariance to generalise this statement to any reference frame, by promoting the partial derivative to the covariant derivative $\partial_\mu \rightarrow \nabla_\mu$. Now we can recast the baryon number conservation expressed in Eq. (A.5) into the equivalent form

$$0 = u^\mu \nabla_\mu n + n \nabla_\mu u^\mu, \quad (\text{A.8})$$

which is an expression we soon will find use for.

To analyze the ideal fluid, we start from the first law of thermodynamics

$$dE = -pdV + TdS. \quad (\text{A.9})$$

Here, dE and dS denote the change of energy and entropy inside a volume V . dV denotes a change of the volume. If we make use of baryon conservation, N is constant, then we can write $dE = \epsilon dV + V d\epsilon$, $dV = -\frac{V}{n} dn = -\frac{N}{n^2} dn$ and $dS = N ds$. We find

$$\frac{N}{n} d\epsilon - \epsilon \frac{N}{n^2} dn = p \frac{N}{n^2} + TN ds, \quad (\text{A.10})$$

where we can cancel N in all terms and multiply by n , which brings

$$d\epsilon = \frac{\epsilon + p}{n} dn + T ds \quad (\text{A.11})$$

If we parameterise the change of these quantities with the proper time τ of the fluid element, we get

$$\frac{d\epsilon}{d\tau} = \frac{\epsilon + p}{n} \frac{dn}{d\tau} + T \frac{ds}{d\tau}. \quad (\text{A.12})$$

We want to rewrite this in terms of covariant derivatives and the four-velocity instead of the proper time τ . To achieve this, we consider an observer following a streamline and measuring the energy density.

Sitting in the rest frame of a fluid element, the observer measures $\epsilon(\tau)$. This is illustrated in Figure A.2 We wish to express this in terms of the spacetime coordinates x^μ , namely $\epsilon(x^\mu)$. The path of the streamline can be parameterised by the eigentime τ .

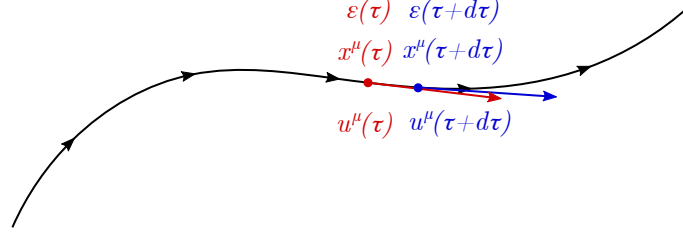


Figure A.2: An illustration of the flow of an observer measuring the energy-density $\epsilon(\tau)$ as he moves along a streamline with coordinates $x^\mu(\tau)$. The observer is marked by a dot. Everything coloured red corresponds to the proper time τ , and the blue to proptime $\tau + d\tau$. For a small step $d\tau$, the observer flows in the direction of $u^\mu(\tau)$. The change in ϵ as we vary τ slightly, is therefore proportional to the direction of the flow u^μ .

Thus, we can write $\epsilon(\tau) = \epsilon(x^\mu(\tau)) = \epsilon(ct(\tau), x(\tau), y(\tau), z(\tau))$. Next, we apply the chain rule as we take the derivative

$$\frac{d\epsilon(\tau)}{d\tau} = \frac{d}{d\tau}\epsilon(ct(\tau), x(\tau), y(\tau), z(\tau)) = c \frac{\partial\epsilon}{\partial t} \frac{dt}{d\tau} + \frac{\partial\epsilon}{\partial x} \frac{dx}{d\tau} + \frac{\partial\epsilon}{\partial y} \frac{dy}{d\tau} + \frac{\partial\epsilon}{\partial z} \frac{dz}{d\tau} = u^\mu \partial_\mu \epsilon. \quad (\text{A.13})$$

Of course, this holds not only for ϵ , but for any quantity we would measure along the stream. This argument only holds in the rest frame of the fluid element, but by the principle of general covariance, we can generalise it to

$$\frac{d}{d\tau} = u^\mu \nabla_\mu, \quad (\text{A.14})$$

which also holds in curved spacetime. The first law of thermodynamics now reads

$$u^\mu \nabla_\mu \epsilon = \frac{\epsilon + p}{n} u^\mu \nabla_\mu n + T n u^\mu \nabla_\mu s. \quad (\text{A.15})$$

In addition, we make use of Eq. (A.8) to eliminate $u^\mu \nabla_\mu n$.

$$u^\mu \nabla_\mu \epsilon = (\epsilon + p) \nabla_\mu u^\mu + T n u^\mu \nabla_\mu s. \quad (\text{A.16})$$

We have now found a description of how ϵ changes along a streamline, but we can in fact determine an even stricter condition. For this we take a look at energy-momentum conservation as expressed in Eq. (B.12), and apply this to the energy-momentum tensor for an ideal fluid in Eq. (A.4). In addition, we contract the free index with u_ν

$$\begin{aligned} 0 &= u_\nu \nabla_\mu T^{\mu\nu} \\ &= \frac{u_\nu u^\nu}{c^2} \nabla_\mu u^\mu (\epsilon + p) + \frac{u_\nu u^\mu}{c^2} \nabla_\mu u^\nu (\epsilon + p) + \frac{u_\nu u^\nu}{c^2} u^\mu \nabla_\mu (\epsilon + p) - u_\nu g^{\mu\nu} \nabla_\mu p \\ &= \nabla_\mu u^\mu (\epsilon + p) + u^\mu \nabla_\mu (\epsilon + p) - u^\mu \nabla_\mu p + \frac{u^\mu}{c^2} u_\nu \nabla_\mu u^\nu (\epsilon + p) \\ &= \nabla_\mu u^\mu (\epsilon + p) + u^\mu \nabla_\mu \epsilon. \end{aligned} \quad (\text{A.17})$$

In the last step, we have used that $u_\nu \nabla^\mu u^\nu = 0$. To see this, we note that $u_\nu u^\nu = c^2$. Taking the covariant derivative of this, we find $0 = \nabla_\mu (u_\nu u^\nu) = 2u_\nu \nabla_\mu u^\nu$. From comparing this to Eq. (A.16), we see that they are identical if we set $ds = 0$. The conclusion is that there can be no change in entropy per

baryon along a streamline of the ideal fluid. Returning to Eq. (A.11), we set $ds = 0$, which is true along any streamline. This is equivalent to saying

$$\frac{d\epsilon}{d\tau} = \frac{\epsilon + p}{n} \frac{dn}{d\tau}. \quad (\text{A.18})$$

The last thing we mention here, is the adiabatic index γ , which is a quantity which is useful for the radial perturbation analysis in Section 6.2. Its definition [5] (p. 692) is

$$\gamma \equiv \left(\frac{\partial \log(p)}{\partial \log(n)} \right)_s = \frac{n}{p} \left(\frac{\partial p}{\partial n} \right)_s. \quad (\text{A.19})$$

When we subscript the partial differentiation with s , it means that we are keeping s fixed in the differentiation. As we have discussed above, the change of the entropy is zero along the streamlines. Due to L'Hopital's rule and that $\frac{d}{d\tau}$ takes us along the streamline, we can rewrite the derivative above in the following way

$$\left(\frac{\partial p}{\partial n} \right)_s = \frac{\frac{dp}{d\tau}}{\frac{dn}{d\tau}} = \frac{\epsilon + p}{n} \frac{\frac{dp}{d\tau}}{\frac{d\epsilon}{d\tau}} = \frac{\epsilon + p}{n} \left(\frac{\partial p}{\partial \epsilon} \right)_s. \quad (\text{A.20})$$

Here we also used the just derived Eq. (A.18). Substituting this back into the expression for the adiabatic index, we find γ expressed in terms of ϵ and p .

$$\gamma = \frac{\epsilon + p}{p} \left(\frac{\partial p}{\partial \epsilon} \right)_s. \quad (\text{A.21})$$

These are all the quantities we need for the analysis of an ideal neutron star.

Appendix B

Energy-Momentum Conservation

The main goal in this appendix is to derive a mathematical expression for energy-momentum conservation. At first, we derive the Euler-Lagrange equation through the principle of least action. This we will do for a scalar field in a flat spacetime, i.e. described with the metric $\eta_{\mu\nu}$. Then we show that spacetime translation symmetries gives rise to conservation laws. These have the physical interpretation of being the conservation of energy and momentum. Finally, we argue that the result can be generalised to hold for curved spacetimes.

B.1 The Euler-Lagrange Equation

In mechanics, we seek to find the equations governing the motion of a system. One formalism for doing so is Lagrangian mechanics, where the equations of motion are derived from the Euler-Lagrange equation. This formalism is especially powerful when we are dealing with the dynamics of fields. To begin our search for the Euler-Lagrange equation, we define the Lagrangian L as

$$L = T - U, \tag{B.1}$$

where T describes the kinetic energy and U is the potential energy. Defining the Lagrangian of a system is the starting point of finding its dynamics. For a point particle of mass m and velocity v , we can insert for the kinetic energy $T = \frac{1}{2}mv^2$. The potential energy will depend on what system we are considering. For a field $\phi(x^\mu)$, we can assign a Lagrangian density \mathcal{L} to each point in spacetime and thus find the total Lagrangian by integrating over the volume of the system

$$L = \int_V dV \mathcal{L} = \int_V dV \mathcal{T} - \mathcal{U}, \tag{B.2}$$

where \mathcal{T} is the kinetic energy density and \mathcal{U} is the potential energy density. For ϕ , the kinetic energy reads $\frac{1}{2}\partial_\mu\phi\partial^\mu\phi$. We assume that \mathcal{L} only depends on $\partial_\mu\phi$, ϕ , and the spacetime coordinate x^μ . Next, we define the action $S[\phi]$ as the functional that integrates $L(\partial_\mu\phi, \phi, t)$ from t_0 to t_1

$$S = \int_{t_0}^{t_1} dt L(\partial_\mu\phi, \phi, t). \tag{B.3}$$

By letting $t_0 \rightarrow -\infty$ and $t_1 \rightarrow \infty$, we integrate \mathcal{L} over all spacetime.

$$S = \int dt \int dV \mathcal{L} = \int d^4x \mathcal{L}(\partial_\mu\phi, \phi, x^\mu), \tag{B.4}$$

where d^4x denotes a spacetime measure. An arbitrary field ϕ has infinitely many degrees of freedom. In fact, it can take any value at any spacetime coordinate, meaning that ϕ has one degree of freedom for every point in spacetime! In order to constrain so many degrees of freedom, we need a powerful restriction. This is exactly what the principle of least action gives us. It states that a system will take the configuration which minimises the action. That is, for a given start configuration $\phi_0 = \phi(t_0)$ and an end configuration $\phi_1 = \phi(t_1)$, we can predict how $\phi(t)$ will vary in between those two points: It will vary precisely such that S takes its minimal value. The next task is formulating this in a way suited for performing calculations. We find this by noting that a minimum of a functional is a stationary point of the variable ϕ , just as for a function is for a coordinate x . Therefore, the principle of least action can be stated mathematically as

$$\delta S [\partial_\mu \phi, \phi] = S [\partial_\mu(\phi + \delta\phi), \phi + \delta\phi] - S [\partial_\mu \phi, \phi] = 0, \quad (\text{B.5})$$

where $\delta\phi$ denotes an arbitrary infinitesimal variation of the field ϕ . Note that we are treating $\partial_\mu \phi$ and ϕ as independent fields, although they are in fact strongly connected. We also note that we cannot perform just any variation, as we have fixed the field at $t = t_0$ and $t = t_1$. This means that $\delta\phi(t = t_0) = 0$, and $\delta\phi(t = t_1) = 0$. In addition, we assume that the variation disappears as we move towards spatial $\pm\infty$. After all, a variation of ϕ which does not disappear towards spatial infinity would not be an infinitesimal variation of S . With this, we can write a variation in S as

$$\begin{aligned} \delta S &= \int d^4x \mathcal{L}(\partial_\mu \phi + \delta\partial_\mu \phi, \phi + \delta\phi, x^\mu) - \mathcal{L}(\partial_\mu \phi, \phi, x^\mu) \\ &= \int d^4x \mathcal{L}(\partial_\mu \phi, \phi, x^\mu) + \frac{\partial \mathcal{L}(\partial_\mu \phi, \phi, x^\mu)}{\partial(\partial_\mu \phi)} \delta\partial_\mu \phi + \frac{\partial \mathcal{L}(\partial_\mu \phi, \phi, x^\mu)}{\partial \phi} \delta\phi - \mathcal{L}(\partial_\mu \phi, \phi, x^\mu) \end{aligned} \quad (\text{B.6})$$

$$= \int d^4x \frac{\partial \mathcal{L}(\partial_\mu \phi, \phi, x^\mu)}{\partial(\partial_\mu \phi)} \partial_\mu(\delta\phi) + \frac{\partial \mathcal{L}(\partial_\mu \phi, \phi, x^\mu)}{\partial \phi} \delta\phi \quad (\text{B.7})$$

In the last equality we have cancelled two terms, and we have changed the ordering of δ and ∂_μ . Assuming that the two operations commute might at first seem strange, and not true in general. This is, however, only an artificial problem stemming from the fact that we are treating $\partial_\mu \phi$ and ϕ as independent fields. Realising that they are in fact related, we understand that the variation we perform must also be related. The variation on $\partial_\mu \phi$ must be dependent on the variation on ϕ such that $\delta\partial_\mu \phi = \partial_\mu(\delta\phi)$ if we are dealing with only one physical field. To save us some writing, we omit the dependencies of \mathcal{L} from now on, as it is the same in every term. We continue the calculation of the variation in the action

$$\begin{aligned} \delta S &= \int d^4x \frac{\partial \mathcal{L}}{\partial(\partial_\mu \phi)} \partial_\mu(\delta\phi) + \frac{\partial \mathcal{L}}{\partial \phi} \delta\phi \\ &= \int d^4x \partial_\mu \left(\frac{\partial \mathcal{L}}{\partial(\partial_\mu \phi)} \delta\phi \right) + \int d^4x \frac{\partial \mathcal{L}}{\partial \phi} \delta\phi - \partial_\mu \frac{\partial \mathcal{L}}{\partial(\partial_\mu \phi)} \delta\phi \\ &= \int d^4x \left(\frac{\partial \mathcal{L}}{\partial \phi} - \partial_\mu \frac{\partial \mathcal{L}}{\partial(\partial_\mu \phi)} \right) \delta\phi. \end{aligned} \quad (\text{B.8})$$

In the second equality, we have added and subtracted $\partial_\mu \frac{\partial \mathcal{L}}{\partial(\partial_\mu \phi)} \delta\phi$ in order to rewrite the first part of the integrand as a total derivative. In the third equality, we have made use of the vanishing of $\delta\phi$ at spatial and temporal infinity to set the integral with the total derivative to zero. As the $\delta\phi$ can be an arbitrary variation, setting the variation of the action to zero is equivalent to requiring that the integrand must be equal to zero for all spacetime coordinates

$$\partial_\mu \frac{\partial \mathcal{L}}{\partial(\partial_\mu \phi)} - \frac{\partial \mathcal{L}}{\partial \phi} = 0. \quad (\text{B.9})$$

This is the famous Euler-Lagrange equation for a scalar field.

B.2 Spacetime Translation Symmetry

A transformation which does not change S is called a symmetry of the action. A particularly important symmetry of the action is a translation of spacetime, i.e. keeping the fields fixed but translating the

coordinate system. We require this to be a symmetry, as moving our reference point should not change the physics. Put differently, moving our coordinate system by an infinitesimal δx^μ should leave S as before. Letting $x^\mu \rightarrow x'^\mu = x^\mu + \delta x^\mu$, we express the fields in terms of the translated coordinates $\phi'(x'^\mu) = \phi(x^\mu + \delta x^\mu) + \delta\phi$, where $\delta\phi = -\partial_\sigma\phi\delta x^\sigma$. We can see this from noting that we want ϕ to remain unchanged as we translate the coordinates. If we consider $\phi'(x^\mu) = \phi(x^\mu - \delta x^\mu)$, we will find $\phi'(x^\mu) = \phi(x^\mu + \delta x^\mu - \delta x^\mu) = \phi(x^\mu)$, which is what we wanted. Consequently Taylor-expanding ϕ' around x^μ to linear order in δx^μ gives $\phi'(x^\mu) = \phi(x^\mu) - \partial_\sigma\phi(x^\mu)\delta x^\sigma$. In total, invariance under translations gives

$$\begin{aligned}
 0 &= \int d^4x \mathcal{L}(\partial_\mu(\phi + \delta\phi), \phi + \delta\phi, x^\mu + \delta x^\mu) - \mathcal{L}(\partial_\mu\phi, \phi, x^\mu) \\
 &= \int d^4x \frac{\partial\mathcal{L}}{\partial(\partial_\mu\phi)}\partial_\mu(\delta\phi) + \frac{\partial\mathcal{L}}{\partial\phi}\delta\phi + \partial_\sigma\mathcal{L}\delta x^\sigma \\
 &= \int d^4x \frac{\partial\mathcal{L}}{\partial(\partial_\mu\phi)}\partial_\mu\delta\phi + \partial_\mu\frac{\partial\mathcal{L}}{\partial(\partial_\mu\phi)}\delta\phi + \partial_\sigma\mathcal{L}\delta x^\sigma \\
 &= \int d^4x \left\{ -\partial_\mu\left(\frac{\partial\mathcal{L}}{\partial(\partial_\mu\phi)}\partial_\sigma\phi\right) + \partial_\sigma\mathcal{L} \right\} \delta x^\sigma.
 \end{aligned} \tag{B.10}$$

From the second to the third line, we used Eq. (B.9) and in the last line, we have inserted the expression for $\delta\phi$. Again, we argue that the δx^σ can be arbitrary, and therefore we must require that the bracket vanishes for all x^μ . This leaves us four constraints on the system, one for each σ . The translational symmetry thus imposes important conditions on ϕ . But we can go a little further. Raising σ in the brackets (thus also lowering it for δx^σ) allows us to write

$$\begin{aligned}
 0 &= \partial_\mu\left(\frac{\partial\mathcal{L}}{\partial(\partial_\mu\phi)}\partial^\sigma\phi\right) - \partial^\sigma\mathcal{L} = \partial_\mu\left(\frac{\partial\mathcal{L}}{\partial(\partial_\mu\phi)}\partial^\sigma\phi\right) - \eta^{\sigma\mu}\partial_\mu\mathcal{L} \\
 &= \partial_\mu\left(\frac{\partial\mathcal{L}}{\partial(\partial_\mu\phi)}\partial^\sigma\phi - \eta^{\mu\sigma}\mathcal{L}\right) \equiv \partial_\mu T^{\mu\sigma}.
 \end{aligned} \tag{B.11}$$

In the final line, we define the energy-momentum tensor as a tensor with vanishing divergence. Inserting $\sigma = 0, 1, 2, 3$ we can check that this actually corresponds to energy ($\sigma = 0$) and momentum ($\sigma = 1, 2, 3$) conservation.

From the principle of general covariance as discussed briefly in the section on GR, we can turn this equation into the more general equation for curved space time

$$\nabla_\mu T^{\mu\nu} = 0. \tag{B.12}$$

We have not yet argued why this conserved tensor in fact is the energy-momentum tensor. To do so, can consider its components. We will not do this for all of them, but we exemplify the procedure with $(\mu, \sigma) = (0, 0)$

$$\begin{aligned}
 T^{00} &= \frac{\partial\mathcal{L}}{\partial(\partial_0\phi)}\partial^0\phi - \eta^{00}\mathcal{L} = \pi\dot{\phi} - \mathcal{L} \\
 &= \mathcal{H},
 \end{aligned} \tag{B.13}$$

where we have used that $\partial_0 = \partial^0$ in flat space and defined the canonical momentum $\pi \equiv \frac{\partial\mathcal{L}}{\partial\dot{\phi}}$. In the last equality, we have recognised that what we have, is the Hamiltonian density for the system. In classical mechanics, we relate the energy density and the Hamiltonian density. Continuing to this for other indices, we will see that the tensor we have defined is the familiar energy-momentum tensor.

Time-Dependent Schwarzschild Metric

When we consider a radially pulsating compact star, we need a spherically symmetric time-dependent metric. It can be shown that any spherically symmetric spacetime can be described with the Schwarzschild metric, see [5]. The line element becomes

$$ds^2 = \alpha(t, r)c^2 dt^2 - \beta(t, r)dr^2 - r^2 d\Omega^2. \quad (\text{C.1})$$

This expression is similar to Eq. (2.2), the metric is still diagonal with the standard angular part, but the functions appearing in front of dt^2 and dr^2 are now time-dependent. As a result of the time dependency, we find three new non-zero the Christoffel symbols. In the calculation below, a prime ' denotes the partial derivative with respect to r as before, and we introduce a dot $\dot{\cdot}$ to denote the partial derivative with respect to time. Calculating the symbols according to Eq. (2.11), we find

$$\begin{aligned} \Gamma_{tt}^t &= \frac{1}{2}g^{t\sigma}(\partial_t g_{t\sigma} + \partial_t g_{t\sigma} - \partial_\sigma g_{tt}) = \frac{1}{2}\frac{1}{\alpha}(\partial_t \alpha + \partial_t \alpha - \partial_t \alpha) \\ &= \frac{\dot{\alpha}}{2\alpha}, \end{aligned} \quad (\text{C.2})$$

$$\begin{aligned} \Gamma_{rr}^t &= \frac{1}{2}g^{t\sigma}(\partial_r g_{r\sigma} + \partial_r g_{r\sigma} - \partial_\sigma g_{rr}) = \frac{1}{2}\frac{1}{\alpha}(-\partial_t(-\beta)) \\ &= \frac{\dot{\beta}}{2\alpha}, \end{aligned} \quad (\text{C.3})$$

$$\begin{aligned} \Gamma_{rt}^r &= \frac{1}{2}g^{r\sigma}(\partial_r g_{t\sigma} + \partial_t g_{r\sigma} - \partial_\sigma g_{rt}) = \frac{1}{2}\frac{-1}{\beta}(\partial_t(-\beta)) \\ &= \frac{\dot{\beta}}{2\beta}. \end{aligned} \quad (\text{C.4})$$

It can be checked that all the other terms given in Eq. (2.23) remain the same. All the new terms contain a time-derivative. This is as expected, because that would make the new terms disappear if we let $\alpha(r, t) \rightarrow \alpha(r)$ and $\beta(r, t) \rightarrow \beta(r)$, which takes us back to the stationary spherically symmetric spacetime. The new non-zero Christoffel symbols give rise to some changes in the components of the

Ricci tensor. It turns out that $R_{\theta\theta}$ remains unchanged, however, R_{tt} and R_{rr} obtain some new terms.

$$\begin{aligned}
 R_{tt} &= \partial_t \Gamma_{\sigma t}^\sigma - \partial_\sigma \Gamma_{tt}^\sigma + \Gamma_{t\sigma}^\rho \Gamma_{\rho t}^\sigma - \Gamma_{tt}^\rho \Gamma_{\rho\sigma}^\sigma \\
 &= \partial_t (\Gamma_{tt}^t + \Gamma_{rt}^r) - \partial_t \Gamma_{tt}^t - \partial_r \Gamma_{tt}^r + \Gamma_{tt}^t \Gamma_{tt}^t + \Gamma_{tr}^t \Gamma_{tt}^r + \Gamma_{tt}^r \Gamma_{rt}^t + \Gamma_{tr}^r \Gamma_{rt}^r \\
 &\quad - \Gamma_{tt}^t (\Gamma_{tt}^t + \Gamma_{tr}^r) - \Gamma_{tt}^r (\Gamma_{rt}^t + \Gamma_{rr}^r + \Gamma_{r\theta}^\theta + \Gamma_{r\phi}^\phi) \\
 &= \partial_t \Gamma_{rt}^r - \partial_r \Gamma_{tt}^r + \Gamma_{tr}^t \Gamma_{tt}^r + \Gamma_{tr}^r \Gamma_{rt}^r - \Gamma_{tt}^t \Gamma_{tr}^r - \Gamma_{tt}^r (\Gamma_{rr}^r + \Gamma_{r\theta}^\theta + \Gamma_{r\phi}^\phi) \\
 &= \partial_t \left(\frac{\dot{\beta}}{2\beta} \right) - \partial_r \left(\frac{\alpha'}{2\beta} \right) + \frac{\alpha'}{2\beta} \left(\frac{\alpha'}{2\alpha} - \frac{\beta'}{2\beta} - \frac{2}{r} \right) + \left(\frac{\dot{\beta}}{2\beta} \right)^2 - \frac{\dot{\alpha}}{2\alpha} \frac{\dot{\beta}}{2\beta} \\
 &= -\frac{\alpha''}{2\beta} + \frac{\alpha'}{2\beta} \left(\frac{\alpha'}{2\alpha} + \frac{\beta'}{2\beta} \right) - \frac{\alpha'}{r\beta} + \frac{\ddot{\beta}}{2\beta} - \frac{\dot{\beta}}{2\beta} \left(\frac{\dot{\alpha}}{2\alpha} + \frac{\dot{\beta}}{2\beta} \right). \tag{C.5}
 \end{aligned}$$

As for the Christoffel symbols, all new terms come with a derivative with respect to time. Ignoring those terms restores the time independent Schwarzschild metric result given in Eq. (2.24). We now perform the same exercise for R_{rr}

$$\begin{aligned}
 R_{rr} &= \partial_r \Gamma_{\sigma r}^\sigma - \partial_\sigma \Gamma_{rr}^\sigma + \Gamma_{r\sigma}^\rho \Gamma_{\rho r}^\sigma - \Gamma_{rr}^\rho \Gamma_{\rho\sigma}^\sigma \\
 &= \partial_r (\Gamma_{tr}^t + \Gamma_{rr}^r + \Gamma_{\theta r}^\theta + \Gamma_{\phi r}^\phi) - \partial_t \Gamma_{rr}^t - \partial_r \Gamma_{rr}^r + \Gamma_{rt}^t \Gamma_{tr}^t + \Gamma_{rr}^t \Gamma_{tr}^r + \Gamma_{rr}^r \Gamma_{rr}^r + \Gamma_{rt}^r \Gamma_{rr}^t \\
 &\quad + \Gamma_{r\theta}^\theta \Gamma_{\theta r}^\theta + \Gamma_{r\phi}^\phi \Gamma_{\phi r}^\phi - \Gamma_{rr}^t (\Gamma_{tt}^t + \Gamma_{tr}^r) - \Gamma_{rr}^r (\Gamma_{rt}^t + \Gamma_{rr}^r + \Gamma_{r\theta}^\theta + \Gamma_{r\phi}^\phi) \\
 &= \partial_r (\Gamma_{tr}^t + \Gamma_{\theta r}^\theta + \Gamma_{\phi r}^\phi) - \partial_t \Gamma_{rr}^t + \Gamma_{rt}^t \Gamma_{tr}^t + \Gamma_{rr}^r \Gamma_{tr}^r + \Gamma_{r\theta}^\theta \Gamma_{\theta r}^\theta + \Gamma_{r\phi}^\phi \Gamma_{\phi r}^\phi - \Gamma_{rr}^t \Gamma_{tt}^t \\
 &\quad - \Gamma_{rr}^r (\Gamma_{rt}^t + \Gamma_{r\theta}^\theta + \Gamma_{r\phi}^\phi) \\
 &= \partial_r \left(\frac{\alpha'}{2\alpha} + \frac{2}{r} \right) - \partial_t \left(\frac{\dot{\beta}}{2\alpha} \right) + \left(\frac{\alpha'}{2\alpha} \right)^2 + \frac{\dot{\beta}}{2\alpha} \left(\frac{\dot{\beta}}{2\beta} - \frac{\dot{\alpha}}{2\alpha} \right) + \frac{2}{r^2} - \frac{\beta'}{2\beta} \left(\frac{\alpha'}{2\alpha} + \frac{2}{r} \right) \\
 &= \frac{\alpha''}{2\alpha} - \frac{\alpha'}{2\alpha} \left(\frac{\alpha'}{2\alpha} + \frac{\beta'}{2\beta} \right) - \frac{\beta'}{r\beta} - \frac{\ddot{\beta}}{2\alpha} + \frac{\dot{\beta}}{2\alpha} \left(\frac{\dot{\beta}}{2\beta} + \frac{\dot{\alpha}}{2\alpha} \right). \tag{C.6}
 \end{aligned}$$

For completion, we also show that $R_{\theta\theta}$ remains unchanged.

$$\begin{aligned}
 R_{\theta\theta} &= \partial_\theta \Gamma_{\sigma\theta}^\sigma - \partial_\sigma \Gamma_{\theta\theta}^\sigma + \Gamma_{\theta\sigma}^\rho \Gamma_{\rho\theta}^\sigma - \Gamma_{\theta\theta}^\rho \Gamma_{\rho\sigma}^\sigma \\
 &= \partial_\theta (\Gamma_{\phi\theta}^\phi) - \partial_r \Gamma_{\theta\theta}^r + \Gamma_{\theta\theta}^r \Gamma_{r\theta}^\theta + \Gamma_{\theta r}^\theta \Gamma_{\theta\theta}^r + \Gamma_{\theta\phi}^\phi \Gamma_{\phi\theta}^\phi - \Gamma_{\theta\theta}^r (\Gamma_{rt}^t + \Gamma_{rr}^r + \Gamma_{r\theta}^\theta + \Gamma_{r\phi}^\phi) \\
 &= \partial_\theta \left(\frac{\cos(\theta)}{\sin(\theta)} \right) - \partial_r \left(-\frac{r}{\beta} \right) - \frac{r}{\beta} \frac{2}{r} + \left(\frac{\cos(\theta)}{\sin(\theta)} \right)^2 + \frac{r}{\beta} \left(\frac{\alpha'}{2\alpha} + \frac{\beta'}{2\beta} + \frac{2}{r} \right) \\
 &= -\frac{\sin(\theta)}{\sin(\theta)} - \frac{\cos^2(\theta)}{\sin^2(\theta)} + \frac{1}{\beta} - \frac{r\beta'}{\beta^2} - \frac{2}{\beta} + \frac{\cos^2(\theta)}{\sin^2(\theta)} + \frac{r}{\beta} \left(\frac{\alpha'}{2\alpha} + \frac{\beta'}{2\beta} \right) + \frac{2}{\beta} \\
 &= \frac{1}{\beta} + \frac{r}{\beta} \left(\frac{\alpha'}{2\alpha} - \frac{\beta'}{2\beta} \right) - 1, \tag{C.7}
 \end{aligned}$$

which is exactly the expression we stated earlier, in Eq. (2.26). Additionally, we find a non-zero off-diagonal Ricci tensor element R_{rt}

$$\begin{aligned}
 R_{rt} &= \partial_r \Gamma_{\sigma t}^\sigma - \partial_\sigma \Gamma_{rt}^\sigma + \Gamma_{r\sigma}^\rho \Gamma_{\rho t}^\sigma - \Gamma_{rt}^\rho \Gamma_{\rho\sigma}^\sigma \\
 &= \partial_r (\Gamma_{tt}^t + \Gamma_{rt}^r) - \partial_t \Gamma_{rt}^t - \partial_r \Gamma_{rt}^r + \Gamma_{rt}^t \Gamma_{tt}^t + \Gamma_{rr}^t \Gamma_{tt}^r + \Gamma_{rt}^r \Gamma_{rt}^t + \Gamma_{rr}^r \Gamma_{rt}^r \\
 &\quad - \Gamma_{rt}^t (\Gamma_{tt}^t + \Gamma_{tr}^r) - \Gamma_{rt}^r (\Gamma_{rt}^t + \Gamma_{rr}^r + \Gamma_{r\theta}^\theta + \Gamma_{r\phi}^\phi) \\
 &= \partial_r \Gamma_{tt}^t - \partial_t \Gamma_{rt}^t + \Gamma_{rr}^r \Gamma_{tt}^r - \Gamma_{tr}^r (\Gamma_{rt}^t + \Gamma_{r\theta}^\theta + \Gamma_{r\phi}^\phi) \\
 &= \partial_r \left(\frac{\dot{\alpha}}{2\alpha} \right) - \partial_t \left(\frac{\alpha'}{2\alpha} \right) + \frac{\dot{\beta}}{2\alpha} \frac{\alpha'}{2\beta} - \frac{\dot{\beta}}{2\beta} \left(\frac{\alpha'}{2\alpha} + \frac{2}{r} \right) \\
 &= -\frac{\dot{\beta}}{r\beta}.
 \end{aligned} \tag{C.8}$$

We need to test whether or not the new terms contributes to the equations for α and β . First, we check the linear combination performed in Eq. (2.31). The terms in the Ricci tensor components with no time derivative are unchanged, so we can insert half of the calculation directly

$$\begin{aligned}
 \frac{R_{tt}}{2\alpha} + \frac{R_{rr}}{2\beta} + \frac{R_{\theta\theta}}{r^2} &= -\frac{\beta'}{r\beta^2} + \frac{1}{r^2\beta} - \frac{1}{r^2} + \frac{1}{2\alpha} \left(\frac{\ddot{\beta}}{2\beta} - \frac{\dot{\beta}^2}{4\beta^2} - \frac{\dot{\alpha}\dot{\beta}}{2\alpha\beta} \right) + \frac{1}{2\beta} \left(-\frac{\ddot{\beta}}{2\alpha} + \frac{\dot{\beta}^2}{4\alpha\beta} + \frac{\dot{\alpha}\dot{\beta}}{4\alpha^2} \right) \\
 &= -\frac{\beta'}{r\beta^2} + \frac{1}{r^2\beta} - \frac{1}{r^2}.
 \end{aligned} \tag{C.9}$$

Luckily, we find that all the new terms with time derivatives appearing in R_{tt} and R_{rr} cancel each other out in this particular linear combination. R_{tt} and R_{rr} were combined in the same way, i.e. respectively divided by α and β in addition to some common factor ($\frac{1}{2}$ above), when we searched for a condition for α in Eq. (2.43). Thus, this equation is still valid for the time-dependent metric, and therefore also Eq. (2.44) is still valid in the time-dependent case.

Appendix D

Numerical Methods of Part I

In this appendix we show the code that has been used to generate solve the TOV-system of equations numerically in Section 5.2. We also add the code that has been used to find the eigenfrequencies for the normal modes in Section 6.3. The code will also be available at https://github.com/carlfand/project_and_master from the first of August, 2023.

D.1 Numerical Solution to the TOV-system of Equations

For the cases when we have an analytic expression for $\epsilon = \epsilon(p)$, we have used the following code. To integrate the differential equation, we have used the standard Runge-Kutta 4 method. Before we have started numerically integrating, we have rewritten the TOV-equation slightly. The one we have computed numerically reads

$$\frac{d\bar{p}}{dr} = -\frac{G\varepsilon_g\bar{M}\bar{\epsilon}}{r^2c^2} \left[1 + \frac{\bar{p}}{\bar{\epsilon}}\right] \left[1 + \frac{4\pi r^3\bar{p}}{\bar{M}c^2}\right] \left[1 - \frac{2G\varepsilon_g\bar{M}}{rc^2}\right]^{-1} \quad (\text{D.1})$$

The bar, e.g. in \bar{p} , denotes that we have divided by ε_g . This means that \bar{p} and $\bar{\epsilon}$ are in their dimensionless form.

```
import numpy as np
from matplotlib import pyplot as plt
from scipy.optimize import bisect
import numba
np.seterr(all="raise")

# Here are the relevant dimesionless equations of state for the different expansions
def EoS_UR_improved(p_bar):
    try:
        return 3 * p_bar + np.sqrt(3 * p_bar)
    except FloatingPointError:
        return 0

def EoS_NR(p_bar):
    try:
        return 15 ** (3/5) / 3 * p_bar**(3/5)
    except FloatingPointError:
        return 0
```

```

def EoS_NR_improved(p_bar):
    try:
        return 15 ** (3/5) / 3 * p_bar**(3/5) + 18/7 * p_bar
    except FloatingPointError:
        return 0

def TOV_expansion(p_bar, r, M_bar, EoS, eps_g, c, G):
    """TOV equation for the expansions."""
    eps_bar = EoS(p_bar)
    try:
        return -(G * eps_g * M_bar * eps_bar) / (r ** 2 * c ** 2) * \
            (1 + p_bar / eps_bar) * (1 + (4 * np.pi * r ** 3 * p_bar) / \
                (M_bar * c ** 2)) / \
            (1 - (2 * G * eps_g * M_bar) / (r * c ** 2))
    except FloatingPointError:
        # Handling the exceptions
        if eps_bar == 0:
            return 0
        elif r == 0:
            return 0
        elif M_bar == 0:
            return 0

def runge_kutta4(func, y, x, stepsize, *params):
    """Standard RK4. y is a vector, x is an evolving parameter."""
    f1 = stepsize * func(y, x, *params)
    f2 = stepsize * func(y + f1/2, x + stepsize/2, *params)
    f3 = stepsize * func(y + f2/2, x + stepsize/2, *params)
    f4 = stepsize * func(y + f3, x + stepsize, *params)
    return y + f1/6 + f2/3 + f3/3 + f4/6

def coupled_derivative(vec, r, EoS, eps_g, c, G):
    # The coupled differential equations
    p_bar, M_bar = vec
    return np.array([TOV_expansion(p_bar, r, M_bar, EoS, eps_g, c, G),
        4 * np.pi * r**2 / c**2 * EoS(p_bar)])

def mass_radius_pressure(p_c_bar, EoS, stepsize):
    """Returns the mass, radius and central pressure of a neutron star of
    central pressure p_c."""
    # The constants relevant for a neutron star
    eps_g, c, G = 1.646776 * 10 ** 36, 3 * 10 ** 8, 6.674 * 10 ** (-11)
    # Initialising parameters:
    r, M = 0, 0
    # Introducing counter to stop while-loop after n_max iterations
    n, n_max = 0, 100000
    # Initialising list of pressure values:
    p_bar = [p_c_bar]
    while p_bar[-1] > 0 and n < n_max:
        p_next, M = runge_kutta4(coupled_derivative, np.array([p_bar[-1], M]),
            r, stepsize, EoS, eps_g, c, G)
        p_bar.append(p_next)
        r += stepsize

```

```

n += 1
if n >= n_max:
    print(" Pressure not dropped to zero {0} steps. Returning values "
          "for the pressure up to r = {1}".format(n, n * stepsize))
return M, r, p_c_bar
    
```

For the case of solving the equation of state with the analytic equations for $\epsilon = \epsilon(x_F)$ and $p = p(x_F)$, we have chosen to rewrite the TOV-equation to rather be solved for x_F .

$$\frac{dp(x_F)}{dr} = \frac{dp(x_F)}{dx_F} \frac{dx_F}{dr} = \frac{\epsilon_g x_F^4}{3\sqrt{1+x_F^2}} \frac{dx_F}{dr}. \quad (\text{D.2})$$

Doing so, we find the differential equation for x_F

$$\frac{dx_F}{dr} = -\frac{3\sqrt{1+x_F^2}}{x_F^4} \frac{G\epsilon_g \bar{M} \bar{\epsilon}}{r^2 c^2} \left[1 + \frac{\bar{p}}{\bar{\epsilon}}\right] \left[1 + \frac{4\pi r^3 \bar{p}}{\bar{M} c^2}\right] \left[1 - \frac{2G\epsilon_g \bar{M}}{rc^2}\right]^{-1} \quad (\text{D.3})$$

This saves us a lot of computation time, as we do not have to numerically find $\bar{\epsilon}$ each time we are at a new \bar{p} . The following code has been used

```

@numba.njit
def epsilon_exact(x_F):
    return 1 / 8 * (2 * x_F**3 * np.sqrt(1 + x_F**2) + x_F * np.sqrt(1 + x_F**2)
                  - np.arcsinh(x_F))
    
```

```

@numba.njit
def p_exact(x_F):
    return x_F**3 * np.sqrt(1 + x_F**2)/12 + 1/8 * (np.arcsinh(x_F)
                                                  - x_F * np.sqrt(1 + x_F**2))
    
```

```

@numba.njit
def TOV_x_F(x_F, r, M_bar, eps_g, c, G):
    eps_bar, p_bar = epsilon_exact(x_F), p_exact(x_F)
    if x_F < 0:
        return 0
    elif r == 0:
        return 0
    elif M_bar == 0:
        return 0
    else:
        return - 3 * np.sqrt(1 + x_F ** 2) / x_F ** 4 * (G * eps_g * M_bar * eps_bar) / \
            (r ** 2 * c ** 2) * (1 + p_bar / eps_bar) * \
            (1 + (4 * np.pi * r ** 3 * p_bar) / (M_bar * c ** 2)) / \
            (1 - (2 * G * eps_g * M_bar) / (r * c ** 2))
    
```

```

def coupled_derivative_x_F(vec, r, eps_g, c, G):
    x_F, M_bar = vec
    return np.array([(TOV_x_F(x_F, r, M_bar, eps_g, c, G),
                     4 * np.pi * r ** 2 / c**2 * epsilon_exact(x_F))])
    
```

```

def integrate(p_c_bar, eps_g, c, G, step, bisection_rel_error):
    # Find first a relevant interval of x_F
    x_max = 1.0
    x_min = 1/2
    
```

```

while p_c_bar < p_exact(x_min):
    # If the guessed x_max and x_min were too large
    x_min *= 1/2
    x_max *= 1/2
while p_c_bar > p_exact(x_max):
    # If the guessed x_max and x_min were too small
    x_max *= 2
    x_min *= 2
M_bar, r = 0, 0
# Find numerically the correct value for x_F, given the central pressure
x_F = bisect(f=lambda x: p_exact(x) - p_c_bar, a=x_min, b=x_max,
            xtol=x_min * bisect_rel_error)
x_Fs, x_F_diffs, M_bars = [], [], []
# Introducing cut off, to avoid being stuck in the while loop
n, n_max = 0, 150000
while x_F > 0 and n < n_max:
    x_Fs.append(x_F), M_bars.append(M_bar)
    x_F, M_bar = runge_kutta4(coupled_derivative_x_F,
                             [x_Fs[-1], M_bars[-1]], r, step, eps_g, c, G)
    x_F_diffs.append(coupled_derivative_x_F([x_Fs[-1], M_bars[-1]],
                                           r, eps_g, c, G)[0])

    r += step
    n += 1
    if not n % 10000:
        print(n)
if n >= n_max:
    print("Did not converge after {} steps.".format(n_max))
return np.array(x_Fs), np.array(x_F_diffs), np.array(M_bars), r - step

def triplet(p_min, p_max, step, n, rel_acc):
    """Generate an array of (M_bar, R, p_c)-triplets for the exact EoS
    for the ideal neutron star."""
    # Constants:
    eps_g, c, G = 1.646776 * 10 ** 36, 3 * 10 ** 8, 6.674 * 10 ** (-11)
    # Constructing logspace
    p_cs = np.array([10 ** pwr for pwr in np.linspace(np.log10(float(p_min)),
                                                    np.log10(float(p_max)), n)])

    # Initialising array for mrp-triplets
    mass_radius_p_c_triplets = np.zeros((n, 3))
    for i, p_c in enumerate(p_cs):
        # Performing integration
        x_Fs, x_F_diffs, M_bars, R = integrate(p_c/eps_g, eps_g, c, G, step=step,
                                             bisect_rel_error=rel_acc)

        # Saving only relevant data
        mass_radius_p_c_triplets[i, :] = np.array([M_bars[-1], step * len(x_Fs), p_c])
    return mass_radius_p_c_triplets

```

The @numba.njit speed the calculation up. Additionally, we supply an example of how to run the code for a simple plot

```

# Natural constants
eps_g = 1.646776 * 10 ** 36
solar_mass = 1.989 * 10 ** 30
# Choosing range of data:
log_p_min, log_p_max = 34, 38

# Generating logspace
p_cs = [10 ** pwr for pwr in np.linspace(log_p_min, log_p_max, 20)]

```

```

improved_NR_mrp_array = np.array([mass_radius_pressure(p_c / eps_g, EoS_NR_improved, 0.5)
                                   for p_c in p_cs])
exact_mrp_array = triplet(10 ** log_p_min, 10 ** log_p_max, 0.5, 20, 10**(-8))
improved_UR_mrp_array = np.array([mass_radius_pressure(p_c / eps_g, EoS_UR_improved, 0.5)
                                   for p_c in p_cs])
NR_mrp_array = np.array([mass_radius_pressure(p_c / eps_g, EoS_NR, 0.5) for p_c in p_cs])

plt.figure()
plt.plot(improved_NR_mrp_array[:, 1], improved_NR_mrp_array[:, 0] * eps_g / solar_mass)
plt.plot(exact_mrp_array[:, 1], exact_mrp_array[:, 0] * eps_g / solar_mass)
plt.plot(improved_UR_mrp_array[:, 1], improved_UR_mrp_array[:, 0] * eps_g / solar_mass)
plt.plot(NR_mrp_array[:, 1], NR_mrp_array[:, 0] * eps_g / solar_mass)
plt.show()
    
```

D.2 Eigenfrequencies for the Radially Oscillating Ideal Neutron Star

In Section 6.2.3 found an equation for the radial part of the perturbation u . When we insert the equation of state for the ideal neutron star, we find the following expression

$$\begin{aligned}
 u_n'' = - & \left\{ \frac{\bar{p}'_0}{\bar{\epsilon}_0 + \bar{p}_0} \left(4 + \frac{5}{x_F^2} \right) - \frac{3}{r} + \frac{\exp(2\lambda_0)}{r} + \frac{4\pi G}{c^4} \varepsilon_g \exp(2\lambda_0) r (3\bar{p}_0 + \bar{\epsilon}_0) \right\} u_n' \\
 & - \frac{1}{\gamma_0 \bar{p}_0} \left[\frac{(\bar{p}'_0)^2}{\bar{\epsilon}_0 + \bar{p}_0} - \frac{4\bar{p}'_0}{r} - \frac{8\pi G}{c^4} \varepsilon_g \exp(2\lambda_0) \bar{p}_0 (\bar{\epsilon}_0 + \bar{p}_0) \right] u_n - \frac{\omega_n^2}{c^2} \frac{3(1+x_F^2)}{x_F^2} \exp(2\lambda_0 - 2\nu_0) u_n.
 \end{aligned} \tag{D.4}$$

We have already introduced the dimensionless energy density $\bar{\epsilon}$ and pressure \bar{p} . Before we tackle this numerically we make some slight redefinitions.

$$\hat{\kappa}_1 = \frac{\varepsilon_g G r_0^2}{c^4}, \tag{D.5}$$

$$\hat{\kappa}_2 = \frac{\varepsilon_g G}{c^2 r_0}, \tag{D.6}$$

$$\hat{\omega}^2 = \frac{\omega^2 r_0^2}{c^2} \tag{D.7}$$

$$\hat{r} = \frac{r}{r_0}. \tag{D.8}$$

$\hat{\kappa}_1$ appears in the expression for u'' and $\hat{\kappa}_2$ in the expression for ν . $\hat{\omega}^2$ is the dimensionless frequency which we shoot for in the code below. In the end, we must restore its dimension. Where we have written omega in the code, we are really referring to $\hat{\omega}^2$. \hat{r} is the dimensionless radius, where we choose $r_0 = 10\text{km}$ as a natural length scale. Substituting these into the Eq. (D.4), and having found the equilibrium solution already, we are ready to shoot for the eigenvalues.

```

@numba.njit
def alpha(r_hat, p_bar_diff_hat, p_bar, eps_bar, M_bar, Kappa_2_hat):
    nu_arr = np.zeros_like(r_hat)
    stepsize = r_hat[1] - r_hat[0]
    for n in range(1, len(r_hat)):
        nu_arr[n] = nu_arr[n-1] + stepsize / 2 * \
            (-p_bar_diff_hat[n] / (eps_bar[n] + p_bar[n]) -
             p_bar_diff_hat[n-1] / (eps_bar[n-1] +
                                   p_bar[n-1]))
    nu_arr = nu_arr - nu_arr[-1] + 1 / 2 * np.log(1 - 2 * M_bar[-1]
                                                  * Kappa_2_hat / r_hat[-1])
    
```

```

return np.exp(2 * nu_arr)

@numba.njit
def beta(r_hat, M_bar, kappa_2_hat):
    """ Finds beta or equivalently  $\exp(2 \lambda_0)$  """
    beta_arr = np.zeros_like(r_hat)
    # we set beta(r=0) = 1 manually to avoid "division by zero"-problems
    beta_arr[0] = 1
    beta_arr[1:] = 1 / (1 - 2 * M_bar[1:] * kappa_2_hat / r_hat[1:])
    return beta_arr

@numba.njit
def gamma(x_F):
    """ Returns the 0th order adiabatic index.
    dp/depilon =  $x_F^{**2} / (3(1 + x_F^2))$  """
    return (epsilon_exact(x_F) + p_exact(x_F)) / p_exact(x_F) * \
        1/3 * x_F ** 2 / (1 + x_F**2)

@numba.njit
def u_coefficients(r, x_F, p_bar, p_bar_diff, eps_bar, alphas, betas,
                  omega_bar, kappa_bar):
    # u_coeffs[0, :] are for u'. u_coeffs[1, :] are for u.
    u_coeffs = np.zeros((2, len(r)))
    # Avoiding division by zero error, therefore cutting of the first point.
    u_coeffs[0, 1:] = (-p_bar_diff[1:] / (eps_bar[1:] + p_bar[1:]) *
                      (4 + 5/x_F[1]**2) + 3 / r[1:] - betas[1:]/r[1:]
                      - 4 * np.pi * kappa_bar * r[1:] *
                      (3 * p_bar[1:] + eps_bar[1:]) * betas[1:])

    u_coeffs[1, 1:] = (- 3 * (1 + 1/x_F[1]**2) *
                      (p_bar_diff[1]**2/((eps_bar[1:] + p_bar[1:]**2) -
                      4 * p_bar_diff[1:]/(r[1:] * (eps_bar[1:] + p_bar[1:]))) -
                      8 * np.pi * kappa_bar * betas[1:] * p_bar[1:] +
                      omega_bar * betas[1:] / alphas[1:]))

    return u_coeffs

@numba.njit
def find_nodes(omega_trial, r_hat, kappa_hat, kappa_2_hat, x_F,
              p_bar_diff_hat, M_bar):
    # Hard coded parameters:
    # When u has become larger than this, we assume it has diverged
    max_u = 50000
    pad1, pad2 = 0.001, 0.001
    p_bar, eps_bar = p_exact(x_F), epsilon_exact(x_F)
    alphas = alpha(r_hat, p_bar_diff_hat, p_bar, eps_bar, M_bar, kappa_2_hat)
    betas = beta(r_hat, M_bar, kappa_2_hat)
    # Getting coefficients
    u_coeffs = u_coefficients(r_hat, x_F, p_bar, p_bar_diff_hat,
                             eps_bar, alphas, betas, omega_trial, kappa_hat)

    # Initialising arrays with u
    u = np.zeros_like(r_hat) # u
    u_diff = np.zeros_like(r_hat) # u'
    u_curve = np.zeros_like(r_hat) # u''

```

```

step = r_hat[1] - r_hat[0] # Equidistant r

# Shooting once
# At first , u = r**3
n = 0
while n * step < pad1 * r_hat[-1]:
    u[n] = (n * step) ** 3
    u_diff[n] = 3 * (n * step) ** 2
    u_curve[n] = 6 * n * step
    n += 1

# Entering area when we integrate normally
for i in [j for j in range(n, len(r_hat))]:
    if j * step < (1 - pad2) * r_hat[-1]:
        u[i] = u[i - 1] + u_diff[i - 1] * step + \
            (step ** 2) / 2 * u_curve[i - 1]
        u_diff[i] = u_diff[i - 1] + step * u_curve[i - 1]
        u_curve[i] = u_coeffs[0, i - 1] * u_diff[i - 1] + \
            u_coeffs[1, i - 1] * u[i - 1]
        if u[i] > max_u:
            break

# At last , counting nodes.
nodes = 0
for k in range(1, len(u)):
    if u[k] * u[k - 1] < 0:
        nodes += 1

return nodes

def eigenfreq(n, x_F, p_bar_diff, M_bar, step_SI, accuracy):
    """Find the n-th eigenfrequency squared for a given
    star-configuration."""
    # The usual constants:
    eps_g, c, G = 1.646776 * 10 ** 36, 3 * 10 ** 8, 6.674 * 10 ** (-11)
    # Setting a new natural length scale r_0
    r_0 = 10 ** 4
    # Defining constants for use in
    kappa_hat, kappa_2_hat = G * eps_g / c ** 4 * r_0 ** 2, \
        G * eps_g / (c ** 2 * r_0)

    p_bar_diff_hat = p_bar_diff * r_0

    r = np.array([n * step_SI for n in range(0, len(x_F))])
    r_hat = r / r_0

    # At first , we must find two limiting omegas.
    omega_upper = 1
    omega_lower = -1
    while find_nodes(omega_upper, r_hat, kappa_hat,
                    kappa_2_hat, x_F, p_bar_diff_hat, M_bar) <= n:
        omega_upper *= 2
    while find_nodes(omega_lower, r_hat, kappa_hat,
                    kappa_2_hat, x_F, p_bar_diff_hat, M_bar) > n:
        omega_lower *= 2

```

```

# Run until the error is less than accuracy
while omega_upper - omega_lower > accuracy:
    omega_trial = (omega_upper + omega_lower) / 2
    nodes_trial = find_nodes(omega_trial, r_hat, kappa_hat,
                             kappa_2_hat, x_F, p_bar_diff_hat, M_bar)

    if nodes_trial <= n:
        omega_lower = omega_trial
    else:
        omega_upper = omega_trial

# Choose the middle value as our best guess for omega^2
omega_guess = (omega_upper + omega_lower) / 2
return omega_guess

def find_modes(n_modes, n_p_c, p_c_min, p_c_max, stepsize=0.5):
    c, G = 3.0 * 10 ** 8, 6.674 * 10 ** (-11)
    eps_g = 1.646776 * 10 ** 36
    solar_mass = 1.989 * 10 ** 30
    bisect_err = 10**(-8)
    omega_err = 10 ** (-4)
    r_0 = 10000

    # Making logspace with n_p_c elements in [p_c_min, p_c_max]
    p_cs = np.array([10 ** pwr for pwr in
                     np.linspace(np.log10(float(p_c_min)),
                                 np.log10(float(p_c_max)), n_p_c)])
    # Initialising an array of tuples (p_c, omega_1, ... omega_n, M, R)
    return_arr = np.zeros((n_p_c, n_modes + 3))
    for i, p_c in enumerate(p_cs):
        return_arr[i, 0] = p_c
        x_F, x_F_diff, M_bar, R = integrate(p_c / eps_g, eps_g, c, G,
                                             stepsize, bisect_err)
        p_bar_diff = x_F ** 4 / (3 * (np.sqrt(1 + x_F**2))) * x_F_diff
        for n in range(n_modes):
            return_arr[i, 1 + n] = eigenfreq(n, x_F, p_bar_diff, M_bar,
                                              stepsize, omega_err)
        return_arr[i, n_modes + 1] = M_bar[-1] * eps_g / solar_mass
        return_arr[i, n_modes + 2] = R / r_0
    return return_arr

# Example of running the code:
# freq_arr = find_modes(2, 10, 10 ** 34, 10 ** 38)
# plt.figure()
# plt.plot(np.log10(freq_arr[:, 0]), freq_arr[:, 1], color="blue")
# plt.plot(np.log10(freq_arr[:, 0]), freq_arr[:, 2], color="red")
# plt.show()

```

Appendix **E**

Gaussian Integrals

E.1 Ordinary Gaussian Integrals

Gaussian integrals play an essential role in QFT. The reason for this, is that Gaussian path integrals are the only class of path integrals we can solve analytically. Therefore, we need to develop an understanding of how we can solve these integrals. To achieve this, we start from the one-dimensional case and move on to the more general N -dimensional case. From there, we can take the continuum limit and solve the Gaussian path integral.

We take the one dimensional Gaussian integral to be well known. The square of the integral becomes analytically solvable, once we perform a change from Cartesian coordinates into polar coordinates.

$$\begin{aligned} \int dx \exp(-ax^2) &= \left(\int dx dy \exp(-a[x^2 + y^2]) \right)^{\frac{1}{2}} \\ &= \left(\int_0^{2\pi} d\varphi \int_0^\infty dr r \exp(-ar^2) \right)^{\frac{1}{2}} = \left(2\pi \int_0^\infty du \frac{1}{2} \exp(-au) \right)^{\frac{1}{2}} \\ &= \sqrt{\frac{\pi}{a}}. \end{aligned} \tag{E.1}$$

If we add a term linear to the exponent, e.g. bx , we can simply complete the square and perform the same calculation. The most general case of a one-dimensional Gaussian integral is

$$\int dx \exp(-ax^2 + bx + c) = \exp\left(\frac{b^2}{4a} + c\right) \int dx \exp\left(-a\left(x - \frac{b}{2a}\right)^2\right) = \sqrt{\frac{\pi}{a}} \exp\left(\frac{b^2}{4a} + c\right). \tag{E.2}$$

The one-dimensional case will be important when we have reduced the multidimensional Gaussian integral into several independent one dimensional ones. The next task is to calculate

$$I_N = \int dx_1 \dots dx_N \exp(-x_k a_{km} x_m + b_k x_k + c) \tag{E.3}$$

In the exponential in the line above, we have written $-\mathbf{x}^T \mathbf{A} \mathbf{x} + \mathbf{b} \cdot \mathbf{x} + c$ in component form. a_{km} denotes the matrix elements of A , an $N \times N$ matrix. \mathbf{x} is a vector whose N components we integrate over. \mathbf{b} is a constant vector of N components and c is a constant. We cannot simply integrate out one x_i due to the cross terms $x_k a_{km} x_m$, $k \neq m$. In order to calculate Eq. (E.3), we need to remember a few results from linear algebra. First of all, we may take the matrix A to be symmetric. This allows us to use some important relations of symmetric matrices later on. Any matrix A can be split into a symmetric part,

A_s , and an anti-symmetric part, A_{as} . Let the components be denoted a_s^{nm} and a_{as}^{nm} , respectively. We can calculate

$$\begin{aligned} \mathbf{x}^T A \mathbf{x} &= \mathbf{x}^T A_s \mathbf{x} + \mathbf{x}^T A_{as} \mathbf{x} = \mathbf{x}^T A_s \mathbf{x} + \sum_{n,m=1}^N x_n x_m a_{as}^{nm} \\ &= \mathbf{x}^T A_s \mathbf{x} + \sum_{n>m} x_n x_m (a_{as}^{nm} + a_{as}^{mn}) = \mathbf{x}^T A_s \mathbf{x}, \end{aligned} \quad (\text{E.4})$$

where we twice have used the anti-symmetric property $a_{as}^{nm} = -a_{as}^{mn}$. Firstly, we needed it to neglect the diagonal $n = m$, and secondly to cancel the rest of the terms stemming from the anti-symmetric part of A . We also assume that A is invertible. It follows that we can diagonalise it, $A = P \Lambda P^{-1}$, where, Λ is a diagonal matrix with the eigenvalues of A along its diagonal, and P is the matrix of the eigenvectors of A . When we write λ_i , we refer to the i -th eigenvalue. It is also useful to have a notation for the components of Λ , which we write λ_{ij} . The diagonal components of λ_{ij} is simply the vector λ_i , and $\lambda_{ij} = 0$ when $i \neq j$. Using the symmetry property, we find

$$P \Lambda P^{-1} = A = A^T = (P \Lambda P^{-1})^T = (P^{-1})^T \Lambda P^T, \quad (\text{E.5})$$

$$A^{-1} = (P \Lambda P^{-1})^{-1} = P \Lambda^{-1} P^{-1} = P \Lambda^{-1} P^T. \quad (\text{E.6})$$

Eq. (E.5) means that the eigenvector matrix is orthogonal $P^{-1} = P^T$. We know that these orthogonal matrices are the group of rotations and inversions. In Eq. (E.6), we have used the orthogonality property to rewrite the inverse of A in terms of the diagonal matrix Λ and the eigenvector matrix P . We know that the determinant does not change when we transpose a matrix. This means that we can write

$$1 = \det(\mathbb{1}) = \det(P P^{-1}) = \det(P P^T) = \det(P) \det(P^T) = \det(P)^2, \quad \text{i.e.} \quad |\det(P)| = 1. \quad (\text{E.7})$$

Now we know enough to handle Eq. (E.3). The trick is to introduce \mathbf{x}' such that $\mathbf{x} = P \mathbf{x}'$. From the interpretation of P above, \mathbf{x}' simply corresponds to a rotated and possibly inverted \mathbf{x} . We can thus rewrite the integrand into a diagonal form

$$\begin{aligned} \exp(-\mathbf{x}^T A \mathbf{x} + \mathbf{b} \cdot \mathbf{x} + c) &= \exp(-\mathbf{x}'^T P^T P \Lambda P^{-1} P \mathbf{x}' + \mathbf{b}^T P \mathbf{x}') \\ &= \exp(-\mathbf{x}'^T \Lambda \mathbf{x}' + \mathbf{b}^T P \mathbf{x}' + c) = \exp(-(x'_k)^2 \lambda_k + b_n P_{nk} x'_k + c) \\ &= \exp(c) \prod_{k=1}^N \exp(-x_k'^2 \lambda_k + b_n P_{nk} x'_k). \end{aligned} \quad (\text{E.8})$$

In the second line written in component form, we see that we have eliminated all cross terms in the form $x_i x_j a_{ij}$ when $i \neq j$. This means that we can separate the integrand to a product of exponentials, each exponential only containing one integration variable x'_i . We have written this out explicitly in the last line. Before we can use Eq. (E.2) on each x_i , we must change the measure. For a linear transformation of the variables represented by the matrix P , the Jacobi determinant is simply $\det(P)^{-1}$. Therefore, we write $dx_1 \dots dx_N \rightarrow dx'_1 \dots dx'_N \det(P)^{-1}$. If we assume $\det(P) = 1$, there is no change of the measure. This means that the transformation P is a pure rotation. Rotating the vector \mathbf{x} into \mathbf{x}' solves the multidimensional Gaussian integral

$$\begin{aligned} \int dx_1 \dots dx_N \exp(-x_k a_{km} x_m + b_k x_k + c) &= \int dx'_1 \dots dx'_N \exp(c) \prod_{k=1}^N \exp(-(x_k)^2 \lambda_k + b_m P_{mk} x_k) \\ &= \exp(c) \prod_{k=1}^N \sqrt{\frac{\pi}{\lambda_k}} \exp\left(\frac{(b_m P_{mk})^2}{4 \lambda_k}\right). \end{aligned} \quad (\text{E.9})$$

We would prefer not having any appearances of the eigenvalues and the eigenvectors. We can go a little further by noting that we can write

$$\frac{(b_m P_{mk})^2}{\lambda_k} = b_m P_{mk} b_n P_{nj} \lambda_{kj}^{-1} = b_m P_{mk} \lambda_{kj}^{-1} P_{jn}^T b_n = \mathbf{b}^T P \Lambda^{-1} P^T \mathbf{b} = \mathbf{b}^T A^{-1} \mathbf{b} \quad (\text{E.10})$$

In the last equality, we have used Eq. (E.6). We may also rewrite the product of the square roots in Eq. (E.9). The product of the eigenvalues is equal to the determinant of the eigenvalue matrix, which again is equal to the determinant of A . As another note, it is common to add a factor of $\frac{1}{2}$ in the quadratic terms in the Lagrangian density. This motivates us to add the same factor to our calculation here. The result remains the same, except for the appearance of a factor 2π instead of π in the square root, and $\frac{1}{4}$ turns into $\frac{1}{2}$ in the exponential term. This is easy to verify letting $A \rightarrow \frac{1}{2}A$ in the calculations above. The N dimensional Gaussian integral then reads

$$I_N = \int dx_1 \dots dx_N \exp\left(-\frac{1}{2}\mathbf{x}^T A \mathbf{x} + \mathbf{b} \cdot \mathbf{x} + c\right) = \det\left(\frac{A}{2\pi}\right)^{-\frac{1}{2}} \exp\left(\frac{1}{2}\mathbf{b}^T A^{-1} \mathbf{b} + c\right). \quad (\text{E.11})$$

As a last note upon the N -dimensional solution, we see that we can rewrite the solution in terms of the fixed point of the integrand. Let \mathbf{X} be defined as

$$\begin{aligned} \partial_{x_i} \left(-\frac{1}{2} x_m A_{mk} x_k + b_k x_k \right) \Big|_{x_i = X_i} = 0, \quad \text{which yields} \\ X_i = A_{im}^{-1} b_m. \end{aligned} \quad (\text{E.12})$$

We now reexpress Eq. (E.11) with the fixed point \mathbf{X}

$$I_N = \det\left(\frac{A}{2\pi}\right)^{-\frac{1}{2}} \exp\left(\frac{1}{2}\mathbf{b}^T \mathbf{X} + c\right). \quad (\text{E.13})$$

In Section 9, we developed the notion of a bosonic path integral, Eq. (9.45). Although being an interesting concept, it would not be worth a lot if we could not calculate anything with it. The point of calculating these N -dimensional Gaussian integrals, was to enable us to calculate the path integral. In the derivation of the path integral, we had a measure of N degrees of freedom $d\phi_n$ and an exponential. If we assume that the function in the exponent is quadratic, it is very similar to what we calculated above. Since we can solve the integral for each N , we can solve the path integral as the continuum limit of such N -degree integrals. In the continuum limit, the vector of coordinates \mathbf{x} have turned into a function ϕ , and the matrix has turned into an operator acting on the function, that is $x_n \rightarrow \phi(t)$ and $A_{n,m} \rightarrow \hat{A}(t, t')$. The discrete indices n, m turns into continuous indices t, t' . Naturally, the sum over the discrete indices goes to an integral over the continuous labels. In the continuum limit, we write the measure $\prod_{i=1}^N d\phi_i \rightarrow \mathcal{D}\phi$. The new expression reads

$$\begin{aligned} I_{\text{continuum}} &= \int \mathcal{D}\phi \exp\left(-\frac{1}{2} \int dx dy \phi(y) A(y, x) \phi(x) + \int dx b(x) \phi(x) + c\right) \\ &= \det\left(\frac{A}{2\pi}\right)^{-\frac{1}{2}} \exp\left(c + \frac{1}{2} \int dx dy b(y) A^{-1}(y, x) b(x)\right) \end{aligned} \quad (\text{E.14})$$

$$= \det\left(\frac{A}{2\pi}\right)^{-\frac{1}{2}} \exp\left(c + \frac{1}{2} \int dx dy b(y) \Phi(x)\right). \quad (\text{E.15})$$

Strangely, we have a determinant of an infinite dimensional "matrix", or the determinant of an operator. Often, this does not pose a problem, as the determinant in those cases is not dependent on any fields, and it is removed in the normalisation. If, however, we need to consider it, we can use $\det[\exp(A)] = \exp[\text{Tr}(A)]$. In the last line, we have included the continuum version of Eq. (E.13). This means that $\Phi(x)$ is the stationary point when we take the functional derivative

$$\frac{\delta}{\delta\phi(x)} \left(-\frac{1}{2} \int dx dy \phi(y) A(y, x) \phi(x) + \int dx b(x) \phi(x) + c \right) \Big|_{\phi(x) = \Phi(x)} = 0. \quad (\text{E.16})$$

A particular example of a matrix A is the identity matrix, $\mathbf{1}_{N \times N}$. In the continuum limit, $\mathbf{1}_{N \times N}$ will be represented by a delta function $\delta(y - x)$. To make everything a bit more tangible, we may calculate

an example by considering a Hamiltonian density for a free particle ϕ . In this exercise, we are using the path integral

$$\int \mathcal{D}\phi \mathcal{D}\pi \exp\left(\frac{i}{\hbar} S(\phi)\right) = \int \mathcal{D}\phi \mathcal{D}\pi \exp\left(i \int dx \pi \frac{\dot{\phi}}{c} - \mathcal{H}(\pi, \phi)\right). \quad (\text{E.17})$$

Remember that we introduced the slashed differential \mathcal{D} as having absorbed a factor of $\frac{1}{2\pi}$ into each degree of freedom. This means that we must reintroduce $\frac{1}{2\pi}$ at some point when performing the integration. The expression above is the path integral that is ordinarily derived in QFT, in the same fashion as we did for the thermal field theory. We insert the form of the Hamiltonian we know from classical field theory

$$\mathcal{H}(x) = \frac{1}{2} [\pi^2(x) + (\nabla\phi(x))^2 + m^2\phi^2(x)]. \quad (\text{E.18})$$

Here, x denotes a spacetime coordinate. In this example we have two fields ϕ and π , that is, there is two Gaussian integrals at play here. In order to bring the Hamiltonian above into something similar to the form in Eq. (E.14), we partially integrate to change $[\nabla\phi(x)]^2$ into $-\phi(x)\nabla^2\phi(x)$. We assume that the fields vanish at infinity, so there is no surface term. We must, however, take into account that we pick up a sign. In addition, we introduce a $\delta(y-x)$ which we integrate over to make Eq. (E.17) look like Eq. (E.14). The equivalent Hamiltonian density reads density

$$\mathcal{H} = \int dy \frac{1}{2} \pi(y) \delta(y-x) \pi(x) + \frac{1}{2} \phi(y) \delta(y-x) (-\nabla^2 + m^2) \phi(x). \quad (\text{E.19})$$

We now substitute this into Eq. (E.17). In addition, we apply Eq. (E.11) to integrate out π . We identify $b(x) \rightarrow i\dot{\phi}(x)$ and $A(y, x) \rightarrow i\delta(y-x)$.

$$\begin{aligned} & \int \mathcal{D}\phi \mathcal{D}\pi \exp\left(i \int dx dy \left\{ -\frac{1}{2} \pi(y) \delta(y-x) \pi(x) \right\} + i \int dx \pi \dot{\phi} - i \frac{1}{2} \int dx dy \phi(y) \delta(y-x) (-\nabla^2 + m^2) \phi(x)\right) \\ &= \det(2\pi i \delta(y-x))^{-\frac{1}{2}} \int \mathcal{D}\phi \exp\left(i \frac{1}{2} \int dx dy \frac{\phi}{c}(y) \delta(y-x) \frac{\dot{\phi}}{c}(x) - \phi(y) \delta(y-x) (-\nabla^2 + m^2) \phi(x)\right) \\ &= \det(2\pi i \delta(y-x))^{-\frac{1}{2}} \int \mathcal{D}\phi \exp\left(-\frac{i}{2} \int dx dy \phi(y) \delta(y-x) (\partial_t^2 - \nabla^2 + m^2) \phi(x)\right) \\ &= \det(2\pi i \delta(y-x))^{-\frac{1}{2}} \det\left(\frac{i\delta(y-x)(\partial_t^2 - \nabla^2 + m^2)}{2\pi}\right)^{-\frac{1}{2}} = \det(i\delta(y-x))^{-\frac{1}{2}} \det(\partial_t^2 - \nabla^2 + m^2)^{-\frac{1}{2}}. \end{aligned} \quad (\text{E.20})$$

Impressively, the Gaussian integral has allowed us to solve the path integral! From the first to the second line, we have integrated out π . Unlike previously, the factor 2π does not appear in the denominator in the determinant. This is because we have taken into account the factor of $\frac{1}{2\pi}$ hiding behind the slash in \mathcal{D} . From the second to the third line, we have partially integrated to let $\dot{\phi}(y)\delta(y-x)\dot{\phi}(x) \rightarrow \phi(y)\delta(y-x)(-\partial_t^2)\phi(x)$. Finally, we can integrate out ϕ too, and arrive at the last determinant expression. In this example, we do not strive to give this somewhat strange result an interpretation, but we will interpret the results in the thermal field theoretical case, and find that they are sensible.

E.2 Grassmannian Gaussian Integrals

In describing fermions, we had to introduce Grassmann numbers. This we did in Section 9.3.1. Here, we will further elaborate upon Grassmannian calculation by finding how to solve Grassmannian Gaussian integrals. To have non-vanishing terms in the exponential, we must use a collection of Grassmann variables and their complex conjugate. This is what appears in the derivation of the fermionic path integral. For a collection of N Grassmann numbers ξ_n and ξ_n^* , we can write a Gaussian integral

$$I_N^{\text{Grass}} = \int d\xi_1 d\xi_1^* \dots d\xi_N d\xi_N^* \exp(\xi_k^* A_{km} \xi_m) \quad (\text{E.21})$$

We will show later that linear terms $b_k \xi_k$ and $c_k \xi_k^*$ will not contribute, so we stick to only the quadratic ones to begin with. Since we treat ξ and ξ^* independently of each other, we can transform only ξ , keeping ξ^* unchanged. In Eq. (9.66), we showed how the measure changes when we linearly transform a set of Grassmannian variables. We now let $\xi = A\xi'$. With this, we can continue the line above as

$$I_N^{\text{Grass}} = \int d\xi'_1 d\xi_1^* \dots d\xi'_N d\xi_N^* \det(A) \exp(\xi_k^* \xi'_k) \quad (\text{E.22})$$

To proceed, we need to think a little about which terms give non-zero contributions when we perform an expansion of the exponential. As we need to have exactly one of each ξ'_i and ξ_i^* , the only contribution we find from the exponential above is the one stemming from the N -th order of the expansion. We continue the calculation

$$\begin{aligned} I_N^{\text{Grass}} &= \int d\xi'_1 d\xi_1^* \dots d\xi'_N d\xi_N^* \det(A) \frac{1}{N!} (\xi^* \xi')^N = \int d\xi'_1 d\xi_1^* \dots d\xi'_N d\xi_N^* \det(A) \frac{1}{N!} (\xi_1^* \xi'_1 + \dots + \xi_N^* \xi'_N)^N \\ &= \det(A) \end{aligned} \quad (\text{E.23})$$

In the parenthesis, there are $N!$ combinations of $\prod_{i=1}^N \xi'_i \xi_i^*$ with different orderings. Luckily, pairs of Grassmann numbers commute, so we do not have to worry about signs. This allows us to arrive at the final equality, by the cancelling of $N!$ and performing the integration. Now, we may actually apply the result above to the more general case of

$$\begin{aligned} I_N^{\text{Grass2}} &= \int d\xi_1 d\xi_1^* \dots d\xi_N d\xi_N^* \exp(\xi^\dagger A \xi + \mathbf{b} \cdot \xi + \mathbf{c} \cdot \xi^*) \\ &= \int d\xi'_1 d\xi_1^* \dots d\xi'_N d\xi_N^* \det(A) \exp(\xi^\dagger \xi') \exp(\mathbf{b}^T A^{-1} \xi' + \mathbf{c} \cdot \xi^*) \\ &= \det(A) + \int d\xi'_1 d\xi_1^* \dots d\xi'_N d\xi_N^* \exp(\xi^\dagger \xi') \sum_{i=1}^N \left\{ \sum_{n=1}^N b_i A_{im}^{-1} \xi'_m + c_i \xi_i^* \right\} = \det(A). \end{aligned} \quad (\text{E.24})$$

The linear terms do not contribute to the Gaussian! From the first to the second, we performed the linear transformation we also did previously, as well applying the exponential property we derived in Eq. (9.60). From the second to the third, we expanded the last exponential and performed the integration which is the same as Eq. (E.23). At last, we realise that the other term only has odd numbers of ξ'_i and ξ_i^* , resulting in its vanishing under the integral.

Appendix **F**

Noether's Theorem

Symmetries lie at the heart of QFT. Continuous symmetries give rise to conserved currents, which are integral parts in constructing interaction terms between matter fields and gauge fields in Lagrangian densities. Noether's theorem tells us how to relate a symmetry to a conserved current. As this theorem is so important, we take a few moments to derive it here.

First of all, a continuous symmetry transformation can always be taken to be infinitesimal. If we can show that an infinitesimal transformation is a symmetry, we know we can build finite transformations from the infinitesimal ones. We consider a collection of fields ϕ_i which transform infinitesimally, and we assume that the Lagrangian will at most obtain a total derivative. This total derivative will only contribute with a surface term after integration. The surface term vanishes at infinity and the total derivative will therefore not contribute to the action (or grand canonical partitionfunction). We write an infinitesimal transformation

$$\phi_i \rightarrow \phi_i + \delta\phi_i = \phi_i + \epsilon F_i[\phi_j, \partial_\mu\phi_j] \quad \text{and} \quad \mathcal{L} \rightarrow \mathcal{L}' = \mathcal{L}(\phi_j, \partial_\mu\phi_j) \rightarrow \mathcal{L}(\phi_j, \partial_\mu\phi_j) + \epsilon \partial_\mu K^\mu(\phi_j, \partial_\mu\phi_j), \quad (\text{F.1})$$

where F and K^μ are some functions depending on the fields and their derivatives. Putting these two transformation properties together, we get the following equality

$$\begin{aligned} \mathcal{L}' - \mathcal{L} &= \mathcal{L}' - \mathcal{L} \\ \frac{\partial \mathcal{L}}{\partial \phi_i} \delta\phi_i + \frac{\partial \mathcal{L}}{\partial(\partial_\mu\phi_i)} \delta\partial_\mu\phi_i &= \epsilon \partial_\mu K^\mu, \quad \text{which implies} \\ \partial_\mu \left(\frac{\partial \mathcal{L}}{\partial(\partial_\mu\phi_i)} \right) \delta\phi_i + \frac{\partial \mathcal{L}}{\partial(\partial_\mu\phi_i)} \partial_\mu(\delta\phi_i) - \epsilon \partial_\mu K^\mu &= 0 \\ \partial_\mu \left(\frac{\partial \mathcal{L}}{\partial(\partial_\mu\phi_i)} F_i[\phi_j, \partial_\mu\phi_j] - K^\mu \right) &= 0. \end{aligned} \quad (\text{F.2})$$

In this calculation, we have used the Euler-Lagrange equation to go from the second to the third line. In addition, we have commuted δ and the partial derivative ∂_μ , just like we did when we derived the Euler-Lagrange equation. In the last line, we can identify the conserved current. This theorem is particularly useful, because it shows the existence of a conserved current *and* it tells us how to calculate it. We name the current j^μ .

$$j^\mu = \frac{\partial \mathcal{L}}{\partial(\partial_\mu\phi_i)} F_i[\phi_j, \partial_\mu\phi_j] - K^\mu. \quad (\text{F.3})$$

Each conserved current j_i^μ has its conserved charge Q_i . We find the conserved charge from integrating

j_i^0 over space

$$Q_i = \int d\mathbf{x} j_i^0, \quad \text{where} \quad \frac{dQ}{dt} = \int d\mathbf{x} \partial_t j^0 = - \int d\mathbf{x} \nabla \cdot \mathbf{j} = 0. \quad (\text{F.4})$$

The vanishing of the last integral happens after we apply Stokes' theorem and use the fact that the current vanish at spatial infinity. We see now that the charge Q_i is conserved. The remaining job is just to identify F and K^μ for a given \mathcal{L} . To familiarise ourselves with procedure, we may consider the Lagrangian of a free fermion under a U(1) symmetry transformation

$$\mathcal{L} = \Psi^\dagger \gamma_0 (i\gamma^\mu \partial_\mu - m)\Psi \quad \text{with} \quad \Psi \rightarrow \exp(i\theta)\Psi, \quad \Psi^\dagger \rightarrow \Psi^\dagger \exp(-i\theta), \quad (\text{F.5})$$

where θ is a number. It is easy to see that the exponential factors cancel, rendering this transformation a symmetry of \mathcal{L} . In other words, we may set $K^\mu = 0$. For an infinitesimal transformation, i.e. infinitesimal θ , we may write $\Psi \rightarrow \Psi + i\theta\Psi$. Now we have identified F as $i\Psi$. When we substitute this into Eq. (F.3), we find the conserved current

$$j^\mu = \Psi^\dagger \gamma^0 i\gamma^\mu i\Psi = -\Psi^\dagger \gamma^0 \gamma^\mu \Psi. \quad (\text{F.6})$$

Feynman Diagrams

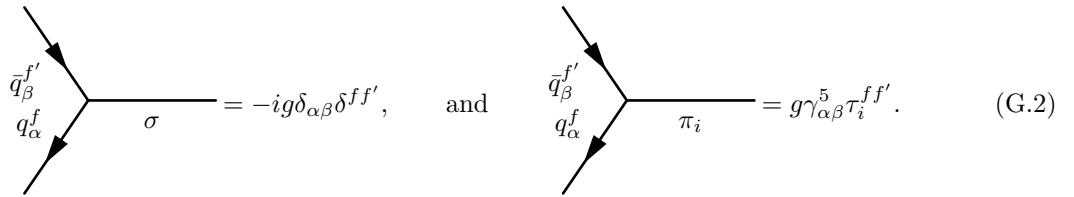
We find explaining the Feynman rules for the QM model slightly outside the scope of this thesis. However, as we have mentioned renormalising and quantum corrections a couple of times, it would be a pity to leave the diagrammatic calculations altogether. Therefore, we calculate one of the mesonic self-energy diagrams we presented in Section 11.5.

G.1 Feynman Rules for the Quark-Meson Model

We start by drawing up the vertices and their Feynman rules. Next, we state the propagators for this theory. Note that we will calculate the self energy in the vacuum, namely that $\mu = 0$. The relevant interaction terms from the fermionic sector are an index-mess

$$\mathcal{L}_{\text{int, q}} = -g\bar{q}_\alpha^f \sigma q_\alpha^f - ig\bar{q}_\alpha^f \gamma^5 q_\alpha^{f'} \tau_i^{ff'} \pi_i. \quad (\text{G.1})$$

f, f' are flavour indices and α, β are indices of the four components of the quarks. We have suppressed the colour indices, as there are no colour interactions. We would not want more indices in there now! In the end, we must simply remember to sum over colour, giving a factor N_c . They give rise to the following interaction vertices:

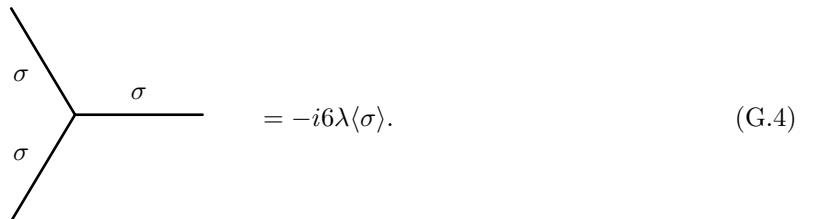


$$\begin{array}{c} \swarrow \\ \bar{q}_\beta^{f'} \\ \searrow \\ q_\alpha^f \end{array} \begin{array}{c} \text{---} \\ \sigma \\ \text{---} \end{array} = -ig\delta_{\alpha\beta}\delta^{ff'}, \quad \text{and} \quad \begin{array}{c} \swarrow \\ \bar{q}_\beta^{f'} \\ \searrow \\ q_\alpha^f \end{array} \begin{array}{c} \text{---} \\ \pi_i \\ \text{---} \end{array} = g\gamma_{\alpha\beta}^5 \tau_i^{ff'}. \quad (\text{G.2})$$

For the diagram we are going to calculate, we need the three-point σ -interaction. The Lagrangian density term reads

$$\mathcal{L}_\sigma^3 = -\lambda\langle\sigma\rangle\sigma_1^3. \quad (\text{G.3})$$

This yields a vertex rule of



$$\begin{array}{c} \swarrow \\ \sigma \\ \searrow \\ \sigma \end{array} \begin{array}{c} \text{---} \\ \sigma \\ \text{---} \end{array} = -i6\lambda\langle\sigma\rangle. \quad (\text{G.4})$$

Note that it is common to define the interaction terms with $\frac{1}{n!}$. In this case, $n = 3$, and we omitted the factorial, producing an extra factor of 6. In addition to knowing the vertices, we must identify the propagators. For the fermions, we include the indices

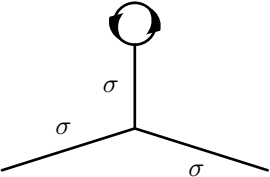
$$\alpha, f \longrightarrow \beta, f' = \frac{i(\gamma^\mu k_\mu + g\langle\sigma\rangle)_{\alpha\beta}}{k^2 - g^2\langle\sigma\rangle^2} \delta^{ff'}, \quad (\text{G.5})$$

where we have used k for the momentum. The mesonic propagators do not have internal indices, and are thus simpler on the form

$$\text{---}\sigma\text{---} = \frac{i}{k^2 - m_\sigma^2} \quad \text{and} \quad \text{---}\pi_i\text{---} = \frac{i}{k^2 - m_{\pi_i}^2}. \quad (\text{G.6})$$

G.2 Diagram Calculation

In Section 11.5, we stated the Feynman-diagrams we must calculate to properly renormalise the theory. We tackle one of them, in order to not leave the diagrams entirely untouched. Firstly, why do we calculate these diagrams, specifically? We say that the propagator, $\tilde{\Delta}(p)$, has a pole at the particle mass. Taking the propagator directly from the free theory or model is what is called tree-level, as the Feynman graphs have no loops. In the tree-level approximation, we get the masses m_σ and m_π for the meson. This we can see from finding the pole at $p^2 = m_\sigma^2$ in the σ -propagator above. We used the tree-level mass in Section 11.4. The loop diagrams we must calculate, are corrections to the propagator – meaning that they move pole of the propagator, shifting the particle mass. As seen from the diagrams we take into account, there are always two external mesons: The loops contribute with corrections to the mesonic propagators. Put differently, adding propagator contributions takes into account that we are dealing with particles that interact, not just free particles. We tackle one of these contributions



$$= L_\sigma^2. \quad (\text{G.7})$$

Tracing the diagram from the lower interaction, we get a three-point σ -interaction vertex factor, a σ -propagator of $p = 0$, a σ - q -vertex factor and a fermion propagator. As the fermion propagator connects to the same vertex, we trace over the flavour, colour and quark indices. In addition, we get a -1 from the fermion loop. We calculate

$$\begin{aligned} L_\sigma^2 &= -i6\lambda\langle\sigma\rangle \frac{i}{-m_\sigma^2} (-ig) \int (-1) d^d k \text{Tr} \left[\frac{i(\gamma^\mu k_\mu + g\langle\sigma\rangle)}{k^2 - g^2\langle\sigma\rangle^2} \right] \\ &= (-1)^4 i^4 \frac{\lambda g^2 \langle\sigma\rangle^2}{m_\sigma^2} 6 \cdot 4N_c N_q \int \frac{d^d k}{(2\pi)^d} \frac{1}{k^2 - g^2\langle\sigma\rangle^2} \\ &= -24N_c N_q \lambda \frac{g^2 \langle\sigma\rangle^2}{m_\sigma^2} \int \frac{d^d k}{(2\pi)^d} \frac{1}{k^2 - g^2\langle\sigma\rangle^2} \end{aligned} \quad (\text{G.8})$$

We recognise the integral as perfectly ready for dimensional regularisation, which we deal with in Appendix H. Peeking a little ahead, this integral is what we call $I_{2,d}^0$, with $\Delta = g\langle\sigma\rangle$. These are the main ingredients for calculating the rest of the meson one loop self-energy diagrams. We leave the rest of the calculations for Ref. [48]. Note that the definitions of the coupling coefficients vary from there to here.

Appendix H

Dimensional Regularisation

When we arrive at results stemming from a path integral, we often encounter formally divergent integrals. In this section, we shall develop a way to make sense of these integrals. The technique we shall use is called dimensional regularisation. For instance, we found the integral

$$I_{-1/2,0}^3 = \int d^3k \sqrt{k^2 + m^2}, \quad (\text{H.1})$$

when we calculated the grand partition function in the mean field approximation in Section 11.2. The notation $I_{-1/2,0}^3$ might seem a bit strange, but it becomes meaningful at once we derive how to perform dimensional regularisation on a class of integrals on the form

$$I_{a,b}^d = \int d^d k \frac{k^b}{(k^2 + \Delta)^a}, \quad (\text{H.2})$$

where $k = |\mathbf{k}|$. We recognise $I_{-1/2,0}^3$ above as one particular member of this class of integrals. We now seek to solve Eq. (H.2) for any a, b and d . Since this integral has spherical symmetry in d -dimensions, we may perform a change of coordinates into a spherical coordinate system. This means that

$$\int d^d k \rightarrow \int d\Omega_d \int_0^\infty dk k^{d-1}, \quad (\text{H.3})$$

where $d\Omega_d$ denotes an infinitesimal element ("solid angle") of the $d-1$ -dimensional sphere, S^{d-1} . Looking at the integrand, we expect $I_{a,b}^d$ to be finite when a is large enough. Specifically, for large k , we see that the k -dependent integrand goes like

$$k^{d-1} \frac{k^b}{(k^2 + \Delta)^a} \stackrel{k \gg \Delta}{\approx} k^{d+b-2a-1}. \quad (\text{H.4})$$

For the integral to be convergent we must require that the integrand goes to zero faster than k^{-1} , giving the restriction

$$a > \frac{b+d}{2}. \quad (\text{H.5})$$

For the case of $a = -\frac{1}{2}$, $b = 0$ and $d = 3$, this is clearly not satisfied.

The integral over $d\Omega_d$ yields the total surface of a $d-1$ -dimensional unit sphere. Naturally, for $d = 2$ and S^1 , this corresponds to the "surface area" of a unit radius circle, 2π . For $d = 3$ and S^2 , we get the surface area of a unit sphere, 4π . Now, we wonder what the "surface area" of a general $d-1$ -dimensional sphere might be, S^{d-1} . Stranger still, we want this to be sensible even for a non-integer d . In order to

answer this question, we start from the Gaussian integral we calculated in Eq. (E.2), setting $a = 1$ and going the other way around. We exponentiate with d to find

$$\begin{aligned}\sqrt{\pi}^d &= \left(\int dx \exp(-x^2) \right)^d = \int d^d x \exp(-x_1^2 - \dots - x_d^2) \stackrel{\substack{\uparrow \\ x = |\mathbf{x}|}}{=} \int d\Omega_d \int_0^\infty dx x^{d-1} \exp(-x^2) \\ &\stackrel{\substack{\uparrow \\ u = x^2}}{=} \frac{1}{2} \int d\Omega_d \int_0^\infty du u^{\frac{d}{2}-1} \exp(-u) = \frac{\Gamma(\frac{d}{2})}{2} \int d\Omega_d.\end{aligned}\quad (\text{H.6})$$

Due to the spherical symmetry of the integrand, we used Eq. (H.3) to split the angular part and the radial part of the integral. After that, we performed the substitution $u = x^2$, which allowed us to recognise the radial integral as the definition of the Γ -function.

The Γ -function will play an important role in this section, so we take some time to recapitulate some of its essential properties.

$$\begin{aligned}(1) \quad & \Gamma(z) = \int_0^\infty du u^{z-1} \exp(-u), & z \in \mathbb{C} \mid \text{Re } z > 0 \\ (2) \quad & \Gamma(z+1) = z\Gamma(z), \\ (3) \quad & \Gamma(n) = (n-1)!, & n \in \mathbb{N}.\end{aligned}\quad (\text{H.7})$$

Property (1) is simply the definition of the Γ -function when the real part of the argument z is greater than zero. In this case, the integral is convergent. The second property holds whenever $\text{Re } z > 0$, as we can show by partial integration

$$\begin{aligned}\Gamma(z+1) &= \int_0^\infty du u^z \stackrel{\substack{t' = \exp(-u) \\ s = u^z}}{=} - \left[u^z \exp(-u) \right]_{u=0}^{u=\infty} + z \int_0^\infty u^{z-1} \exp(-u) \\ &= z\Gamma(z).\end{aligned}\quad (\text{H.8})$$

Property (3) follows from subsequent use of (2) and the fact that $\Gamma(1) = 1$, which is easily verified by the definition (1). We also note that $\Gamma(\frac{1}{2}) = \sqrt{\pi}$. This is also verifiable by (1) and using the substitution $u = x^2$ to find a Gaussian integral. Another important remark is that $\Gamma(z)$ is also defined for $\text{Re } z < 0$. In this case, the integral in (1) is no longer valid, and the $\Gamma(z)$ is defined as the analytic continuation of (1). We will not dwell further on this topic. The important fact is that property (2) still holds. This causes $\Gamma(z)$ to have poles in $z = 0, -1, -2, \dots$. A last important remark about $\Gamma(z)$, is its Weierstrass form. This is an equivalent form, and we will use it to expand the function around its pole in $z = 0$. It reads

$$\Gamma(z) = \frac{\exp(-\gamma_E z)}{z} \prod_{n=1}^{\infty} \left(1 + \frac{z}{n} \right)^{-1} \exp\left(\frac{z}{n}\right).\quad (\text{H.9})$$

Here, γ_E is the Euler-Mascheroni constant. We now consider $\Gamma(\epsilon)$, where we take ϵ to be small so we neglect all terms which are proportional to ϵ . We expand the terms in orders of ϵ to find

$$\begin{aligned}\Gamma(\epsilon) &= \frac{\exp(-\gamma_E \epsilon)}{\epsilon} \prod_{n=1}^{\infty} \left(1 + \frac{\epsilon}{n} \right)^{-1} \exp\left(\frac{\epsilon}{n}\right) \\ &= \frac{1}{\epsilon} \left[1 - \gamma_E \epsilon + \mathcal{O}(\epsilon^2) \right] \prod_{n=1}^{\infty} \left(1 - \frac{\epsilon}{n} + \mathcal{O}(\epsilon^2) \right) \left(1 + \frac{\epsilon}{n} + \mathcal{O}(\epsilon^2) \right) \\ &= \frac{1}{\epsilon} (1 - \gamma_E \epsilon) + \mathcal{O}(\epsilon) = \frac{1}{\epsilon} - \gamma_E + \mathcal{O}(\epsilon).\end{aligned}\quad (\text{H.10})$$

We see that the $\Gamma(\epsilon)$ has a simple pole when $\epsilon \rightarrow 0$. In addition, there is a constant non-diverging term of γ_E . This is the final Γ -function property we will need here.

We now return again to Eq (H.6). A simple reshuffling of the terms gives us the surface area of a $d - 1$ -dimensional sphere

$$S_{d-1} = \int d\Omega_d = \frac{2\pi^{\frac{d}{2}}}{\Gamma(\frac{d}{2})}. \quad (\text{H.11})$$

We see that for $d = 2$, we get the surface area $S_1 = \frac{2\pi}{1!} = 2\pi$, exactly like we expected. For $d = 3$, we find $S_2 = \frac{2\pi^{\frac{3}{2}}}{\Gamma(1+\frac{1}{2})} = \frac{4\pi^{\frac{3}{2}}}{\pi^{\frac{1}{2}}} = 4\pi$, again in accordance with what we expected. Eq. (H.11) takes care of the angular part of Eq. (H.2). Continuing from here, we find

$$I_{a,b}^d = \int d\Omega_d \int_0^\infty dk \frac{k^{b+d-1}}{(k^2 + \Delta)^a} = \frac{2\pi^{\frac{d}{2}}}{\Gamma(\frac{d}{2})} \underbrace{\int_0^\infty dk \frac{k^{b+d-1}}{(k^2 + \Delta)^a}}_{\text{Radial integral}}. \quad (\text{H.12})$$

Next, we tackle the radial part. In order to do so, we perform a clever substitution

$$l = \frac{\Delta}{k^2 + \Delta}, \quad \text{or} \quad k^2 = \frac{\Delta}{l} - \Delta. \quad (\text{H.13})$$

We seek to eliminate k in favour of l in the radial integral. We are able to do this now, but we must also find how the measure dl relates to dk . In addition, we need to express the integration boundary for l . The results are

$$\frac{dl}{dk} = -\frac{2k}{\Delta} \frac{\Delta^2}{(k^2 + \Delta)^2} = -\frac{2k}{\Delta} l^2 \quad \text{which means} \quad dk = -\frac{\Delta}{2kl^2} dl. \quad (\text{H.14})$$

The boundaries become $l(k = 0) = 1$ and $l(k \rightarrow \infty) = 0$. Equipped with this substitution, we start to calculate

$$\begin{aligned} \int_0^\infty dk \frac{k^{b+d-1}}{(k^2 + \Delta)^a} &= -\frac{1}{2} \int_1^0 dl \frac{\Delta}{kl^2} \frac{k^{b+d-1}}{\Delta^a} \frac{\Delta^a}{(k^2 + \Delta)^a} && \text{(by (H.14))} \\ &= \frac{\Delta^{-a+1}}{2} \int_0^1 dl \left(\frac{\Delta}{l} - \Delta \right)^{\frac{b+d}{2}-1} l^{a-2} && \text{(by (H.13))} \\ &= \frac{\Delta^{\frac{b+d}{2}-a}}{2} \int_0^1 dl (1-l)^{\frac{b+d}{2}-1} l^{a-\frac{b+d}{2}-1} = \frac{\Delta^{\frac{b+d}{2}-a}}{2} I^{\frac{b+d}{2}, a-\frac{b+d}{2}}. && (\text{H.15}) \end{aligned}$$

In the last equality, we have defined a new class of integrals, $I^{\alpha,\beta}$. In order to arrive at a final form for the radial integral, we must be able to calculate

$$I^{\alpha,\beta} = \int_0^1 dt (1-t)^{\alpha-1} t^{\beta-1}. \quad (\text{H.16})$$

Luckily for us, these types of integrals are also related to the Γ -function through an identity. To see this identity, we start by considering the product of $\Gamma(\alpha)$ and $\Gamma(\beta)$. We insert the definition and rearrange some terms

$$\begin{aligned} \Gamma(\alpha)\Gamma(\beta) &= \left(\int_0^\infty du u^{\alpha-1} \exp(-u) \right) \left(\int_0^\infty dv v^{\beta-1} \exp(-v) \right) \\ &= \int_0^\infty \int_0^\infty du dv u^{\alpha-1} v^{\beta-1} \exp(-u-v). \end{aligned} \quad (\text{H.17})$$

Now we are going to perform a change of variables $s = s(u, v)$ and $t = t(u, v)$. Motivated by having a single integration variable in the exponent, we try $s = u + v$. With this, the values of s range from 0

to ∞ . With this substitution, we can eliminate u in favour for s . Considering ourselves done with the exponent term, the remainder of the integrand now looks like

$$u^{\alpha-1}v^{\beta-1} = (s-v)^{\alpha-1}v^{\beta-1} = s^{\alpha+\beta-2} \left(1 - \frac{v}{s}\right)^{\alpha-1} \left(\frac{v}{s}\right)^{\beta-1}. \quad (\text{H.18})$$

In this form, it is certainly tempting to let $t = \frac{v}{s} = \frac{v}{u+v}$. The values of t lie in the interval $[0, 1]$. Naturally, we must take into consideration the Jacobian. We find the following

$$\det J = \begin{vmatrix} \frac{\partial s}{\partial t} & \frac{\partial s}{\partial v} \\ \frac{\partial u}{\partial t} & \frac{\partial u}{\partial v} \end{vmatrix} = \begin{vmatrix} 1 & 1 \\ -\frac{v}{(u+v)^2} & \frac{1}{u+v} - \frac{v}{(u+v)^2} \end{vmatrix} = \frac{1}{u+v} - \frac{v}{(u+v)^2} + \frac{v}{(u+v)^2} = \frac{1}{s}. \quad (\text{H.19})$$

Now we are ready to insert the substitution into Eq. (H.17)

$$\begin{aligned} \Gamma(\alpha)\Gamma(\beta) &= \int_0^\infty ds \int_0^1 dt |\det J|^{-1} s^{\alpha+\beta-2} (1-t)^{\alpha-1} t^{\beta-1} \exp(-s) \\ &= \int_0^\infty ds \int_0^1 dt s^{\alpha+\beta-1} (1-t)^{\alpha-1} t^{\beta-1} \exp(-s) = \int_0^\infty ds s^{\alpha+\beta-1} \exp(-s) \int_0^1 dt (1-t)^{\alpha-1} t^{\beta-1} \\ &= \Gamma(\alpha + \beta) \int_0^1 dt (1-t)^{\alpha-1} t^{\beta-1}. \end{aligned} \quad (\text{H.20})$$

We recognise the last integral to be exactly on the form of Eq. (H.16). Thus the solution reads

$$I^{\alpha, \beta} = \frac{\Gamma(\alpha)\Gamma(\beta)}{\Gamma(\alpha + \beta)}, \quad (\text{H.21})$$

which is the identity we were hinting at earlier. Everything is now ready to be applied to calculate $I_{a,b}^d$,

$$I_{a,b}^d = \frac{2\pi^{\frac{d}{2}}}{\Gamma\left(\frac{d}{2}\right)} \frac{\Delta^{\frac{b+d}{2}-a}}{2} \frac{\Gamma\left(\frac{b+d}{2}\right) \Gamma\left(a - \frac{b+d}{2}\right)}{\Gamma(a)}. \quad (\text{H.22})$$

As stated earlier, we expect $I_{a,b}^d$ to be finite whenever Eq. (H.5) is satisfied. This is also reflected in the solution above, as $\Gamma(z)$ diverges as $z \rightarrow 0$ or a negative integer. For instance, if we let $a \rightarrow \frac{b+d}{2}$, we get a divergence in the last Γ -function in the numerator above. To analyse further the divergences which may occur, we will use property (2) in Eq. (H.7) in combination with our description of the divergence at $z = 0$ given by Eq. (H.10). This is where the name dimensional regularisation starts making sense: We "perturb" our dimensionality of the integral $I_{a,b}^d$, that is, instead of letting d be an integer, we write it $d \rightarrow d - 2\epsilon$, where d_{int} is the integer dimension, and 2ϵ is some small perturbation. We may now insert the perturbed dimension into the Γ s, as these functions are also defined for non-integer arguments. The integral will no longer be divergent for the non-integer d . Specifically, we may now split the formally divergent integral into one part which diverges as we let d approach an integer value and other finite parts. We say that we have regulated the integral. However, upon perturbing the dimension by 2ϵ , we must add a constant customarily called $\mu^{2\epsilon}$ to the integral. This is in order to keep the dimension of the integral. The measure is dimensionful, and to counteract its dimensional perturbation we need a dimensionful μ . This is a very important property, as μ will scale whenever we scale our units. We write $d^d k \rightarrow \mu^{2\epsilon} d^{d-2\epsilon} k$.

Finally, we puzzle every piece in this chapter together to meaningfully solve formally divergent integrals on the form $I_{a,b}^d$. By perturbing the dimension of the measure, we get

$$I_{a,b}^d \xrightarrow{\text{dim.reg.}} \mu^{2\epsilon} I_{a,b}^{d-2\epsilon} = \mu^{2\epsilon} \frac{\pi^{\frac{d}{2}-\epsilon}}{\Gamma\left(\frac{d}{2}-\epsilon\right)} \frac{\Gamma\left(\frac{b+d}{2}-\epsilon\right) \Gamma\left(a - \frac{b+d}{2} + \epsilon\right)}{\Gamma(a)} \Delta^{\frac{b+d}{2}-a-\epsilon} \quad (\text{H.23})$$

In the special case of $b = 0$, this expression simplifies slightly. As this case will be useful in Section 11.2, we state the result

$$I_{a,0}^d \xrightarrow{\text{dim.reg.}} \mu^{2\epsilon} \pi^{\frac{d}{2}-\epsilon} \frac{\Gamma\left(a + \epsilon - \frac{d}{2}\right)}{\Gamma(a)} \Delta^{\frac{d}{2}-a-\epsilon}. \quad (\text{H.24})$$

Numerical Methods of Part II

In this Appendix, we explain some of the numerical procedures we perform in Part II. We also provide the python code for some calculations we find to be the most crucial. The complete code for both the project and Master's thesis will be available from the first of August, 2023 at

https://github.com/carlfand/project_and_master.

I.1 Dimensionless Form of Ω

In Section 11.5, we state the renormalised expression for the grand potential. We wish to express everything on a dimensionless form, and we use f_π as our dimensionful scale. An overline, e.g. \overline{m}_π , denotes that we have removed the dimensionality by dividing by f_π . We note two relations in particular

$$\overline{m}_q = \frac{gf_\pi}{f_\pi} = g, \quad \text{and} \quad \frac{\Delta}{m_q} = \frac{g\langle\sigma\rangle}{gf_\pi} = \overline{\langle\sigma\rangle}. \quad (\text{I.1})$$

The expression underneath is what we have used in the numerical implementation, where our quantities are dimensionless.

$$\begin{aligned} \frac{\Omega_0}{f_\pi^4} = \overline{\Omega}_0 &= \frac{3\overline{m}_\pi^2}{4} \left[1 - \frac{g^2 N_c}{4\pi^2} G(m_\pi^2) \right] \overline{\langle\sigma\rangle}^2 \\ &- \frac{\overline{m}_\sigma^2}{4} \left[1 + \frac{g^2 N_c}{4\pi^2} \left\{ \left(1 - \frac{4g^2}{\overline{m}_\sigma^2} \right) F(m_\sigma^2) + \frac{4g^2}{\overline{m}_\sigma^2} - F(m_\pi^2) - G(m_\pi^2) \right\} \right] \overline{\langle\sigma\rangle}^2 \\ &+ \frac{\overline{m}_\sigma^2}{8} \left[1 - \frac{g^2 N_c}{4\pi^2} \left\{ \frac{4g^2}{\overline{m}_\sigma^2} \ln(\overline{\langle\sigma\rangle}^2) - \left(1 - \frac{4g^2}{\overline{m}_\sigma^2} \right) F(m_\sigma^2) + F(m_\pi^2) + G(m_\pi^2) \right\} \right] \overline{\langle\sigma\rangle}^4 \\ &- \frac{\overline{m}_\pi^2}{8} \left[1 - \frac{g^2 N_c}{4\pi^2} G(m_\pi^2) \right] \overline{\langle\sigma\rangle}^4 - \overline{m}_\pi^2 \left[1 - \frac{g^2 N_c}{4\pi^2} G(m_\pi^2) \right] \overline{\langle\sigma\rangle} + \frac{3g^2}{4} \frac{g^2 N_c}{4\pi^2} \overline{\langle\sigma\rangle}^4. \end{aligned} \quad (\text{I.2})$$

with

$$F(m^2) = 2 - 2 \left[\frac{4g^2}{m^2} - 1 \right]^{\frac{1}{2}} \arctan \left(\left[\frac{4g^2}{m^2} - 1 \right]^{-\frac{1}{2}} \right), \quad (\text{I.3})$$

$$G(m^2) = \frac{4g^2 \overline{m}_\pi^2}{m^4} \left[\frac{4g^2}{m^2} - 1 \right]^{-\frac{1}{2}} \arctan \left(\left[\frac{4g^2}{m^2} - 1 \right]^{-\frac{1}{2}} \right) - \frac{\overline{m}_\pi^2}{m^2}. \quad (\text{I.4})$$

We also write down the derivative with respect to $\overline{\langle\sigma\rangle}$, which gives terms which appear in the constraint equations to find μ_u and μ_d .

$$\begin{aligned}
 \frac{\partial\overline{\Omega}_0}{\partial\overline{\langle\sigma\rangle}} &= \frac{3\overline{m}_\pi^2}{2} \left[1 - \frac{g^2 N_c}{4\pi^2} G(m_\pi^2) \right] \overline{\langle\sigma\rangle} \\
 &\quad - \frac{\overline{m}_\sigma^2}{2} \left[1 + \frac{g^2 N_c}{4\pi^2} \left\{ \left(1 - \frac{4g^2}{\overline{m}_\sigma^2} \right) F(m_\sigma^2) + \frac{4g^2}{\overline{m}_\sigma^2} - F(m_\pi^2) - G(m_\pi^2) \right\} \right] \overline{\langle\sigma\rangle} \\
 &\quad + \frac{\overline{m}_\sigma^2}{2} \left[1 - \frac{g^2 N_c}{4\pi^2} \left\{ \frac{4g^2}{\overline{m}_\sigma^2} \ln(\overline{\langle\sigma\rangle}^2) - \left(1 - \frac{4g^2}{\overline{m}_\sigma^2} \right) F(m_\sigma^2) + F(m_\pi^2) + G(m_\pi^2) \right\} \right] \overline{\langle\sigma\rangle}^3 \\
 &\quad - \frac{\overline{m}_\pi^2}{2} \left[1 - \frac{g^2 N_c}{4\pi^2} G(m_\pi^2) \right] \overline{\langle\sigma\rangle}^3 - \overline{m}_\pi^2 \left[1 - \frac{g^2 N_c}{4\pi^2} G(m_\pi^2) \right] + \frac{g^4 N_c}{2\pi^2} \overline{\langle\sigma\rangle}^3 \\
 &= 0.
 \end{aligned} \tag{I.5}$$

I.2 Construction of Interpolating Polynomials in a Unified Equation of State

In Section 12.3 we unify two equations of state by introducing an interpolating function. The simplest strategy to try (at least the first one that we arrived at) was fitting a polynomial between the nucleon and quark equations. For this section, let a subscript N denote the last of the nucleon phase quantities, and q the first of the quark quantities. For example, the chemical potential μ_N denotes the final chemical potential for which we take the APR-data to be valid. Fixing the number density n_N where we no longer trust APR, we may find μ_N and $p_N(\mu_N)$ which correspond to n_N . μ and n denote the baryonic chemical potential and the baryonic number density, i.e. we skip the subscript B in this section. Similarly, we can fix a number density n_q where we no longer trust the QM-model results and identify μ_q and p_q at that point. We neglect the electrons in this section, as they hardly contributed at all to the grand potential. Recalling Eqs. (3.6) and (9.4), we write

$$n = -\frac{\partial\Omega}{\partial\mu} = \frac{\partial p}{\partial\mu}, \quad (\text{definition})$$

$$1 < \frac{\partial\epsilon}{\partial p} = \frac{\partial}{\partial p}(-p + \mu n) = -1 + \frac{\partial\mu}{\partial p} \frac{\partial}{\partial\mu}(\mu n) = -1 + \frac{1}{n} \left(n + \mu \frac{\partial n}{\partial\mu} \right) = \frac{\mu}{n} \frac{\partial n}{\partial\mu}. \quad (\text{causality condition})$$
(I.6)

We are trying to construct a second-order phase transition. This means that $p(\mu)$ and its derivative, $n(\mu)$, must be continuous. In contrast, the *hybrid* equation of state we worked with in Section 12.2 gave us a discontinuous number density $n(\mu)$. Given the values of the pressure and number density at the two end points, this uniquely determines a third degree polynomial. It is tempting to just find such a polynomial, however, it allows for $\frac{\partial n}{\partial\mu} < 0$. We cannot accept such an interpolating equation of state, as it violates causality. We may introduce a fourth-degree polynomial, and try to use the degree of freedom in the last polynomial coefficient to assert that the causality condition holds, however, this does not give causal equations of state either. Instead of going to even higher order, we may consider the possibility of splitting the interval $[\mu_N, \mu_q]$ at some μ_m , and assigning one lower order (than 4) polynomial for each segment. Naturally, we must impose boundary conditions at μ_m . The chemical potential μ_m is ours to pick, giving us some freedom to select the "most pleasing" interpolating polynomials which satisfies the causality condition. The simplest possible solution, is to choose two second-degree polynomials. This approach will in general give three kinks of the unified $n(\mu)$ at μ_N , μ_m and μ_q . This "kinked" behaviour does not seem very realistic. We can remedy this by going to higher order in each of the polynomials, at the cost of making the determination of coefficients somewhat more tedious. In the end, we settled for introducing two *third*-degree polynomials. The first polynomial, r , is valid from μ_N to μ_m , and the second one, q , from μ_m to μ_q . To fully constrain the total of 8 coefficients, we require that $p(\mu)$ is continuous (3 conditions), $n(\mu)$ is continuous (3 conditions) and that $n'(\mu)$ is continuous through μ_N (1 condition), removing one kink. At last, we fix the eighth coefficient by choosing $n(\mu_m) = n_m$. With this construction, a kink in $n(\mu)$ may occur at μ_m and μ_q . We seek to tune the parameters μ_m and $n(\mu_m)$ to both make the resulting equation of state causal, but also to make n_m as smooth as possible.

First we look at some technicalities of the polynomials, then we plot what a few of them look like. To make the boundary conditions easy to implement, we define r and q in the following way

$$r(x) = a + bx + cx^2 + dx^3, \quad x \in [0, \mu_m - \mu_N], \quad (\text{I.7})$$

$$q(u) = e + fu + gu^2 + hu^3, \quad u \in [\mu_m - \mu_q, 0], \quad (\text{I.8})$$

where we must linearly shift μ before passing it as an argument to r and q . Note that the linear shift is not the same for r as for q . The different shifts read

$$x(\mu) = \mu - \mu_N, \quad \mu \in [\mu_N, \mu_m] \quad \text{and} \quad u(\mu) = \mu - \mu_q, \quad \mu \in [\mu_m, \mu_q]. \quad (\text{I.9})$$

This linear shift gives boundary conditions which are easy to use to eliminate the set of coefficients. Most

of the equations are even uncoupled.

$$\begin{aligned}
 r(x(\mu_N)) &= p_N(\mu_N) & r'(x(\mu_N)) &= n_N, & r''(x(\mu_N)) &= \frac{\partial n_N}{\partial \mu}, \\
 r(x(\mu_m)) &= q(u(\mu_m)), & q(u(\mu_q)) &= p_q, & q'(u(\mu_q)) &= n_q, \\
 r'(x(\mu_m)) &= n_m & q'(u(\mu_m)) &= n_m. & &
 \end{aligned} \tag{I.10}$$

Fixing (μ_m, n_m) , we may evaluate them. For example, we fix $n_m = \frac{n_N + n_q}{2}$, and vary μ_m . The differences are best illustrated in a plot of the number densities, as seen in Fig. I.1.

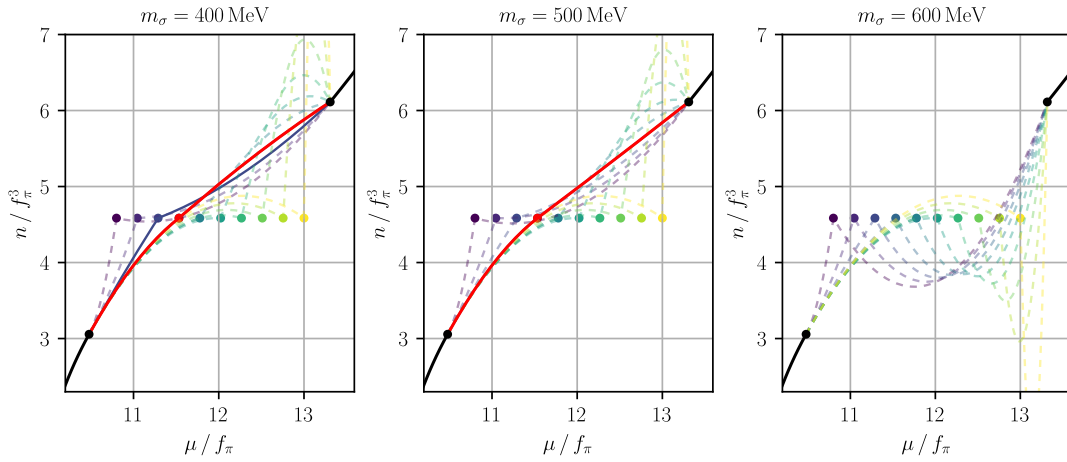


Figure I.1: The panels display the polynomials that interpolate between the number densities of the nucleon phase (lower left black) with the quark phase (upper right black) with boundary conditions as given in Eq. (I.10). The faded, dashed lines represent non-physical equations of state. The full lines are physically acceptable, based on the causality. The red line represents the favoured polynomial, judged by its smoothness. The coloured dots mark the point we force the polynomials to run through, namely (μ_m, n_m) . The colours other than the red one, are added only to make visual separation of curves easier. There are only causality breaking polynomials for $m_\sigma = 600$ MeV.

With boundary conditions in Eq. (I.10) and the chosen set of (μ_m, n_m) , we see that there are possible polynomials for a causal equation of state for $m_\sigma \in \{400, 500\}$ MeV. On the other hand, no polynomial does the trick for $m_\sigma = 600$ MeV. We must investigate whether we even can find polynomials when we extend our search to include variations of μ_m as well. We have visualised our findings in Fig. I.2.

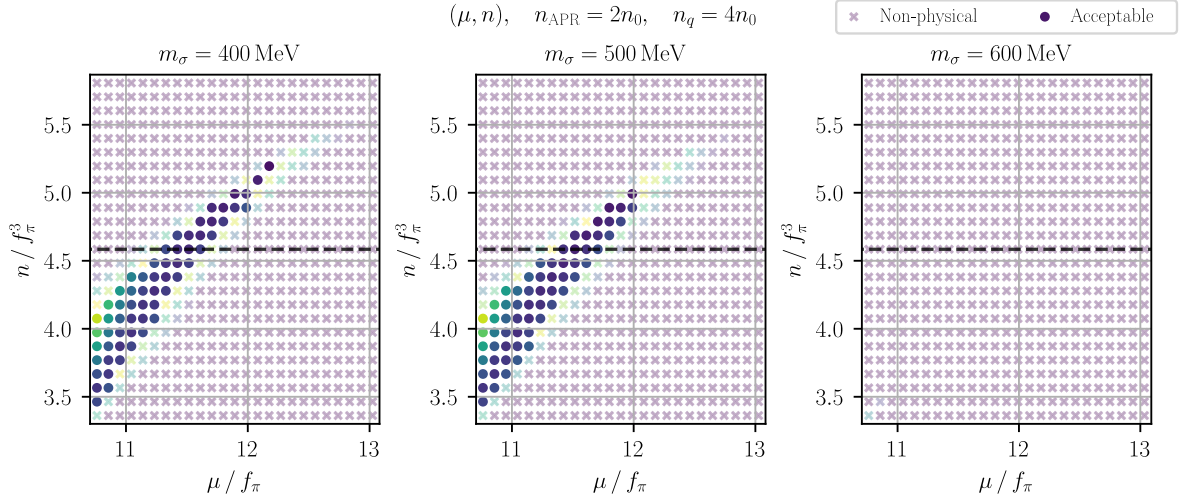


Figure I.2: The panels display a discrete set of choices for (μ_m, n_m) where the derivative of two third degree polynomials connect. The colouring of the dots indicates a measure of "kinkedness". The yellow means that the curves have a high degree of "kinkedness", while the darker and bluer the colour, the less kink is there to find at μ_m and μ_q . n_{APR} and n_q indicate at which number density we no longer trust the APR equation of state and the quark equation of state, respectively. The nuclear saturation density is as usual denoted by n_0 . The crosses represents the interpolations which yield non-causal equations of state. The more yellow the cross, the closer it is to be causal.

Each dot in the panels in the figure above represents a point where we force the polynomial construction through. Note the dashed horizontal line in Fig. I.2. The dots in Fig. I.1 lie on that dashed line, and we see what happens to the polynomials as we change μ_m . Unfortunately, it may seem that we cannot fit a polynomial for $m_\sigma = 600$ MeV. However, we may be less strict in our boundary conditions. By not enforcing that the second derivative is continuous through $\mu_{B,l}$, i.e. the top right boundary condition in Eq. (I.10), we may actually find causal interpolations. In the end, we found that modifying the second derivative boundary condition to

$$r''(x(\mu_N)) = 0.605 \frac{\partial n_N}{\partial \mu}, \quad (\text{I.11})$$

gave us a few choices of (μ_m, n_m) . Now we have found causal interpolating polynomials in the $m_\sigma = 600$ MeV-case too. This is displayed in Fig. I.3.

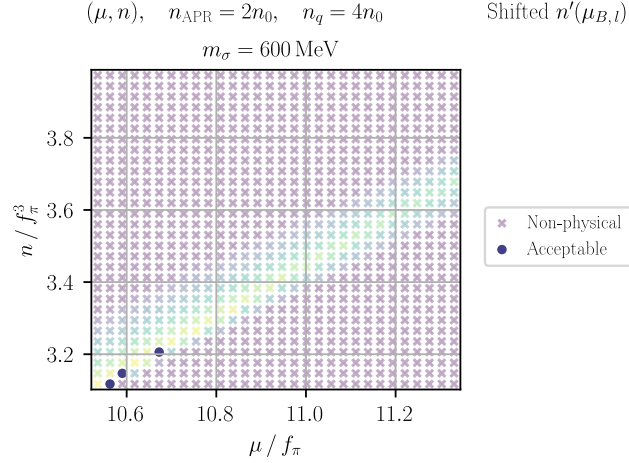


Figure I.3: Choices for (μ_m, n_m) . The colouring scheme is the same as in Fig. I.2, however, for this plot we have changed the boundary conditions as written down in Eq. (I.11). We have also narrowed down the search to a smaller range of μ and n , as there are no solutions elsewhere.

At last, we choose the polynomial fit with the least kink for each of the three values for m_σ . The selections are displayed in the main part of the thesis in Fig. 12.4. Explicitly, the choices for (μ_m, n_m) are shown in Table I.1

m_σ [MeV]	μ_m [MeV]	n_m [fm^{-3}]
400	1135	0.55
500	1127	0.53
600	982	0.33

Table I.1: The values of (μ_m, n_m) which give the smoothest interpolating polynomials for $n(\mu)$ with our chosen set of boundary conditions. These values yield the polynomials in Fig. 12.4.

As an important note on the interpolation, it should be mentioned that our fixing of the boundary conditions *and* using two third-degree polynomials are somewhat arbitrary choices. Of course, had the final results been unsatisfactory, we would have chosen other boundary conditions and/or different order polynomials. The point being: There may be better choices, however, determining them are hard to do in a rigorous way.

Finally, we would like to illustrate the polynomial interpolation procedure also for other parameters. We would like to use the actual APR-value for the neutron mass, $m_n = 936 \text{ MeV}$. In addition, we increase our scepticism towards the QM equation of state by one notch, setting $n_q = 6n_0$. Running our numeric set-up for these values, we find the physically reasonable set of (μ_m, n_m) as shown in Fig. I.4.

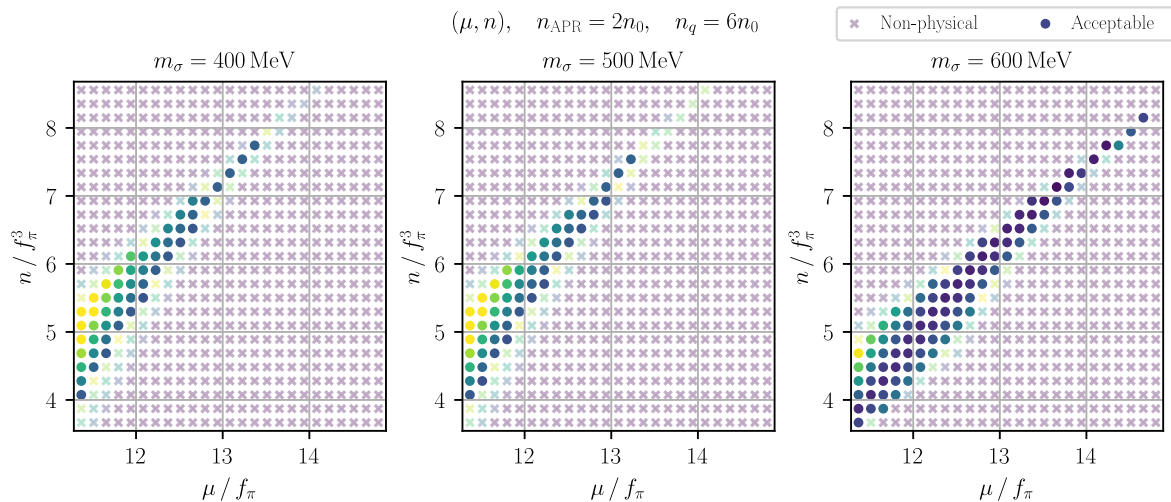


Figure I.4: Similar panels as in Fig. I.2, but this time we have increased the lower value where the quark phase start by modifying $n_q = 4n_0 \rightarrow n_q = 6n_0$. In addition, we have not shifted the neutron mass, such that it now corresponds to the APR-value, $m_n = 939.6$ MeV. This time, it seems $m_\sigma = 600$ MeV yields the smoothest interpolating functions.

In the end, for the unshifted m_n , $n_N = 2n_0$, and $n_q = 6n_0$, we find the best parameters (μ_m, n_m) to be the ones presented in Table I.2.

m_σ [MeV]	μ_m [MeV]	n_m [fm^{-3}]
400	1101	0.53
500	1057	0.42
600	1277	0.75

Table I.2: The values of (μ_m, n_m) that gives the smoothest interpolating polynomials for $n(\mu)$ with $m_n = 939.6$ MeV, $n_N = 2n_0$, and $n_q = 6n_0$. These values yield the polynomials in Fig. 12.7.

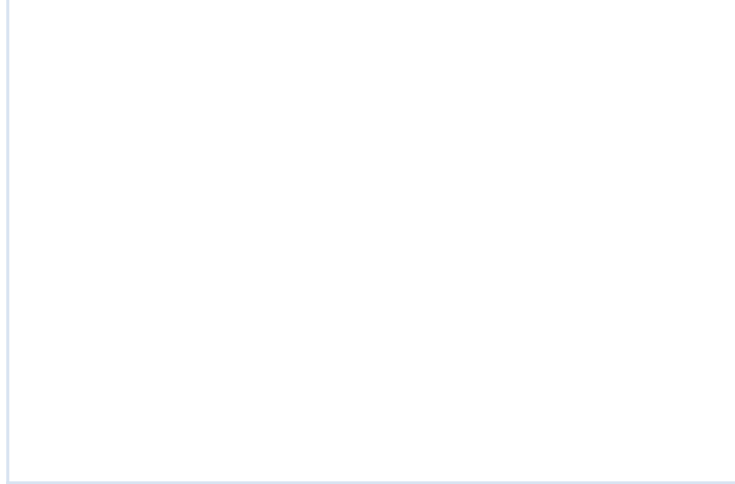
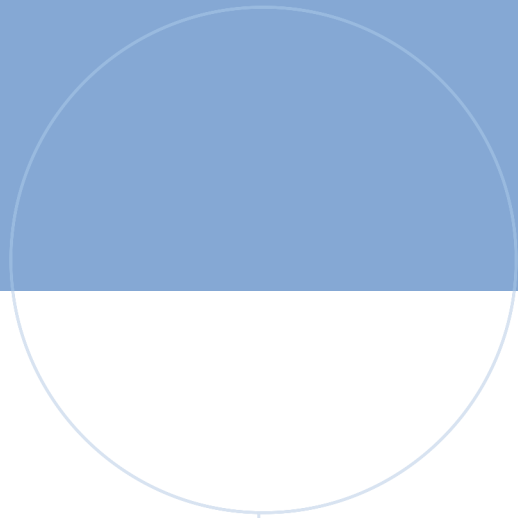
Bibliography

- [1] Sletmoen, H. (2022) *Quark and Hybrid Stars with the Quark-Meson Model*. Master's Thesis, NTNU, Trondheim, Norway.
Retrieved from: <https://github.com/hersle/master-thesis>
- [2] Tondeur, F., Berdichevsky, D., & Farine, M. (1986) *Nuclear Matter Saturation Density: From Finite Nuclei to Infinite Matter*.
Zeitschrift für Physik A Atomic Nuclei **325** pp. 405–413.
- [3] IAU Working group. *Numerical Standards for Fundamental Astronomy*.
Accessed: 26.06.2023
https://iau-a3.gitlab.io/NSFA/NSFA_cbe.html#GMS2012
- [4] Glendenning, N. K. (2000) *Compact Stars: Nuclear Physics, Particle Physics and General Relativity*.
New York: Springer-Verlag
- [5] Misner, C. W., Thorne, K. S., Wheeler, J. A. (1973) *Gravitation*.
San Fransisco: W. H. Freeman and Company
- [6] d'Inverno, R. (1992) *Introducing Einstein's Relativity*.
Oxford: Oxford University Press
- [7] Weinberg, S. (1972) *Gravitation and Cosmology*.
Canada: John Wiley & Sons, Inc.
- [8] Wald, R. M. (1984) *General Relativity*.
Chicago and London: The university of Chicago Press
- [9] Oppenheimer, J. R., Volkoff, G. M. (1939) *On Massive Neutron Cores*.
Phys. Rev. Vol. 55, pp. 374-381
- [10] Shibata, M., Zhou, E., Kiuchi, K., Fujibayashi, S. (2019) *Constraint on the Maximum Mass of Neutron Stars Using GW170817 Event*.
Physical Review D 100.2, p. 023015
- [11] Pasechnik, R., Šumbera, M. (2017) *Phenomenological Review on Quark-Gluon Plasma: Concepts vs. Observations*.
Universe 3
- [12] Chandrasekhar, S. (1964) *Dynamical Instabilities of Gaseous Masses Approaching the Schwarzschild Limit in General Relativity*.
Phys. Rev. Vol. 12, Nr. 4

-
- [13] Bardeen, J. M., Thorne, K. S., Meltzer, D. W. (1966) *A Catalogue of Methods for Studying the Normal Modes of Radial Pulsation of General-relativistic Stellar Models*. Astrophysical Journal, vol. 145, pp. 505-513
- [14] Chin, S. A., Walecka, J. D. (1974) *An Equation of State for Nuclear and Higher-density Matter Based on a Relativistic Mean-field Theory*. Physics Letters, vol.52B, no. 1
- [15] Polyanin, A. D., Zaitsev, V. F. (2003) *Handbook of Exact Solutions for Ordinary Differential Equations*. Florida: Chapman & Hall/CRC.
- [16] Hewish, A., Bell, S. J., Pilkington, J. D. H., Scott, P. F., & Collins, R. A. (1968) *Observation of a Rapidly Pulsating Radio Source*. Nature **217**
- [17] Özel, F. & Freire, P. (2016) *Masses, Radii, and the Equation of State of Neutron Stars*. Annu. Rev. Astron. Astrophys. 54 pp 401–440.
<https://doi.org/10.48550/arXiv.1603.02698>
- [18] *Fermi LAT Multiwavelength Coordinating Group*
Accessed: 26.06.2023.
<https://confluence.slac.stanford.edu/display/GLAMCOG/Fermi+LAT+Multiwavelength+Coordinating+Group>
- [19] Antoniadis, J. et al. (2013) *A Massive Pulsar in a Compact Relativistic Binary*. Science, vol. 340 6131, pp. 448-502.
<https://doi.org/10.48550/arXiv.1304.6875>
- [20] Özel, F., Psaltis, D., Ransom, S., Demorest, P., & Alford, M. (2010) *The Massive Pulsar PSR J1614-2230: Linking Quantum Chromodynamics, Gamma-ray Bursts, and Gravitational Wave Astronomy*. ApJL **724** L199
<https://doi.org/10.48550/arXiv.1010.5790>
- [21] Romani, R. W., Kandel, D., Filippenko, A. V., Brink, T. G., & Zheng, W. (2022) *PSR J0952–0607: The Fastest and Heaviest Known Galactic Neutron Star*. ApJR **934** L17
<https://doi.org/10.48550/arXiv.2207.05124>
- [22] Laine, M. & Vuorinen, B. (2022) *Basics of Thermal Field Theory*. Lect. Notes Phys. **925**
<https://doi.org/10.48550/arXiv.1701.01554>
- [23] Sakurai, J. J. (1967) *Advanced Quantum Mechanics*. Pearson Education, inc.
- [24] Kardar, M. (2007) *Statistical Physics of Particles*. New York: Cambridge University Press.
- [25] Zee, A. (2010) *Quantum Field Theory in a Nutshell*. New Jersey: Princeton University Press.
- [26] Dirac, P. A. M. (1928) *The Quantum Theory of the Electron*. Proc. Roy. Soc. Lond. A **117** pp. 610–624. <https://doi.org/10.1098/rspa.1928.0023>
- [27] Peskin, M. E. & Schroeder, D. V. (1995) *An Introduction to Quantum Field Theory*. Addison-Wesley Publishing Company.
- [28] Tetradis, N. (2003) *The Quark-Meson Model and the Phase Diagram of Two-Flavour QCD*. Nucl.
-

- Phys A**726**, pp. 93–119. <https://doi.org/10.1016/S0375-9474%2803%2901624-5>
- [29] Adhikari, P., Andersen, J. O., & Kneschke, P. (2017) *Inhomogeneous Chiral Condensate in the Quark-Meson Model*.
Physical review D 96, p 016013.
<https://doi.org/10.1103/PhysRevD.96.016013>
- [30] Weinberg, S. (2021) *On the Development of Effective Field Theory*.
Eur. Phys. J. H 46:6.
<https://doi.org/10.1140/epjh/s13129-021-00004-x>
- [31] Gómes Nicola, A. (2020) *Aspects on Effective Theories and the QCD Transition*.
Symmetry 12 6, 945.
<https://doi.org/10.48550/arXiv.2005.08234>
- [32] Schwartz, M. D. (2014) *Quantum Field Theory and the Standard Model*.
New York: Cambridge University Press.
- [33] Erdmann, K. & Wildon, M. J. (2006) *Introduction to Lie Algebra*.
London: Springer-Verlag.
- [34] Bodmer, A. R. (1971) *Collapsed Nuclei*.
Phys. Rev. D 4, 1601.
<https://doi.org/10.1103/PhysRevD.4.1601>
- [35] Witten, E. (1984) *Cosmic Separation of Phases*.
Phys. Rev. D 30, 272.
<https://doi.org/10.1103/PhysRevD.30.272>
- [36] Particle Data Group (2022) *Review of Particle Physics*.
Progress of Theoretical and Experimental Physics, Volume 2022.
<https://doi.org/10.1093/ptep/ptac097>
- [37] Schaefer, B.-J. & Wambach, J. (2006) *Susceptibilities near the QCD (tri)Critical Point*.
Phys. Rev. D 75, 085015
<https://doi.org/10.1103/PhysRevD.75.085015>
- [38] Eickmann, G. (2020) *Chiral Effective Field Theories*. Lecture notes.
<http://cftp.ist.utl.pt/~gernot.eichmann/lecture-notes>
- [39] Chodos, A., Jaffe, R. L., Johnson, K., Thorn, C. B., & Weisskopf, V. F. (1974) *New Extended model of Hadrons*.
Phys. Rev. D **9** 3471 <https://doi.org/10.1103/PhysRevD.9.3471>
- [40] Griffiths, D. J. (1987) *Introduction to Elementary Particles*.
John Wiley & Sons, Inc.
- [41] Gasser, J., & Zarnauskas, G.R.S. (2010) *On the Pion Decay Constant*.
Phys. Lett. B **693** 2, pp. 122-128. <https://doi.org/10.48550/arXiv.1008.3479>
- [42] Pogliano, F. (2017) *Neutron Stars – Study of the Mass-Radius Relation and Mean-Field Approaches to the Equation of State*. Master’s Thesis.
Norwegian University of Science and Technology.
- [43] Baym, G., Hatsuda, T., Kojo, T., Powell, P. D., Song, Y. & Takatsuka T. (2018) *From Hadrons to Quarks in Neutron Stars: A Review*.
Rep. Prog. Phys. 81 056902.
<https://doi.org/10.1088/1361-6633/aaae14>

- [44] Akmal, A., Pandharipande, V. R. & Ravenhall, D. G. (1998) *Equation of State of Nucleon Matter and Neutron Star Structure*.
Phys. Rev. C 58, 1804-28.
- [45] Douchin, F & Haensel, P. (2001) *A Unified Equation of State of Dense Matter and Neutron Star Structure*.
A&A 380, pp. 151-167. <https://doi.org/10.1051/0004-6361:20011402>
- [46] Baym, G., Pethick, C. & Sutherland, P. (1971) *The Ground State of Matter at High Densities: Equation of State and Stellar Models*.
Astrophysics Journal, 170, pp. 299-317.
<https://dx.doi.org/10.1086/151216>
- [47] Typel, S., Oertel, M. & Klähn, T. (2015) *CompOSE CompStar Online Supernova Equations of State Harmonising the Concert of Nuclear Physics and Astrophysics compose.obspm.fr*.
Phys. Part. Nuclei 46, 633-664.
<https://doi.org/10.1134/S1063779615040061>
(Data explanation on pp. 644-645)
- [48] Folkestad, Å. S. (2018) *Effective Polyakov Loop Modeling of QCD – A Field Theoretical Study of the Phase Diagram of Quark Matter*. Master's Thesis.
Norwegian University of Science and Technology.



 **NTNU**

Norwegian University of
Science and Technology